Taming *Vibrio cholerae* with cationic polymers: engineering bacterial physiology by interfering with communication and virulence.

Nicolás Pérez-Soto.

A thesis submitted to the University of Birmingham for the degree of DOCTOR OF PHILOSOPHY.

Institute of Microbiology and Infection
School of Biosciences
College of Life and Environmental Sciences
University of Birmingham

May 2018

UNIVERSITY^{OF} BIRMINGHAM

University of Birmingham Research Archive

e-theses repository

Abstract

The Gram-negative *Vibrio cholerae* is native to aquatic environments and an important human pathogen causing cholera disease. The induction of virulence in this bacterium is subjected to a wide variety of stimuli including environmental cues and quorum sensing. In this study, non-bactericidal cationic polymers were designed to capture *Vibrio cholerae* into clusters resulting in physiological changes. Poly(*N*-(3-aminopropyl) methacrylamide) (P1), poly(*N*-[3-dimethylamino)propyl] methacrylamide) (P2) or poly(acryloyl hydrazide) imidazole (P3) were synthesised via free radical polymerisation displaying amine groups that cluster cells mediated by electrostatic interactions. This binding resulted in a forced transition from planktonic to a sessile lifestyle. The clustering is accompanied by reduced motility, increased biofilm synthesis and repression of virulence since the expression cholera toxin was down-regulated. This avirulent phenotype was defective to colonise intestinal epithelial cells and the zebrafish digestive tract. Since the cell density increases locally as a result of the clustering, a quorum-sensing-controlled phenotype was observed as the *lux* operon was actively expressed. Overall, the bacterial physiology was modulated without genetic modification preventing virulence as the pathogen adapt its lifestyle during clustered lifestyle. This thesis highlights the use of polymeric materials as a mean to control pathogens beyond the use antibiotics.

Acknowledgements

The PhD process has been a stimulating, yet challenging journey. However, the people I met along the way were essential in supporting me to accomplish this endeavour.

Table of contents

List of tables

List of figures

List of abbreviations

ACVA	4,4'-azobis(4-cyanovaleric acid); V501	GPC	Gel permeation chromatography
AHL	Acyl homoserine lactone	H-NS	Histone-like nucleoid-structuring protein
AI-2	Auotinducer -2	HEPES	4-(2-hydroxyethyl)-1-piperazineethanesulfonic acid
AIBN	Azobisisobutyronitrile		
BHI	Brain-heart infusion		
BMSU	Biomedical services unit	LPS	Lipopolysaccharide
bp	base pair	MOI	Multiplicity of infection
c-di-GMP	cyclic diguanylate	NMR	Nuclear magnetic resonance
CAI-1	Cholera autoinducer 1	NPN	N-phenyl-1-naphthylamine
cAMP	cyclic adenosine monophosphate	OD	Optical density
		ONPG	ortho-Nitrophenyl-β-galactopiranoside
CFU	Colony forming units		
CRP	cAMP receptor protein	P1	Poly(N-(3-aminopropyl)-methacrylamide
CTx	Cholera toxin		
D_2O	Deuterium oxide	P2	Poly(N-[3-dimethylamino]-propyl)-methacrylamide
DIC	Differential interference contrast		
		P3	Poly(acryloyl hydrazide)
DMEM	Dulbecco's modified Eagle's medium	PFA	Parafomaldehyde
		PTU	N-phenylthiourea
DMSO	Dimethyl sulfoxide	SAM	S-adenosyl methionine
DPD	(S)-4,5-dihydroxy-2,3-pentanedione	TCBS	Thiosulfate-citrate-bile salts-sucrose
ELISA	Enzyme-linked immunosorbent assay	TCP	Toxin co-regulated pilus
		VBNC	Viable but nonculturable
FACS	Fluorescence-activated cell sorting	VPS	*Vibrio* polysaccharide
		VPI	*Vibrio* pathogenicity island
FMN	Flavin mononucleotide		

Chapter 1: General Introduction

1.1 Background

Bacterial infections are an increasingly common threat over recent years. Diseases related to pathogens have a critical impact at an economic level on health systems especially in developing countries, and directly on the quality of life of the population (Allegranzi *et al.*, 2011). According to the National Health Service (NHS), in the United Kingdom alone, 44,000 people die from sepsis every year, which are more deaths than from lung or bone cancers (England, 2015, Shahin *et al.*, 2012), and nearly 17 million around the world (WHO, 1996). Many of these deaths have in common the presence of multidrug-resistant bacteria as their cause. The abuse of antibiotics is speeding up the development of so-called "superbugs" therefore, the development of new strategies to treat bacterial infections is urgently needed. New approaches are desired that target and intefere with cellular functions that are not essential to the bacterial physiology, and at the same time, are cheap, to replace or enhance current treatments and produce no selective pressure. Synthetic polymers appear to be an excellent alternative to attack this problem as the physical capturing of microorganism can result bactericidal (Yang *et al.*, 2017) or induce controlled phenotypes (Lui *et al.*, 2013).

1.2 The bacterial cell envelope

In order to understand the dynamics between polymeric materials and bacterial cells, it is necessary to give an overview of the bacterial cell envelope structures. The cell membrane is the separation between the extracellular environment with the inner compartment of both eukaryotic and prokaryotic cells. It's a complex structure essential to maintain the inner homeostasis while being selectively permeable to nutrients from the outside and waste from the inside (Silhavy *et al.*, 2010). An additional layer of phospholipids and polysaccharides

covering the cell membrane has allowed classifying a vast number of bacteria into two major groups according to the intensity of the Gram staining. Gram-positives are characterised by the lack of an outer membrane. Instead, they have a thicker peptidoglycan that retains crystal violet dye. Gram-negatives present an outer membrane and a thinner peptidoglycan that retain less crystal violet dye. In Gram-negatives, the envelope is thin with sub-compartments in it. It is composed of three layers, the outer membrane, the peptidoglycan layer and the inner membrane; the space between each layer is the periplasm. The cell wall in Gram-positives is relatively big compared with Gram-negatives as the absence of outer membrane is compensated with layers of peptidoglycan. The composition of peptidoglycan is similar to Gram-negatives with linear glycan strands of *N*-acetylglucosamine and *N*-acetylmuramic acid and peptide stems (Silhavy *et al.*, 2010). The Gram-positive cell wall is also composed of anionic polymers known as teichoic acids that maintain rigidity and regulate the net charge in the cell wall (Marquis *et al.*, 1976). Many proteins are decorating the cell wall, and while in Gram-negatives these proteins are assembled in the outer membrane, in Gram-positives proteins are anchored to the peptidoglycan or teichoic acids by covalent or non-covalent binding (Dramsi *et al.*, 2008).

1.2.1 Outer membrane

The outer membrane is the most external layer of Gram-negatives and is in contact with the extracellular environment. It is an asymmetric phospholipid bilayer that in its outer leaflet is covered with lipopolysaccharide (LPS). The lipopolysaccharide is composed of three main parts; the most external corresponds to the O-antigen which is highly immunogenic and elicit a strong innate immune response, followed by the LPS core and finally the lipid A is embedded in the outer membrane. The core is divided in inner and outer core according to the sugar

composition and the O-antigen is a variable glycan structure useful to classify strains (Chatterjee and Chaudhuri, 2003). The lipopolysaccahride plays an important role in defense against antimicrobial compounds. In *V. cholerae*, the modification of the lipid A anchoring complex with glycine and diglycine, modulates the net of charges of the bacterial cell envelope resulting in reduced susceptibility to cationic compounds such as polymixin B (Hankins *et al.*, 2012).

Beside the LPS, the outer membrane exhibits different lipoproteins and porins, which allow selective permeability for small molecules by passive diffusion (Silhavy *et al.*, 2010). An example of this is the *Vibrio cholerae* porins OmpU and OmpT that control the passage of hydrophilic solutes such as deoxycholate when exposed to bile salts which is crucial during infection. Their expression is dictated by the virulence regulator ToxR, and the ratio between OmpU/OmpT impacts on the strain virulence, since strains expressing more OmpT instead of OmpU are deficient to colonise the digestive tract. Conversely, major expression of OmpU resulted in high tolerance to deoxycholate (Provenzano and Klose, 2000, Wibbenmeyer *et al.*, 2002). Despite these observations, the role of these porins in virulence remains unclear.

1.2.2 Peptidoglycan and periplasm

The peptidoglycan is a rigid layer composed by long glycan chains consisting of N-acetyl glucosamine-N-acetyl muramic acid disaccharide cross-linked by peptide stems. This repetitive array of glycans protects the cell from osmotic shocks while at the same time gives the bacterial cell its shape. Depending on the glycan chain length and the angle at which these polymers are crosslinked the cell will be shaped (Gan *et al.*, 2008). *V. cholerae* cells are "comma-shaped" which allows an optimum movement when swimming in viscous environments. The peptidoglycan is located in the aqueous space between the outer and inner

membranes named periplasm. The periplasm is important for several cellular functions since it is a space full of enzymes that resemble lysosomal functions as in eukaryotic cell to degrade potentially harmful molecules. Also, components of the cell wall are synthesised and translocated from here during envelope biogenesis (Silhavy *et al.*, 2010). Also, periplasmic elements help to determine the cell shape. *V. cholerae* expresses a periskeletal element, CrvA, which assembles into rigid filaments located in the periplasmic space at the inner curvature that model the curved cell shape (Bartlett *et al.*, 2017).

1.2.3 Inner membrane

Between the periplasm and the cytoplasm is the inner membrane. This phospholipid bilayer has many of the proteins essential for bacterial physiology, such as energy production, protein and lipid synthesis and export.

It is well known that the membrane has a negative net charge (Shai, 2002). In Gram-negatives more than the LPS, is the inner membrane the structure that contributes to maintain a net negative charge (Silhavy *et al.*, 2010).

The bacterial cell envelope of Gram-positives and Gram-negatives is depicted below (Fig. 1.1).
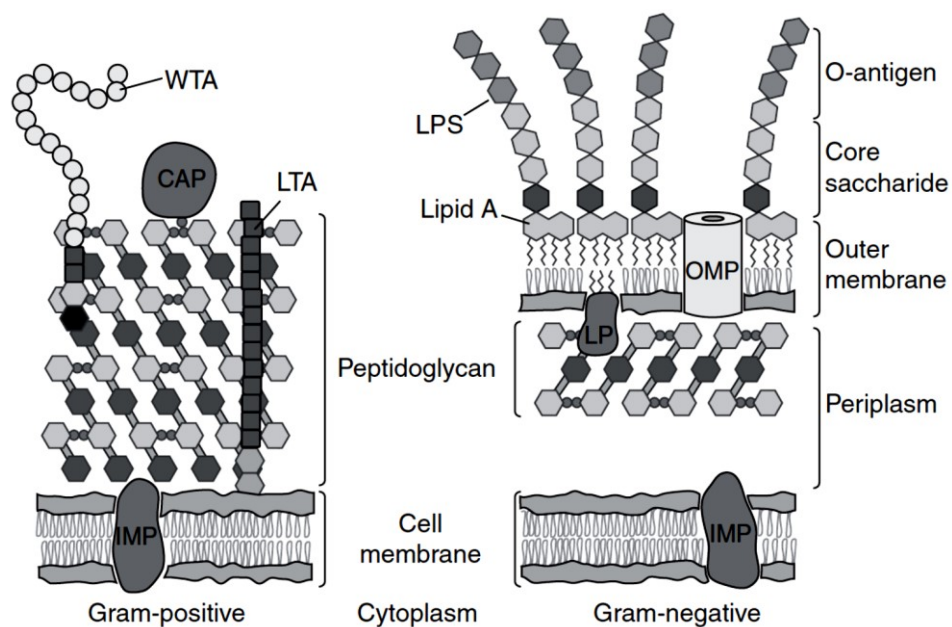
Figure 1.1. Diagram of Gram-positive and Gram-negative bacterial cell envelopes. WTA, wall teichoic acid; CAP, covalently attached protein; LTA, lipoteichoic acid; IMP, integral membrane protein, LPS, lipopolysaccharide, OMP, outer membrane protein and LP, lipoprotein (modified from Silhavy *et al.*, 2010).

1.3 Introduction to synthetic polymers as nanomaterials

Polymers are long repetitions of a monomer (homopolymers) or a combination of usually two monomers (copolymers); this combination could be statistically or randomly distributed (statistical or random copolymers), or one type of monomer on each side (block copolymers) (Wang and Grayson, 2012). The synthesis of these materials is relatively easy, the production easily scalable, and their length and composition can be precisely controlled (Müller and Matyjaszewski, 2009). The polymer carbon-based chemistry allows to rationally design the molecular structure, adapting the material to different environments and purposes. These attributes make polymers attractive for biomedical applications. However, polymers are not new in medicine since they are already the material of choice for sutures, prosthetics and implants (Maitz, 2015). In this respect, biodegradable materials are used as they could be soluble or can be enzymatically degraded (Langer, 2000). Further, the development of modern medicine has opened new possibilities to the use polymers in more specific manners, such as nanomaterials. As the name implies, nanomaterials are structures with dimensions at the nanoscale (10^{-9}), allowing their interactions with cellular structures at the molecular level. With this in mind, most of the relevant applications are focused on enhanced drug delivery methods, regeneration of tissue by tissue engineering, as synthetic vectors for gene therapy, and as matrices to control bacterial infections (Griffith, 2000).

The use of polymers as drug delivery carriers aims to improve the pharmacokinetics and biodistribution of drugs used in traditional treatments (Allen and Cullis, 2004). Biodegradable polymers are often used as the periodic release of the drug can be controlled. The most used polymers for this application are poly(glycolic acid), poly(lactic acid) and poly(lactic acid-co-glycolic acid) copolymers. The biological, thermal and mechanical properties can be modulated by changing the stereochemistry of the material (Pillai and Panchagnula, 2001). Non-

degradable polymers are also used to create porous matrices that contain the drug controlling the release by passive diffusion (Kumar and Kumar, 2013).

Stimuli-responsive nanomaterials take advantage of the environmental conditions such as body organs or cellular compartments, to react and reshape. In these applications, biologically active groups are hidden until conditions allow the polymer to expose them. Usually, these conditions are pH or temperature (Schmaljohann, 2006) but in sophisticated applications can be the presence of a particular catalytic activity (Hu *et al.*, 2012) or the redox potential (Mathiowitz *et al.*, 1997).

Polymer design can be challenging but is also flexible; this is relevant to increase the specificity of the delivery method. Polymers can be coupled to adapters that respond to the triggering condition. For example, *Pseudomonas aeruginosa* has been controlled with antimicrobial particles, consisting of a combination of a polycation complex with a peptide specific for the bacterial protease LasB, avoiding degradation by human elastase (Insua *et al.*, 2016).

The use of polymers in tissue engineering faces the necessity to develop prosthetics or artificial tissue that can remain in the body without side effects. This application is particularly challenging since it is necessary to understand the complexity of the cellular interactions. The principle here is to use polymeric materials as scaffolds for cells to spatially arrange themselves, and also control the cell density. Essentially, the control of cellular behaviours is achieved by coupling the polymer with bioactive ligands such as proteins that mediate cell adhesion (Wheeldon *et al.*, 2011). Hydrogels are among the most used type of polymers in this application due to their ability to control ligand concentration and also the movement of these ligands uniformly (Zahouani *et al.*, 2017). Other approaches to control the concentration of ligands is by using self-assembly materials to coat surfaces. Here, hydrophobicity controls the

concentration of polymers to attach to a surface, consequently controlling the concentration of ligands coupled to polymers (Griffith, 2000).

The application of polymers in gene therapy derives from the drug delivery strategies due to the importance to cross cellular barriers. Here, polymers are designed to carry DNA and target cellular compartments where the DNA is processed. Although polymers as synthetic vectors lack several functions compared to viruses, the uptake occurs through endocytic pathway and the "proton-sponge" hypothesis may explain how the DNA could be delivered. Once the material is internalised via endolysosomal vesicles, ATPases pump protons into the vesicle to compensate the increase in pH as the secondary and tertiary amines in these polymers get protonated at lysosomal pH. This effect also is accompanied by movement of water which ultimately causes an osmotic shock, liberating the polyplexes into the cytosol (Pack *et al.*, 2005). Cationic polymers are especially important in this area as DNA can be coupled by binding to the phosphate groups. Low molecular weight polymers such as polyethylenimines useful to couple DNA, however the rate of transfection is low (Moghimi *et al.*, 2005).

1.3.1 Cationic polymers to control bacterial pathogens

Bacteria develop resistance to antibiotics faster than our capacity to develop new antibiotics. Polymeric materials offer an opportunity to control pathogens by targeting virulence at the regulatory level, or by competing for attachment sites. Compared with single molecules, polymers can be multivalent which allows them to target multiple ligands enhancing, tightening and outcompeting the binding for a particular membrane protein, component of the lipopolysaccharide or toxin (Van Dongen *et al.*, 2014). Many reports have demonstrated the potential of polymers in antimicrobial applications (Timofeeva and Kleshcheva, 2011, Muñoz-Bonilla and Fernández-García, 2012, Siedenbiedel and Tiller, 2012). Within this group, the

vast majority are cationic polymers since they are attracted to the negatively charged membrane phospholipids. These polymers kill the bacteria upon contact with the membrane in a similar way as antimicrobial peptides (Tiller *et al.*, 2001). On Gram-negative membranes, the contact with the material may perturb the membrane, inducing a collapse in the electrolyte gradient resulting in cell death by osmotic shock (Chen and Cooper, 2002). In Gram-positives it would follow a similar pathway, facilitated by the absence of the outer membrane. These antimicrobial polymers are diverse in structure but share similarities in the chemical properties of their backbone or side groups. Munoz-Bonilla (Muñoz-Bonilla and Fernández-García, 2012) grouped several antimicrobial polymers according to their biologically active group as described below. This type of polymer is mostly used to functionalise surfaces of medical devices resulting in a reduction in the bacterial burden and the amount of biofilm as well (Tiller *et al.*, 2002, Tiller *et al.*, 2001).

Polymers with quaternary nitrogen atoms are widely used in antimicrobial applications. The protonated nitrogen atom confers the biocidal property, and the backbone is modified to modulate the material solubility (Muñoz-Bonilla and Fernández-García, 2012). However, the balance between hydrophobicity from the backbone and the net charge conferred by the lateral side chains can determine their toxicity.

The easiest cationic polymers to prepare are acrylate and methacrylate derivatives, as many monomers are commercially available. Polymers prepared from polystyrene or poly(vinyl pyridine) backbones are also easy to prepare and widely used. Nevertheless, the biocompatibility of these polymers is a drawback, and most applications are focused on coating surfaces to prevent bacterial adhesion or other *ex vivo* applications (Tiller *et al.*, 2002). Other preparations involve polyelectrolytes to increase the number of double bonds in the backbone, polysiloxanes which produce flexible backbones, dendrimers, polyoxazolines functionalised

with quaternary ammonium salts and quaternary nitrogen atoms as part of the backbone (Muñoz-Bonilla and Fernández-García, 2012).

At the nanoscale, the mechanisms by which cationic polymers interact with the membrane *in vivo* are not well understood. As the binding occurs by electrostatic forces, cationic groups interact with the phosphate moiety of phospholipids and teichoic acids and the hydrophobicity induces their intercalation inside the membrane. Studies with proteoliposomes have shown that binding to the membrane also clusters membrane proteins (Kozlova *et al.*, 2001). Molecular dynamics studies demonstrated that depending on their hydrophobicity; polymers can easily enter the membrane bilayer and aggregate (Bochicchio *et al.*, 2017). Once inside the membrane, cationic groups, especially protonated amines, rearrange the net charge, moving water molecules to the water/lipid interface due to binding to head groups of anionic lipids slowing down their lateral movement and increasing the membrane permeability (Kostritskii *et al.*, 2016).

1.3.2 Not to kill but deceive

Few reports have addressed the use of polycations at non-toxic concentrations to manipulate bacterial phenotypes. Here, polymers are designed to attack a particular cellular process known as quorum sensing, which in simple words interferes with the communication between bacteria.

To trigger an infective process, the microbes often rely on environmental conditions such as pH, temperature, metal key ions or anions, but also more complex triggers such as the hostile encounter with the immune system (Thomas and Wigneshweraraj, 2014). Nevertheless, equally important as these conditions are the inter-cellular communication system or quorum sensing. Microorganisms (bacteria and fungi) are constantly releasing quorum sensing molecules or autoinducers; when the concentration of these autoinducers surpasses a threshold

given by the cellular density, microbes start to act collectively (Waters and Bassler, 2005). Quorum sensing signalling pathways vary between organisms, but similar features are shared. In Gram-negative organisms, quorum sensing is mediated mainly by acyl-homoserine lactones (AHL) molecules whereas in Gram-positive species short peptide sequences are used (Rutherford and Bassler, 2012). Inner membrane receptors sense these molecules with the potential to start a series of processes resulting in the expression of regulatory molecules. These regulators can modulate innocuous effects such as the production of bioluminescence, synthesis of pigments, or virulence-related processes such as the expression of virulence factors or the production of biofilm (Waters and Bassler, 2005). The quorum sensing cascades will be discussed in detail in Section 1.5 and Chapter 6.

Mainly, two ways in which polymers interfere with the communication have been used, arresting/interfering the signalling molecule (quorum quencher), or as an aggregative cell agent. However, worth to mention that not all the strategies to interfere with quorum sensing are polymer-based, also nanoparticles have been used successfully. The virulence of *V. cholerae* has been modulated by the external addition of controlled quantities of autoinducers through autoinducer-loaded nanoparticles though a technique called Flash NanoPrecipiation, where autoinducers are encapsulated with a lipophilic co-core surrounded by amphiphilic PEG (Lu *et al.*, 2015). Similarly, the quorum quencher quercetin has been encapsulated in chitosan, sulfo-butyl-ether-β-cyclodextrin and/or pentasodium tripolyphosphate though ionotropic gelation to produce nanoparticles with the ability to control quorum sensing in *Escherichia coli* (Thanh Nguyen and Goycoolea, 2017).

1.3.3 Depletion of autoinducers by synthetic polymers

At early stages of infection, it becomes critical for microbes to form tight and specific interactions with the host to increase the density of cells. At the same time, quorum sensing

24

signalling is still weak due to low concentration and rapid diffusion of signal molecules (Lui *et al.*, 2013). For some pathogens, such as *P. aeruginosa* or *Staphylococcus aureus,* the induction of virulence is coupled with the activation of quorum sensing (Rutherford and Bassler, 2012). Polymers have potential to reduce the concentration of autoinducers, by incorporating functional groups able to interact with and sequester autoinducers. Compared with small soluble "quorum-quencher" molecules, polymers can be attached to surfaces interfering with the attachment and ultimately biofilm formation. Together with their intrinsic multivalence, increase their efficacy in this application compared with small molecules.

Quorum quenchers combined with polymers have been used to inhibit expression of the quorum-dependent *agr*-system of *S. aureus (Kratochvil et al., 2015)*. Using a nanoporous superhydrophobic film to coat surfaces, water-labile peptidic analogue autoinducers can be coupled and used to compete with the natural signal molecules for their receptors. This approach has been shown to inhibit quorum sensing, and quorum quenchers were detected after eight months (Kratochvil *et al.*, 2015). Similarly, dendrimeric scaffolds exposing an antagonist of AI-2 reduced quorum-sensing in *Salmonella enterica Typhimurium* in a concentration-dependent manner by direct interaction with quorum sensing sensors (Garner *et al.*, 2011).

Molecularly imprinted polymers (MIP) have been shown to be effective disrupting effects on the quorum sensing signal of *P. aeruginosa* PAO1, reducing the biofilm formation by around 80% (Piletska *et al.*, 2011). This approach is relevant since *P. aeruginosa* is commonly found attached to catheters and medical devices as a biofilm. Interruption of communication by arresting AHL has been achieved using the marine pathogen *Vibrio fischeri,* resulting in a reduction in the emission of bioluminescence (Piletska *et al.*, 2010). *Vibrio* species use a second quorum sensing signal molecule derived from 4,5-dihydroxy-2,3-pentaedione (DPD) and $B(OH)_3$ known as AI-2. Poly(vinyl alcohol)s easily quench AI-2, reducing the natural luminescence of *Vibrio harveyi* (Lui *et al.*, 2013). Other types of structures have been used to

quench quorum sensing signals. AHL from the opportunistic pathogen *Serratia marcescens* was sequestered by cyclodextrin molecules, reducing the formation of pigments (Kato *et al.*, 2006).

1.3.4 Clustering bacterial cells with cationic polymers

Microorganisms have evolved their quorum sensing routes independently, some regulating the production of virulence factors opposite to the cell density such as *V. cholerae*. Since virulence is activated at low cell density, the clustering of cells will increase the local concentration of autoinducers within the cluster. Few studies have dealt with this idea, observing the induction of high cell density phenotypes in the bioluminescent bacterium *V. harveyi*. Polymers exposing cationic binding groups can cluster bacterial cells and induce the bioluminescence (Lui *et al.*, 2013, Louzao *et al.*, 2015, Leire *et al.*, 2016). However, electrostatic interactions may present the challenge of bacterial toxicity since many antimicrobial structures display cationic groups to damage the membrane. Therefore it is important to explore different binding groups.

As exposed on this work, the polymers used here were designed to capture bacteria in cell aggregates or clusters. The decision to use this type of polymers was based on previous works that demonstrate that amine groups were suitable to cluster bacterial cells without compromising its viability significantly. At physiological pH, the degree of protonation of the amines exposed by P1, P2 and P3 will differ, therefore the binding to the bacterial cells and the toxicity will be different as well. Experiences of clustering bacterial cell has been achieved and characterised for Gram-positive S. aureus and Gram-negatives *E. coli*, *P. aeruginosa* and *V. harveyi* with P2 (Louzao *et al.*, 2015) whereas the clustering of the primary amine of P1 has been studied using *V. harveyi* coupled with a dendrimers scaffold (Leire *et al.*, 2016). Bacteria quickly form clusters upon contact with the polymer, while physiological response related to a high cell density phenotype has been observed when clustering *V. harveyi* (Lui *et al.*, 2013).

On the other side, P3 or its binding group has not been used against bacterial cells, but the backbone allows the use of different binding molecules in order to fabricate polymer libraries by adding aminoaldehydes (Crisan *et al.*, 2017). The interaction at the polymer-membrane interface is still matter of research and what is known is discussed in chapter 4**.**

1.3.5 Potential sources of resistance

Modulating virulence though non-essential pathways is still a significant challenge and more research on the field is required. Bacteria can quickly develop resistance to small antimicrobial molecules such as antibiotics through overexpressing drug efflux pumps, modifying the structure of targeted enzymes or by blocking the drug's biological activity (Clatworthy *et al.*, 2007). Similar pathways to resistance have been identified in the case of quorum quenchers. In this respect, multidrug-resistant *P. aeruginosa* is well known to expose multiple drug efflux pumps that help to eliminate toxic compounds. An example of this is the efflux pumps MexR and NalC that move quorum quenchers outside the cell (Contreras *et al.*, 2013). On the other hand, use of polymeric structures interacting with membranes may elicit less resistance, as they cannot be subject to efflux and act extracellularly. However, resistance to antimicrobial peptides has been reported in *S. aureus*. This occurs through a similar mechanism as mupiricin resistance, where the anionic moiety of the teichoic acid is chemically modified to result in physicochemical surface changes (Peschel, 2002). More studies need to address potential pathways to resistance against these compounds.

There is not yet a clear picture of how these materials interact with bacterial communities in order to develop potential drugs to treat infections. As discussed above, quorum sensing circuits are diverse between organisms: while in some bacteria virulence is activated by quorum sensing in others it is repressed. Therefore, specificity against particular pathogens is critical

especially when localised in their niche. At the same time, pathogens need to be localised on specific tissues to initiate attachment and infection, then delivery of the compounds is also a key factor together with the toxicity against host cells.

Examples of these nanomaterials and relevant applications are summarised below (Fig 1.2).
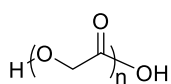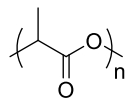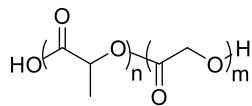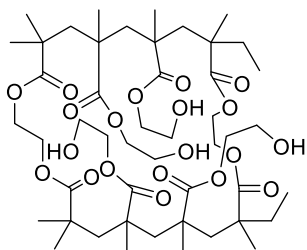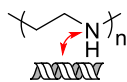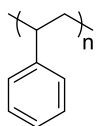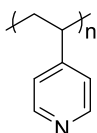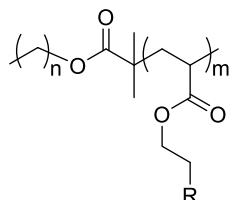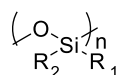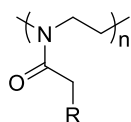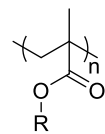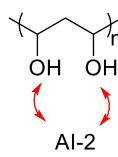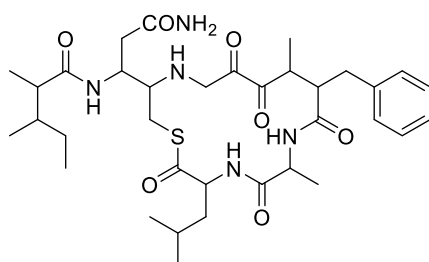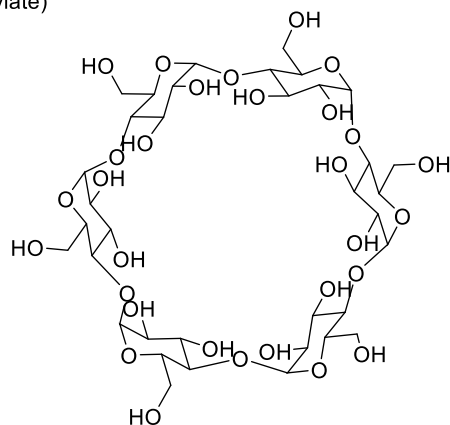
Figure 1.2. Examples of synthetic polymer backbones and nanomaterials, and relevant applications. AI-2 correspond to Autoinducer-2, discussed in detail in section 1.5 and chapter 6.

1.4 Vibrio cholerae and cholera disease

Cholera disease has been depicted in many forms throughout history. It was the hallmark of the early days of globalisation associated with the movement of people (Barnett and Collection, 2014). Even today, cholera disease remains a significant public health issue especially in poor areas and conflict zones around the world. Annually, more than 142,000 people are estimated to die while several million contract the disease (Lewnard *et al.*, 2016). Cholera disease is attributable to *V. cholerae*; a motile "comma-shaped" Gram-negative usually found in tropical estuaries or associated with aquatic organisms bound to chitinous surfaces (Tarsi and Pruzzo, 1999). Until today, seven pandemics have been recorded, the most recent being associated with the biotype El Tor (Prouty and Klose, 2006). *V. cholerae* is an exceptionally successful human pathogen due to the integration of genetic elements in the control of quorum sensing, expression of virulence factors, chitin breakdown and DNA exchange.

During the infective cycle, *V. cholerae* exhibits a wide variety of adhesion molecules and virulence factors. The expression of these genes is tightly coordinated since virulence overlaps with other cellular functions such as biofilm synthesis, quorum sensing or chemotaxis (Liu *et al.*, 2008, Teschler *et al.*, 2015, Matson *et al.*, 2007). *V. cholerae,* as a free-living cell, is highly susceptible to environmental conditions. For example, it tolerates a narrow range of pH being not successful to overcome the low gastric pH (Cash *et al.*, 1974). Nevertheless, there are less susceptible and more infective phenotypes known as "viable-but not culturable" (VBNC) or "hyperinfectous" cells which can be found as cells contained within biofilms or cells derived from microcolonies respectively (Almagro-Moreno *et al.*, 2015a). Usually, virulence in *V. cholerae* is expressed when bacterial density is low and is repressed when it reaches high cell density in response to quorum sensing (Hammer and Bassler, 2003). It is hypothesised that this

is a dissemination strategy for the expulsion of unattached bacteria through diarrhoea that maximises the cell number in the environment (Prouty and Klose, 2006).

V. cholerae has two major virulence factors, cholera toxin (CTx) which is responsible for the characteristic symptom, a rice water stool, and the toxin co-regulated pilus (TCP), a type IV bundle-forming pilus. Besides CTx, *V. cholerae* secretes another toxin named RTX that targets actin and can form pores on the epithelial cell membrane, although its physiological impact *in vivo* is minor (Fullner and Mekalanos, 2000). At the genomic level, these enzymes are grouped in the *Vibrio* pathogenicity island (VPI) and the cholera pro-phage (CTxΦ). Many other enzymes and extracellular proteins that help during infection are encoded in different loci along the genome, and their functions are to facilitate the movement across protective mucus layers, uncover potential attachment sites and establish a tight binding with the epithelial surface. The most significant ones during infection are discussed below.

The intestinal lumen is covered with a protective layer of a heterogeneous matrix of polysaccharides and proteins known as mucus, with mucins being the major gel-forming proteins (Corfield *et al.*, 2000). *V. cholerae* secretes the metalloprotease hemagglutinin/protease HapA, which degrades the mucus layer during infection. Mucin serves as a cue for *V. cholerae* to induce the expression of *hapA* and is used as carbon source due to its high sugar content (Almagro-Moreno and Boyd, 2009b). The solubilised mucin gives the white colour of cholera associated diarrhoea (Ritchie *et al.*, 2010). Once the mucus layer is dissolved, *V. cholerae* uses a second protease known as TagA to remove the remaining mucin on the cell surface (Szabady *et al.*, 2011). The host surface also contains sialic acid, a family of nine-carbon ketosugars that few pathogens including *V. cholerae* can use it as carbon source (Almagro-Moreno and Boyd, 2009a). Sialic acid is hydrolysed by NanH neuraminidase encoded in a pathogenicity island (VPI-2) of 57-kb, together with a sialic acid transporter and catabolism-related genes (Almagro-Moreno and Boyd, 2009b).

The bacterial adhesion process involves a series of interactions with the host cell surface and progresses from weak interactions such as electrostatic forces to stronger and specific ones such as lipid-protein and protein-protein interactions. Membrane proteins are essential to establish adhesion, especially adhesins that can be specific or non-specific. During infection, *V. cholerae* expresses an adhesin known as multivalent adhesion molecule 7 (MAM-7) that establishes protein-protein interactions with fibronectin and protein-lipid interactions with phosphatidic acid (Krachler *et al.*, 2011). At the same time, *V. cholerae* is able to bind polysaccharides using GbpA, a GlcNAc-binding protein that helps the bacteria to bind both cell surfaces and chitinous surfaces in aquatic environments (Kirn *et al.*, 2005).

1.4.1 Vibrio cholerae virulence cascade

Most of the virulence factors are encoded in a region known as the *Vibrio* pathogenicity island 1 (VPI-1) (Fig. 1.3). This region encompasses a section of the chromosome of about 41.2 kb flanked by phage-like integrase sequences, the transposase-like gene *vpiT* and the phage-like attachment site *att* (Rajanna *et al.*, 2003). As a mobile element, the VPI can be excised, circularised and transferred to non-toxigenic *V. cholerae* cells turning them virulent. Within the island are located the *acf* genes (accessory colonisation factors), the TCP operon and other genes with indirect relation to virulence (Rajanna *et al.*, 2003). The *acf* genes are involved in the synthesis of the colonisation factor. They are A, B, C and D, all of them regulated by ToxR, encoded in the TCP operon. An insertion in the *acf* genes generates a mutant with reduced colonisation properties (Parsot and Mekalanos, 1992).
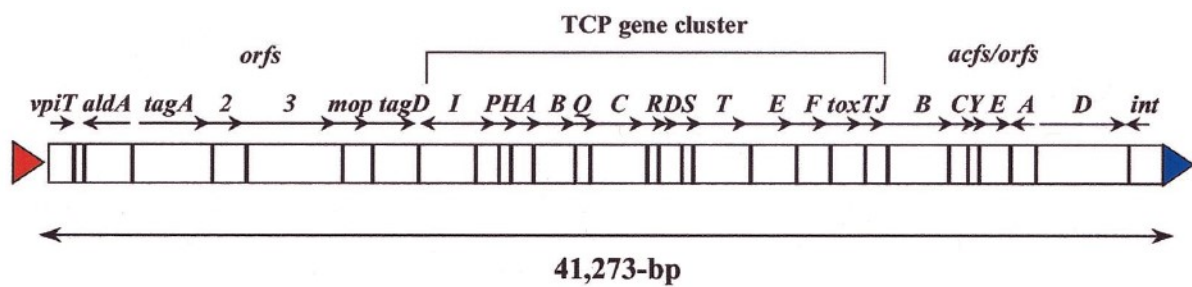
Figure 1.3. Organisation of the *Vibrio* Pathogenicity Island of *V. cholerae*. Indicated are genes related to virulence highlighting the TCP operon (mofidied from Rajanna *et al.*, 2003).

The *tcp* operon comprises a set of 15 genes; some encode membrane proteins with diverse functions while others are subunits of a type-IV bundle-forming pilus (Brown and Taylor, 1995) important for colonisation. Like the *acf* genes, these genes are regulated by ToxR. The genetic network that *tcp* genes form is key to understanding the regulation of virulence. TcpA is the main structural subunit of the pilus. The gene encodes a protein of 20.5 kDa that multimerises to form a filament of 7 nm diameter (Li *et al.*, 2008). Although TcpB shares similarity with TcpA, its function is not clear, but it most likely interacts with TcpA to form the filament as a basal component (Manning, 1997). TcpC serves to anchor lipoproteins to the outer membrane (Ogierman and Manning, 1992) while TcpF is a colonisation factor released from the TCP pilus during infection (Rajanna *et al.*, 2003, Brown and Taylor, 1995). Accordingly to the sequence of these proteins, *tcpD*, *E*, *J*, *P* and *R* are all predicted to be located in the inner membrane. TcpE helps the ATP-binding protein TcpT to be anchored to the inner membrane. TcpJ is a signalling peptidase that processes TcpA for its export (Kaufman *et al.*, 1991, Rajanna *et al.*, 2003). TcpP is also a relevant regulator of virulence as its presence upregulates the expression of virulence factors through ToxT (Häse and Mekalanos, 1998). TcpH, Q and S are all predicted to be periplasmic or exported. From this group, TcpH seems to contribute to activating virulence by preventing the degradation of TcpP (Manning, 1997, Beck *et al.*, 2004). TcpI is predicted to be a chemotaxis-related protein. Although its function is unknown, it is possibly related to the sensing of chemoattractant and transduction of signalling for the expression of TcpA (Harkey *et al.*, 1994). TcpT is predicted to be an ATP-binding protein located in the inner membrane. Mutants in this gene are unable to translocate monomers of TcpA via TcpE (Manning, 1997) (Fig. 1.4).

TCP is the second most important virulence factor of *V. cholerae*. This structure is synthesised during infection however its role is unclear as it is not participating directly in host cell interactions (Childers and Klose, 2007). However, it is necessary for virulence associated

phenotypes such as the formation of microcolonies (Jude and Taylor, 2011). TCP mediates the secretion of the colonisation factor TcpF (Kirn *et al.*, 2005). Also, the bacteriophage CTxФ uses TCP as a receptor in non-toxigenic strains to internalise its genome (Waldor and Mekalanos, 1996). Due to its importance in virulence, this pilus has attracted the attention of vaccine developers as a functional target. Although vaccines against TCP are protective in mouse models, it is biotype-restricted as the immunity cannot challenge heterogeneous biotypes (Attridge *et al.*, 1999).

Another group of virulence associated genes includes the *aldA* and the ToxR-activated genes (*tag*), which are related to diverse cellular processes during infection but most of the functions are predicted based on sequence homology. The cytoplasmic aldehyde dehydrogenase AldA may be related to virulence as it is activated during infection by ToxT (Withey and Dirita, 2005). Nonetheless, environmental cues also activate its expression, indicating that other regulators may be implicated in its transcription and share a divergent promoter with *tagA* (Withey and Dirita, 2005). Functions associated with *tag* genes include an extracellular protease that cleaves mucin residues (Szabady *et al.*, 2011), a putative-fimbriae structural protein (Hughes *et al.*, 1994) and *tagB* which shares a high level of identity with *tcpI* (Harkey *et al.*, 1994).

Lastly, *toxT* encodes an AraC-family transcriptional activator known as the master regulator of virulence. The presence of this regulator is associated with virulent phenotypes in *V. cholerae* since it activates the transcription of *acfD*, *tagD, aldA* and most of the TCP operon genes. It also promotes the transcription of *ctxA* and *ctxB*, the structural components of the cholera toxin (Weber and Klose, 2011). ToxT usually binds directly to the toxboxes, AT rich regions located at -35 and -10 regions of targeted gene promoters and interacts with the ribosome. Although the toxboxes are present in virulence-related gene promoters, these regions are not particularly

conserved, and it is common to find one or two with different orientations (Withey and DiRita, 2006).

Together with TCP, cholera toxin is considered the major virulence factor of *V. cholerae*. Cholera toxin is an ADP-ribosyltransferase associated with the AB_5 family (Kaper *et al.*, 1995) composed of a pentamer of B subunits of 12 kDa each and an A subunit of 20 kDa, resulting in an 80 kDa toxin complex (Prouty and Klose, 2006). During infection, cholera toxin attached to the host surface undergoes a proteolytic cleavage on the subunit A by HapA protease leading to the internalising of the cytoplasmic A_1 subunit that catalyses the ribosylation of $G_s a$ protein, resulting in uncontrollable high levels of intracellular cAMP (Glineur and Locht, 1994). High levels of cAMP are accompanied with the expulsion of Cl^-, resulting in an osmotic imbalance as the cell moves water to the lumen. Although the extreme dehydration is the principal cause of mortality in cholera disease, the tissue damage during infection is minimal (Millet *et al.*, 2014). During many years, the upregulation of *nanH* by sialic acid and the presence of sialic acid on the monosialotetrahexosyl (GM1) ganglioside was believed to be the point of entry for A_1 as cholera toxin interacts with it when added into rabbit ileon (Holmgren *et al.*, 1975). Moreover, the high affinity for GM1 of the related heat-labile toxin B-subunit from *E. coli* (Spangler, 1992) and the enhanced response of cholera toxin when GM1 is exogenously added to murine and human cell lines (Fishman *et al.*, 1976, Yu *et al.*, 2016) strongly supports this idea. However, the GM1-deficiency in C6 rat glioma cells exposed to cholera toxin did result in GM1 ganglioside-independent toxicity with the toxin binding to the fucosylated moiety of the blood group Lewis[X], a histo blood group antigen (HBGA) abundant in the intestinal epithelium together with other HBGAs (Cervin *et al.*, 2018). Genetically, the cholera toxin genes are encoded in the genome of CTxΦ bacteriophage, a lysogenic phage capable of avoiding superinfection immunity, therefore, some strains can have multiple lysogens (Casas

and Maloy, 2011) increasing the toxicity of a strain or inducing virulence in non-virulent populations.
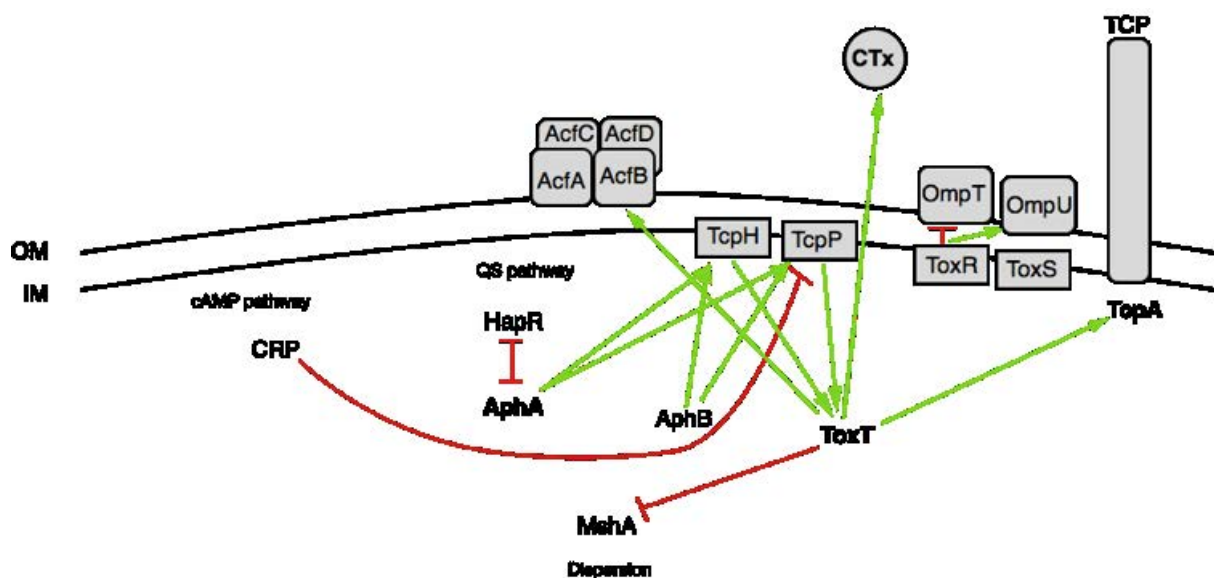
Figure 1.4. Summary of the virulence regulatory pathway in *V. cholerae*. Pathway regulators and virulence factors are indicated together with important pathways that also modulate virulence. In bold (AphA, ToxT, TcpA and CTx) are key members of which transcription was analysed in this work. Green arrows indicate induction while red indicates repression (Kanehisa *et al.*, 2016).

1.4.2 Vibrio cholerae synthesis of biofilm

Another important aspect of virulence in *V. cholerae* is the synthesis of biofilm as infective cells are usually found associated with biofilms. Biofilm, by definition, is a community of organisms living embedded into a matrix of polysaccharides, proteins and DNA. Compared with *E. coli* biofilm, *V. cholerae* biofilm is mainly composed of sugars termed *Vibrio* polysaccharide (VPS) (Reichhardt *et al.*, 2015). Analysis of the matrix composition revealed that the main component is the polysaccharide -4)-α-Gul*p*NAcAGly3OAc-(1-4)-β-D-Glc*p*-(1-4)-α-Glc*p*-(1-4)-α-D-Gal*p*-(1- (Yildiz *et al.*, 2014). All the components required for biofilm synthesis are located in the *vps* clusters, two arrays of genes divided into six subclasses depending on the catalytic activity of the encoded enzymes (Fong *et al.*, 2010).

During motility, *V. cholerae* scans the surface with two distinct patterns of movement, roaming and orbiting; the bacteria use the mannose-sensitive haemagglutinin (MSHA) pili to find mannose or mannose derivatives. Theoretical modelling has suggested that surface scanning occurs by the body rotation of the bacterium with periodic mechanical contact with the surface to find non-metabolisable mannose derivatives (Utada *et al.*, 2014). This contact is enough to arrest cell motility and start adhesion, as MSHA pili deficient mutants fail to initiate attachment (Watnick *et al.*, 1999). The immobilisation of the bacteria through mechanosensing interactions lead to the loss of flagellar function which has been identified as a cue to initiate biofilm production. The absence of structural components or the entire polar flagella results in cell shape and colony morphology differences (Watnick *et al.*, 2001).

At the transcriptional level, biofilm synthesis is not regulated by virulence activators and virulence, nor by biofilm regulators, but both routes are regulated by the global regulators histone-like nucleoid-structuring protein (H-NS), cyclic adenosine monophosphate receptor protein (cAMP-CRP or CRP) PhoB-P and the quorum sensing related regulators HapR and AphA (Silva and Benitez, 2016). Genes from *vps* clusters are directly activated by the binding

of VpsR and VpsT when c-di-GMP is elevated. Both regulators bind to c-di-GMP, yet only VpsR is affected to activate *vpsT* and *aphA* expression (Srivastava *et al.*, 2011) (Fig. 1.5).

During the synthesis of the biofilm matrix, three structural proteins serve as a scaffold to add the sugar branches; these are RbmA, RbmC and Bap1. RbmA is secreted opposite to the polar flagella and enables cell-cell adhesion; Bap1 promotes the adhesion to surfaces as well as the expansion of the biofilm matrix, while RbmC coats the bacteria forming an envelope to start adding VPS (Berk *et al.*, 2012). RbmA plays a significant role in inciting the process of biofilm formation since its proteolytic cleavage is the signal to recruit other bacteria and reinforce the matrix structure (Smith *et al.*, 2015). These structural proteins are all delivered to the external matrix through a type II secretion system (Johnson *et al.*, 2014). Within the matrix, communication between cells is enhanced, and DNA is exchanged.
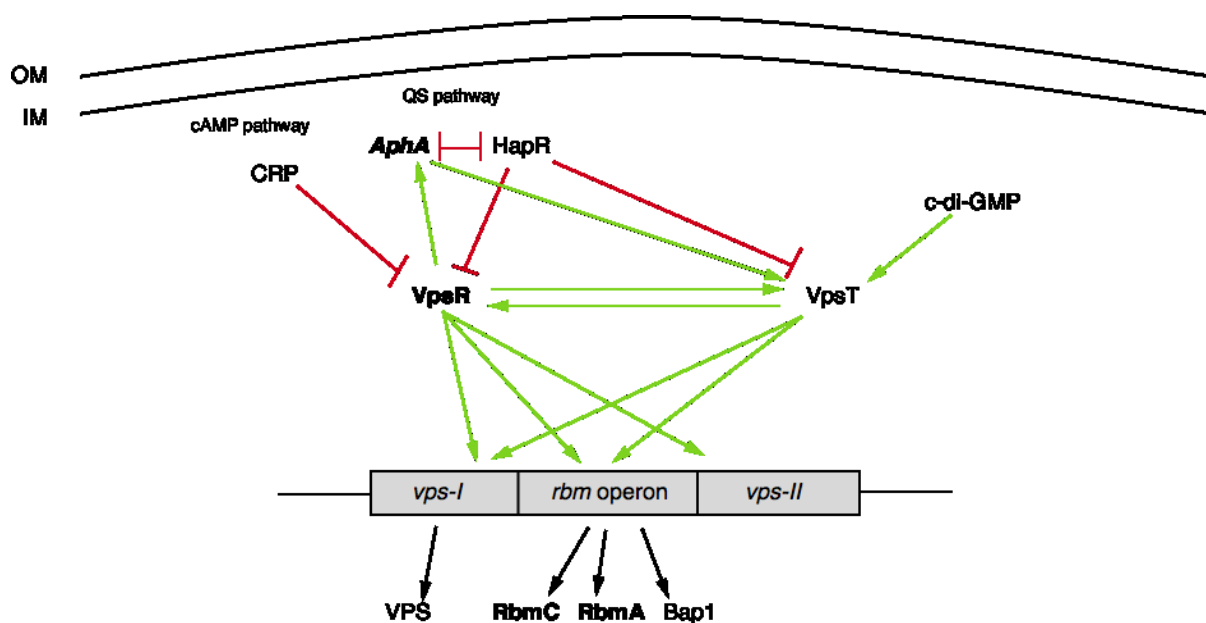
Figure 1.5. Summary of the biofilm regulatory pathway in *V. cholerae*. Pathway regulators and relevant clusters are indicated together with the main structural components. Also, important pathways that also modulate biofilm are indicated. In bold (AphA, VpsR, RbmC and RbmA) are key members of which transcription was analysed in this work. Green arrows indicate induction; red lines indicate repression (Kanehisa *et al.*, 2016).

1.5 Vibrio cholerae quorum sensing

Recently, quorum sensing has dragged the attention because of its overlap with many cellular functions and it is a potential target to control virulence. In *V. cholerae* at least four parallel quorum sensing routes have been identified (Jung *et al.*, 2015) but the two best characterised are the major contributors to bacterial communication. One of the ligands, (S)-3-hydroxytridecan-4-one (CAI-1), is synthesised by CqsA by coupling S-adenosyl methionine (SAM) with decanoyl-coenzyme A (Rutherford and Bassler, 2012) and is believed to be responsible for intra-species communication. The second autoinducer, autoinducer-2 (AI-2), is synthesised by LuxS by converting the S-ribosyl homocysteine cycle from SAM to (S)-4,5-dihydroxy-2,3-pentadione (DPD) with the release of homocysteine. DPD spontaneously converts into autoinducer-2 (AI2; (2S,4S)-2-methyl-2,3,3,4-tetrahydroxytetrahydrofuran-borate or S-THMF-borate) (Rutherford and Bassler, 2012). As LuxS is present in several other Gram-negatives and Gram-positives, it is responsible for inter-species communication (Waters and Bassler, 2005). Receptors for these ligands are in the inner membrane, CqsS for CAI-1 and LuxPQ for AI-2. Both sensory signalling systems converge in the phosphotransferase LuxU that phosphorylates LuxO. At low cell density, autoinducers are diluted which reduces the number of molecules being sensed by CqsS and LuxPQ, resulting in the phosphorylation of LuxO by LuxU. The phosphorylation of LuxO results in the expression of four small RNAs, Qrr1-4, that repress the expression of HapR by pairing at the mRNA 5' untranslated region (UTR). This is helped by the RNA chaperone Hfq blocking the ribosome binding site (RBS) (Bardill *et al.*, 2011). Through the same mechanism the RBS from *aphA* mRNA is exposed, resulting in accumulation of AphA regulator (Shao and Bassler, 2012). Conversely, during high cell density, the autoinducers accumulate above the quorum sensing threshold leading to the LuxO dephosphorylation and the absence of Qrr1-4, resulting in the accumulation of HapR (Lenz *et al.*, 2004). Footprint analysis of the *aphA* promoters has revealed that HapR binds to

a region between -85 and -58 in the promoter region which represses the transcription under not yet known conditions as HapR was unable to bind to a 360 bp fragment of the *aphA* promoter (Jobling and Holmes, 1997, Kovacikova and Skorupski, 2002b). The AphA/HapR interplay, allows for the regulation of multiple genes including virulence, biofilm, uptake of nutrients and competence accordingly to the cell density (Lenz *et al.*, 2004, Zhu and Mekalanos, 2003, Suckow *et al.*, 2011) (Fig. 1.6).

The control of virulence through quorum sensing is not yet entirely understood and remains controversial. Usually pathogens upregulate virulence genes during high cell density however, in *V. cholerae,* the opposite happens. AphA can repress the transcription of ToxR and ToxT by direct interaction with the DNA motif at the promoter. In the same line, other regulators such as the biofilm-related regulator VpsR, similarly regulate ToxR (Ritchie and Waldor, 2009). On the other hand, the regulation of virulence in toxigenic and non-toxigenic strains of *V. cholerae* in relation to HapR is influenced by the binding affinity to its motif. The toxigenic El Tor biotype has a frameshift mutation in *hapR* reducing the affinity of HapR. Therefore, virulence cannot be properly downregulated at high cell density (Joelsson *et al.*, 2006). At the same time, the release of HapR from the promoter can be mediated by RpoS independent of cell density (Nielsen *et al.*, 2006).
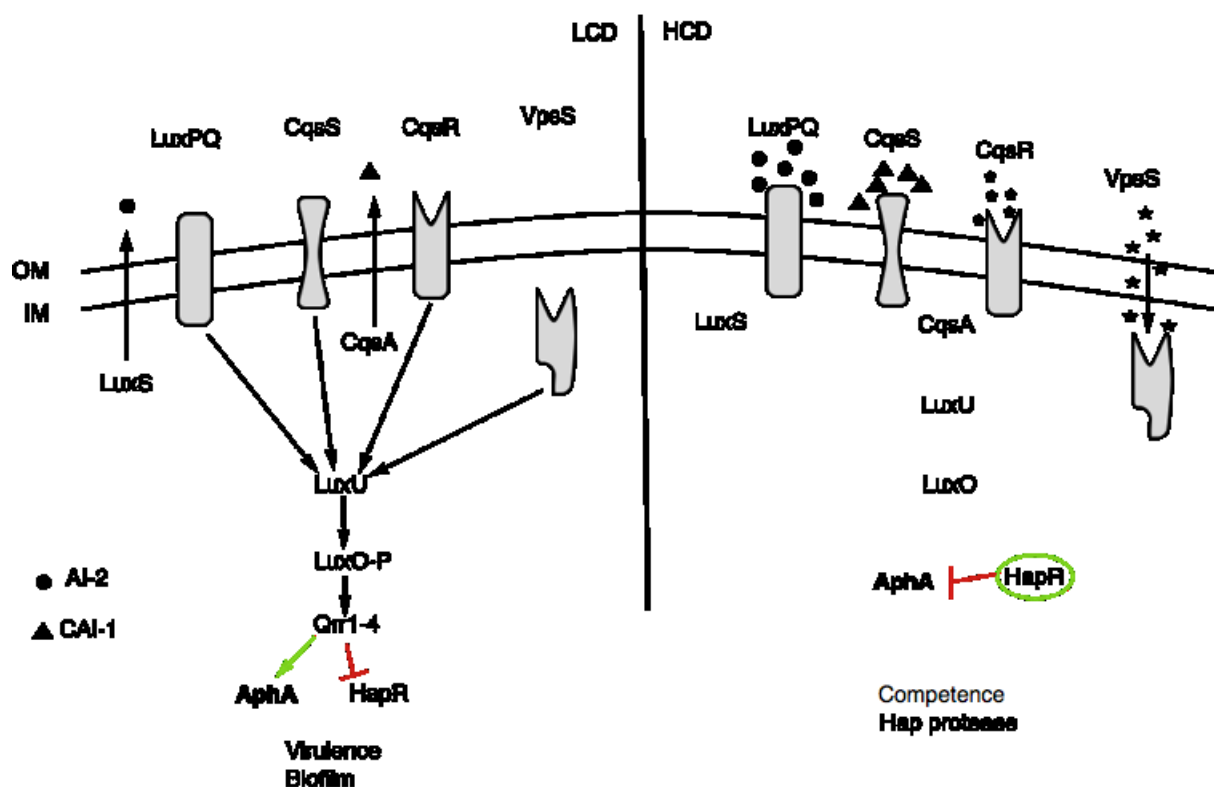
Figure 1.6. Summary of the quorum sensing regulatory pathway in *V. cholerae* during high and low cell density. Pathway regulators indicated with their functions during high cell density (HCD) and low cell density (LCD). At low cell density, the reduced content of autoinducers in the extracellular environment maintains phosphorylated LuxO via the kinase LuxU. The signal transduction results in the expression of the Qrr1-4 sRNA which dictates the expression of AphA or HapR. Meanwhile, during high cell density, the accumulation of autoinducers in the extracellular environment is sensed by LuxPQ, CqsS, CqsR and intracellularly VpsS resulting in the dephosphorylation of LuxO, and in the expression of HapR over AphA. In bold (AphA) is the low cell density regulator of which transcription was analysed in this work. Green arrows indicate induction; red lines indicate repression; black arrows indicate signal transduction (Kanehisa *et al.*, 2016).

44

1.6 Aims

Our current understanding of the non-bactericidal properties of cationic polymers is limited as most of the applications are focused on their antimicrobial potential. This work set out to address key questions regarding the impact on critical cellular functions during polymer-induced clustering of *Vibrio cholerae*. If polymers are able to cluster bacteria, then virulence genes might be downregulated as result of a controlled high cell density phenotype expressed locally whitin the clusters.

This thesis aims to investigates:

1) Cationic polymers with amines as binding groups to induce the cell clustering via electrostatic interactions were synthesised .

2) The polymer mediated clustering of *V. cholerae* as well as their non-bactericidal properties were evaluated.

3) The switch to a sessile lifestyle during the cell clustering was evaluated.

4) A controlled quorum sensing-phenotype induced by clustering was dissected.

5) The impact of clustering over *V. cholerae* virulence expression was characterised by transcriptional and phenotypical assays.

Chapter 2: Materials and Methods

2.1 Polymer synthesis

2.1.1 Polymerisation reagents

Monomers used to synthesise P1 and P2 were *N*-(3-aminopropyl)methacrylamide and *N*-[3-(dimethylamino)propy]methacrylamide respectively. Initiator agents were 4,4'-azobis(4-cyanovaleric acid) (ACVA) for P1 and 2,2′-azobis(2-methylpropionitrile) (AIBN) for P2, while the chain transfer agent was 2-thioethanol for both polymerisations.

2.1.2 Polymerisation reaction

2.1.2.1 P1 synthesis

N-(3-aminopropyl)methacrylamide hydrochloride (505 mg), 4,4'-azobis(4-cyanovaleric acid) (ACVA) (12.4 mg) and 2 thioethanol (1 µL) were dissolved in MiliQ water (2.2 mL). The solution was degassed with argon for 10 minutes and then heated at 70 ℃ under stirring for 17 hours. The tube was opened, and polymer was precipitated three times with diethyl ether (50 mL). Precipitate was freeze-dried, yielding a white crystalline solid (70 mg) (Fig. 2.1).

2.1.2.2 P2 synthesis

The polymerisation reaction was carried out before this work by L. Moule (an undergraduate summer student), and the resulting product was characterised as part of the work described here. *N*-[3-(dimethylamino)propy]methacrylamide (2.2 mL), 2,2′-azobis(2-methylpropionitrile) (AIBN) (19.6 mg) and 2 thioethanol (4 µL) were dissolved in toluene (9.5 mL). The solution was degassed with argon for 10 minutes and then heated at 70 ℃ under stirring for 17 hours. The tube was opened and polymer was precipitated initially with diethyl

ether (200 mL) and then into a 1:1 mixture of diethyl ether:hexane (100 mL). The precipitate was freeze-dried, yielding a white crystalline solid (1.6 g) (Fig. 2.1).

2.1.2.3 P3 synthesis

The polymerisation reaction and characterisation of the poly(acryloyl hydrazide) were carried out prior to this work by D. Crisan (Crisan *et al.*, 2017), and the resulting material was used as a backbone to produce P3. For the preparation of P3, one equivalent of backbone (15 mg) was mixed with two equivalents (33.48 mg) of 4-imidazolecarboxaldehyde in 3 mL H_2O and heated for 2 hours at 60 ℃ stirring (Fig. 2.1).
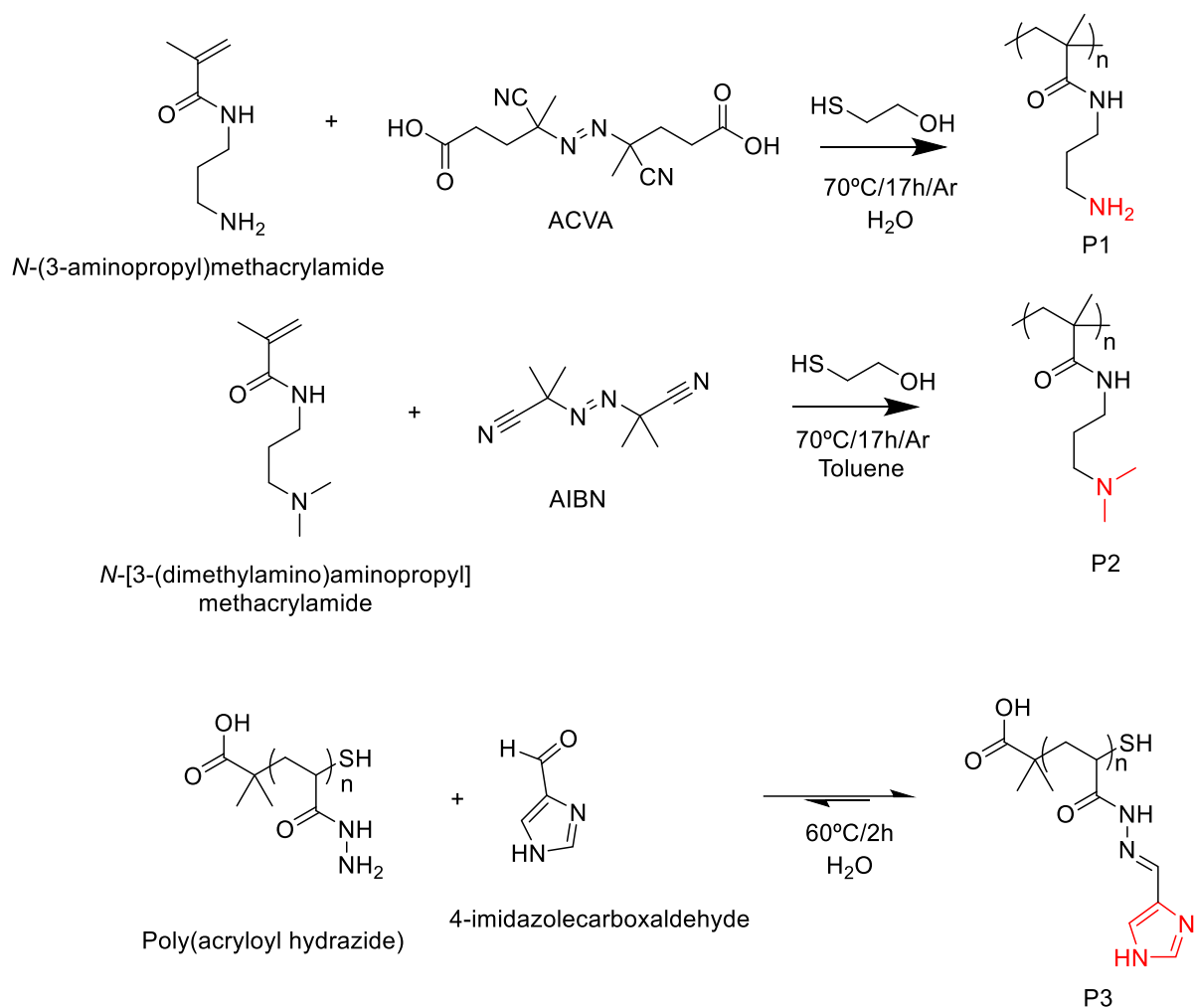
Figure 2.1. Polymerisation reactions for poly(*N*-(3-aminopropyl) methacrylamide) (P1), poly(*N*-[3-dimethylamino)propyl] methacrylamide) (P2) or poly(acryloyl hydrazide) coupled with imidazolecarboxaldehyde (P3). Synthesis route and conditions for the polymerisation of P1, P2 and P3. In red is indicated the amine group corresponding to the polymer.

2.1.3 Polymer characterisation - Instrumentation

Characterisation of polymers was done by Nuclear Magnetic Resonance (NMR) and Gel Permeation Chromatography (GPC). NMR spectra were recorded using a Bruker Avance III spectrometer at 300 MHz and fitted with a 5 mm broadband fluorine observation (BBFO) probe. Chemical shifts are reported in ppm (δ) references to corresponded solvents: DMSO-*d6* (δ = 2.50) and D_2O (δ = 4.79). GPC was done using a Shimadzu Prominence LC-20A, fitted with a Shodex Asaphipak GF-510 HQ (300 x 7.5 mm, 5 μm) and a GF-310 HQ (300 x 7.5 mm, 5 μm) column in series, and equipped with a Thermo Fisher Refractomax 512 detector. Solvents used with the GPC were 100 mM acetate buffer at pH 2.9 as eluent at 40 ºC with a flow rate of 0.6 mL/min. Molecular weights were calculated from a calibration curve made with polyethyleneglycol oligomers.

2.2 Bacterial culture conditions

V. cholerae El Tor strains used in this study (Table 2.1) were derived from N16961 (Heidelberg et al., 2000) and E7946 (Miller et al., 1989). El Tor biotype is responsible for the ongoing *V. cholerae* pandemic, replacing the Classical biotype. As discussed later (Chapter 8), the virulence associated to El Tor biotype is different to Classical and not many works have been done with these strains, which highlights the importance to use this the N16961 strain. Nevertheless, since genetic modification of N16961 is challenging, used mutant derived from E7946 and contrasted with the clean background. The *E. coli* K12 strains JCB387 (Page et al., 1990), DH5α (Taylor et al., 1993) and SM10 λpir (Simon et al., 1983) were used for general cloning and conjugation procedures. Strains were propagated at 37 ºC in lysogeny broth (LB) either liquid or agar, supplemented with 10 μg/μL tetracycline or 30 μg/μL kanamycin for selection when required. Conjugation experiments were done in Brain-Heart Infusion (BHI)

agar, while selection in M9 or thiosulfate-citrate-bile salt-sucrose (TCBS) agar with a required antibiotic. Minimal media Dulbecco's Modified Eagle's Medium (DMEM) and artificial marine water media were used during exposition of *V. cholera* to polymers. Cultures were incubated at 37 ºC with shaking at 200 rpm. Bacterial stocks were frozen down at -80 ºC in 30 % glycerol.

Table 2.1. Showing strains used in this study.

Strain	Description or genotype	Source or Reference
Vibrio cholerae		
N16961	Wildtype; O1 biovar El Tor	(Heidelberg *et al.*, 2000)
E7946	Wildtype; Ogawa biovar El Tor	(Miller *et al.*, 1989)
623-39	non-O1/non-O139	
BH1651	*luxO*^{D47E}	(Ng and Bassler, 2009)
BH1578	Δ*luxS*Δ*cqsA*	(Ng and Bassler, 2009)
WN1103	Δ*luxQ*Δ*cqsA*	(Ng and Bassler, 2009)
DH231	Δ*luxS*Δ*cqsS*	(Ng and Bassler, 2009)
E7946 Δ*crp*	Δ*crp* Kan^R	Gift from D. Grainger
NP5001	N16961 pRW50-oriT promoterless; Tet^R	This study
NP5002	N16961 pRW50-oriT containing upstream region of toxT promoter; Tet^R	This study
NP5003	N16961 pRW50-oriT containing upstream region of ctxAB promoter; Tet^R	This study
NP5004	N16961 pRW50-oriT containing upstream region of tcp*A* promoter; Tet^R	This study
NP5005	N16961 pRW50-oriT containing upstream region of *aphA* promoter; Tet^R	This study
NP5006	N16961 pRW50-oriT containing upstream region of *flaA* promoter; Tet^R	This study
NP5007	N16961 pRW50-oriT containing upstream region of *flaE* promoter; Tet^R	This study
NP5008	N16961 pRW50-oriT containing upstream region of *vpsR* promoter; Tet^R	This study
NP5009	N16961 pRW50-oriT containing upstream region of *rbmA* promoter; Tet^R	This study
NP5010	N16961 pRW50-oriT containing upstream region of *rbmC* promoter; Tet^R	This study
NP5011	N16961 pRW50-oriT containing upstream region of *chiS* promoter; Tet^R	This study
NP5012	N16961 pRW50-oriT containing upstream region of *chiA1* promoter; Tet^R	This study

NP5013	N16961 pRW50-oriT containing upstream region of *chiA2* promoter; Tet^R	This study
NPMW1	N16961 carrying pMW-*gfp* plasmid; Spect^R	(Ritchie *et al.*, 2012)
	Escherichia coli	
DH5α	Donor and maintenance of pBB1 and pMW-*gfp*	(Taylor *et al.*, 1993)
JCB387	Donor and maintenance of pRW50 oriT	(Page *et al.*, 1990)
SM10	Helper strain; λ*pir* pRK2013; Kan^R	(Simon *et al.*, 1983)

2.3 Epithelial cell culture conditions

The epithelial cell line Caco-2 (ATCC® HTB-37™) derived from human colorectal adenocarcinoma cells was used for cytotoxicity and attachment assays. Cells were kept at 37 °C under 5 % CO_2 in low glucose (1 g/L) DMEM with phenol red as pH indicator. The media was supplemented with 10 % foetal bovine serum (FBS), 100 units/mL streptomycin, 100 units/mL penicillin and 2 mM L-glutamine. Cells were subcultured after thawing from frozen stocks successive times until passage 15. Briefly, attached cells were washed once with PBS and 1 mL of trypsin-EDTA solution was added for 3 to 5 minutes at 37 °C. Then, 9 mL of fresh coloured-DMEM was added, and aliquots were used to seed new flasks.

2.4 Zebrafish culture conditions.

Zebrafish (*Danio rerio*) wildtype strain AB was kept under a 14 h/10 h light/dark cycle in a recirculating tank system at 28 °C at the Biomedical Service Unit (BMSU) facility at University of Birmingham. Zebrafish care, breeding and experiments were done in accordance with the Animal Scientific Procedure Act 1986, under the Home Office Project License 40/3681. Adult fish were gathered in groups of 4 females and 3 males in breeding tanks for 16 hours at 26 °C. After the 16 hours incubation, adult fish were returned to their respective husbandry tanks while the eggs were washed in E3 media and collected in Petri dishes.

Zebrafish eggs were kept under a 14 h/10 h light/dark cycle at 33 °C in E3 media. E3 media composition was 292 mg/L NaCl, 13 mg/L KCl, 44 mg/L $CaCl_2$, 81 mg/L $MgSO_4$ and 477 mg/L HEPES at pH 7.0. To avoid fungal contamination, methylene blue was added at 0.00003 % for 8 hours and then larvae were kept in fresh E3 up to day five post-fertilisation, the experimental endpoint according to Home Office license requirements. For imaging, embryos were treated with 26.6 µg/mL 1-phenyl-2-thiourea (PTU) to inhibit melanisation. Anaesthetising and euthanising were done with buffered tricaine solution at 160 µg/mL and 1.6 mg/mL respectively (Westerfield, 1995).

2.5 Molecular biology

2.5.1 Primer design

Upstream regions of selected genes were retrieved from the *V. cholerae* N16961 genome submitted on EnsemblBacteria (www.bacteria.ensembl.org). The genes were *aphA* (VC_2647), *ctxAB* (VC_1457), *toxT* (VC_0838), *tcpA* (VC_0828), *rbmA* (VC_0928), *rbmC* (VC_0930), *vpsR* (VC_0665), *flaA* (VC_2188), *flaE* (VC_2144), *chiS* (VC_0622), *chiA1* (VC_1952) and *chiA2* (VC_A0027). Primers were designed to amplify a region that contains regulatory elements and finishing at the transcription starting codon. Primers contained restriction sites for EcoR1, HindIII or BamHI for cloning, plus four random nucleotides at the 5' end to facilitate digests. The length and GC content were adjusted in order to anneal around 20 nucleotides and achieved melting temperatures between 58 °C to 60 °C. Primers are listed in Table 2.2.

Table 2.2. Showing primer sequences used in this study**.** In red, EcoRI restriction site is highlighted; in green, HindIII restriction site is highlighted; in yellow, BamHI restriction site is highlighted.

Primer	Sequence (5'-3')
pRW50 F	GTTCTCGCAAGGACGAGAATTTC
pRW50 R	AATCTTCACGCTTGAGATAC
aphApF1	TGCAGAATTCCTGGTTAACAAATCGCTAAATGTCAG
aphApR1	ATTCAAGCTTGTGTGGTAATGACATGTCTTCAATC
toxTpF1	TGTAGAATTCGATAAGATAACAGCCATATTCGTGG
toxTpR1	GATCAAGCTTTCCCAATCATTGCGTTCTACTC
ctxABpF1	GCTTGAATTCCTGTGGGTAGAAGTGAAACGG
ctxABpR1	TCATAAGCTTTATCTTTACCATATAATGCTCCCTTTG
tcpApF1	CTTAGAATTCGGTCTTATCATGAGCCGCC
tcpApR1	TGATAAGCTTTGCATATTTATATAACTCCACCATTTGTG
flaApF1	ATCTGAATTCGTCAGCGGCAAAATGGATTG
flaApR1	GTCAAAGCTTCATAGTTTGCTCTCCTATCGAGTTC
flaEpF1	ATCTGAATTCGATCACGGCCTACTGTTTATTG
flaEpR1	GTCAAAGCTTATTTACCGTCATGGCCATGG
rbmApF1	TGTAGAATTCCTTTGGGTGAAAAAATAAAC
rbmApR2	GATCAAGCTTCCATTTGTTTTTACAACTGGC
rbmCpF1	TGTAGAATTCTAGAAAATGCTTCTTGAAAAAGAG
rbmCpR2	GATCAAGCTTTTGTAAGACTCCCTTTACCTTG
vpsRpF1	TGTAGAATTCACTGTAGATTGATTAAAAAGCC
vpsRpR2	GATCAAGCTTCCTATATTCCTTATTTTTATTGTTAC
chiA1pF1	TCAGGATCCTTGATTGGTGGTTTGGGTAGC
chiA1pR1	CTTAAGCTTCGCTTCATGTTTCTCTCCTGTATTAG
chiA2pF1	TCAGGATCCTATTTCGTTCTGTGACGAGCG
chiA2pR1	CTTAAGCTTAAGTTTTCTCTCTCTTCCTTAGATGTTTC
chiSpF1	CTTGGATCCTCATATTGAGTTAGAGATGACAGACATCAG
chiSpR1	CTGAAGCTTGCAAAAAACGTGAGGAGAATGC

2.5.2 Polymerase chain reaction (PCR)

DNA fragments were amplified using Phusion High-Fidelity DNA polymerase (NEB) and genomic DNA from *V. cholerae* N16961 as a template. The PCR mixture contained 0.5 μM of forward and reverse primers, respectively, 1X Phusion HF Buffer, 3 % DMSO, 200 μM dNTP mix and 0.02 units of polymerase in a final volume of 50 μL. The temperature program consisted of a first denaturation round for 2 min at 95 °C, then, 30 cycles of denaturation at 95 °C for 30 seconds followed by annealing at primer-specific temperature for 30 seconds at temperatures around 60 °C, and extension at 72 °C for 30 to 60 seconds depending on the

length of the fragment. A final extension step was included at 72 °C for 10 minutes. Fragments were separated by 1 % agarose gel electrophoresis in Tris/borate/EDTA (TBE) buffer.

2.5.3 pRW50-oriT plasmids construction.

The amplified fragments were cloned into pRW50-oriT vector (Gift from D. Grainger) (Lodge *et al.*, 1992). This vector is a pRW50-derivative which has been modified by inserting the oriT sequence from the broad-host plasmid pRK2 (Figurski *et al.*, 1982). Amplified fragments were digested and ligated into pRW50-oriT specific sites (Fig. 2.2).

The cloning procedure consisted of double digestion of 1 µg of amplified fragments with 10 units of EcoRI, HindIII or BamHI for 2 hours at 37 °C followed by denaturation at 80 °C for 20 minutes. Digested fragments were purified again to remove short overlapping fragments and ligation was done by incubating digested vector and fragments with 1 unit of T4 DNA ligase, incubating at 16 °C 16 hours. The ligation product was used for transformation into *E. coli* DH5α or JCB387 by heat-shock method.
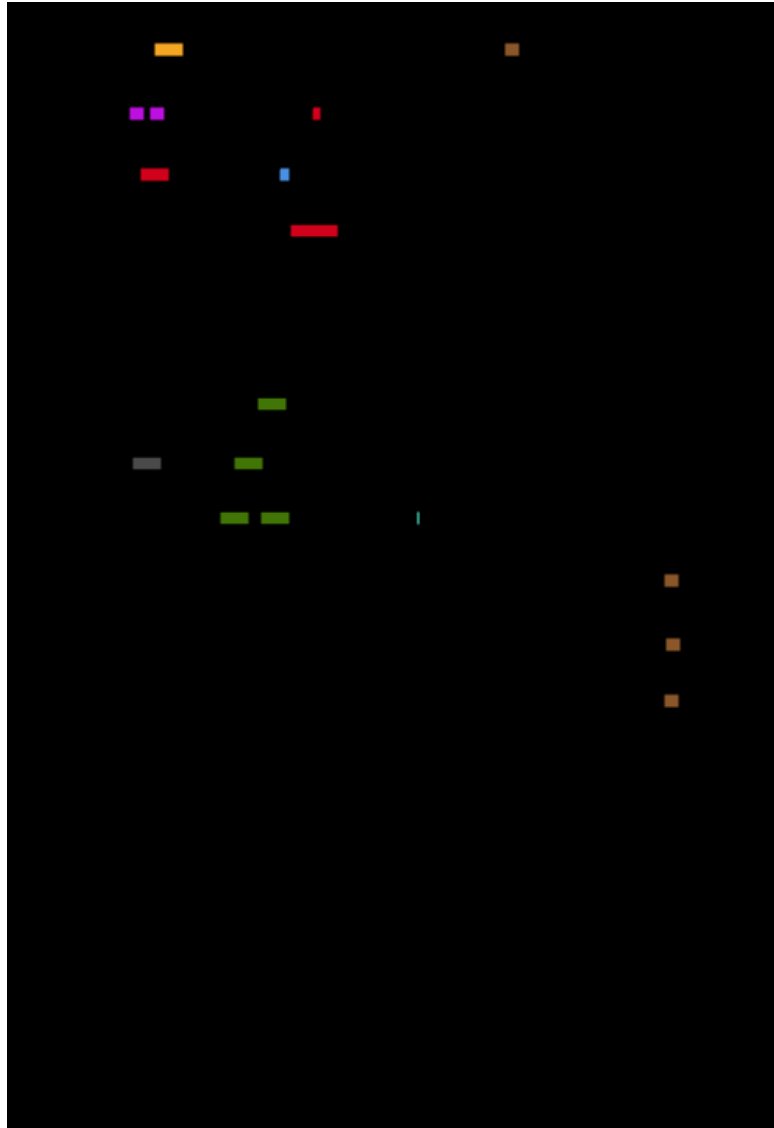
Figure 2.2. pRW50-oriT vector diagram and cloned fragments. A schematic depiction of the reporter plasmid and the promoter regions used in this work for virulence (*toxT*, *ctxAB* and *tcpA*), biofilm (*vpsR*, *rbmA* and *rbmC*), quorum sensing (*aphA*), flagellum (*flaA* and *flaE*) and chitin utilisation (*chiS*, *chiA1* and *chiA2*). Numbering refers to base number relative to the transcriptional start site and promoter binding sites for important regulators of virulence, biofilm and quorum sensing pathway, respectively. Induction of flagellar genes is mediated by sigma factors, while genes from the chitin utilisation program are induced by chitinous oligomers. All the regions as indicated were cloned at 5' through an EcoR1 while the 3'site was HindIII, except *chiA1*, *chiA2* and *chiS* where it was a BamHI site.

2.5.4 E. coli heat-shock transformation

E. coli strains were transformed by heat-shock transformation. Bacterial competence was induced by incubating 30 mL of mid-log phase (OD_{600} 0.6) cultures on ice replacing the LB media with the same volume of ice-cold 100 mM $CaCl_2$, by centrifuging at 3000 rpm for 10 minutes. During the last washing step, bacteria were resuspended in 3 mL of ice-cold 100 mM $CaCl_2$.

100 μL of bacteria solution was mixed with 5 μL of ligation reaction and incubated 30 minutes on ice, followed by a heat-shock of 30 seconds at 37 °C and re-incubating on ice for 2 minutes. 1 mL of LB was added and then, the transformed sample was incubated at 37 °C for 45 minutes with shaking. 100 μL of the transformation sample was plated onto LB agar with antibiotic while the rest of the reaction was centrifuged at 7000 rpm for 5 minutes and resuspended in 100 μL of LB to be plated onto LB plate with antibiotics. Plates were incubated at 37 °C 16 hours.

2.5.5 pRW50 oriT and pBB1 plasmid extraction

pRW50-oriT and pBB1 were extracted by Maxiprep following the manufacturer's instructions (Qiagen). Briefly, 100 mL of 16 hours culture in LB were centrifuged, and vectors were extracted by modified alkaline lysis and DNA precipitated with isopropanol and eluted with Tris-EDTA buffer. The purity of the precipitate was checked by 1 % agarose gel electrophoresis in TBE buffer.

2.5.6 Vibrio cholerae conjugation by triparental mating

pBB1, pMW-*gfp*, pRW50-oriT and its derivatives were mobilised into *V. cholerae* strains by triparental mating (Goldberg and Ohman, 1984). *V. cholerae* recipient strains, *E. coli* SM10

pRK2013 helper strains and *E. coli* DH5α carrying pRW50-oriT or pBB1 donor strain were propagated 16 hours in LB media with antibiotics. Then, volumetric aliquots were mixed in a ratio of 1:2:2 of recipient:helper:donor respectively, in 250 µL. The mixture was vortexed and 100 µL was spotted on a BHI plate to be incubated 16 hours at 37 °C. The spot was dislodged from the plate by adding 3 mL of PBS and helping with a scraper to plate onto M9 or TCBS agar. GFP fluorescence was checked under UV light and by fluorescence microscopy, while pRW50-oriT constructs were checked by PCR with external primers.

2.6 GFP-based growth curves

GFP fluorescence was used as a proxy of the bacterial growth instead of OD_{600}. Following 16 hours of growth cultures of GFP-tagged *V. cholerae* were diluted to an initial OD_{600} of 0.02 in DMEM with 50 µg/µL of spectinomycin. Polymers were added at a range of concentrations starting from 0.00005 mg/mL to 0.5 mg/mL in 200 µL using a 96-well plate. To reduce evaporation, the plate was covered with a BEM-1 breathe easy gas-permeable membrane (Sigma) and incubated at 37 °C. GFP fluorescence was recorded every 30 minutes for 24 hours using a FLUOstar Omega plate reader.

2.7 Membrane Integrity

2.7.1 LIVE/DEAD staining coupled with fluorescent activated cell sorting

V. cholerae membrane integrity was determined by fluorescent activated cell sorting (FACS) using the LIVE/DEAD *Bac*Light™ kit (Thermo Scientific). Following 16 hours of growth, cultures of *V. cholerae* were adjusted to an OD_{600} 1.0 in 1 mL of colourless DMEM. Polymers were added at concentrations of 0.00005 mg/mL to 0.5 mg/mL and cultures were incubated for

20 hours. Then, bacterial samples were stained following the manufacturer's instructions. Readings were taken at a flow of 100 µL/min counting up to 10,000 events using an Attune Flow Cytometer. As "LIVE" control, bacteria were incubated without polymer, while bacteria treated with 70 % v/v 2-propanol were used as a "DEAD" control but 2-propanol was replaced with DMEM after treatment due to the incompatibility of the 2-propanol with the dyes.

2.7.2 Outer membrane permeability – N-Phenyl-1-naphthylamine assay

Permeability of the outer membrane was assessed using N-Phenyl-1-naphthylamine (NPN) as previously described (Helander and Mattila-Sandholm, 2000). Briefly, *V. cholerae* 16 hours culture was diluted to an OD_{600} of 0.5 in 5 mM 4-(2-hydroxyethyl)-1-piperazineethanesulfonic acid (HEPES) pH 7.2 and incubated with P1 and P2 at concentrations from 0.005 mg/mL to 0.5 mg/mL, 16 hours at 30 ºC. NPN solution was prepared in acetone and added to 1 mL of clustered bacteria to give a final concentration of 10 µM. 200 µL aliquots were transferred into a 96-well glass bottom plate, and fluorescence was measured using a FLUO Star plate reader exciting at 355 nm and emitting at 460 nm.

2.8 Bacterial clustering

2.8.1 Imaging of bacterial clustering

V. cholerae cultures grown in LB for 16 hours were diluted to an OD_{600} of 1.0 in clear DMEM and polymers were added at concentrations of 0.005 mg/mg, 0.05 mg/mL and 0.5 mg/mL. Images of the clustering were taken after 5, 15, 30 and 60 minutes by mounting 10 µL of sample on microscopy slides visualising at 60X/1.4 NA oil objective using a Differential Interface Contrast (DIC) filter on a Nikon TE200-U microscope, and images were acquired with Nikon

NIS-Elements software. Five pictures per sample were taken and processed with ImageJ software.

2.8.2 Cluster size estimation by laser diffraction

Sizes of P1-induced clusters were measured by laser diffraction using a MasterSizer 3000 (Malvern) laser diffraction size analyser following the manufacturer's instructions. The size distribution of bacterial clusters was measured after 5 minutes of P1 addition at concentrations of 0.005 mg/mL, 0.05 mg/mL and 0.5 mg/mL to a 10 mL chamber with bacteria diluted to 0.1 in OD_{600}. Stirring was constant, and particle diffraction was recorded and plotted as diffraction relative intensity. For clustering kinetics, recorded particle diffraction over time for 10 minutes was plotted as percentage of the particles with a diameter larger than 2 μm. The cutoff size for clusters versus individual bacteria was determined by the median diameter of particles from a sample containing no polymer (2 μm).

2.8.3 Motility assay on polymer-captured V. cholerae

Motility assay was done as previously described (Moisi *et al.*, 2009). *V. cholerae* at an OD_{600} of 1.0 was clustered with P1 and P2 at concentrations from 0.005 mg/mL to 0.5 mg/mL in 1 mL clear DMEM. An aliquot of 1 μL taken from the sample clustered bacteria portion was used to pierce the agar in a LB 0.4 % agar plate. At the same time, the remaining clustered bacteria were washed with high salt PBS (200 mM NaCl) and 1 μL was used to pierce semisolid LB agar plates. Plates were incubated 16 hours at 37 ℃ and images were taken afterwards using a Chemidoc MP system (BioRad) and images processed with ImageJ.

2.9 Biofilm assays

2.9.1 Biofilm measurement by crystal violet assay

Biofilm formation was quantified by crystal violet assay, as previously described (O'Toole, 2011). *V. cholerae* at an OD_{600} of 0.2 in clear DMEM was clustered with P1, P2 or P3 at concentrations ranging from 0.005 mg/mL to 0.5 mg/mL and incubated in 200 µL using a 96-well plate at 37°C with shaking at 200 rpm 16 hours. Then, bacteria were removed, and wells were washed with sterile PBS to remove unattached cells. 200 µL of 1 % crystal violet solution in water was added to each well and removed after 30 minutes. Wells were rinsed again with PBS to remove unattached dye; once the PBS was clean, 200 µL of 95 % ethanol was added and absorbance of the resulting coloured solution was measured at 595 nm using a FLUOstar Omega plate reader.

2.9.2 Biofilm DNAse I digestion and imaging

GFP-labelled *V. cholerae* N16961 was incubated in 200 µL using a glass bottom 96-well plate containing bacteria at an OD_{600} of 0.2 in DMEM with P1 or P2 at concentrations from 0.005 mg/mL to 0.5 mg/mL, in similar conditions described above. In the case of DNAse I treated samples, 2 units of DNAse I were added and the plate was incubated again for 2 hours at 37 ºC. Then, samples were washed with PBS and fixed with 4 % formaldehyde in PBS for 15 minutes and washed again with PBS. Extracellular DNA was stained with 10 µg/mL Hoechst for 10 minutes. Samples were visualised with a Zeiss Axio Observer.Z1 microscope using a Zeiss 40x/1.4 plan Apochromat objective and a Hamamatsu ORCA-Flash 4.0 camera. Images were captured with ZEN 2.0.0.10 software and processed with ImageJ.

The relative pixel intensity of the blue channel was used to estimate the corresponding amount of extracellular DNA. Five images per sample were taken using a Nikon-Eclipse TE2000-U

microscope with a 100x Plan Apo objective and captured with a Digital Sight DS-Qi1MC camera. Image acquisition was done using Nikon NIS-Elements software and final images processed with ImageJ.

2.10 Transcriptional assay: β-galactosidase assay

Reporter strains were used to monitor the expression of relevant genes by measuring the β-galactosidase activity as previously described (Bell *et al.*, 1989). Following 16 hours of growth, cultures of *V. cholerae* reporter strains were used to infect Caco-2 cell monolayer at a multiplicity of infection (MOI) of 10. Prior to the infection bacteria were clustered at sublethal polymer concentrations and incubated for 30 minutes in 1 mL DMEM at 30 ℃. Clustered bacteria were transferred to the Caco-2 cells and infection was incubated for 7 hours at 37 ℃. Then, cells were washed with 1 mL PBS and homogenised with 1 mL of 0.5 % triton X-100 in PBS for five minutes. β-galactosidase activity was measured by disrupting cells with a drop of toluene and a drop of 1 % sodium deoxycholate and tubes were vortexed and left open for 30 minutes to let the toluene evaporate at room temperature. 100 μL of the lysate was added to 2.5 mL of ortho-nitrophenyl-β-galactosidase (ONPG) solution and reactions were stopped when yellow colour developed, recording the reaction time and the absorbance at 420 nm using a Jenway 6305/UV Visible spectrophotometer. Transcriptional activity was calculated as follows:

$$\beta galactosidase\ activity\ (Miller\ Units) = \frac{1000 * 2.5 * total\ Rx\ volume * Abs\ 420nm}{4.5 * time * lysis\ volume * OD600}$$

, where 1000/4.5 is a conversion factor used to convert Abs_{420} into moles of o-nitrophenol (yellow) and 2.5 correspond to a conversion factor used to convert OD_{600} into mg of dry protein

based on the assumption that an OD_{600} of 1.0 is 0.4 mg/mL of dry bacterial mass. Time is expressed in minutes and volumes (lysis and Rx – reaction volume) are in mL.

2.10.1 β-galactosidase assay from sessile bacteria

β-galactosidase assay was done in sessile (clustered and attached) bacteria. Cultures of reporter strains for *rbmA*, *rbmC* and *vpsR* were grown for 16 hours and diluted to an OD_{600} of 0.2 in clear DMEM. Small cultures in Petri dishes were set in 3 mL final volume with clear DMEM, and polymers P1 and P2 added at sublethal concentrations of 0.005 mg/mL and 0.05 mg/mL and incubated for 16 hours at 37 ℃ with shaking. Then, samples were assayed for β-galactosidase activity using bacteria from the supernatant and bacteria clustered (formations on top of plate bottom). Clustered bacteria were washed with high salt PBS (200 mM NaCl) to disrupt electrostatic bounds and OD_{600} can be measured.

For reporters of chitin utilisation-related genes *chiS*, *chiA1* and *chiA2*, following 16 hours of growth cultures were adjusted to OD_{600} 0.2 and bacteria added to 1 mL of artificial marine water containing 10 mg of chitin flakes or 100 μL of chitin bead suspension. Two sets of samples prepared in parallel were incubated at 30 ℃ for 16 hours without shaking. Then, one set of samples was thoroughly washed with artificial marine water and plated onto TCBS and OD_{600} was estimated from CFU counting assuming the relationship that OD_{600} of 1.0 is equal to 10^9 CFU/mL, while the other set was used for the β-galactosidase assays.

2.11 Luminescence assay

2.11.1 Plate-based luminescence assay

Luminescence assays were done using *V. cholerae* pBB1 transconjugants. The pBB1 cosmid (Bassler *et al.*, 1993) was introduced into *V. cholerae* strains by triparental mating in the same conditions as used for pRW50-oriT. Following 16 hours of growth, cultures of *V. cholerae* pBB1 were adjusted to OD_{600} of 0.5, 0.2 and 0.02 in artificial marine water by dissolving sea salts at a concentration of 40 g/L (Sigma) with 10 μg/μL of tetracycline. Polymers P1 and P2 were added at concentrations of 0.005 mg/mL, 0.05 mg/mL and 0.5 mg/mL, in 200 μL final volume using a dark wall clear bottom 96-well plate. The plate was incubated for up to 15 hours at 37 ℃ with shaking at 200 rpm, while luminescence and OD_{600} were recorded every 30 minutes using a FLUOstar Omega plate reader. The following assays were done with bacterial cultures with OD_{600} adjusted to 0.2. Cells were recovered after the assay and washed with PBS containing 200 mM NaCl and plated onto LB with tetracycline to determine the viability. Plates were imaged using a BioRad Gel Doc XR System and images were processed with ImageJ.

2.11.2 Luminescence assay - time-lapse imaging

Following 16 hours of growth, cultures of *V. cholerae* N16961 pBB1 were diluted to an OD_{600} of 0.2 in artificial marine water and clear DMEM with 10 μg/μL of tetracycline, and polymers at concentrations of 0.005 mg/mL, 0.05 mg/mL and 0.5 mg/mL. Samples were prepared in 200 μL using a glass-bottom 96-well plate. Images were taken every 30 minutes with 10 seconds of exposure at 40X magnification, using an Evolve 512 EMCCD camera mounted on a Nikon-Eclipse TE2000-U microscope. Image acquisition was done using Nikon NIS-Elements

software and final images processed with ImageJ. Pixel intensity was determined from several clusters within frame using ImageJ.

2.11.3 Luminescence assay of V. cholerae BH1578 pBB1 with supernatant and co-cultured

V. cholerae BH1578 pBB1 was used to determine the effect of polymers on the production of autoinducers. *V. cholerae* strains at an OD_{600} of 0.2 were clustered for 16 hours with polymers at concentrations of 0.005 mg/mL, 0.05 mg/mL and 0.5 mg/mL in 1 mL artificial marine water. Supernatants were recovered by centrifuging cells and used to resuspend *V. cholerae* BH1578 pBB1 previously adjusted at an OD_{600} of 0.2 in 200 µL. Luminescence was recorded for 15 hours at 37 ℃ using a FLUO Star Omega plate reader

Similarly, *V. cholerae* strains and *V. cholerae* BH1578 pBB1 were co-cultured in 200 µL final volume and polymers added at concentrations of 0.005 mg/mL, 0.05 mg/mL and 0.5 mg/mL in artificial marine water. Both strains were adjusted to a final OD_{600} of 0.1. Incubation was done at 37 ℃ with shaking a 200 rpm while luminescence and OD_{600} were measured every 30 minutes.

2.13 Caco-2 infection

2.13.1 Lactate dehydrogenase assay

Cytotoxicity was determined by following the release of lactate dehydrogenase enzyme from the cytoplasm of host cells using a LDH cytotoxicity detection kit (Takara Clontech). During the detection, the lactic acid is converted to pyruvate by the LDH with reduction of NAD^+. This

reaction is coupled with a second reaction were a diaphorase converts tetrazolium which is yellow into formazan which is red, with oxidation of the NADH molecule. The intensity of the red colour was measured at 420 nm. Epithelial cell line Caco-2 was seeded at a concentration of 75,000 cells/mL in a 24-well plate. Plates were incubated until confluence was around 80 % to start the assay. Following 16 hours of growth, a culture of *V. cholerae* pMW-*gfp* was diluted in clear DMEM to end up with an MOI of 10 according to the formula:

$$MOI\ 10\ (\mu L) = \frac{OD600}{3}$$

To synchronize the infection, the plate was centrifuged at 1000x g for 5 minutes at 20 °C and incubated for 7 hours. The lysis control was prepared by replacing the DMEM with 1% triton X-100 for 10 minutes before sampling the supernatant.

At the time of the assay, 200 µL of each sample was transferred to a 96-well plate in triplicate (600 µL in total) to have technical triplicates for each independent biological replicate. The plate was centrifuged again, and 100 µL was transferred to a new 96-well plate which was mixed with 100 µL of the LDH reagent mixture according to the manufacturer's recommendation. Absorbance at 490 nm was recorded to calculate the % cytotoxicity following the equation:

$$\%\ Cytotoxicity = 100 * \frac{Abs490\ experimental\ release - Abs490 spontaneous\ release}{Abs490\ maximum\ release - Abs490\ spontaneous\ release}$$

, where spontaneous release corresponds to untreated conditions and maximum release to triton X-100 treatment.

2.13.2 Attachment assay – CFU/mL counting

V. cholerae adjusted to an MOI of 10 were clustered with P1, P2 or P3 at concentrations ranging from 0.005 mg/mL to 0.5 mg/mL in clear DMEM for 1 hour prior to infection of Caco-2 cells, using similar conditions as described above. Caco-2 cells forming a monolayer were exposed

to clustered *V. cholerae* for 7 hours at 37 ºC with 5 % CO_2. Cells were washed with sterile PBS to remove unattached bacterial cells and then were treated with 1 mL of 0.5 % triton X-100 in PBS for 5 minutes. Once the debris was dislodged, serial dilutions were plated onto TCBS plates and incubated at 37 ºC for 16 hours. Colony forming units were expressed as CFU/mL.

2.13.3 Cyclic adenosine monophosphate enzyme-linked immunosorbent assay (cAMP ELISA)

Following 16 hours of growth, cultures of *V. cholerae* N16961 were used to infect Caco-2 as described previously. Cultures adjusted to MOI of 10 were incubated in clear DMEM with P1 or P2 for 1 hour at 30 ºC before infection. Caco-2 cells forming a monolayer were infected with clustered *V. cholerae* for 7 hours at 37 ºC. Cells were washed and disrupted with 50 μL of 100 mM HCl to measure the intracellular cyclic adenosine monophosphate (cAMP) concentration by enzyme-linked immunosorbent assay (ELISA) following manufacturer's instructions (Thermo Scientific). Concentration of cAMP was estimated in pmol/mL from a calibration curve made with pure cAMP.

2.13.4 Imaging V. cholerae pMW-gfp infection on Caco-2 cells.

Visualization of *V. cholerae* infection on epithelial cells was performed by placing coverslips on the bottom of the 24-well plate before seeding cells for the LDH assay. After taking the supernatant, cells were washed gently with 1 mL of PBS twice to remove any unattached cells. Then, 500 μL of 4 % formaldehyde solution in PBS was added and incubated for 15 minutes at room temperature. Fixed cells were washed twice with 1 mL PBS and permeabilization was done with 1 mL of 0.1 % Triton X-100 no more than 5 minutes. Caco-2 staining was done by

adding 250 µL of each dye, rhodamine-phalloidin (66 ng/mL) to stain actin, and Hoechst (10 µg/mL) to stain the nuclei and to incubate for 10 minutes at room temperature in the dark. The coverslips were placed onto a drop of ProLong Gold Antifade Mountant on microscope slides, with the cells facing downwards. Samples were incubated at room temperature for 16 hours in the dark to cure the mountant, and visualisation was done under a Zeiss Axio Observer.Z1 microscope with 63X/1.4 Plan Apocromat objective coupled with Apotome2 (Zeiss). Image acquisition was done with Zen Pro Software (Zeiss) and processed with ImageJ.

2.14 Zebrafish colonisation

2.14.1 Zebrafish infection by submersion and colony forming units counts.

Five days post fertilisation (d.p.f.) zebrafish embryos were exposed to *V. cholerae*. In order to estimate the number of bacteria per OD_{600}, cultures at different OD_{600} were plated out onto TCBS and CFU/mL were estimated. Before the infection, *V. cholerae* 16 hours cultures were adjusted to 10^6 and 10^7 CFU/mL in 2 mL of E3 media. At the same time, *V. cholerae* at this CFU/ mL were clustered with sublethal concentrations of P1 and P2 for 1 hour at 30 ºC before infection. Supernatant was removed not disturbing any precipitate formed, and the volume was replaced with E3. Groups of 5 larvae were added to each sample, incubating them at 25 ºC with constant rotation. Larvae were euthanised with an overdose of Tricaine (1600 µg/mL) and homogenised by washing with PBS and incubating them with 1 % triton X-100 for 30 minutes. Lysate was passed through a needle several times, and serial dilutions were plated onto TCBS agar, incubating 16 hours at 37 ºC and counting the colonies afterwards.

2.14.2 Zebrafish imaging

Under similar infection conditions as described above, larvae were imaged. After 6 hours of exposure to *V. cholerae*, zebrafish embryos were mounted directly into 0.4 % low melting point agarose containing tricaine at a concentration of 160 µg/mL for immobilisation. Samples were visualised at 32 ºC and in 80% humidity, using a Zeiss Axio Observer.Z1 microscope with 10X/1.4 Plan Apocromat objective. Image acquisition was done with Zen Pro Software (Zeiss) and processed with ImageJ. After imaging, embryos were euthanised by putting them in a Petri dish with 20 mL of E3 media buffered with 2 mL of 0.1 M sodium bicarbonate and 1.6 mg/mL of tricaine. *Rigor mortis* was determined by cessation of the heat beat checked under the microscope.

2.15 Statistical analysis.

Statistical analysis of data was completed using GraphPad Prism version 6. Data were analysed for statistical significance with a 2-way analysis of variance (ANOVA) using Tukey's multiple comparison test. Data are presented as means $\pm$ standard error of the mean (s.e.m.) of three biologicals replicates. *p* values for significance are indicated in each case.

Chapter 3: Synthesis and characterization of polymers poly(*N*-(3-aminopropyl) methacrylamide) (P1), poly(*N*-[3-dimethylamino)propyl] methacrylamide) (P2) and poly(acryloyl hydrazide) imidazole (P3)

Part of the results of this chapter has been published as part of a paper (Perez-Soto et al., 2017).

3.1 Background

Polymers are used in many different industries and many applications. The annual production of synthetic polymers rose to 299 million tonnes in 2013 and half of it was produced by free radical polymerisation reaction (PlasticEurope, 2015). Many of these materials are characterised by their strong resistance to environmental degradation, which can be a drawback or an advantage depending on the application.

Polymerisation reactions of carbon-carbon backbone polymers such as polyacrylates commonly occurs by a chain-growth mechanism (Reimschuessel, 1975). Here, the addition of monomers takes place at the chain active end by transfer of free radicals, ions or transition metals (Hacker and Mikos, 2011). The reaction involves three necessary steps; initiation, propagation and termination. During initiation, an initiator agent collapses, leaving behind free radicals that mediate the addition of monomers in a chain reaction during the propagation step. The reaction ceases when free radicals pair on terminal carbons, or by removing a proton from the chain. By doing so, there is poor control over the reaction and chains can grow uncontrollably in length and branching. Therefore, "controlled/living radical polymerisation" techniques have been developed to control the composition, length, and polymer structure, at the same time increasing polymerisation yield and lowering polydispersity of the resulting materials (Braunecker and Matyjaszewski, 2007). In order to control the polymerisation process, these controlled reactions adjust the equilibrium between a low concentration of active propagating chains and "dormant" chains which are unable to propagate, neither terminate (Fischer, 2001).

3.1.1 Free Radical Polymerisation

As the name suggests, Free Radical Polymerisation (FRP) involves the formation of free radicals that catalyse the reaction. Free radical formation is achieved by the decomposition of an initiation molecule through the application of an external source of energy such a temperature, ultrasound or radiation, or chemically, for example through the reduction of H_2O_2 by transition metals (Nesvadba, 2012). Free radicals attack carbon-carbon double bonds of the monomer and form a new bond with the fragmented initiator. The free radical at the chain end reacts with the next monomer during the propagation phase. Finally, during termination phase, free radicals at the end of a growing chain can pair with another growing chain, terminating the reaction. The reaction can go through a second mechanism of termination known as disproportionation, where free radical attacks the bond between the hydrogen and the carbon right next to the active end. By doing so, one polymer ends with a CH_3 while the other, free radicals pair and form a double bond at the end of the chain (Fig. 3.1A). In the same manner, free radicals can react with another C-H bond on the structure and branching can occur (Fig. 3.1B). Non-biodegradable C-C backbone polymers synthetized by this method include poly(ethylene), poly(propylene), poly(styrene), and poly(acrylate) derivatives (Tokiwa *et al.*, 2009). However, the inclusion of degradable groups joining chains can improve the backbone degradation. Among these groups disulphides, hemiacetal esters or o-nitrobenzyl esters have been used for a controlled breakdown (Delplace and Nicolas, 2015).

Free radical polymerisation is highly versatile, and allows the engineering of numerous polymer architectures including block (Raether *et al.*, 2002), star-shaped with tri- to multi-arms (Matyjaszewski, 2003) or grafted polymers (Shinoda and Matyjaszewski, 2001) with inorganic or natural components, coating of surfaces or formation of nanoparticles (Zhao and Brittain, 2000, Pyun *et al.*, 2003). Early free radical polymerisation reactions were restricted to the monomer compatibility with solvents. Polymerisation reactions have been adapted to be

performed in water, where the critical factor is the solubility and stability of the initiator or control agent such as RAFT (reversible addition-fragmentation chain-transfer) agent or chain transfer agent, discussed later (Qiu *et al.*, 2001). Other solvents include ionic liquids such as 1-butyl-3-methylimidazolium hexafluorophosphate used for room temperature transition metal mediated living polymerisation of vinyl monomers (Carmichael *et al.*, 2000). Also, free radical polymerisation techniques have been adapted to be used in CO_2 saturated environments with high dispersity (Clark and DeSimone, 1994) while supercritical CO_2 environments have been used to enhance dispersity. The advantage is that there is no chain termination with the solvent, the solvent is of low viscosity, and is environmentally benign.
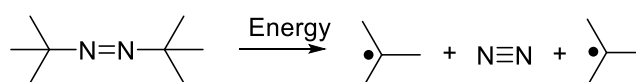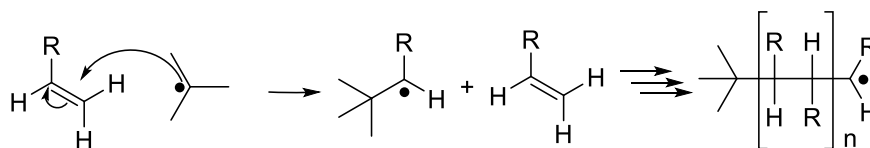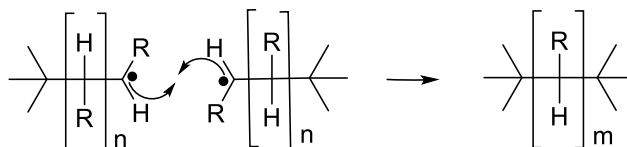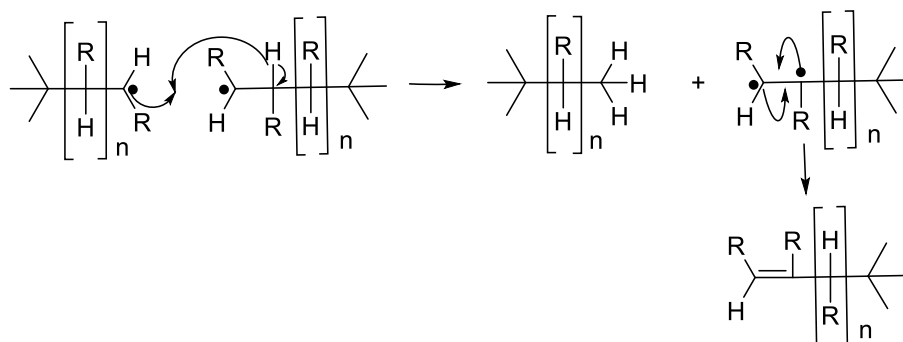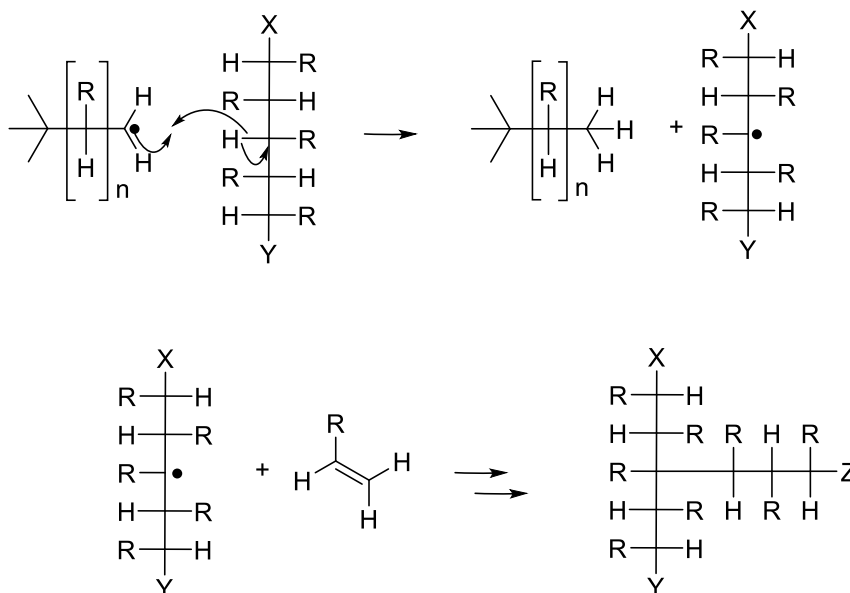
Figure 3.1. Free radical polymerisation reaction. A) Example of free radical polymerisation of substituted ethylene with azobisisobutyronitrile (AIBN) as initiator agent. Reaction steps and two possible termination processes. B) Branching event. Disproportionation but, in another region of the linear chain produce branched structures as monomers can propagate. Normally, FRP does not control the termination rate, therefore new polymerisation techniques apply additional steps to control this rate such as the transference of the free radical to another molecule.

3.1.2 Controlled/Living polymerisation - Chain transfer

The polymerisation reaction can be controlled by controlling the active centre of the growing chain, in other words, the free radical is transferred to another molecule or site in the polymer, and the reaction terminates (Colombani, 1997). By doing so, the contribution of chain breaking processes is low compared to the propagating chains when reaction conditions are favourable, the propagation rate is uniform and the molecular weight, the dispersity and the addition of monomers or specific functional groups are controlled (Qiu *et al.*, 2001). A chain transfer event can occur by removal of the free radical by virtually any C-H bond in the reaction mixture such as the solvent, monomers or polymer. However, molecules with a weaker C-H bond simplify the chain transfer reaction and are known as chain transfer agents. A common chain transfer agent is thiol, since the CH_3S-H bond has a bond enthalpy of 368 kJ/mol compared to 431 kJ/mol for CH_3-H (Dean and Lange, 1973). A variation of this technique is RAFT polymerisation which allows designing different polymeric architectures while being compatible with polymerisation of most of the monomers polymerisable by radical polymerisation. The difference is that a molecule containing a dithioester group, known as RAFT agent, meditates the free radical transfer. The reaction starts with the formation of free radicals by the initiator molecules and propagating rapidly just attacking the monomer. By chance, the active centre of the chain will attack a RAFT agent, and a new type of initiator is generated. Since the RAFT agent is in excess compared with the initiator, the rest of the reaction is driven by this new initiator. A re-initiation step begins, and the RAFT main equilibrium is reached when the dithioester group binds two chains by weak single bonds that can dissociate, forming an active chain and a chain coupled with the thioester. Addition of external energy such as heat can control the dissociation. Finally, "dead" chains are formed by chains that undergo termination, but the vast majority are "dormant" chains that in the presence of monomer and optimal

reaction conditions can start another living polymerisation reaction (Fig. 3.2) (Chiefari *et al.*, 1998).

Other examples of controlled living polymerisation are nitroxide-mediated radical polymerisation and atom transfer radical polymerisation (ATRP). In the first, a nitroxide jumps in and jumps out the chain, generating an active centre in the chain where propagation occurs. However, the reaction has important limitations, such as slow polymerisation kinetics, side reactions when polymerising methacrylate monomers, and the difficulty of synthesising the nitroxide group, resulting in few commercially available options (Grubbs, 2011). The ATRP mechanism is similar to nitroxide-mediated radical polymerisation but is more versatile due to the reactant chemistry. During the "dormant" state, polymers have attached a halogen group, commonly bromide, and a copper catalyst. The capturing of the bromide generates a free radical at the end of the chain where monomers can be added. However, the balance of the reaction tends to go to the reactants or "dormant" species, preparing the chain for the next monomer addition (Tang *et al.*, 2006). In summary, the overall aim of living free radical polymerisation techniques is to control the polymerisation rate by favouring a dormant state of the chain by reversible deactivation.
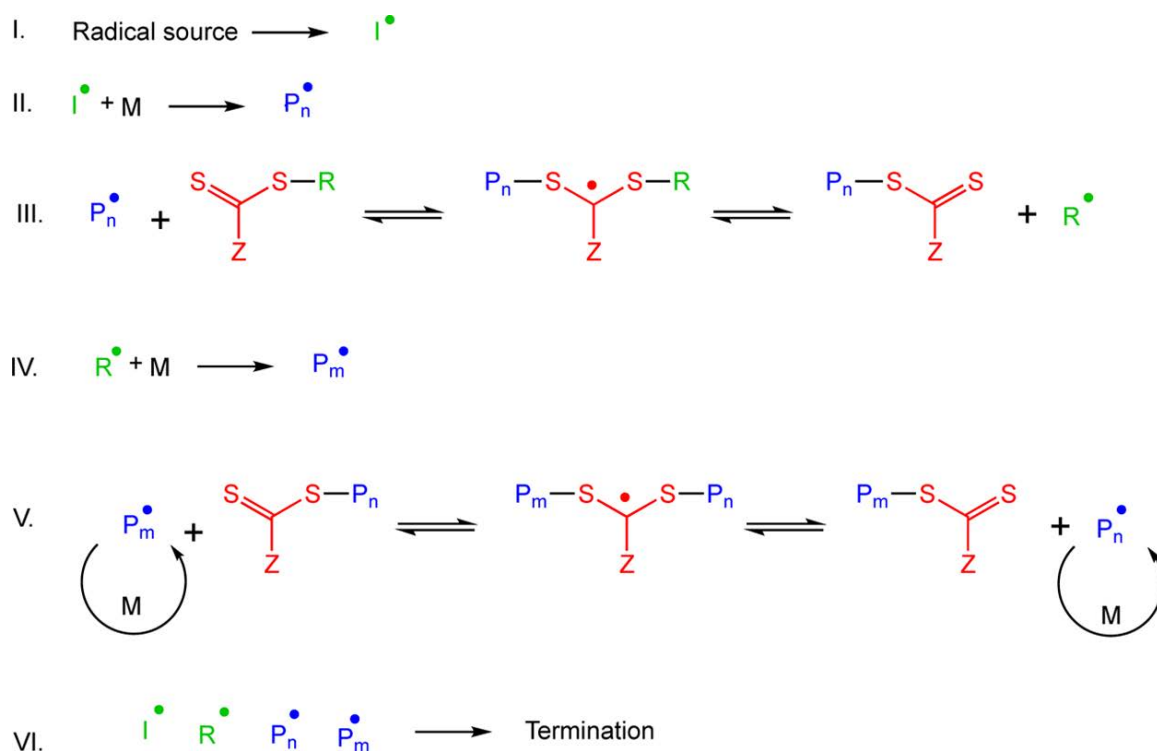
Figure 3.2. Scheme of the Controlled Radical Polymerisation RAFT mechanism. In step I the radical is formed by dissociation of the initiator (I). During step II, the radical is transferred to a monomer (M) forming an activate polymer chain ($P^\bullet_n$). In step III, the radical from $P^\bullet_n$ specie is transferred to the RAFT agent allowing to form an equilibrium between active and dormant species, this is noted as the RAFT pre-equilibrium. A new specie $P^\bullet_m$ is formed by the fragmentation of the RAFT agent and activating a new monomer during step IV and the main equilibrium of the reaction is reached in step V. As the RAFT agent is in excess compared with the initiator, $P^\bullet_m$ will be the main chain transfer agent. Finally, termination occurs when two radicals encounter in step VI (Perrier, 2017).

3.2 Results

3.2.1 Polymerisation of P1 and P2 by free radical polymerisation

Poly(aminopropyl) methacrylamide (P1) and poly(dimethyl)propyl methacrylamide (P2) were synthesised from the commercially available monomers *N*-(3-aminopropyl)methacrylamide hydrochloride and *N*-[3-(dimethylamino)propyl] methacrylamide, respectively. At physiological pH, the overall charge of P1 and P2 should be cationic as P1 exposes a primary amine (pK_a 10.4 (Perrin *et al.*, 1981)) and P2 exposes tertiary amine residues (pK_a 9.61 (Perrin *et al.*, 1981)).

3.2.1.1 Synthesis and characterisation of P1

P1 was polymerised from *N*-(3-aminopropyl)methacrylamide and initiator agent was 4-4'-azobis(4-cyanovaleric acid) (ACVA) in water as a solvent. The reaction was kept 18 h at 70 ℃ with stirring in a Argon-degased environment. The reaction resulted in proton nuclear magnetic resonance (^{1}H NMR) spectrum shifts between monomer and polymer. Clearly, peaks corresponding to the double bond environment disappeared from the 5.5 ppm region, and a new peak appeared at nearly 0.5 ppm region for the polymer (Fig. 3.3A). Other peaks did not change between monomer and polymer and remained in the same areas but changed in intensity. Of note that broadening of the peaks base in polymer ^{1}H NMR spectra resulted from the overlapping of the proton environment which is characteristic of polymeric structures. The integration of peaks resulted in the following as predicted locations were determined using ChemDraw:

Table 3.1. ^{1}H NMR integrations for P1.

δ ppm	Environment	Predicted region
3.11	3H	$CH_{3 \text{ backbone}}$
2.93	2H	CO-NH-$\underline{CH_2}$
1.78	2H	-$\underline{CH_2}$-NH$_2$
1.63	2H	-$\underline{CH_2}$-CH$_2$-NH$_2$
0.98	1H	$CH_{2 \text{ backbone}}$
0.83	1H	$CH_{2 \text{ backbone}}$

Gel permeation chromatography (GPC) analysis was done at a flow of 0.6 mL/min at 40 ºC using 100 mM acetate buffer at pH 2.9. Two hydrophilic interaction column in tandem separated the samples, a Shodex Asahipak GF-510 HQ and a GF-310 HQ. The analysis demonstrated that the retention times for monomer and polymer were different. The GPC profile showed the monomer eluting at 28.4 minutes, while reaction product eluted at 17.4 minutes (Fig. 3.3B). The theoretical molecular weight (Mn) of the polymer was determined as 46,997 g/mol, and the calculated dispersity ($Đ_M$) was 1.16.

The yield of the reaction was 14%, as from 500 mg of monomer only 70 mg of product was recovered after precipitation with diethyl ether and freeze-drying.

Together, these results suggest that *N*-(3-aminopropyl)methacrylamide polymerised into P1. ^{1}H NMR analysis showed a shift in the peak pattern suggesting a new molecule and GPC show that this new molecule is larger compared with the monomer with a low yield for the reaction.

A)
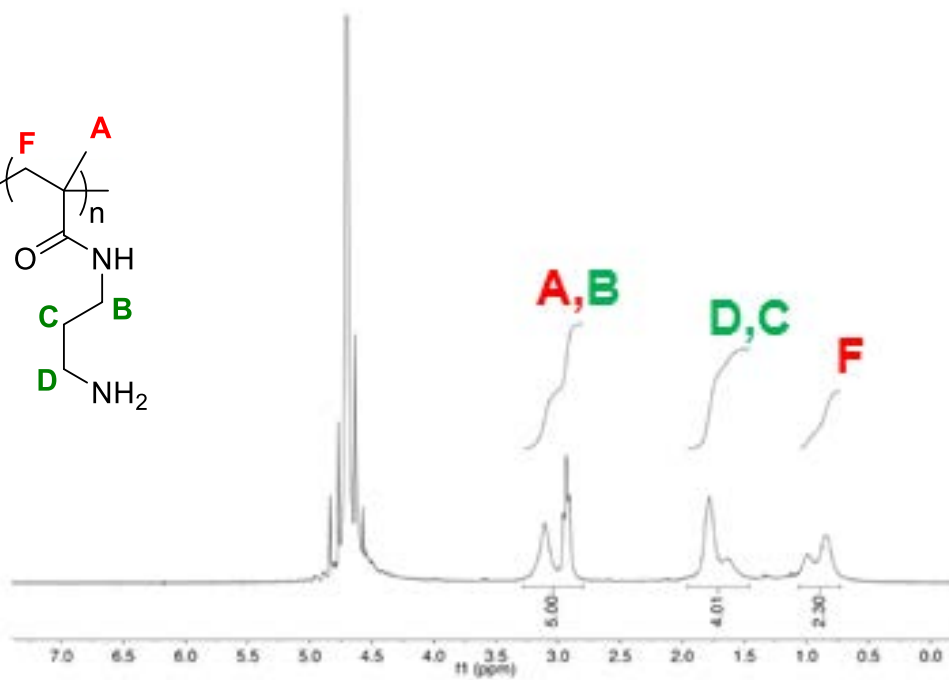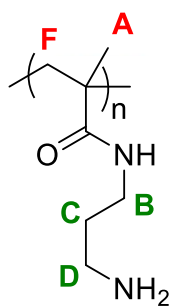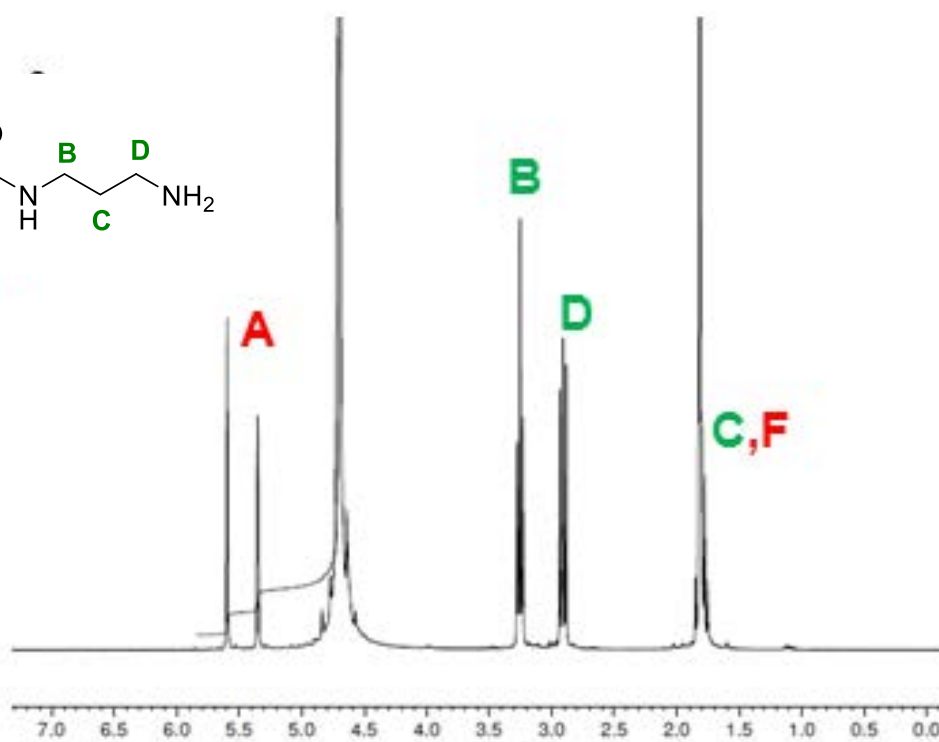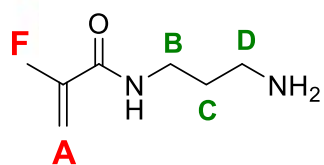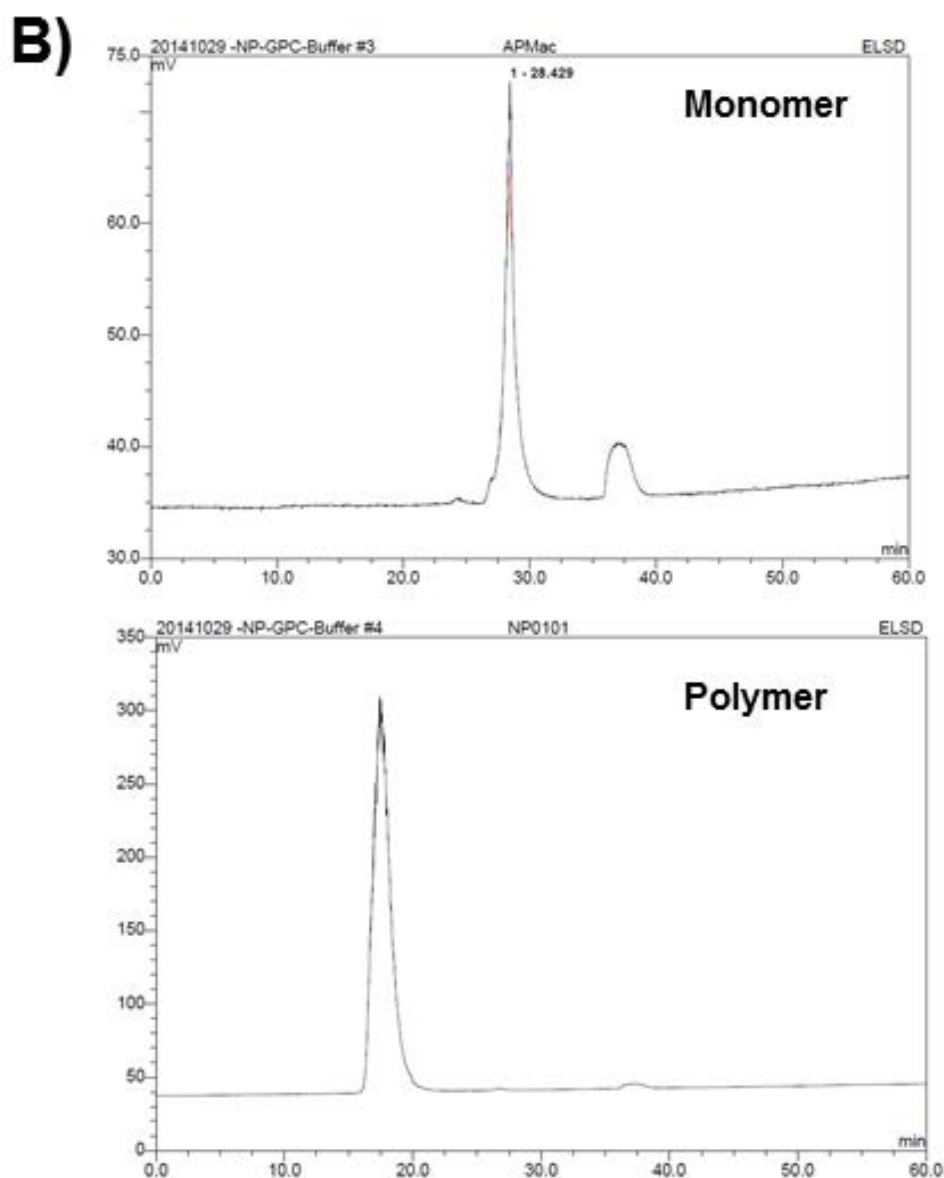
Figure 3.3. ^{1}H NMR spectrum and GPC for *N*-(3-aminopropyl)methacrylamide and P1. A) ^{1}H NMR spectrum for monomer and polymer; NMR was operating at 300 MHz and samples dissolved in D_2O (δ 4.79), and characterisation was done by predicting the shifts with ChemDraw and integration with MestreNova. In red letters are indicated the predicted environments of the molecule that change from monomer to polymer. In green proton environments that do not change from monomer to polymer. B) GPC was done in 100 mM acetate buffer pH 2.9 at 40 ºC and a flowrate of 0.6 ml/min. Samples were detected using an evaporative light scattering detector (ELSD). Upper panel corresponds to the monomer while the bottom panel corresponds to the resulted polymer.

P2 was polymerised from *N*-[3-(dimethylamino)propyl] methacrylamide, with azobisisobutyronitrile (AIBN) as an initiator and toluene as a solvent. The polymerisation reaction was carried out prior to this work by L. Moule, and the resulting product was characterised as part of the work described here. The reaction resulted in proton nuclear magnetic resonance (^{1}H NMR) spectrum shifts between monomer and polymer. Peaks corresponding to the double bond environment disappeared from the 5.5 ppm region similarly as the P1 reaction, and a new peak appeared at nearly 0.5 ppm region for the polymer (Fig. 3.4A)

According to the prediction by ChemDraw, the peaks corresponding to P2 and their integrations were the following:

Table 3.2. ^{1}H NMR integrations for P2.

δ ppm	Environment	Predicted region
7.51	1H	CO-NH
2.96	2H	CO-NH-$\underline{CH_2}$
2.19	5H	$\underline{CH_2}$-N-$(CH_3)_2$ + $CH_{3\ backbone}$
2.11	6H	N-$(CH_3)_2$
1.50	2H	$\underline{CH_2}$-CH_2-N
0.78	2H	$CH_{2\ backbone}$

For GPC, the retention time of the reaction product was 20 minutes (Fig. 3.4B), with an average molecular weight of 46,331 g/mol and a calculated $Đ_M$ of 1.14. The yield of the reaction was 87 %, as 1.66 g of product was recovered from 2 g (ρ 0.94 g/mL) of monomer. Together, these

results suggest that *N*-[3-(dimethylamino)propyl] methacrylamide polymerised into P2. ^{1}H NMR analysis and prediction of proton environment peaks suggest the formation of a new molecule as broad bases were observed in the ^{1}H NMR spectra, at the same time that GPC analysis resulted in the synthesis of a large molecule with a high reaction yield compared with P1.

A)
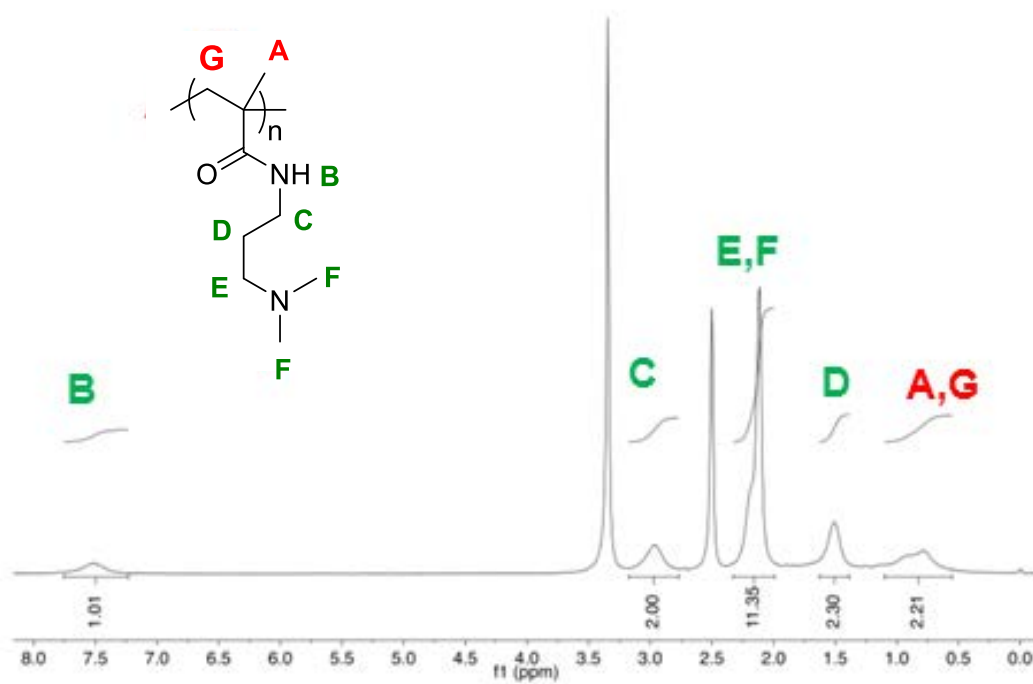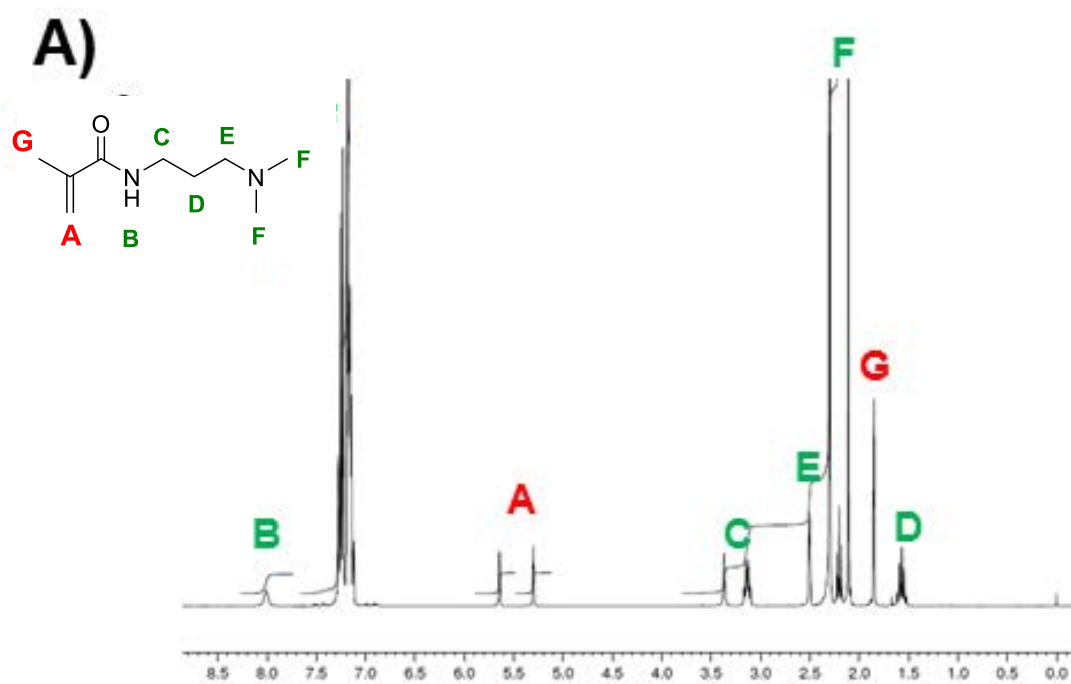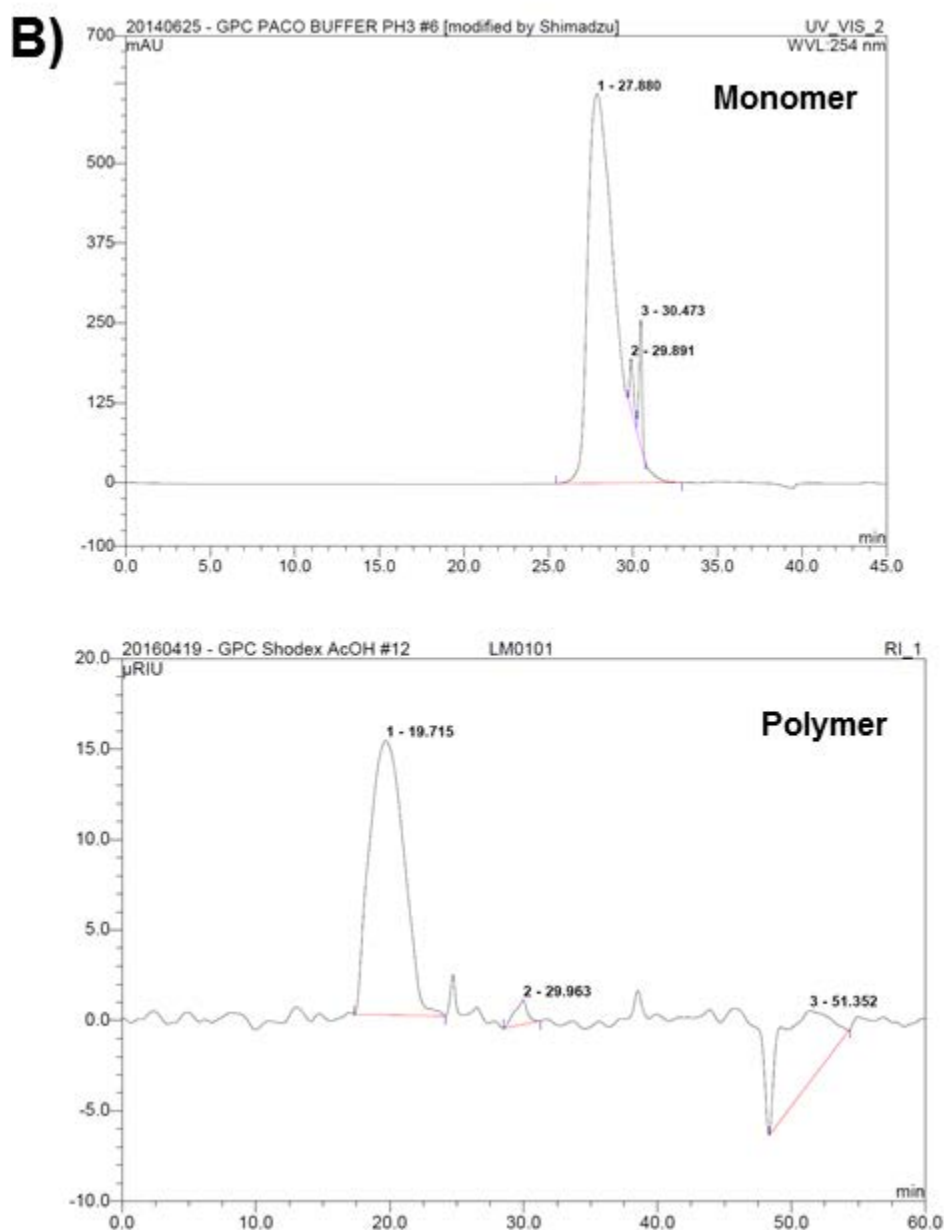
Figure 3.4. ¹H NMR spectrum and GPC for *N*-[3-(dimethylamino)propyl] methacrylamide and P2. A) ¹H NMR spectrum for monomer and polymer; NMR was operating at 300 MHz and samples dissolved in D2O (δ 4.79), and characterisation was done by predicting the shifts with ChemDraw and integration with MestreNova. In red letters are indicated the predicted environments of the molecule that change from monomer to polymer. In green proton environments that do not change from monomer to polymer. B) GPC was done in 100 mM acetate buffer pH 2.9 at 40 ℃ and a flowrate of 0.6 ml/min. Monomer sample (Upper panel) was detected using a UV/VIS detector at 254 nm while polymer sample (bottom panel) was detected by refractive index (RI) detector.

3.2.2 Synthesis and characterization of P3

The synthesis and characterisation of the P3 backbone, poly(acryloyl hydrazide), was reported previously together with the conjugation of soluble and insoluble aldehydes (Crisan *et al.*, 2017). P3 backbone was produced by reverse addition-fragmentation chain transfer (RAFT) which can be conjugated with soluble aldehydes in aqueous conditions. Taking advantage of this, P3 was generated by conjugating 2-imidazolecarboxaldehyde (pK_a 6.95 (Perrin *et al.*, 1981)) with the existing poly(acryloyl hydrazide) backbone at a ratio of 2:1, and the reaction was incubated for 2 hours at 60 ℃. Crisan et al. reported 74 % of aldehyde coupling in aqueous conditions. P3 was prepared immediately prior to experiments and used without further purification, to avoid spontaneous decoupling of the aldehyde during prolonged storage (Fig. 2.1).

3.3 Discussion

This chapter discusses the synthesis and characterisation of the polymers poly(*N*-(3-aminopropyl) methacrylamide) (P1), poly(*N*-[3-dimethylamino)propyl] methacrylamide) (P2) or poly(acryloyl hydrazide) imidazole (P3) which were subsequently used to cluster bacteria. All of these polymers expose different amines that should be protonated at physiological pH, resulting in a cationic net charge. According to the amine structure, polymer polarity could be classified as P1>P2>P3. Although their synthesis route is different, all three polymers share features at their backbones. Therefore, any differences in effects they exert over bacterial cells will be due to differences in the interactions between the bacterial surface and the polymer's lateral groups. P1 and P2 differ in the amine exposed at the end of the side group whereas P3 differ in the amine group and a double bond resulted from the imidazole ring coupling (Fig. 2.1). This structure could potentially be an issue for long-term stability of the material, as P3 imidazole group could be decoupled after longer periods. When preparing polymer solutions, P1 was readily solubilised in any of the tested media, P2 was soluble as well, but it took longer to be completely dissolved. In the case of P3, after the coupling and for almost 48 hours the solution was translucid, and after that white precipitates were formed at the bottom of the tube when it was prepared in DMEM media. For this reason, P3 was prepared and used immediately before each experiment.

The final yields for P1 and P2 polymerisation differed which can be the result of a poor performance of the material under the reaction conditions, or material was lost during post-reaction processing such as dialysis steps. Polymerisation is expected to yield molecules with different physicochemical properties as their monomers. Therefore the behaviour of the molecule in the reaction or the purification solvent might be different (Taylor and Nasr-El-Din, 1998). A typical change from monomer to polymer is the increase in viscosity of the final

product, as multiple factors including temperature, pressure, molecular structure or the auxiliary processing additives affect polymer viscosity (Burow *et al.*, 1964).

Despite the low yield for P1, both polymers in aqueous solutions exhibit patterns on the ^{1}H NMR spectrum associated to polymers. For both materials, ^{1}H NMR peaks corresponding to backbone or side chain protons are broad in their bases as environments overlap (Fig. 3.3A and 3.4A bottom panels). Despite this overlap, the estimation of proton per environments can be done under the conditions used in this study. The study of polymers through NMR is challenging, but some strategies have been developed to distinguish changes in the structure of polymer. High-resolution NMR can identify head to tail arrangement from head to head units which are…-CH_2-CHR'-CH_2-CHR-… to …-CH_2-CHR-CHR-CH_2-… when polymerising vinyl monomer of the type $H_2C=CHR$ (Saalwächter and Reichert, 2010). Also, the kinetics of monomer-to-polymer transition helps to study the rate of monomer conversion (Colombani *et al.*, 2010)

The GPC analysis showed the shift in retention time between monomer and polymer (Fig 3.3B and 3.4B). Estimated values for the Mn and dispersity were calculated against polyethyleneglycol oligomers standard curve. Since the monomers for P1 and P2 differ just in the amine groups, under similar reaction conditions, the product is similar as well. Both polymers exhibit similar Mn (46,000-47,000) and similar calculated $Đ_M$ (1.16 and 1.14, respectively) resulting in a calculated molecular weight of around 50000, estimated from the relation $Đ_M=M_w/M_n$. However, these values are calculated, and $Đ_M$ close to 1 is unrealistic for FRP reactions since many terminations occur and chains do not elongate at the same rate. During a controlled radical polimerisation reaction, the control over the elongation rate could result in values close to 1. Nevertheless, under the reaction conditions used in this study, is expected to have values larger than 1. Possibly, this could be a result of a poor separation of the polymer sample under the flow conditions that resulted in a fast and low resolutive elution,

as peaks, especially in P1, are narrow. Poor control over the reaction results in broad-base peaks as many terminations occur, in other words polymers of different lengths are formed.

The synthesis of P3 was different from P1 and P2. Here, the polymer backbone was synthesised by RAFT, having in mind the capacity to be coupled with different binding groups though a modulator group at the side chain composed by a hydrazide group. These groups can be stably conjugated with aldehydes at neutral pH which allows developing polymer libraries. This approximation allows screening different groups with relevance in biomedical applications. In this work, P3 was included in some experiments to explore the potential to cluster bacteria after the coupling of an imidazole ring which shows a pK_a of 6.95, lower than the other two polymers. However, although P3 was able to cluster bacterial cells without compromising the cell integrity (as discussed later in chapter 4), its use was restricted to some experiments mainly due to the limited impact on cellular functions described in the following chapters when compared with P1 or P2.

Chapter 4: *Vibrio cholerae* cells are captured by cationic polymers and form clusters.

4.1 Background

Numerous studies have been focused on maximising the antimicrobial properties of cationic polymers (Kuroda and Caputo, 2013, Scott *et al.*, 2008, Som *et al.*, 2008). Recent articles have explored the capacity to capture bacterial cells into clusters and immobilizing them while they are still viable (Lui *et al.*, 2013, Xue *et al.*, 2011, Louzao *et al.*, 2015). By displaying cationic groups on polymers, binding occurs though non-specific electrostatic interactions with the bacterial cell envelope, possibly to teichoic acid in Gram-positives and phospholipids along with the LPS in Gram-negatives (Louzao *et al.*, 2015). Polymers have been used as antifouling surfaces inhibiting the adhesion of pathogens directly or displaying ligands to compete for the site of attachment disrupting bacterial adhesion (Hook *et al.*, 2012). However, poly(*N*-(3-aminopropyl) methacrylamide) (P1), poly(*N*-[3-dimethylamino)propyl] methacrylamide) (P2) or poly(acryloyl hydrazide) imidazole (P3) fall into a third group; materials that induce a specific microenvironment for the bacterial cell through clustering. The polymer-mediated immobilisation of bacterial cells into clusters has been studied in species such as the Gram-positive *S. aureus* and the Gram-negatives *E. coli*, *P. aeruginosa* and *V. harveyi* (Louzao *et al.*, 2015). The multivalence of the materials plays an important role in these applications to tighten the binding when bacteria are immobilised into clusters. However, the aggregation of cells into clusters has suggested that diffusion of nutrients and other relevant molecules, such as quorum sensing autoinducers, could be affected (Lui *et al.*, 2013).

The clustering of *V. harveyi* induces controlled phenotypes as polymers are designed to have dual action over quorum sensing signal molecules; on one hand autoinducer-2 (AI-2) was arrested through a poly(vinyl alcohol) and on the other, clustering was achieved with poly(dimethyl)propyl methacrylamide (Lui *et al.*, 2013). Similarly, multibranched dendrimers have been used to capture *V. harveyi* into clusters, inducing a quorum sensing-controlled

phenotype as bioluminescence is increased while viability is maintained. Here, the dendrimer exposes primary amines similar to P1 (Leire *et al.*, 2016). The physical capturing of the bacterial cell also implies a transition from a planktonic to sessile-like lifestyle, interfering with cellular processes such as motility.

4.1.2 Motility as virulence factor in pathogenic Vibrio species.

Motility is often related to chemotaxis as bacteria moves toward nutrients or chemical gradients. The movement is mediated by specialised surface appendices where the flagellum is an essential structure. The flagellum is a rotatory organelle consisting of a molecular motor anchored to the inner membrane, a basal hook complex where the self-assembled rotatory filament protrudes (Josenhans and Suerbaum, 2002). The direction of the rotation dictates repulsion or attraction since the machinery is linked to the chemotactic signalling cascade (Moisi *et al.*, 2009). In *E. coli* the power to move the flagella comes from the H^+ gradient across the membrane when H^+ from outside moves inside the cells through specialised proteins MotA and MotB that move a protein rotor (Kojima and Blair, 2004). In *V. cholerae*, the force to rotate the polar flagella is driven by a Na^+ motor allowing a maximum speed of 100 µm/s (36 cm/h) (Utada *et al.*, 2014). During motility, *V. cholerae* mechanically scans the surface where adhesion will be established by exhibiting two patterns of movement; roaming, where the cell rotates following wavy trajectories leading to skim large areas, and orbiting, where the cell moves in tightly curved trajectories to scan small surfaces (Teschler *et al.*, 2015). The movement is accompanied by the extension of pili from the surface to detect substrates where to initiate adhesion. A theoretical model of *V. cholerae* motility demonstrated a synergistic effect between the flagella and pili during motility as the friction expected by the movement over a surface favours the action of sensory pili (Utada *et al.*, 2014). The relationship between

92

pattern of movement and induction of genes has been extensively studied in the important human pathogen and related *Vibrio* species *Vibrio parahaemolyticus*. This pathogen possesses a dual flagellar system that helps the bacteria to "swim" or "swarm". A Na^+-driven polar flagellum similar to *V. cholerae*, is continually produced while H^+-driven lateral flagella is induced when growing over surfaces. The lateral flagella system *laf* is encoded in 38 genes located in two loci with a biphasic type of expression. The transcription of early *laf* genes is mainly controlled by LafK, a σ^{54}-dependent regulator, while the transcription of late *laf* genes is controlled by a lateral-specific σ^{28} regulator (Stewart and McCarter, 2003). Although *V. cholerae* lacks homologous *laf* genes, it is interesting to see that induction of pathogenicity in *V. parahameolyticus* responds to impediment to polar flagella movement as virulent trait are co-regulated with swarming rather than swimming. In addition, the absence of the lateral flagella regulator LafK not only resulted in defective growth over surface but cytotoxicity was diminished (Gode-Potratz *et al.*, 2011). Although motility has been pointed out to be important for *V. cholerae* pathogenicity, the direct implication in the virulence induction remains unclear (Gardel and Mekalanos, 1996). Unlike previous reports that non-motile V. cholerae were unable to colonise the host tissue, Millet *et al.* demonstrate that non-motile bacteria cannot colonise the proximal section of the small intestine, but colonisation occurs at the distal portion (Millet *et al.*, 2014). Moreover, the change in the colonisation patter is not due by the lack of FlaA, but the absence of MotB from the flagellar rotatory machinery. An article has pointed out that the σ^{54} factor RpoN is a central regulator of the flagellar genes ensuring the balance between flagella biosynthesis and expression of colonisation factors during infection. The absence of RpoN or its constitutive expression resulted in deficient colonisation of the small intestine in mice (Prouty *et al.*, 2001).

In this chapter, the cationic polymers poly(*N*-(3-aminopropyl) methacrylamide) (P1), poly(*N*-[3-dimethylamino)propyl] methacrylamide) (P2) or poly(acryloyl hydrazide) imidazole (P3)

were tested to determine if the polymers are able to form bacterial clusters, and if this interaction is not cytotoxic. Moreover, the interaction mediated by electrostatic forces, it was determine if this binding can be disrupted by increasing the ionic force to determine how the clustering impacts on motility.

4.2 Results

4.2.1 Cationic polymers form clusters upon contact with V. cholerae.

Bacterial clustering induced by cationic polymers was described previously in *V. harveyi*, *S. aureus*, *E. coli* and *P. aeruginosa* (Louzao *et al.*, 2015, Lui *et al.*, 2013). In order to investigate the potential of poly(*N*-(3-aminopropyl) methacrylamide) (P1), poly(*N*-[3-dimethylamino)propyl] methacrylamide) (P2) or poly(acryloyl hydrazide) imidazole (P3) to capture *V. cholerae* cells, these cationic polymers were added in solution and the clustering was followed over time. *V. cholerae* cells were adjusted to an OD_{600} 1.0 in 1 mL of clear DMEM media with polymers at concentrations of 0.005 mg/mL, 0.05 mg/mL and 0.5 mg/mL. At different time points (15 and 60 minutes) an aliquot of 10 μL was mounted onto a microscope slide and visualised under a microscope using a differential interference contrast filter at 60x. Cluster formation progressed by immobilisation of an initial group of cells and increased in size as more bacteria were added. No significant differences were observed in the clustering using P1, P2 or P3. Clusters were formed over the 15 minutes and remained stable over the time the experiment took (Fig. 4.1A). Similarly, *V. cholerae* GFP-labelled was clustered with P1 or P2 at 0.5 mg/mL in clear DMEM and clusters were visualised under a spinning disc fluorescence microscope after 15 minutes of incubation. Rendering the Z-projection of the sample, the volume of clusters was observed showing the three-dimensional shape of clusters. No significant differences were observed between using P1 or P2 (Fig. 4.1B).

These results suggest that the clustering is mediated by electrostatic interactions between the positively charged amine and the negatively charged bacteria. *V. cholerae* is captured by the polymer and motility is not observed from the cluster members.
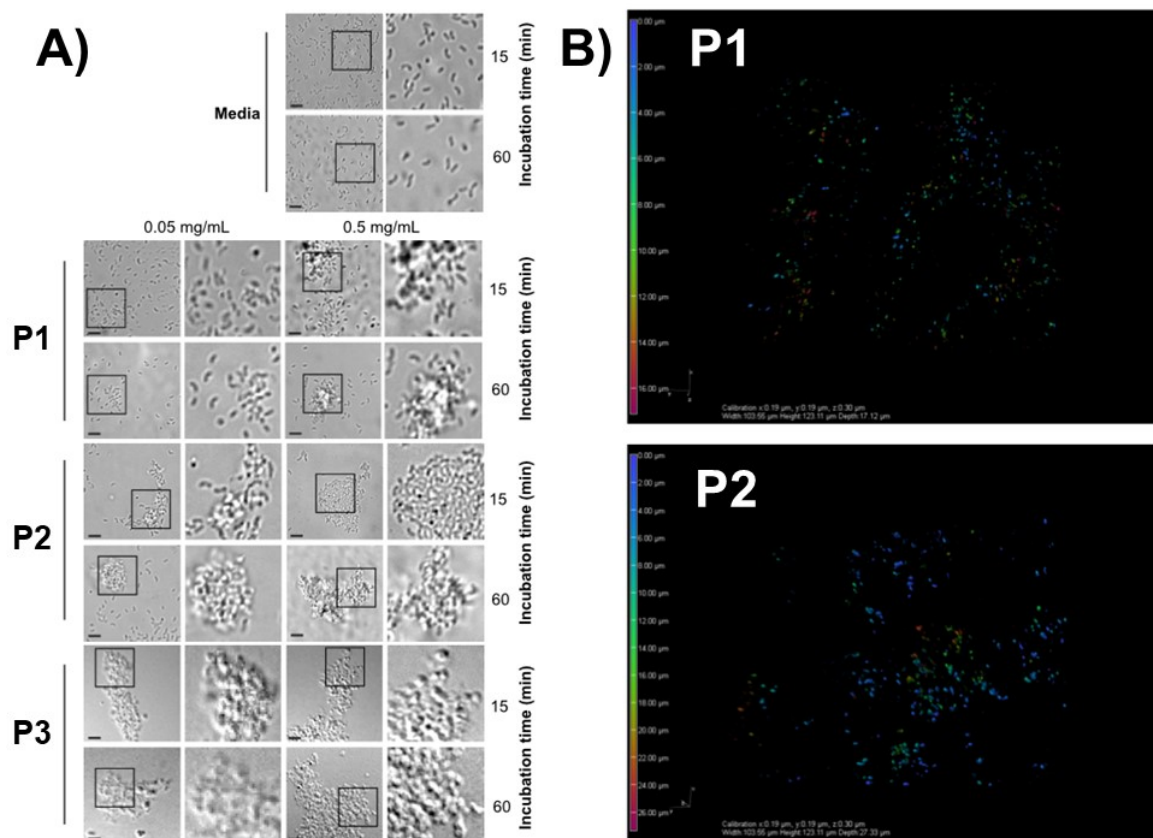
Figure 4.1. Micrographs of *V. cholerae* N16961 in PBS (pH 7.4) with polymers. A) Optical microscopy with DIC filter at 60x of magnification. Poly(*N*-(3-aminopropyl) methacrylamide) (P1), poly(*N*-[3-dimethylamino)propyl] methacrylamide) (P2) or poly(acryloyl hydrazide) imidazole (P3) were added at 0.05 or 0.5 mg/mL and pictures were taken after 15 or 60 minutes of incubation. Scale bar corresponds to 5 μm. B) GFP-labelled *V. cholerae* incubated with P1 or P2 at 0.5 mg/mL for 15 minutes. Images were taken using a spinning disc microscope and z-projection of maximum intensities is shown in different colours according to the z-depth, 17 μm in the P1 sample, and 27 μm in the P2 sample.

4.2.2 P1 clusters V. cholerae in a concentration-dependent manner.

Upon contact poly(N-(3-aminopropyl) methacrylamide) (P1), poly(N-[3-dimethylamino)propyl] methacrylamide) (P2) or poly(acryloyl hydrazide) imidazole (P3) clustered *V. cholerae* rapidly, and no gross differences were observed after 15 minutes (Fig. 4.1A). In order to determine if the polymer concentration is a critical factor to determine the cluster size as well as the speed that the phenomenon occurs, a kinetic clustering analysis was done. The size distribution of bacterial clusters was measured at different concentrations of P1 ranging from 0.005 mg/mL to 0.5 mg/mL in 5.6 mL clear DMEM with *V. cholerae* adjusted to an OD_{600} of 0.5 under stirring. The light diffraction of the clusters was variable depending on the concentration of polymer going from 1 μm when polymer was absence to nearly 10 μm at 0.5 mg/mL with a low proportion of bigger particles (Fig. 4.2A). Similarly, clustering kinetics were followed through the measuring of the size particle for 10 minutes each 30 seconds. *V. cholerae* adjusted to an OD_{600} of 0.5 was exposed to 0.0 mg/mL and 0.5 mg/mL in 5.6 mL of clear DMEM with stirring. In order to determine whether bacteria were clustered, particle diffraction was plotted as a percentage of the particles with a diameter larger than 2 μm (corresponding to the average cell length of *V. cholerae*). The clustering proceeded quickly and reached equilibrium a few minutes after the polymer was added. At 0.05 mg/mL, the equilibrium was reached after nearly 3 minutes while with 0.5 mg/mL it was reached almost immediately (Fig. 4.2B).

These results suggest that the concentration of cationic polymer P1 is a limiting factor of the cluster size and the timing of the clustering process, demonstrating that clustering occurs within minutes of polymer exposure.
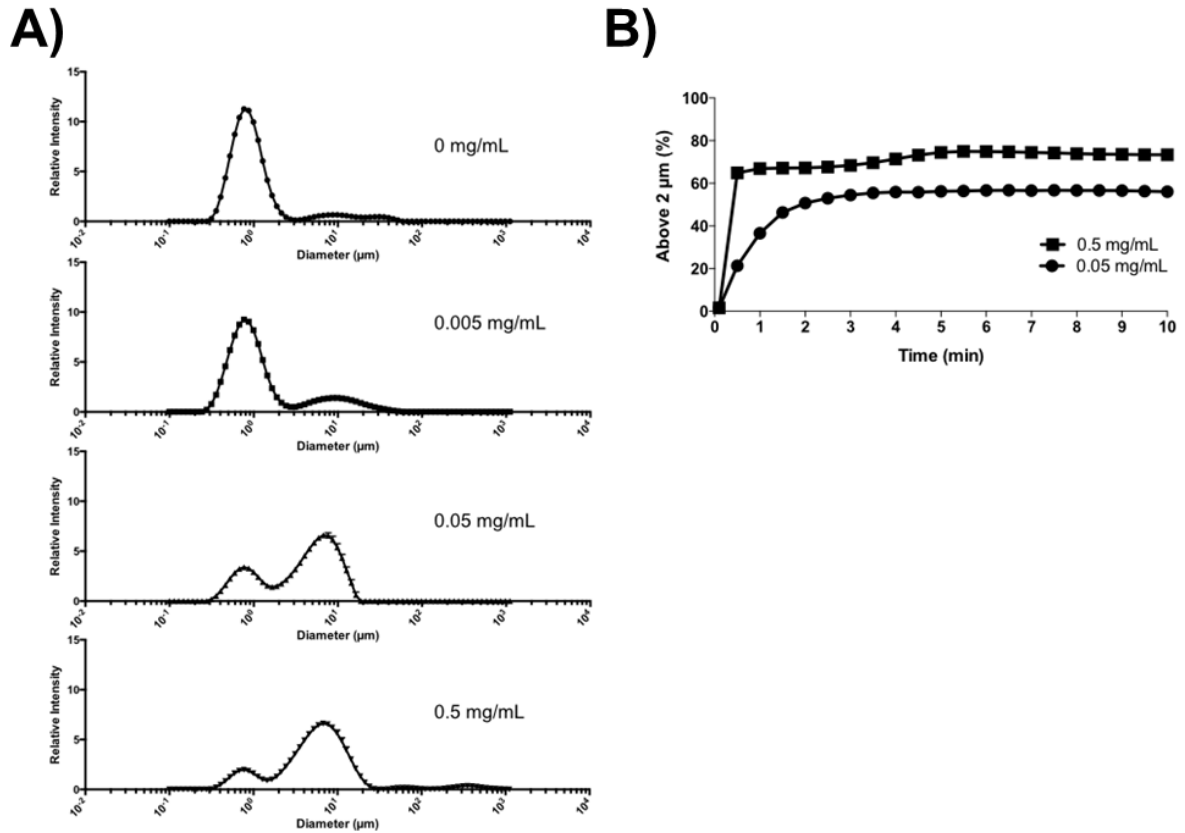
Figure 4.2. Analysis of clustering kinetics and polydispersity by laser diffraction of *V. cholerae* clusters with P1. Analysis was done using a MasterSizer 3000 laser diffractor and data collected by using its proprietary software. A) Average diameter of clusters induced by P1 at concentrations of 0.005 mg/mL, 0.05 mg/mL and 0.5 mg/mL in clear DMEM and bacteria at OD_{600} of 0.5. B) Concentration-dependent kinetics analysis of particle size distribution for P1 induced clustering. Clusters are defined as particles of a mean diameter larger than that of individual bacteria (2 μm).

4.2.3 V. cholerae motility is inhibited by clustering but restored by increasing the ionic strength of the medium.

The physical capturing of *V. cholerae* suggests a detrimental effect on motility as clustering leads to immobilisation. In order to determine if clustering prevents *V. cholerae* to swim in aqueous media a motility assay was done in semisolid LB agar plate. LB plates were prepared with 0.4 % of agar in order to partially restrict the motility of *V. cholerae* to observe impediment of movement as result of the clustering. Bacteria at an OD_{600} of 1.0 were clustered for 16 hours with P1 or P2 at concentrations of 0.005 mg/mL, 0.05 mg/mL and 0.5 mg/mL in 1 mL clear DMEM at 30 ºC with no shaking. Clusters flocculated at the bottom of the tube and 1 µL aliquots from there were used to pierce the agar and deposit the bacteria. The remaining sample was washed with 200 mM NaCl PBS to disrupt electrostatic interactions, and 1 µL was used to pierce another soft agar plate. Both sets of plates were incubated 16 hours at 37 ºC. Images of plates were taken using a ChemiDoc MP System (Bio-Rad) with a ruler as scale. As expected, *V. cholerae* motility was prevented significantly at higher concentrations of P1 and P2, and the effect was concentration-dependent. The disruption of the polymer-bacteria binding resulted in the liberation of bacterial cells, and motility was restored (Fig. 4.3A). Transcriptional analysis of the induction of selected flagellar genes was done in order to detect differences due to the impact of the clustering. *V. cholerae* N16961 was carrying the pRW50-oriT vector. This vector contains the genes from the *lac* operon, a tetracycline resistance and an oriT sequence that was inserted from a broad host plasmid pRK2. Fragments from the upstream region of *flaA* (298 bp upstream from the transcription initiation site) and *flaE* (332 bp upstream from the transcription initiation site), both related to the synthesis of the flagella, were cloned upstream of the *lac* operon. FlaA corresponds to the subunit of the polar flagella whereas FlaE is a component of the basal structure of the flagella (Syed *et al.*, 2009). After a 7 hours incubation with P1 at 0.05 mg/mL or P2 and P3 at 0.5 mg/mL the induction of *lacZ*

reporters was measured from bacteria washed with 200 mM NaCl. There were no large differences at the same time the sample showed variability. In general, P1 down-regulated *flaA-lacZ* and *flaE-lacZ* whereas P3 down-regulated *flaE-lacZ* (Fig. 4.3B-C)

These results suggest that motility of *V. cholerae* is limited upon clustering with cationic polymers while by increasing the ionic strength in the media, the motility is restored confirming that clustering is mediated by electrostatic interactions that can be broken in the presence of competing electrolytes. Polymers showed a mild down-regulation of *fla* genes, especially P1 at 0.05 mg/mL
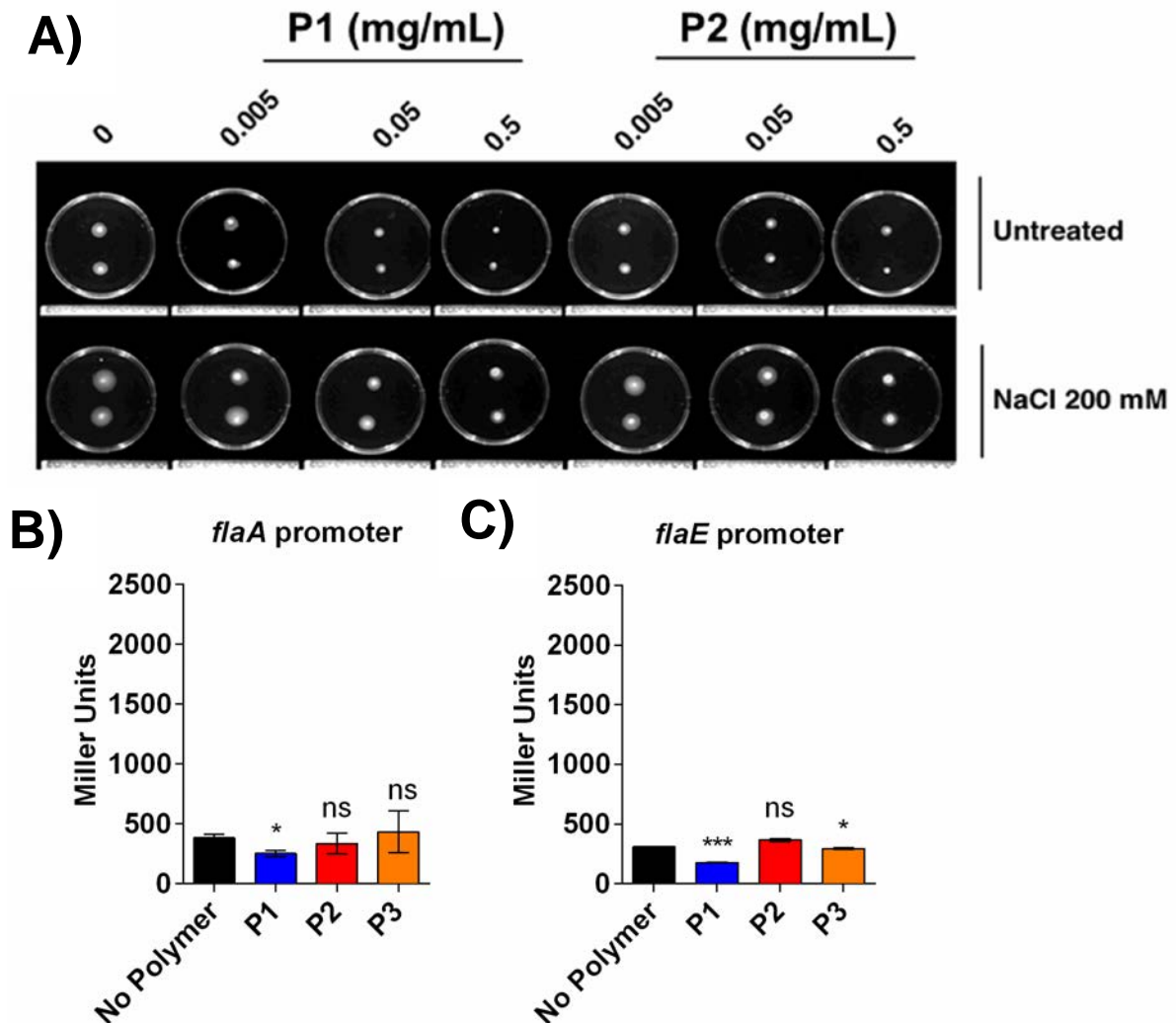
Figure 4.3. Motility of *V. cholerae* in 0.4% agar LB plates and transcription of *fla-lacZ* reporters. A) Polymers were added at indicated concentrations, and clustering was done with bacteria at 1.0 in OD_{600} in clear DMEM and incubated 16 hours at 30 ºC. 1 µL from flocculated bacteria was used to pierce the agar. The rest of the sample was washed with 200 mM NaCl PBS, and 1 µL used to pierce another soft LB plate. After 16 hours incubation at 37 ºC pictures were taken using a ChemiDoc MP System (Bio-Rad). *fla-lacZ* reporters were used to measuring levels of transcription with P1 at 0.05 mg/mL while P2 and P3 were added at 0.5 mg/mL. B) *flaA-lacZ* and C) *flaE-lacZ* were incubated at sublethal concentrations to induce clustering of bacteria at OD_{600} of 0.2. After 7 hours, β-galactosidase activity was measured (section 2.10.1). Each bar corresponds to the mean ± s.e.m. of three biological repetitions. Analysis of variance (ANOVA), followed by Tukey's post hoc test, was used to test for significance. Statistical significance was defined as $p < 0.05$ (*) and $p < 0.005$ (***). For consistency, the Miller Units axis (y-axis) is the same as in virulence β-galactosidase assays.

4.2.4 Polymer-induced clustering does not affect bacterial growth

The effect of cationic polymer on bacterial viability differs significantly according to the charge, hydrophobicity, concentration of material and the bacterial species used (Louzao *et al.*, 2015). Such differences may result in bactericidal activity or merely clustering, as seen with poly(*N*-(3-aminopropyl) methacrylamide) (P1), poly(*N*-[3-dimethylamino)propyl] methacrylamide) (P2) or poly(acryloyl hydrazide) imidazole (P3). To determine if the clustering negatively impacts the bacterial proliferation, growth curves were done. Since OD_{600} measurement relies on light scattering, the formation of clusters may interfere with the measurements. In order to overcome this drawback, fluorescence was used as a proxy of bacterial propagation. GFP-labelled *V. cholerae* carrying pMW-*gfp* was diluted to an OD_{600} of 0.02 in clear DMEM and P1, P2 or P3 were added at a concentration ranging from 0.00005 mg/mL to 0.5 mg/mL in 200 µL using a 96-well plate. The plate was incubated at 37 ºC with 200 rpm shaking, covered with a membrane to avoid evaporation. GFP fluorescence (Excitation 488 nm Emission 509 nm) was recorded every 30 minutes for 25 hours. Bacterial growth was unaffected by clustering, except at 0.5 mg/mL of P1. Moreover, despite 0.5 mg/mL of P1, growth was similar in all the other conditions (Fig. 4.4).

In conclusion, this experiment suggests that the interaction of polymers with the bacteria did not affect the growth significantly. Nevertheless, the GFP signal increases slowly nearly after 5 hours which could be due to another effect of polymers such increase in media viscosity or residual cell damage.
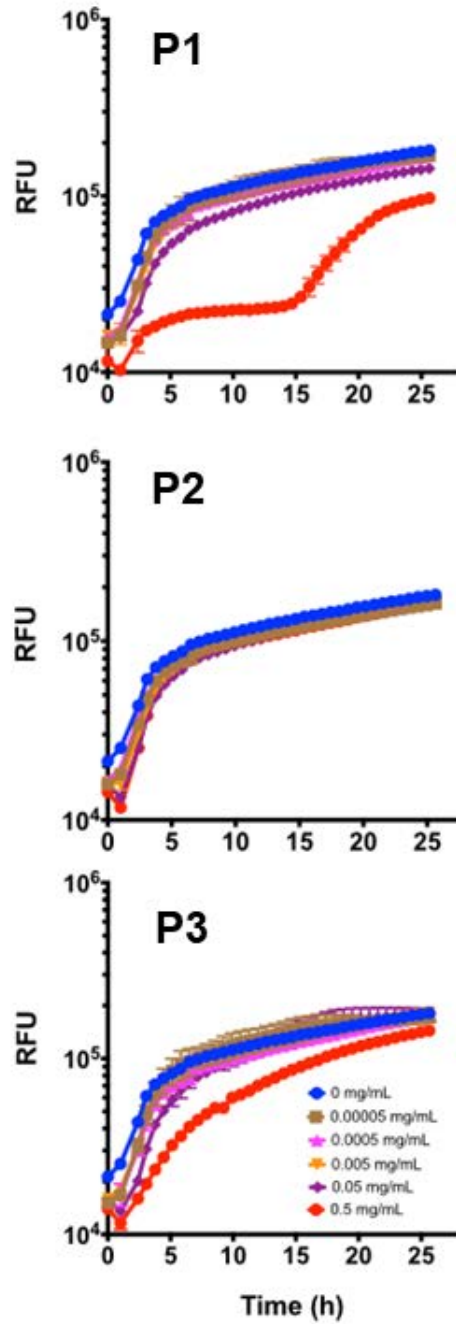
Figure 4.4. Effect of clustering on bacterial growth. GFP-labelled *V. cholerae* carrying pMW-*gfp* was adjusted to an initial OD_{600} of 0.02 and exposed to poly(*N*-(3-aminopropyl) methacrylamide) (P1), poly(*N*-[3-dimethylamino)propyl] methacrylamide) (P2) or poly(acryloyl hydrazide) imidazole (P3) at concentration ranging from 0.00005 mg/mL to 0.5 mg/mL in 200 μL using a 96-well plate. GFP fluorescence, in relative fluorescence units (RFU) was recorded every 30 minutes for 25 hours. Results are plotted as means ± s.e.m. of three independent experiments.

4.2.5 Membrane integrity is not significantly compromised by polymer-induced clustering

Polymers interact directly with the bacterial cell envelope; this interaction may lead to piercing of the bacterial surface (Palermo *et al.*, 2010). Although bacterial propagation is not compromised at most of the tested concentration, it is unclear if there is cellular damage which is commonly associated with cationic polymers. Fluorescent-activated cell sorting (FACS) was used to determine the population of cells that present increased membrane permeability using a differential fluorescent staining. LIVE/DEAD® cell viability staining uses lipophilic SYTO9® which emits green fluorescence and lipophobic propidium iodide (PPi) which emits red fluorescence; both stains bind to bacterial DNA. Every cell will stain with SYTO9® but, membrane perforation allows PPi to reach the bacterial DNA located in internal compartments, displacing the green signal. *V. cholerae* cells were adjusted to an OD_{600} of 1.0 in PBS and incubated with P1, P2 or P3 at concentrations ranging from 0.00005 mg/mL to 0.5 mg/mL, in 1 mL. Samples were kept at 30 ℃ for 16 hours without shaking. 1 μL of 1:1 mixture of dyes was added to 300 μL of clustered bacteria and loaded into FACS. A total of 10,000 events were counted to determine the red and green fluorescence. Gates were adjusted according to "live" population (untreated cells) and "dead" population (cells treated with 70% 2-propanol). Membrane integrity was largely uncompromised except at high concentrations of P1 which is in accordance with the growth curves (Fig. 4.5A).

The interaction at molecular level between cationic polymers with the membrane is not well understood. Studies done on liposomes and molecular dynamics approximations have suggested that the binding of polymers may affect the integrity of the outer membrane (Kozlova *et al.*, 2001). An NPN (N-phenyl-1-naphtylamine) assay was done with *V. cholerae* adjusted to an OD_{600} of 0.5 and clustered with P1 or P2 at 0.005 mg/mL, 0.05 mg/mL or 0.5 mg/mL in 1 mL of 5 mM HEPES pH 7.2. Samples were incubated for 16 hours. NPN was loaded to a

final concentration of 10 μM and end-point fluorescence was measured exciting at 355 nm and emitting at 460 nm. Cells clustered with P1 showed increasing amounts of NPN loaded as the concentration of polymer increased, but this effect was not as clear with P2, where only 0.05 mg/mL showed a significant difference with untreated bacteria (Fig. 4.5B).

These results suggest clustering by poly(*N*-(3-aminopropyl) methacrylamide) (P1), poly(*N*-[3-dimethylamino)propyl] methacrylamide) (P2) or poly(acryloyl hydrazide) imidazole (P3) is largely not detrimental to the membrane integrity as at the concentrations tested the bacterial cell membrane was not compromised except at 0.5 mg/mL of P1. However, the outer membrane is affected to an extent where lipophilic NPN was loaded as result of the clustering which was evident when using P1 as loading was concentration-dependent. Although P1, P2 or P3 are not antimicrobial polymers, it is not possible to rule out if the disruption of the outer membrane may resemble the effect of an actual antimicrobial material.
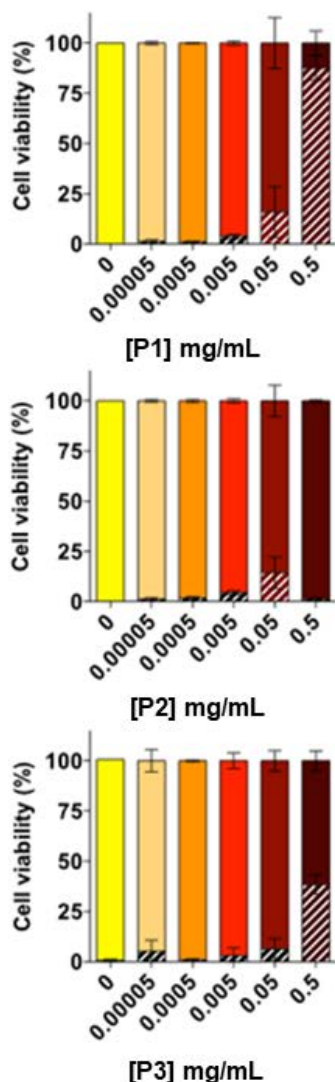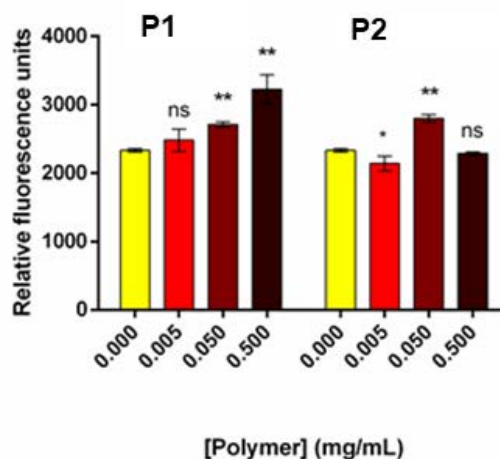
Figure 4.5. Effect of clustering on the bacterial cell wall. A) *V. cholerae* N16961 was incubated for 16 hours with P1, P2 or P3 in serial dilutions. OD_{600} was adjusted at 1.0 and then stained with LIVE/DEAD cell viability kit. The population of "live" bacteria (solid bars) have the membrane intact while "dead" bacteria (dashed bar) allows membrane permeation and DNA binding of the red dye. b) Cells of *V. cholerae* N16961 at an OD_{600} of 0.5 treated with P1 and P2 at different concentrations 16 hours. When outer membrane is disrupted, NPN loads the membrane and fluorescence were recorded at 460 nm. Analysis of variance (ANOVA), followed by Tukey's post hoc test, was used to test for significance. Statistical significance is defined as p<0.05 (*), p<0.002 (**) from three independent measurements.

4.3 Discussion

This chapter describes the effect of physical contact between cationic polymers and the *V. cholerae* cell wall and how this interaction impacts cell viability. Cationic polymers have been reviewed for their antimicrobial properties as an alternative to the use of traditional antibiotics (Muñoz-Bonilla and Fernández-García, 2012, Yang *et al.*, 2017). Their synthesis is cheap and allows to fine-tune features such as charge or hydrophobicity, resulting in changes in their toxicity. Such properties have been highlighted previously for the potential to manipulate bacterial behaviour without compromising the physiology (Lui *et al.*, 2013, Xue *et al.*, 2011). In this line, polymers P1, P2 and P3 were tested to determine their ability to capture bacterial cells into clusters and determine if this clustering affects bacterial viability.

The polymers shared the same backbone but different amines as decorating groups. These amine groups are partially or entirely protonated at physiological pH, driving cellular sequestration by targeting the phosphate moiety of the lipopolysaccharide. Similar to previous studies done in *V. harveyi* (Lui *et al.*, 2013), *V. cholerae* was quickly clustered by all three polymers used (Fig. 4.1A), producing a precipitate. The clustering kinetics by P1 demonstrate the dose-dependence of cluster formation/clustering kinetics as well as cluster size (Fig. 4.2). Since clustering reaches an equilibrium after a few minutes, the clustering may start with the formation of a core that increases in size as more bacteria are being captured.

The capacity of polymers to capture *V. cholerae* into clusters is indicative of the impairment in motility. Since the interaction of cationic groups with the membrane occurs through electrostatic interactions, the motility was fully restored once these bonds were disrupted by increasing the ionic strength of the buffer (Fig. 4.3A). Also, the force transition to a sessile lifestyle impacts the expression of *fla* genes, especially during clustering with P1 (Fig. 4.3B-C). During movement, the bacteria are avid to find sugar-rich surfaces especially ones rich in

mannose, to adhere. Then, once sessile, processes such as infection or production of biofilms are triggered (Silva and Benitez, 2016). Details of the attachment process and biofilm synthesis will be discussed in Chapter 5.

The antimicrobial properties of cationic polymers are mainly due to the interactions established with negatively charged components of the bacterial cell envelope, phospholipid bilayer and anionic sugars of the LPS, followed by intercalation due to the amphiphilic polymer backbone. These dynamics result in critical perturbations of the membrane compromising its integrity (Palermo *et al.*, 2010, Palermo and Kuroda, 2009, Siedenbiedel and Tiller, 2012). Nonetheless, the toxicity of the materials can be balanced by modulating the hydrophobicity and the cationic strength. It has been reported that a low degree of polymerisation and/or adding a hydrophobic tail increases the antimicrobial properties (Grace *et al.*, 2016). Polymers presented here are long and completely substituted, which might be reflected in the little impact on the *V. cholerae* physiology such as growth and cell viability, as they were not affected at most of the tested concentrations.

Since optical density relies on light scattering, following the bacterial growth by OD_{600} during clustering might result in misreading of the growth. For this reason, GFP fluorescence was used as a proxy of growth instead. Growth curves show that only 0.5 mg/mL of P1 have a bactericidal effect while with P2 and P3 the effect is minimal (Fig. 4.4). Although the growth was mostly unaffected by the clustering, this method does not indicate whether bacterial damage is produced which is common when using cationic polymers (Phillips *et al.*, 2017). LIVE/DEAD staining demonstrated that the clustering upon contact with cationic poly(*N*-(3-aminopropyl) methacrylamide) (P1), poly(*N*-[3-dimethylamino)propyl] methacrylamide) (P2) or poly(acryloyl hydrazide) imidazole (P3) had little impact on inner membrane permeability as is not enough to pierce it, except a 0.5 mg/mL of P1 (Fig. 4.5A). Nevertheless, the outer membrane seems to be disturbed as a dose-dependency in the load of NPN is observed when

clustering with P1 (Fig. 4.5B). This dose-dependency was not clear when clustering with P2 as values were variable. Since the binding of the polymers is charge-mediated, the clustering mediated by a net positive charge will be different for each polymer at physiological pH, not considering that the scaffold of P3 is 60 % shorter than the other two polymers. This reduced length might also affect the strength of the binding as well as the effect over the membrane.

This chapter describes the interaction between *V. cholerae* cells with cationic polymers, leading to the formation of clusters with little impact on cell integrity. Since clustering occurs through electrostatic interactions, charge plays a key role in binding to membrane structures. In the case of *V. cholerae*, this binding does not appear to cause significant permeabilisation of the cell envelope, except at a higher concentration of P1 which is the most polar polymer of the group, and to a lesser extent P3. In the next chapter, the effect of clustering on the expression of quorum sensing phenotype of *V. cholerae* is characterised. At the same time polymers can induce phenotypic changes due to signalling tied to sensing of polymers, or due to polymer induced impaired motility, some of which will be discussed in the following chapters.

Chapter 5: Clustering by cationic polymers induces *Vibrio cholerae* biofilm formation

Part of the results of this chapter has been published as part of a paper (Perez-Soto et al., 2017).

5.1 Background

Biofilm communities are associated with numerous species of bacteria embedded in a self-produced exopolysaccharide. Such communities have a large impact on virulence as infection can be developed by few bacteria. At the same time, the extracellular polysaccharide layer protects the community from harsh environments increasing the tolerance of pathogens to antimicrobial compounds (Flemming *et al.*, 2016). During a sessile lifestyle, attached bacteria are allocated within the matrix at different depths depending on their physiological requirements. In a mature biofilm, anaerobes prevail deeper in the matrix where the concentration of oxygen is low, while aerobes are located near the biofilm surface. Between these two groups, fermentative and facultative anaerobes are located. Besides the oxygen gradient, a nutrient gradient dictates the environmental conditions that members of the biofilm community are exposed to where in nutrient-rich areas, cells are metabolically active while in nutrient-poor areas cells are dormant, starving or dead (Flemming *et al.*, 2016). Another phenotype usually associated with biofilms is the "viable-but-not-culturable" (VBNC) state which is characterised by alive bacteria that are not growing or dividing as the metabolic activity is low, and bacteria can remain in this state for long periods (Oliver, 2005). The VBNC phenotype is associated with hypervirulent phenotypes in *V. cholerae* as fewer VBNC cells can start an infection which is critical when a portion of biofilm is ingested by the host (Almagro-Moreno *et al.*, 2015a). Interestingly, the co-culturing of *V. cholerae* O1 or O395 VNBC with eukaryotic cells HT-29, promotes the transition to culturables when human catalase activity is present (Senoh *et al.*, 2015).

Within the biofilm other gradients such as pH, ions or secondary metabolites, help to support the variety of habitats within the biofilm. Biofilm heterogenicity determines the localisation of different physiological states of cells. In monospecies biofilms, different phenotypes are

associated with different depths which also reflects the differential gene expression (Boles *et al.*, 2004). These metabolic interactions organise the biofilm structure to optimise the cellular functions of the members. The highly packed environment helps to increase the efficiency of degradative enzymes. During planktonic lifestyle, extracellular enzymes diffuse rapidly whereas in a biofilm they can accumulate and form external digestive systems that can reutilise matured biofilm components such as extracellular DNA, or digest complex molecules absorbed through the matrix interface (Seper *et al.*, 2011, Tielen *et al.*, 2013).

All of these interactions are favoured by the flexible structure of the biofilm matrix which is constantly reorganised to allow the bacteria to move inside and to reallocate biomass to different layers. The remodelling is essential for biofilm maintenance when members need to disperse or to overcome hydrodynamic shear (Hall-Stoodley and Stoodley, 2005).

5.1.1 Associations between biofilm members

Since several bacterial species can be members of a biofilm, diverse types of interactions and exchange of molecules can occur within a biofilm. Although polymicrobial communities are prevalent in nature, the vast majority of publications on biofilms are on monospecies communities. The proximity between cells and the low diffusion of molecules reinforce the idea that high cell density phenotypes are important during biofilm formation and maintenance. The stratification of the members can be beneficial as metabolic functions associated with bacterial species can be coupled in a food-chain-like manner. An example of this is the nitrite oxidizer bacteria *Nitrospira moscoviensis* that supply ammonia to ammonia oxidiser bacteria through an extracellular urease. Ammonia is transformed into nitrite by these microorganisms, and *N. moscoviensis* receives this nitrite, while at the same time the bacteria couple the formate oxidation reaction with reduction of the nitrite to survive in anaerobic environments as nitrate

is used as a terminal electron acceptor (Koch *et al.*, 2015). As *N. moscoviensis* uses O_2 and nitrate as terminal electron acceptor it can survive where oxygen is much depleted such as in deeper layers of the biofilm (Flemming *et al.*, 2016). Co-evolution has been observed in *Pseudomonas putida* and *Acinetobacter sp.* biofilms. Studying the interaction of both microorganisms revealed that point mutations appear in the genome of *P. putida*, specifically the LPS core biosynthesis-related gene *wapH* when growing in the presence of *Acinetobacter* and the production of exopolysaccharide is enhanced (Hansen *et al.*, 2007). Although the function of the deletion is unclear, a similar phenotype has been observed in *Azospirillum brasilense* where a deletion that resulted in lipopolysaccharide (LPS) core modification also enhanced the production of calcofluor white-stainable polysaccharide (Jofre *et al.*, 2004).

Cooperation and mutualism are essential relations within a biofilm, but also inter-species competition that can be fatal as competition is important to control invaders. For example, *P. aeruginosa* inhibits the attachment and stimulates the dispersion of *Agrobacterium tumefaciens* biofilm using a yet unknown exoproduct (Hibbing and Fuqua, 2012). Another example of competition is the fight for resources or DNA as in the case of *V. cholerae* which is capable of 'stabbing' other bacteria with a type VI secretion system and of taking up their DNA when growing on a chitinous surface (Borgeaud *et al.*, 2015).

5.1.2 Exchange of "information" within a biofilm.

The proximity between cells inside a biofilm favours the exchange of information such as nucleic acids or secondary metabolites such as signalling molecules. Horizontal transfer of DNA is especially predominant in such environments as the cells can be aligned closely enough for the conjugative machinery to move plasmids with high efficiency. At the same time, natural competence has been observed during growth in a biofilm. For *Acinetobacter* biofilms it has

been reported that 15 minutes after addition of the plasmid pGAR1, bacterial cells were transformed. Moreover, small amounts of DNA were enough to detect transformed cells (Hendrickx *et al.*, 2003). The establishment of conjugative machinery also has direct effects on biofilm formation, as the conjugative pili help to stabilise the structure of a newly formed a biofilm. Studies in *E. coli* biofilms have also demonstrated a dual function of the conjugative pili where it is not only used to transfer DNA, but also as an adhesion factor to help bacterial surface attachment (Ghigo, 2001).

5.1.3 Associations between V. cholerae and chitin

Chitin is the second most abundant polysaccharide on earth and the most abundant polysaccharide of animal origin (Sahariah *et al.*, 2015a). It is composed of long chains of *N*-acetylglucosamine and differs from cellulose by a $NHCOCH_3$ group instead of an OH group at the C2 carbon. Chitin is insoluble in water while the derivative chitosan is soluble when it is partially acetylated (Fig. 5.1), (Kubota *et al.*, 2000). Aquatic microorganisms use chitin as carbon and nitrogen source when using chitin to adhere, followed by the breaking down and transporting of the oligomers. Chitin oligomers are then catabolised to produce fructose-6-phosphate, acetate and ammonia (Keyhani and Roseman, 1999). In *V. cholerae* these functions are mediated by chitin-inducible genes under the control of the sensor histidine kinase ChiS. Profiling the expression of the ChiS-regulon by microarray with simple chitin oligomers has shown the coordinated expression of extracellular chitinases, a chitoporin and a PilA-containing type IV pilus, ChiRP, that helps to adhere onto chitin surfaces; N-acetylglucosamine induced the expression of genes related to chemotaxis, adherence, transport and assimilation in order to use N-acetylglucosamine, while dimers of D-glucosamine induced transport and catabolism of non-acetylated chitin. This array of genes are named as the chitin utilisation

program of *V. cholerae* (Meibom *et al.*, 2004). During infection ChiRP pili have a role in colonisation as a deletion in *pilA* prevents *V. cholerae* from colonising the infant mouse intestine (Fullner and Mekalanos, 2000). Moreover, it has been reported that *pilA* is expressed during infection in humans possibly due to the encounter with chitin-derived oligomers but the significance of this during infection remains unclear (Hang *et al.*, 2003). Likewise, the mannose-sensitive haemagglutinin (MSHA) pilus, a type IV pilus, also contributes to chitin binding as mutants in *mshA* are unable to bind to chitin coated beads. This pilus also mediates the attachment to other surfaces, such as silica, to initiate the synthesis of biofilm, suggesting no direct induction by chitin (Watnick *et al.*, 1999, Meibom *et al.*, 2004). Besides this MSHA pili, the N-acetylglucosamine binding protein GbpA plays an important role in *V. cholerae* chitin adherence when is in the environment. At the same time, it mediates the attachment of bacteria to mammalian intestinal mucin during infection. GpbA consists of 4 domains; one strictly binds to chitin while a second one binds to chitin and intestinal mucus. The remaining two domains interact with the bacterial cell envelope (Wong *et al.*, 2012). Comparing the adhesion mediated by MSHA and GbpA, MSHA is far more effective than GbpA to bind to chitinous surfaces and other inorganic surfaces (Stauder *et al.*, 2012).

The sessile growth of *V. cholerae* over chitin also induces the competence proteins ComEA via the competence activator protein TfoX. Although TfoX is the major competence regulator, its presence is insufficient to induce *comEA* transcription. The additional presence of the high cell density regulator HapR promotes the horizontal gene transfer (Ng and Bassler, 2009, Antonova and Hammer, 2011, Meibom *et al.*, 2005).

In this chapter, polymers P1, P2 and P3 were tested to determine whether the immobilisation the bacterial cell leads to the formation of a biofilm structure by inducing the VPS pathway. Additionally, since *V. cholerae* uses chitinous surfaces to adhere when living environmentally, chitinous materials were tested as potential groups to improve selectivity toward *Vibrio* species.
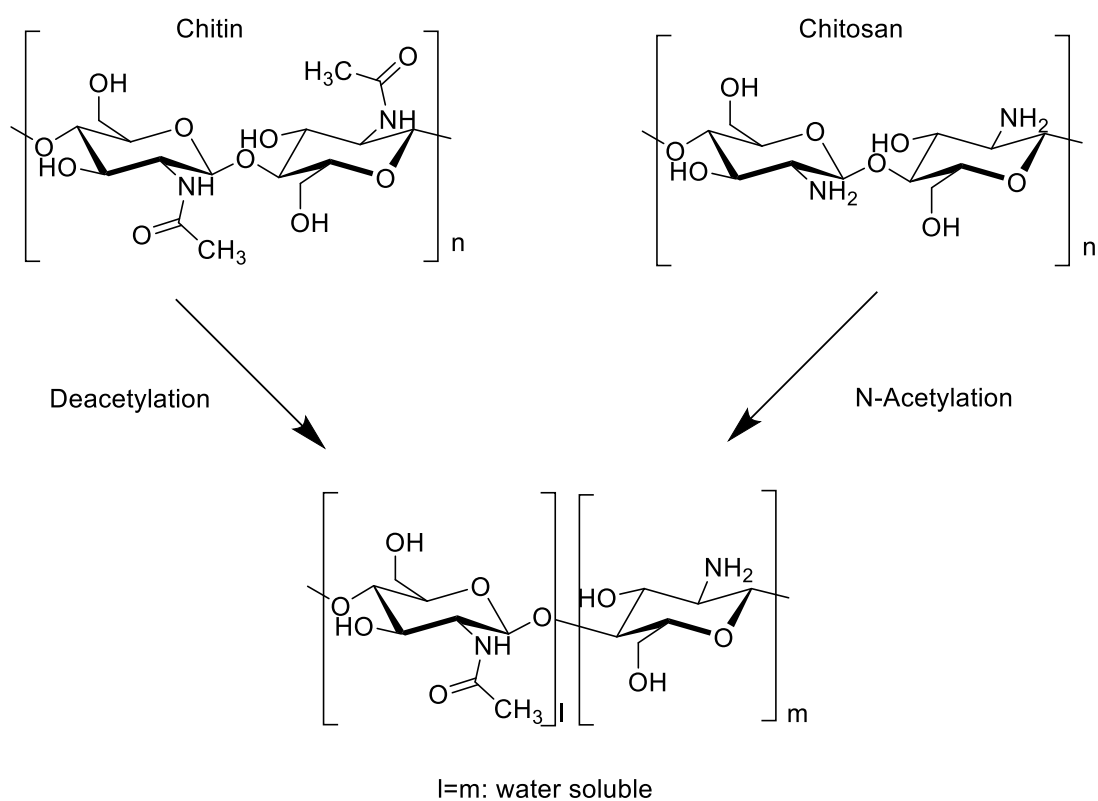
Figure 5.1 Chitin and chitosan. Both materials are insoluble in water but, chitin de-acetylation (or chitosan acetylation) increase the solubility. Soluble chitinous material can be incorporated into polymers to explore sugars as binding groups for *V. cholerae* (Kubota *et al.*, 2000).

5.2 Results

5.2.1 Sequestration of V. cholerae in clusters promotes a biofilm-like state with enhanced biofilm production.

Immobilisation by cationic polymers forces a transition from planktonic to sessile bacterial state which resembles the growth in a biofilm. During biofilm synthesis, *V. cholerae* secretes an exopolysaccharide named *Vibrio* polysaccharide (VPS) that is organised by structural proteins and extracellular DNA (See section 1.4.2). These components are building blocks of the external matrix. In order to determine if the clustering with P1, P2 or P3 resulted in an enhancement of biofilm production, a crystal violet assay was done to measure the amount of biofilm accumulated during clustering. *V. cholerae* N16961 exposed to polymers at concentrations ranging from 0.005 mg/mL to 0.5 mg/mL in 200 μl of clear DMEM were incubated at 37 ℃ for 16 hours to promote the formation of biofilm. Crystal violet assay determine that polymer-induced clustering led to significant production of biofilm in *V. cholerae*, about 3-fold increased (from 0.5 to 1.5 in average, at 595nm) at any concentration of P1 and similarly with P2 at 0.05 mg/mL and 0.5 mg/mL (Fig. 5.2A). The biofilm-induced by cationic polymers was visualised under the microscope. GFP-labelled *V. cholerae* carrying pMW-*gfp* was clustered at 0.05 mg/mL of P1 and 0.5 mg/mL of P2 and P3 under similar conditions indicated above. After 16 hours samples were washed with PBS and fixed with 1 mL of 4% paraformaldehyde for 15 minutes. Then extracellular DNA was stained with Hoechst. The biofilm-induced by clustering was accompanied by release of high levels of extracellular DNA into the biofilm compared with untreated *V. cholerae*. Microscopic sections were acquired throughout the depth of the biofilm in order to render an orthogonal view of the biofilm. When polymers were not present, a uniform layer of bacteria attached to the bottom of the well. The presence of polymers increased the surface-deposition of bacteria at the bottom

into non-defined structures (Fig. 5.2B). Upon clustering with P2, groups of bacteria were scattered across the field of view, and with P1 and P3 larger aggregates were observed. The blue signal of the extracellular DNA was observed outside the bacteria where the groups were located.

These results suggest that clustering *V. cholerae* triggers the productions of biofilm significantly compared with untreated bacteria. The production of biofilm is accompanied by deposition of extracellular DNA surrounding the bacterial cells as Hoechst is mainly located in the biofilm matrix.
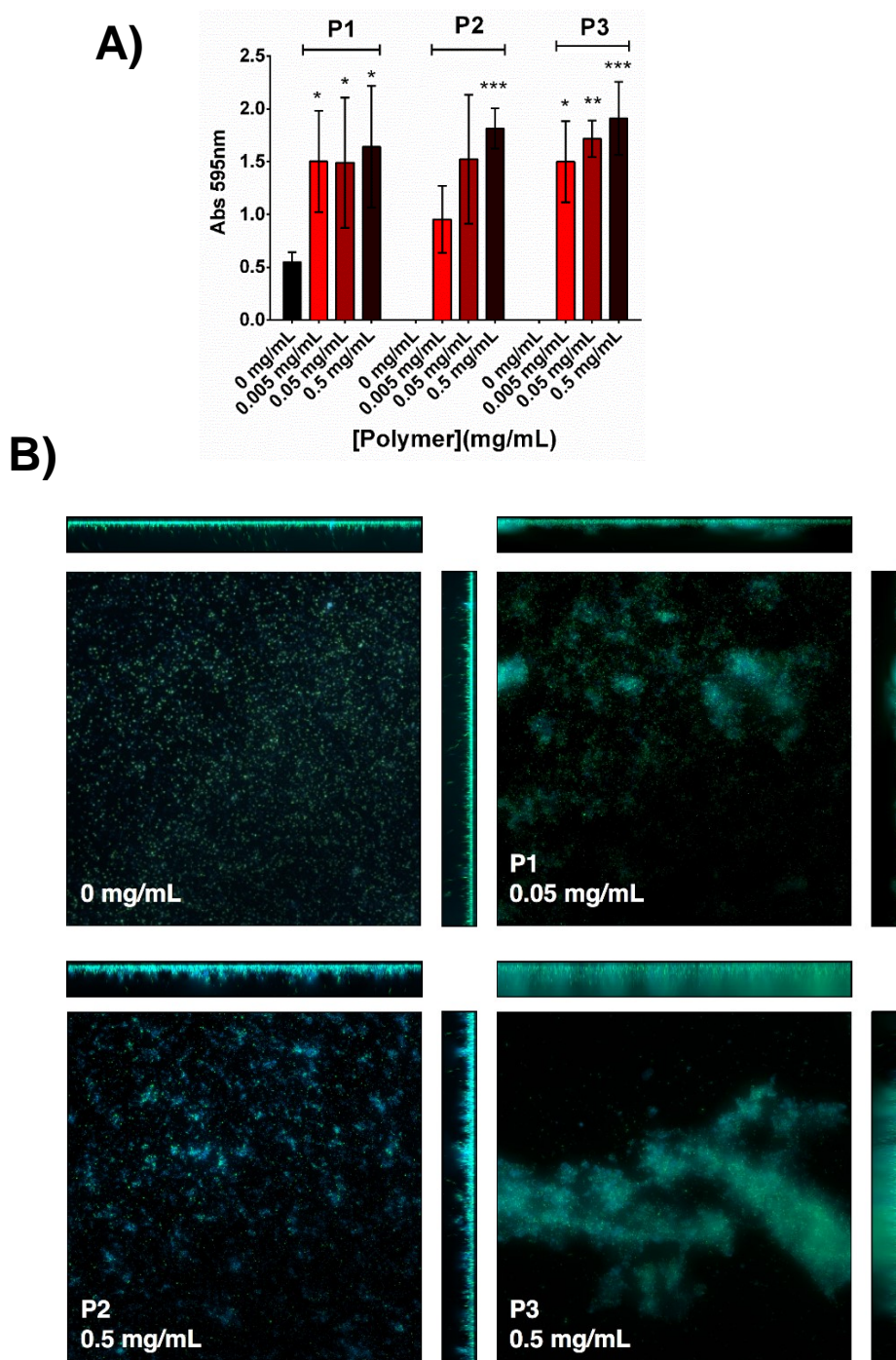
Figure 5.2. Biofilm is accumulated during clustering with polymers. *V. cholerae* N16961 incubated with P1, P2 or P3 increases the synthesis of biofilm. A) Crystal violet assay from 16 hours cultures in clear DMEM with polymers at concentrations ranging from 0.005 - 0.5 mg/mL. Analysis of variance (ANOVA), followed by Tukey's post hoc test, was used to test for significance. Statistical significance was defined as $p<0.05$ (*), $p<0.01$ (**) or $p< 0.001$ (***). B) Micrographs and Z-projections of biofilms formed after clustering of GFP-labelled *V. cholerae* with a sublethal concentration of P1, P2 or P3. Orthogonal views were obtained by taking 30 images in the Z-axis using a range between 8 - 10 µm from the bottom of the well. Extracellular DNA was stained with Hoechst.

5.1.2 Extracellular DNA associated to polymers-induced biofilm is digested by DNAse I

Nucleic acids are structural components of biofilms, but their specific role in biofilm communities is unclear. Studies have assigned them to be important for the early stages of biofilm formation, for bacterial adhesion to surfaces and for controlling the diffusion of cations by chelating them (Okshevsky and Meyer, 2015). Additionally, extracellular DNA has been reported to be a source of phosphate and a dynamic pool of genes for horizontal gene transfer (Vlassov *et al.*, 2007). During the assembly of *V. cholerae* biofilm the nucleases Dns and Xds allow a coordinated accumulation of the biofilm reinforcing the structural role of DNA (Seper *et al.*, 2011).

GFP-labelled *V. cholerae* carrying pMW-*gfp* clustered with P1 or P2 at concentrations ranging from 0.005 mg/mL to 0.5 mg/mL were grown in order to promote clustering and biofilm formation and determine the amount of eDNA present in the biofilm matrix. After 16-hour incubation at 37 ºC, biofilm was washed, and extracellular DNA digested with 2 units of DNAse I. Extracellular DNA was stained with Hoechst and images at 100X were taken detecting fluorescence in green and blue channels. Pixel intensity of different pictures was plotted as pixel intensity versus concentration of polymer. An increase of the blue channel intensity was observed for samples exposed to P1 while with P2 the effect was minor. However, the variability of the samples prevented a more precise quantification of the eDNA produced especially in the samples treated with P2. DNAse I digested the eDNA as treated samples displayed less intensity of the blue channel (Fig. 5.3 upper panels). Also, intensities in the green channel corresponding to the bacterial cells were almost invariable during the experiment. Variations in GFP were only detected between 0.5 mg/mL of P1 in the undigested sample and 0.05 mg/mL of P2 at digested sample (Fig. 5.3 bottom panels). These results suggest that eDNA is a structural component of the biofilm-induced by clustering. However, the addition of

extracellular DNAse activity did not result in biofilm dispersion as suggested for other biofilms (Klare *et al.*, 2016, Harmsen *et al.*, 2010).
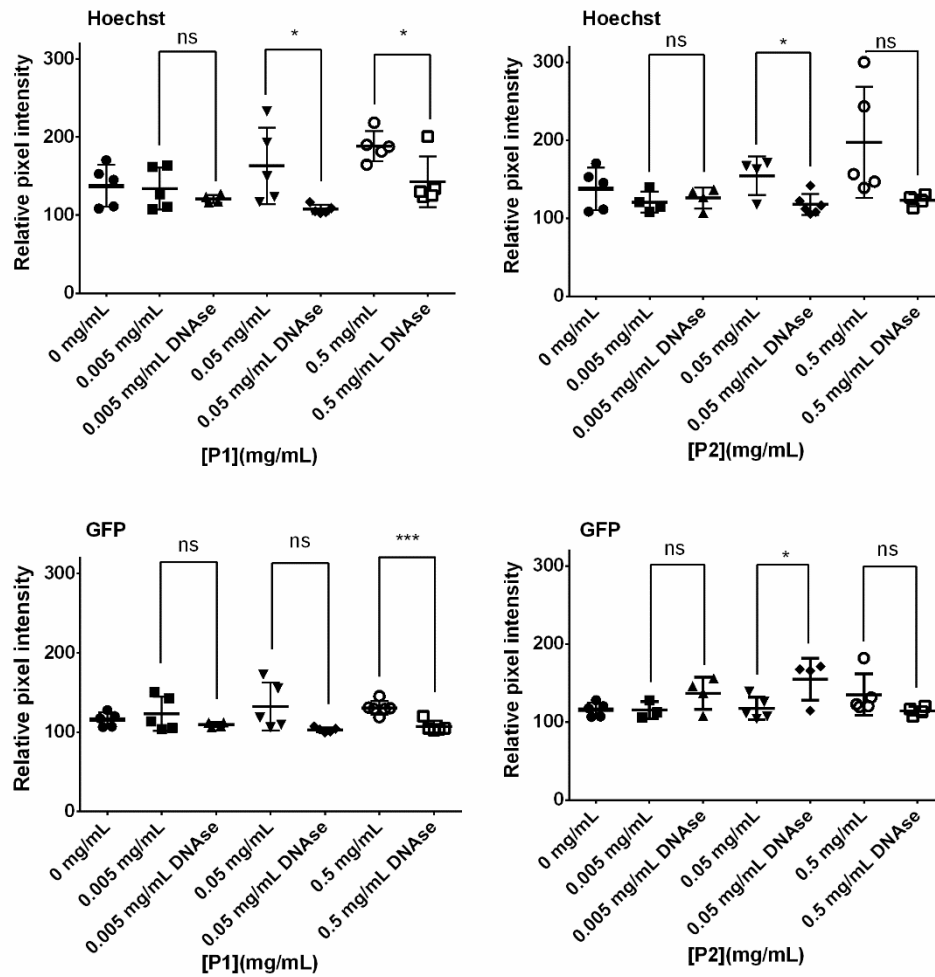
Figure 5.3. Digestion of extracellular DNA with DNAse I. The nuclease DNAse I digest extracellular DNA. GFP -expressing *V. cholerae* was clustered with a sublethal concentration of P1 or P2 and incubated 16 hours in clear DMEM at 37 °C. Once the biofilm was formed the well was washed digestion reaction was done with 2 units of DNAse I. The remaining extracellular DNA was stained with Hoechst and several pictures were taken. The pixel intensity of both channels, blue (DAPI) and green (eGFP) was measured using ImageJ. Analysis of variance (ANOVA), followed by Tukey's post hoc test, was used to test for significance. Statistical significance was defined as $p < 0.05$ (*) or $p < 0.001$ (***).

5.1.3 Transcription of genes encoding for structural proteins RbmA, RbmC and the biofilm regulator VpsR is affected by clustering.

The assembly of *Vibrio* polysaccharide (VPS) is organised by structural proteins RbmA, RbmC and Bap1. The orchestrated function of these proteins is to serve as a scaffold for the sugar matrix, and changes in the expression of any of these proteins resulted in different macroscopic features of the biofilm (Teschler *et al.*, 2015).

Since the polymer-induced clustering stimulates the biofilm formation, transcription of biofilm structural proteins was followed by β-galactosidase assays from planktonic and clustered cells. Reporter strains containing the pRW50-oriT vector containing upstream promoter regions from *vpsR* (273 bp upstream from the transcription initiation site), *rbmA* (195 bp upstream from the transcription initiation site) and *rbmC* (263 bp upstream from the transcription initiation site) (Fig. 2.2) were grown and diluted to an OD_{600} of 0.2 in DMEM with P1 and P2 clustering at sublethal concentrations of 0.005 mg/mL and 0.05 mg/mL during 16 hours at 37 ℃. Then clustered and planktonic cells were separated by removing the supernatant and not disturbing any precipitate formed. OD_{600} was estimated from planktonic cells as well as clustered cells by disrupting the electrostatic interactions with PBS supplemented with 200 mM NaCl. There were differences in the transcription of *vpsR*, *rbmA*, and *rbmC* depending on the bacterial lifestyle (Fig. 5.4). The regulator *vpsR-lacZ* was mostly transcribed when polymers were present, but there were no notable differences between planktonic and clustered bacteria recovered after polymer treatment. However, transcription of *rbmA-lacZ* and *rbmC-lacZ* was high during clustering, especially with P1. The *vps-lacZ* reporter had almost 1-fold increase, *rbmC-lacZ* almost 1.5-fold and *rbmA-lacZ* around 5-fold change with P1 at any concentrations. In contrast, the transcription of these genes was not significantly induced in planktonic cells in the presence of polymers.

These results suggest that induction of biofilm by clustering results in expression of biofilm structural proteins and may do so in a *vps*-dependent manner, as levels of *vpsR* are higher in both planktonic and clustered polymer-treated cells compared to untreated controls. Also, results indicate a strong tendency to the expression of biofilm structural proteins that are under the regulation of VpsR (Fig. 1.5).
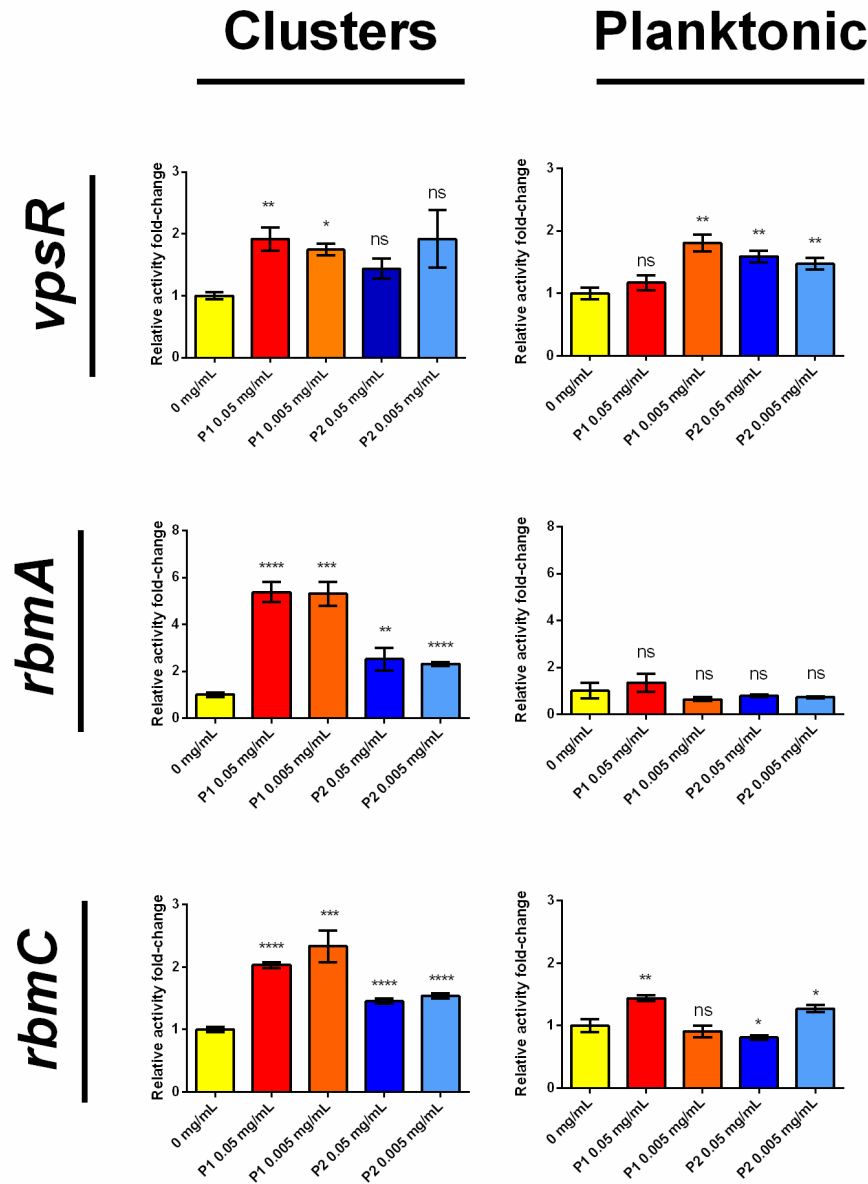
Figure 5.4. Transcription of biofilm-related genes is affected by clustering. *V. cholerae* reporter strains for *rbmA-lacZ*, *rbmC-lacZ* and *vpsR-lacZ* were clustered with P1 and P2 at sublethal concentrations of 0.005 mg/mL and 0.05 mg/mL in DMEM after a 26 hours incubation. Clustered and planktonic cells were separated from each other and clustered cells were washed with 200 mM NaCl PBS to disrupt electrostatics bonds. Activity was measured and calculated in Miller units (Section 2.10.1). Results were expressed in relative fold-changed compared to no polymer condition (0 mg/mL). Analysis of variance, followed by Tukey's post hoc test, was used to test for significance. Statistical significance was defined as $p<0.05$ (*), $p<0.01$ (**), $p< 0.001$ (***) or $p<0.0001$ (****).

5.1.4 Chitinous materials promote attachment and induce chitinases of V. cholerae

V. cholerae is commonly found attached to chitinous surfaces of crustacean exoskeletons. The adhesion is mediated by hydrophobic forces, ionic bonds and lectin-like interactions that enhance the binding specificity (Tarsi and Pruzzo, 1999). Such interactions through chitin-binding-proteins (CBP) could be exploited to develop *Vibrio*-specific polymers. Since polymers arrest bacterial cells through electrostatic interactions mediated by amine groups, chitin seems to be a good candidate to increase the specificity of polymers in the future.

Transcription of *V. cholerae* chitin utilisation genes, encoding sensor histidine kinase (*chiS)* and chitinases (*chiA1* and *chiA2)*, was followed during a longer incubation (40 h) to monitor the response to these materials. *V. cholerae* reporter strains carrying pRW50-oriT with upstream promoter regions of *chiS* (498 bp upstream from the transcription initiation site), *chiA1* (488 bp upstream from the transcription initiation site) and *chiA2* (494 bp upstream from the transcription initiation site) (Fig. 2.2) were tested. There was differential expression of the chitin utilization genes according to the material used for incubation (Fig. 5.5A). A 3-fold induction of *chiA1-lacZ* was observed with both chitin flakes and chitin beads in the first 8 hours (50 MU to 150 MU approximately) and increased to 4-fold at 40 h (about 200 MU), compared with the initial activity. *chiA2-lacZ* was strongly transcribed in the presence of chitin flakes and reached a nearly 3-fold change at 20 hours (50 MU to 150 MU). The *chiS-lacZ* reporter showed a small induction with chitin flakes and chitin beads as a 2-fold change was observed after 40 hours of incubation (50 MU to 100 MU).

Then, in order to determine if a sessile state of *V. cholerae* may have an impact on the transcription of *chiS-lacZ*, *chiA1-lacZ* and *chiA2-lacZ* during interaction with a chitinous surface, reporter strains were clustered at sub-lethal concentrations of polymers, P1 at 0.05 mg/mL and P2 at 0.5 mg/mL in 1 mL of artificial marine water with 10 mg/mL of chitin flakes and incubated for 7 hours at 30 ºC without shaking. Then, bacteria were washed with 200 mM

NaCl PBS, one set of samples were plated onto TCBS while the second set was used for β-galactosidase assays. Overall, there was no significant difference in the expression of *chi-lacZ* reporters during clustering (Fig. 5.5B)

The interaction of GFP-labelled *V. cholerae* carrying pMW-*gfp* was monitored in the presence of chitin flakes and chitin beads. Under conditions explained above, aliquots of 10 µL were mounted on microscope slides directly from the sample and visualised under the fluorescence microscope after 5 minutes and 60 minutes of incubation. Images showed that *V. cholerae* rapidly colonised the surface of this material and the attachment remained stable over the duration of the experiment. (Fig. 5.5C).

Together these results suggest that chitinous materials have the potential to be used as specific-*V. cholerae* binding groups. *V. cholerae* showed induction of genes *chiS*, *chiA1* and *chiA2* which are related to the chitin utilisation program indicating a normal physiological response. Along the same lines, induction of these genes and characterisation of the physiological response has been reported previously with *V. cholerae* in contact with chitin oligomers, and more complex chitinous materials (Meibom *et al.*, 2004). The bacterial clustering with P1 or P2 did not present a challenge for the interaction with chitin as chitin inducible genes were normally transcribed. The adhesion is quick since after 5 minutes a significant bacterial burden is observed attached to chitin flakes and chitin resin.
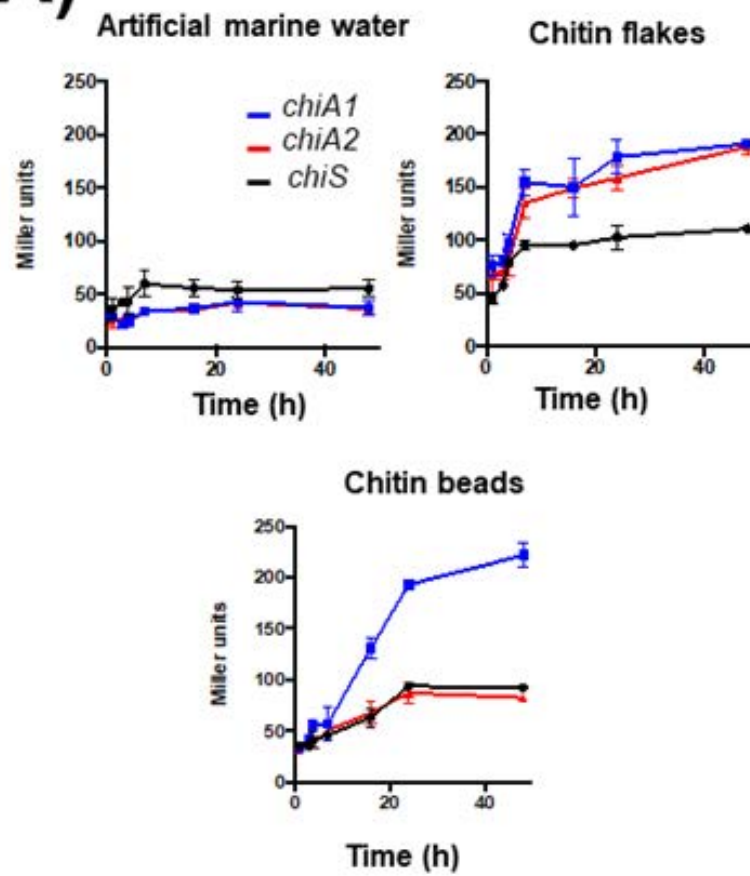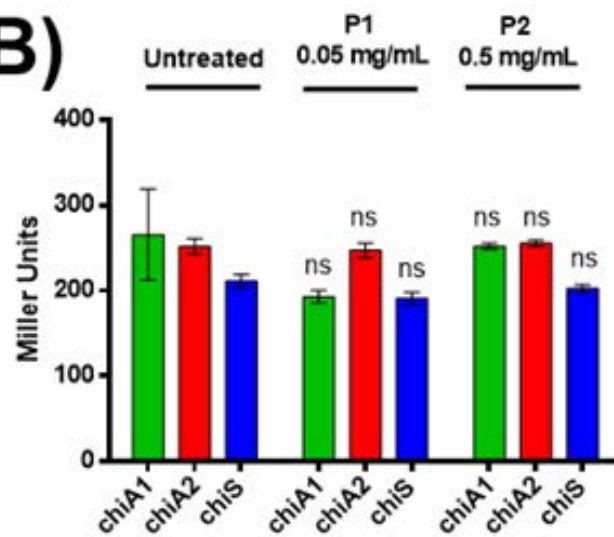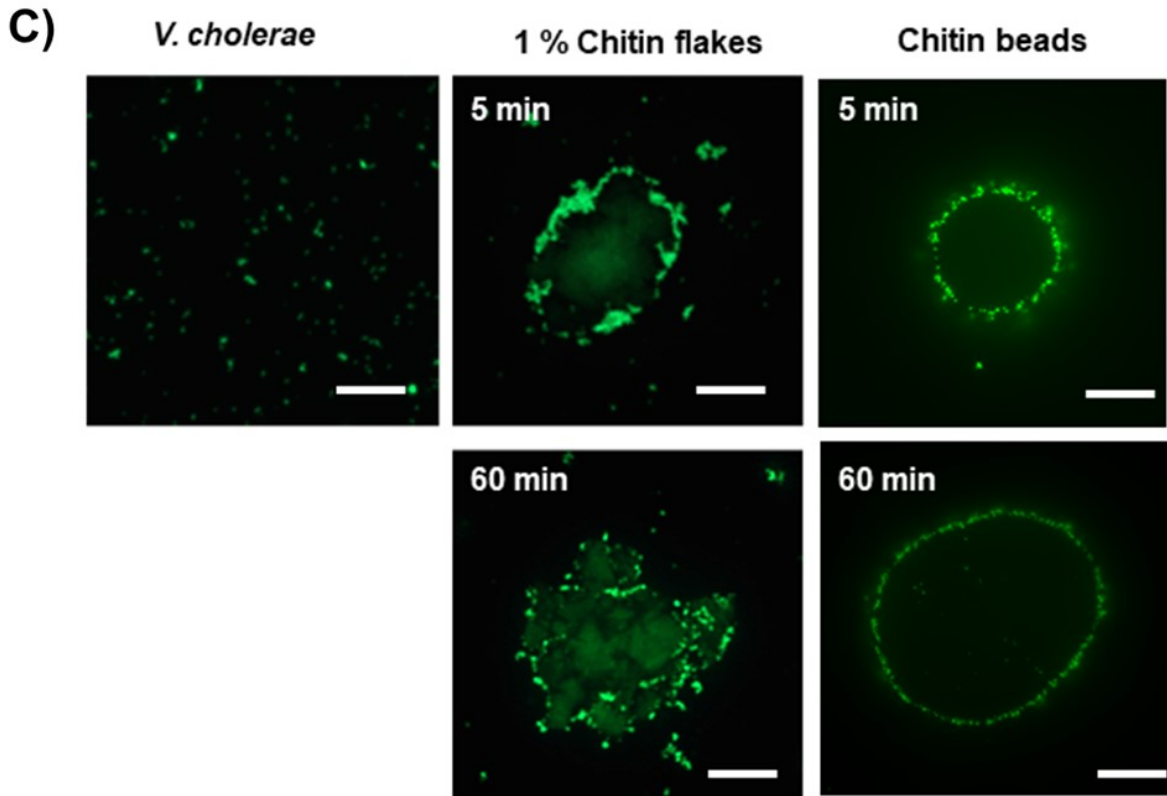
Figure 5.5. Transcription of *chiS-lacZ*, *chiA1-lacZ* and *chiA2-lacZ* in the presence of chitinous materials. A) Promoter regions of *chiS*, *chiA1* and *chiA2* were inserted into pRW50-oriT to determine transcription when reporter *V. cholerae* N16961 strains was exposed to chitinous materials over time. Black line corresponds to *chiS-lacZ*, blue line corresponds to *chiA1-lacZ*, and red line corresponds to *chiA2-lacZ*. Time points were 2, 4, 8, 15, 24 and 48 hours incubated at 30 ºC with no shaking in artificial marine water. Each point corresponds to the mean ± s.e.m. of three independent assays. B) Chitin-utilisation reporter strains were clustered with P1 and P2 at 0.05 mg/mL and 0.5 mg/mL respectively and exposed to 10 mg/mL of chitin flakes for 7 hours in artificial marine water. Activity was measured afterwards; Green *chiA1-lacZ*, red *chiA2-lacZ* and blue *chiS-lacZ*. Each point represents the mean ± s.e.m. of three independent replicates. Analysis of variance, followed by Tukey's post hoc test, was used to test for significance. C) Micrographs of the colonisation of chitin flakes (10 mg/mL) and chitin beads (10-fold diluted from saturated solution) by GFP-labelled *V. cholerae* (OD$_{600}$ 0.2). Images were taken after 5 and 60 minutes of incubation in artificial marine water at 63X magnification. Scale bar corresponds to 10 μm. Images were taken using a Zeiss Axio.Observer microscope, image acquisition on ZenPro (Zeiss) and processing in ImageJ.

5.3 Discussion

In this chapter, the induction of biofilm production upon contact with polymers was tested. Microbes tend to produce biofilm to persist against hydrodynamic forces, to increase the tolerance to toxic compounds or as a response to high cell density. Although exopolysaccharides (EPS) are an important component of biofilms, deletion of components of the EPS synthesis machinery still allows for the formation of EPS-independent biofilm with different structural features and less protective capacity (Davies *et al.*, 1998, Danese *et al.*, 2000). Here, it was observed that *V. cholerae* is organised in a biofilm-like structure during clustering with sub-lethal concentrations of polymers. Possibly, biofilm structural components are allocated alongside the polymers while these are immobilising the cell. Also, the net charge of the polymers impacts the quantity of biofilm as P1 led to higher levels of biofilm at lower concentrations compared with P2 (Fig. 5.2A).

Staining the clusters with Hoechst, extracellular DNA was appreciably surrounding the bacteria. The synthesis and role of eDNA within a biofilm is a matter of ongoing research, but some articles have explored its production, identifying both cell lysis and active secretion as potential sources. Biofilms from different species have been associated with phage-mediated lysis, elevated hydrogen peroxide species, autolysis or lysis induced by subpopulations (Okshevsky and Meyer, 2015). Likewise, when natural competence is induced, *Neisseria gonorrhoeae* actively secretes DNA in coordination with its type IV pili. Mutations in the gene encoding the pili resulted in less eDNA within a biofilm (Salgado-Pabon *et al.*, 2010). These interactions are favoured during high cell density which is a feature associated with the clustering.

The addition of external DNAse activity to biofilm has shown dispersal of the members mediated by the eDNA breakdown. For studies in *Listeria moncytogenes* biofilms, the dispersal was mediated by external addition of DNAse I in microtiter and in flow cell biofilms (Harmsen

et al., 2010). Moreover, studies done on *P. aeruginosa* biofilms reported that DNAse I treatment dispersed immature biofilm (>24 hours) (Klare *et al.*, 2016) but not when growing in flow cells, as more EPS was detectable (Whitchurch *et al.*, 2002). The enzymatic removal of the eDNA showed a significant reduction of the eDNA levels, especially when clustering with P1 (Fig. 5.3 upper panels). Although there was a high level of the eDNA signal at higher concentration of P2, the difference was not significant since individual values had a significant variation making the estimation less accurate. On the other hand, the level of bacterial cells (Fig. 5.3 bottom panels) remained similar across samples suggesting no biofilm dispersion mediated by the external addition of a nuclease. It seems that the addition of DNAse I is not enough to disperse the *V. cholerae* biofilm-induced by the clustering, suggesting that polymers might tighten the structure of the biofilm. In *V. cholerae*, it is known that the breakdown of eDNA helped by Xds and Dns nucleases is involved in dispersion (Seper *et al.*, 2011) but other enzymes may complete the process. Although the presence of eDNA in the *V. cholerae* biofilm matrix is expected, an increased amount of it might help to neutralise the effect of the cationic groups of polymers in a chelator-like manner. An eDNA chelator function has been observed in *P. aeruginosa* biofilm to capture cations that resulted to be cue to modify components of the lipopolysaccharide. Physical alteration of the outer membrane follows, which result in increased tolerance to polymyxin B and aminoglycosides (Mulcahy *et al.*, 2008).

The *vps* operon regulation is remarkably complex as the major regulators VpsR and VpsT are autoregulated, positively regulate each other's expression, and modulate the transcription of the operon by directly binding promoter motifs (Fig. 1.5), but also, indirectly through CdgA, a predicted diguanylate cyclase (Beyhan *et al.*, 2008). During biofilm formation, diguanylate cyclase activity is high, resulting in accumulation of c-di-GMP which interacts with VpsR and VpsT. However, only VpsT needs this interaction to bind with its DNA motif. Instead, VpsR function occurs by the phosphorylation of a conserved aspartate residue (Krasteva *et al.*, 2010,

Teschler *et al.*, 2015). Transcriptional activation targets structural proteins and the *vps* synthesis machinery.

The conditions where clustering was done resemble those of a marine environment, the induction of biofilm observed here seems to be through a *vps*-activation pathway. There is a differential expression between clustered and planktonic cells after 7 hours of incubation especially of the structural proteins. The presence of polymers results in high levels of *vpsR* transcription in both clustered and planktonic cells exposed to the polymers. However, genes encoding for structural proteins, especially *rbmA*, are highly transcribed only in clustered cells (Fig. 5.4 *rbmA* section). RbmA is important for the structure of the biofilm since its dual action involves the direct binding to the VPS reinforcing the matrix structure and recruitment of new cells through its proteolytic cleavage, key events during early stages of biofilm formation (Smith *et al.*, 2015). Although the enhanced expression of *vpsR* may explain the high levels of *rbmA* and *rbmC*, due to its mode of action it would be optimal to measure the expression of *vpsT* as well. By doing so, the hypothesis of activation in a vps-dependent manner could be tested more thoroughly. Unfortunately, the construction of *vpsT* (and *bap1*) *lacZ* transcriptional reporters was unsuccessful.

Chitin is a preferred substrate for adhesion during environmental growth of *V. cholerae,* mediated by specific chitin binding proteins (CBP). Chitin coordinates the induction of important cell functions in *V. cholerae* regarding the utilisation of chitin as carbon source, the natural competence or the growth in biofilm (Meibom *et al.*, 2004). The binding to chitin is established by hydrophobic, ionic and lectin-like interactions to the zooplankton surfaces (Tarsi and Pruzzo, 1999). Since chitin is an insoluble polysaccharide, its soluble form chitosan, has been used to produce polymer backbones with cationic groups with a focus on their antimicrobial properties. The structure of the polymers resulted in changes in the antimicrobial

effect, which increased with increased degree of substitution and decreased with the length of polymers (Sahariah *et al.*, 2015b).

V. cholerae exposed to chitinous materials showed differential expression of the histidine kinase ChiS, and the two extracellular chitinases ChiA1 and ChiA2 when followed over 48 hours. Using chitin beads the induction of *chiA1-lacZ* was predominant compared with *chiA2-lacZ* and *chiS-lacZ*. Unfortunately, neither the composition nor the concentration of the chitin beads is available as it is a secret of trade (NEB), but this difference presumably is related to the complexity of the chitin residues exposed by both materials (Fig. 5.5A). The clustering with P1 and P2 did not result in significant changes regarding the chitinases or the regulator transcription (Fig. 5.5B).

According to Meibom et al. (Meibom *et al.*, 2005), *chiA1* and *chiA2* are inducible by the activation of ChiS located in the inner membrane. ChiS is encoded in a 10-gene cluster together with the cognate periplasmic chitin binding protein (CBP) which senses GlcNAc dimers. The expression of *chiS* requires CBP but not the transport of the $(GlcNAc)_2$ (Li and Roseman, 2004). Under this scheme it seems that the activation of the chitin-inducible genes is independent of the clustering as bacteria can still sense and presumably use chitin as source of nutrients as planktonic cells. Possibly, clustering may not affect important metabolic functions as growth and biofilm formation are not impeded. The quick binding and the innocuous effect of the clustering on the transcription of these genes may suggest that despite the immobilisation bacteria can establish interactions with chitinous surfaces.

The interaction between *V. cholerae* and chitin has been widely investigated (Keyhani and Roseman, 1999, Meibom *et al.*, 2005, Tarsi and Pruzzo, 1999). Along the same lines, these investigations have served to shed light on other *Vibrio* species that develop similar interactions as well. Attachment of the important human pathogen *V. parahaemolyticus* to diatom derived

chitin is mediated by the type IV pili MSHA and PilA (GbpA) similarly as *V. cholerae* (Frischkorn *et al.*, 2013). The opportunistic human pathogen *Vibrio vulnificus* is also associated to chitin through similar structures *as V. parahaemolyticus* and *V. cholerae* (Williams *et al.*, 2014). Similarly, the non-pathogenic *V. harveyi* use extracellular chitinases to degrade the chitinous surfaces where is attached (Svitil *et al.*, 1997). Considering the dynamic interactions that *Vibrio* species establish with chitinous surfaces, chitin not only seems to be a good candidate to enhance the specificity of polymers for *V. cholerae* clustering, but for other *Vibrio* species with relevance in human health. Polymers with chitosan-derived backbones and with no antimicrobial activities seem not to be used as carbon source by pathogens when in contact (Sahariah *et al.*, 2015b). However, it is unclear if in the case of *V. cholerae*, chitinous residues attached to the polymer may activate metabolic processes to facilitate degradation or serve as a carbon source for bacterial growth and this should be subject to further studies.

Chapter 6: Clustering *Vibrio cholerae* induces a quorum sensing controlled phenotype.

6.1 Background

Bacterial cell to cell communication, termed quorum sensing, allows microorganisms to express collective-type behaviours. By releasing small amounts of signalling molecules called autoinducers, cells can analyse the external environment and sense how many of their kind and other kinds of bacteria are around. However, from an evolutionary point of view communication is a drawback as organisms displaying cooperative behaviours can be exploited (Diggle *et al.*, 2007). This dilemma has also raised questions about the nature of this communication mechanism and debate exists around whether secretion of the signalling molecules reflects diffusion of a metabolite without a real communication purpose (West *et al.*, 2012). When talking about quorum sensing, the terminology is fundamental as the empiric definition of signal implies that one organism is trying to share information with another organism through a "signal", in this case, a molecule. Diggle *et al.* (Diggle *et al.*, 2007) postulate that to be a signal, the production of autoinducer should evolve to elicit a response in another organism and not a molecules that elicit a response in the organism that sense it, such as a waste product.

6.1.1 Quorum system circuits overview

Microorganisms, both bacteria and fungi, have evolved different communication systems using several types of signalling molecules. Usually, quorum sensing systems in Gram-positive bacteria use short peptides and amino acids for communication, while Gram-negatives use fatty acid derivatives (Whitehead *et al.*, 2001). These autoinducer molecules are small and can be exported or diffuse freely to accumulate outside the bacteria. Once their concentration is high enough, the quorum sensing threshold is reached, and different cellular

functions are activated while some are repressed according to the cell density phenotype associated.

In most Gram-positives, quorum sensing pathways are mediated by peptidic autoinducers that are synthesized in the cytoplasm as propeptides, becoming biologically active after post-translational processing. This modification can occur either before being secreted or in the extracellular environment. The extracellular peptide is sensed by histidine kinases located at the inner membrane or re-enters the cytoplasm through specialised membrane transporters to reach internal receptors activating the QS regulon (Rutherford and Bassler, 2012). An example of this is the Gram-positive *Bacillus cereus*, where this import is mediated by the oligopeptide permease Opp (Slamti and Lereclus, 2002).

In Gram-negatives, autoinducers are synthesised and diffuse freely through the inner and outer membranes. Then, the autoinducer can diffuse back again to reach cytoplasmic receptors, as in the case of N-acyl homoserine lactone (AHL) or can be sensed by inner membrane histidine kinases that will activate regulators of the quorum sensing regulon as in the case of autoinducer-2 (AI-2; (2S,4S)-2-methyl-2,3,3,4-tetrahydroxytetrahydrofuran-borate or S-THMF-borate) (Rutherford and Bassler, 2012). In *Vibrio* species, the Lux and Cqs pathways have been extensively studied through the bioluminescence response of *Vibrio harveyi* and *Vibrio fischeri* (Lui *et al.*, 2013, Xue *et al.*, 2011). In *V. cholerae* at least four quorum sensing cascades responding to different autoinducers are working in parallel but merge at the LuxU kinase. Traditionally, Lux and Cqs have been described extensively due to the homology with the *V. harveyi* pathways. Together with CqsS and LuxPQ, are CqsR and VpsS histidine kinases that also converge in LuxU (Jung *et al.*, 2015).

6.1.2 Quorum sensing phenotype through the lux operon.

The *lux* operon is a collection of five genes *luxCDABE*, where *luxAB* encode for a luciferase while *luxCDE* encode a fatty acid reductase complex. The reaction of light production occurs with the oxidation of long fatty aldehyde chain and reduction of flavin mononucleotide by the luciferase. Fatty acids are taken from the fatty acid synthesis by LuxD, then the acyl group is activated with AMP by LuxC, and finally, reduced to an aldehyde chain by LuxE (Miyashiro and Ruby, 2012). In *V. fischeri*, another three genes are relevant in the Lux operon which are the *luxG* that encodes a FMN reductase (Nijvipakul *et al.*, 2008), and the pair *luxR-luxI* that encodes the operon regulatory proteins; *luxI* encodes the autoinducer synthetase and *luxR* encodes an autoinducer-dependent transcription factor, and is homologous to HapR in *V. cholerae* (Miyashiro and Ruby, 2012) (Fig. 6.1). HapR actively regulates the *lux* operon during high cell density, which will maintain the bioluminescence until the density is decreased. The entire *lux* operon or enzymes are used as reporters. The pBB1 plasmid developed by B. Bassler (Bassler *et al.*, 1993), contains the *V. harveyi luxCDABE* luciferase operon and tetracycline resistance and is used to trace the different stimuli experienced by the bacterial population and as a read-out of quorum activation through the emission of visible blue light of 490 nm.
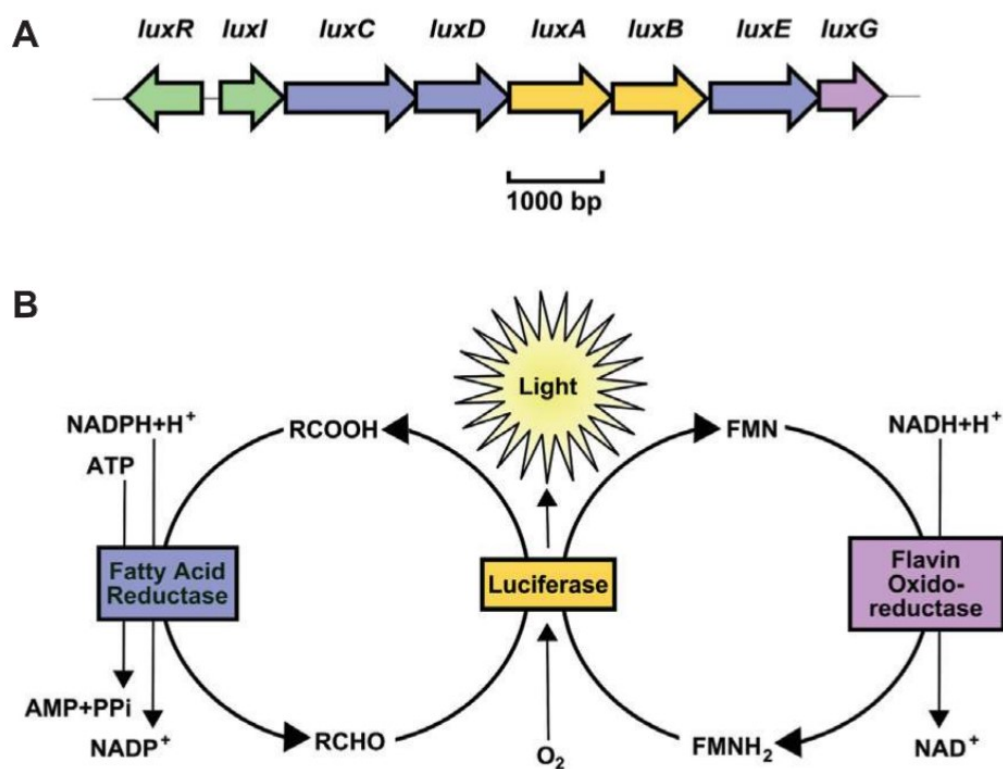
Figure 6.1. *V. fischeri lux* operon and light production mechanism. A) *V. fischeri lux* locus consisting in the *lux* operon (*luxCDABE*), *luxG* and regulatory proteins *luxR* and *luxI*. B) Mechanism of light production by the *lux* operon enzymes. The luciferase emits blue light at 490 nm by oxidising long-chain aldehydes and reducing flavin mononucleotide ($FMNH_2$) (Miyashiro and Ruby, 2012).

6.1.3 Conditions that stimulate quorum sensing dependent phenotypes.

Quorum activation is associated with high cell density as autoinducers are accumulated in the extracellular environment. During stationary phase, where the growth has reached its maximum, the quorum sensing threshold is also surpassed by the accumulation of autoinducers. Simultaneously, bacteria that enter into stationary phase undergoes stress-related processes, especially the lack of nutrients. Starvation activates stress-related repair systems such as the RNA polymerase sigma S factor RpoS (Schellhorn and Stones, 1992) that results in modulation of quorum sensing. Starvation signals are important for quorum sensing activation since integration of the pathways results in an adjustment of the quorum sensing threshold, reaching the quorum with fewer cells (Lazazzera, 2000).

Quorum activation can also be modified by changing the local concentration of autoinducer, either by external addition of autoinducer to a low-density population or by reducing the volume of the bacterial population while maintaining bacterial numbers. *V. cholerae* has been controlled by addition of external S-3-hydroxytridecan-4-one (CAI-1) encapsulated into nanoparticles; the release of the autoinducer resulted in inhibition of biofilm and activation of a *lux* operon reporter (Lu *et al.*, 2015). Induction of quorum sensing in *P. aeruginosa* has been achieved by microencapsulating a single cell in a small volume of media, where autoinducer accumulates quickly (Boedicker *et al.*, 2009).

In this chapter, the quorum sensing was dissected to determine if the clustering results in the activation of the quorum sensing route. For this, mutant strains that fail to produce or sense autoinducers were clustered and luminescence was followed as a read out of quorum sensing.

6.2 Results.

6.2.1 Clustering of V. cholerae by polymers initiates transcription of the lux operon in response to quorum sensing.

Cationic groups attached to linear polymers and dendrimers, have been shown to activate and enhance bioluminescence in *V. harveyi* (Lui *et al.*, 2013, Leire *et al.*, 2016, Xue *et al.*, 2011). Here, cationic polymers were used to determine if clustering resulted in the induction of bioluminescence in *V. cholerae* strain bearing the pBB1 vector as quorum sensing reporter. Initially, OD_{600} of the strain was measured to determine if artificial marine water could serve as a source of nutrients, to determine if changes in bioluminescence could be due to changes in bacterial biomass and/or growth. Compared with DMEM, there was no growth in artificial marine water over 20 hours of incubation at 37 ℃ (Fig. 6.2A). As the induction of luminescence is a quorum sensing dependent phenotype, the luminescence was measured during clustering, starting at different OD_{600}. Polymers at concentration ranging from 0.005 mg/mL to 0.5 mg/mL were added to dilutions of an overnight culture at OD_{600} of 0.5, 0.2 and 0.02 reflecting cells in lag, early and mid-log phase, respectively. The plate was incubated for 20 h at 37 ℃, and luminescence was recorded every 30 minutes. Luminescence induction by polymers presented as a sharp peak during the early hours of incubation which was more pronounced at 0.5 mg/mL of polymers, while lower concentrations did cause a significant increase in luminescence. These peaks in luminescence shifted accordingly as cultures were more diluted: at an OD_{600} of 0.5 the peak appears approximately after an hour of incubation, at an OD_{600} of 0.2 the peak appears at around 4 hours, while at OD_{600} of 0.02 the peak was delayed until 6 hours (Fig. 6.2 B-C). After the peak, bacteria progressively lost luminescence, eventually reaching undetectable levels after 8 hours in the case of high luminescence induction or 6 hours when the induction was low.

The clustering and luminescence enhancement were visualised by clustering *V. cholerae* N16961 bearing pBB1 vector at an OD_{600} of 0.2 and polymers were added to concentrations of 0.005 mg/mL, 0.05 mg/mL and 0.5 mg/mL in 200 µL of artificial marine water. Luminescence was recorded every 30 minutes for 15 hours where each still image was taken with 10 seconds exposure time. Clusters increased the luminescence simultaneously with high intensity at higher concentration of polymer. A pixel intensity analysis from the luminescence on individual clusters showed a correlation with the plate reader assay, where luminescence peaked at nearly 5 hours, and clusters enhanced their luminescence simultaneously (Fig. 6.2H and 21J). The same experiment was done in DMEM as media, which resulted in almost undetectable levels of luminescence as observed from the pictures (Fig. 6.2I). The brightfield images showed no evident increase in the cell density, suggesting that luminescence is not result of more cells per field. Moreover, clusters can be observed (Appendix 1).

These results suggest that polymers induce a quorum sensing controlled phenotype in *V. cholerae* N16961 since luminescence from the *lux* operon reporter is enhanced 100-fold (10^2 RLU to 10^4 RLU) when comparing 0.5 mg/mL of P1 or P2 with the untreated conditions with bacteria at OD_{600} of 0.2. This luminescence induction was not as a result of increased total cell number as no growth was observed in artificial marine. Although artificial marine water is scarce from nutrients, it is rich in salts compared with minimal media DMEM. The production of AI-2 is tied to boron which is absent in DMEM.

H) Artificial marine water

P1

0 mg/mL   0.005 mg/mL   0.05 mg/mL   0.5 mg/mL

P2

0 mg/mL   0.005 mg/mL   0.05 mg/mL   0.5 mg/mL

I) DMEM

P1

0 mg/mL   0.005 mg/mL   0.05 mg/mL   0.5 mg/mL

P2

0 mg/mL   0.005 mg/mL   0.05 mg/mL   0.5 mg/mL

144
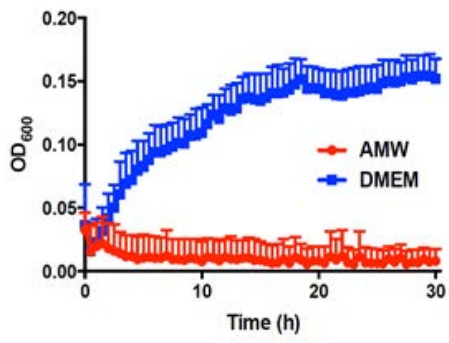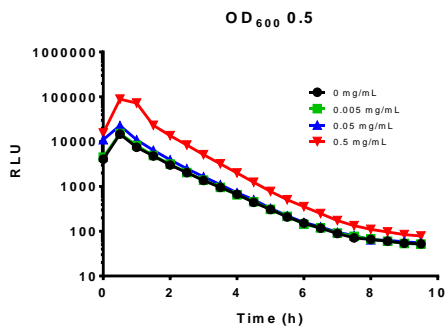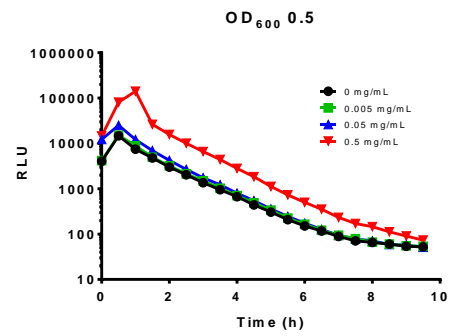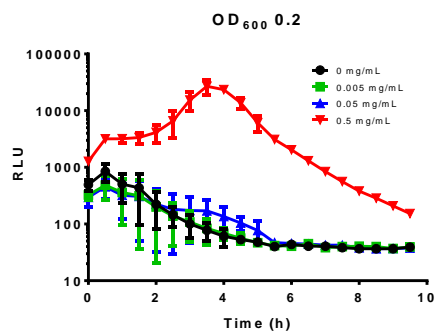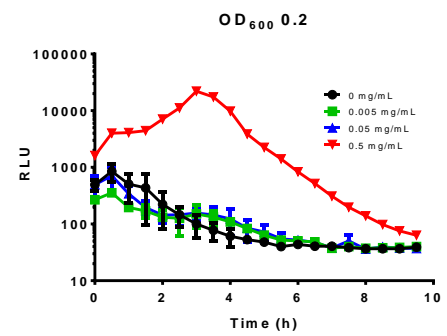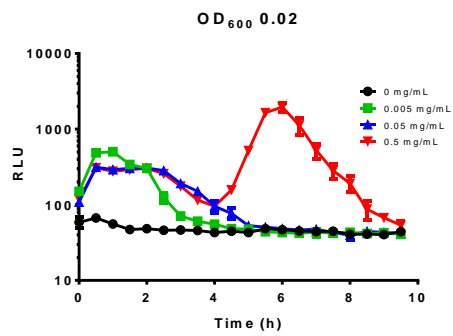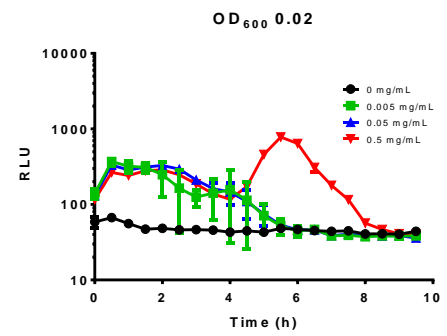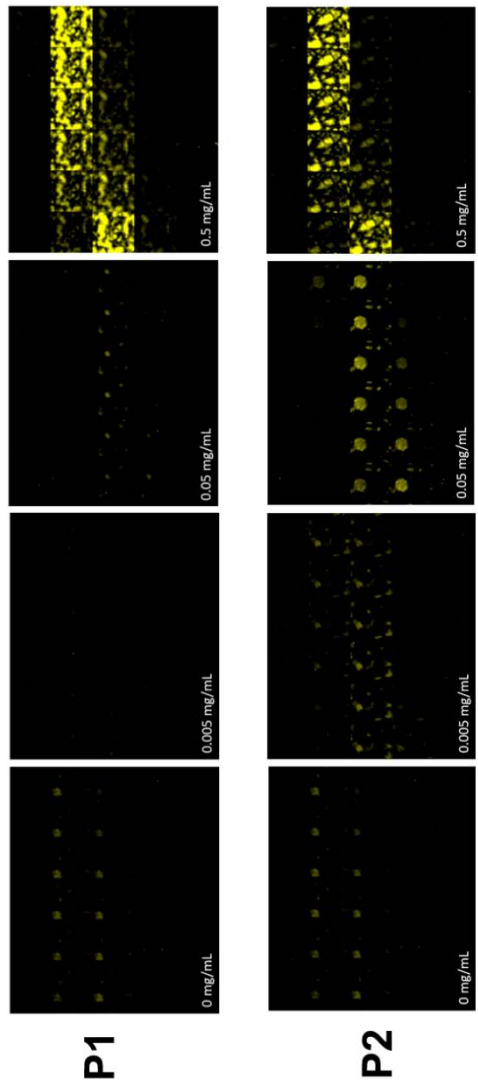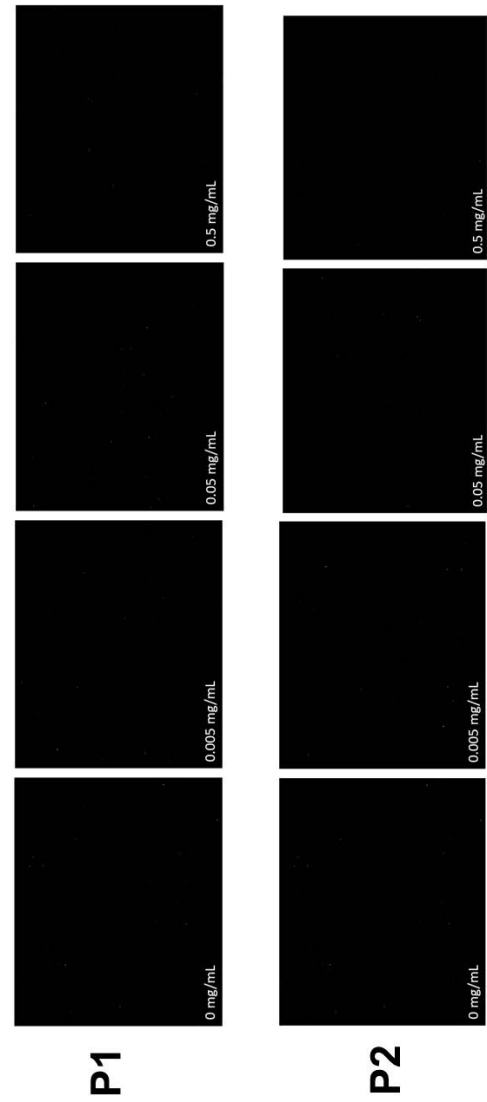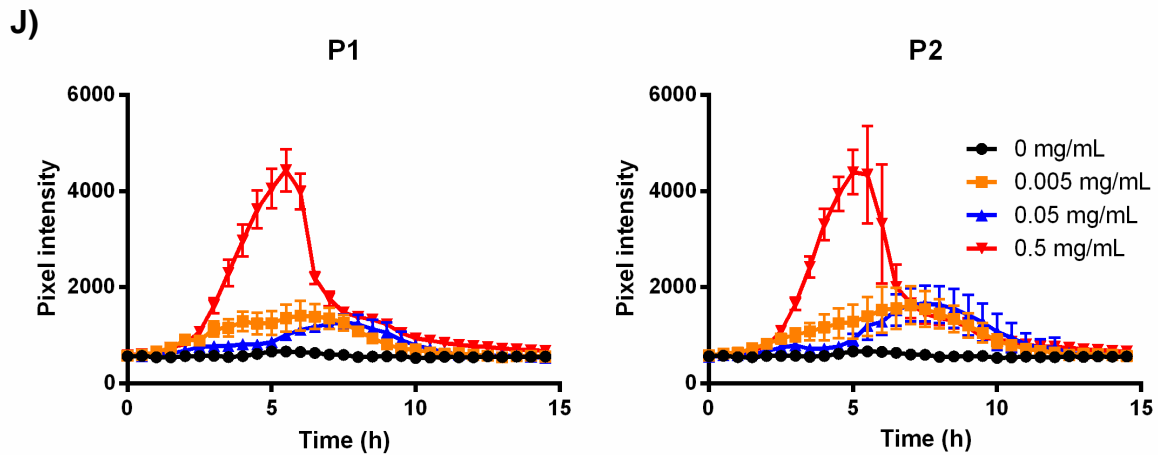
Figure 6.2. Luminescence assay of *V. cholerae* N16961 pBB1 in artificial marine water clustered with P1 or P2. A) Cultures were diluted to an OD_{600} of 0.02 in 200 uL and incubated for 30 hours at 37 ℃ with shaking. Optical density was measured every 30 minutes. Minimal media DMEM stimulates a mild increase in cell density (blue) while no growth was observed in artificial marine water (red). Each point is the means ± s.e.m. of three biological replicates. B-C) 16 hours cultures diluted to an OD_{600} of 0.5 with P1 and P2 at concentrations from 0.005 mg/mL to 0.5 mg/mL, D-E) 16 hours cultures diluted to an OD_{600} of 0.2 with P1 and P2 at concentrations from 0.005 mg/mL to 0.5 mg/mL, F-G) 16 hours cultures diluted to an OD_{600} of 0.02 with P1 and P2 at concentrations from 0.005 mg/mL to 0.5 mg/mL in 200 μL final volume in a 96-well plate. Luminescence was followed every 30 minutes incubating the plate at 37 ℃. Time-lapse of the luminescence assay in artificial marine water (H) and DMEM (I) with polymers at concentrations from 0.005 mg/mL to 0.5 mg/mL, with bacteria diluted to an OD_{600} of 0.2, pictures were taken with a Nikon-Eclipse TE2000-U microscope using an EMCCD camera Evolve 512 at 40X magnification. Each frame corresponds to 10 seconds time of exposure. J) Pixel intensity of single clusters from the time-lapse. Intensity was measured from individual clusters on each frame with ImageJ. Each point corresponds to the mean ± s.e.m. of three individual clusters that were followed throughout the images.

6.2.2 Polymers and amino acids activate bioluminescence in a similar manner.

The induction of luminescence was enhanced when polymers clustered *V. cholerae* in nutrient-poor media. The nutrient limitation enhances the activity of adenylate cyclases leading to the accumulation of cyclic AMP, which in turn is reflected in the activation of the cAMP receptor proteins (CRP) (Lazazzera, 2000). CRP and the quorum sensing route merge during starvation leading to control of the activation of LuxO via modulation of autoinducers synthesis (Liang *et al.*, 2007).

In order to determine if the micro-environment within the cluster resembles a low-nutrient condition that leads CRP to modulate the luminescence, a Δ*crp* background was tested. Since genetic engineering is methods are restricted when using N16961, the El Tor strain E7946 has been modified deleting *crp* open reading frame usign MuGENT method (gift from D. Grainger). The mutant carrying pBB1 at an OD$_{600}$ of 0.2 was clustered with P1 and P2 at concentrations of 0.005 mg/mL, 0.05 mg/mL and 0.5 mg/mL and luminescence was recorded in 200 µL of artificial marine water. No induction of luminescence was observed from E7946 Δ*crp* at any of the tested concentrations with any of the polymers, which is opposite to the effect over the isogenic wildtype strain (E7946) (Fig. 6.3 A-D).

Next, in order to determine if the clustering affects the diffusion of nutrients impacting the activation of quorum sensing, luminescence was measured from clustered bacteria. *V. cholerae* N16961 carrying pBB1 was diluted to an OD$_{600}$ of 0.2 and incubated with P1 and P2 at 0.5 mg/mL respectively in 200 µL of artificial marine water supplemented with 1 % glucose, 1 % peptone or a combination of both. The presence of nutrients resulted in induction of luminescence at higher levels. Of note was that clustering in the presence of peptone resulted in a very significant enhancement of the luminescence compared with the other conditions (Fig. 6.3E-H).

These results indicate that bioluminescence induction is not driven by the limitation of nutrients since the addition of glucose and peptone resulted in even higher luminescence during clustering. At the same time, a Δ*crp* background failed to induce luminescence during clustering which highlights the importance of CRP in modulating the quorum sensing regulon. Also, the induction of luminescence was significant especially in the presence of peptone as the luminescence reached similar levels as without polymers suggesting that amino acids and polymer may share quorum sensing-inducing properties.
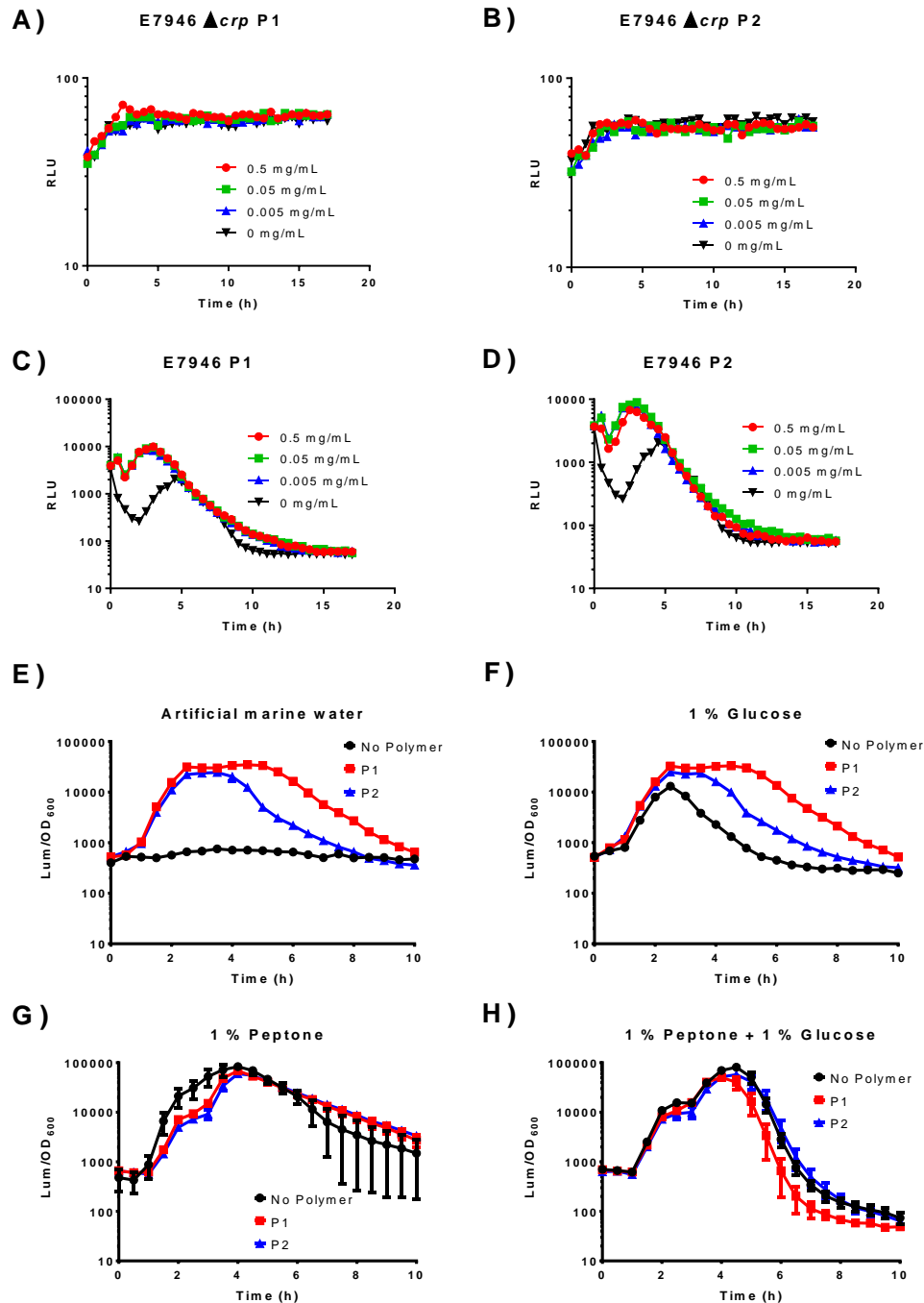
Figure 6.3. Influence of CRP and nutrients on the induction of luminescence in *V. cholerae* E7946 and N16961 pBB1. A-B) *V. cholerae* E7646 Δ*crp* at OD_{600} of 0.2 and polymers added at concentrations ranging from 0.005 to 0.5 mg/mL. C-D) *V. cholerae* E7946 at OD_{600} of 0.2 and polymers added at concentrations ranging from 0.005 to 0.5 mg/mL. During clustering, the availability of nutrients enhanced the luminescence in a clustering-independent manner. *V. cholerae* N16961 in E) artificial marine water, F) artificial marine water supplemented with 1 % glucose, G) artificial marine water supplemented with 1 % peptone and H) artificial marine water with a combination of 1 % glucose and 1 % peptone. The luminescence was recorded every 30 minutes and OD_{600} in the case of E-H. Each point is the mean ± s.e.m. of three independent replicates.

6.2.3 Polymer clustering enhances the production of quorum sensing autoinducers

Previous experiments showed that the clustering increased luminescence as a result of quorum sensing activation in *V. cholerae*. The activation of quorum sensing has a positive feedback in *V. fischeri* as the synthesis of autoinducers is enhanced (Engebrecht *et al.*, 1983). In order to determine if enhancement of autoinducer production is mediated by clustering, a set of strains with mutations in the quorum sensing pathway enzymes were tested. The contribution of autoinducers after clustering was detected using BH1578 ($\Delta luxS\Delta cqsA$) which lacks both autoinducer synthetases LuxS and CqsA, meaning that it can only sense the autoinducers produced by other species (Ng *et al.*, 2012). *V. cholerae* wildtype at an OD_{600} of 0.2 was clustered with P1 or P2 at concentrations from 0.005 mg/mL to 0.5 mg/mL in 1 mL of artificial marine water for 16 hours at 30 ºC. After that, the filtered supernatant was transferred to BH1578 previously adjusted to OD_{600} of 0.2 and the luminescence was recorded. Similar to the behaviour of wildtype bacteria, luminescence was induced at higher concentrations of polymers about 3-fold (50 RLU to 150 RLU) compared with the untreated condition for both polymers (Fig. 6.4A-B). To compare the involvement of either CAI-1 or AI-2 pathways in the induction of luminescence, BH1578 was incubated with supernatant from quorum sensing mutant WN1103 $\Delta luxQ\Delta cqsA$ which is defective in producing CAI-1, and DH231 $\Delta luxS\Delta cqsS$ which is defective in producing AI-2. Strains were incubated in LB media at a starting OD_{600} of 0.2, and then the filtered media was transferred to BH1578 at an OD_{600} of 0.2 as well. The induction of luminescence was stronger than the previous assay, by almost 100-fold (Fig. 6.4C-F). However, the induction of quorum sensing is dominated by CAI-1 as reported before (Rutherford and Bassler, 2012).

In order to determine if during the clustering the production of autoinducers is enhanced, quorum sensing mutants WN1103 and DH231 carrying pBB1 plasmid were co-incubated with wildtype N16961 in a ratio 1:1 to have an OD_{600} of 0.2 and were clustered with P1 at

concentrations from 0.005 mg/mL to 0.5 mg/mL in artificial marine water. The induction of luminescence was higher in response to CAI-1 (being sensed by DH231) by about 100-fold (10^1 RLU to 10^3 RLU) in line with previous assays (Fig. 6.4G-H).

Together these results suggest that the clustering induced the positive feedback of the quorum sensing circuit as autoinducer synthetases produced more autoinducer when bacteria were clustered with P1 and P2. Also, the contribution of CAI-1 and AI-2 was determined by using quorum sensing mutants WN1103 and DH231 and demonstrated that the induction of quorum sensing by clustering followed a similar pattern as in nature, where CAI-1 dominates the activation compared with AI-2 by about 10^2-fold.
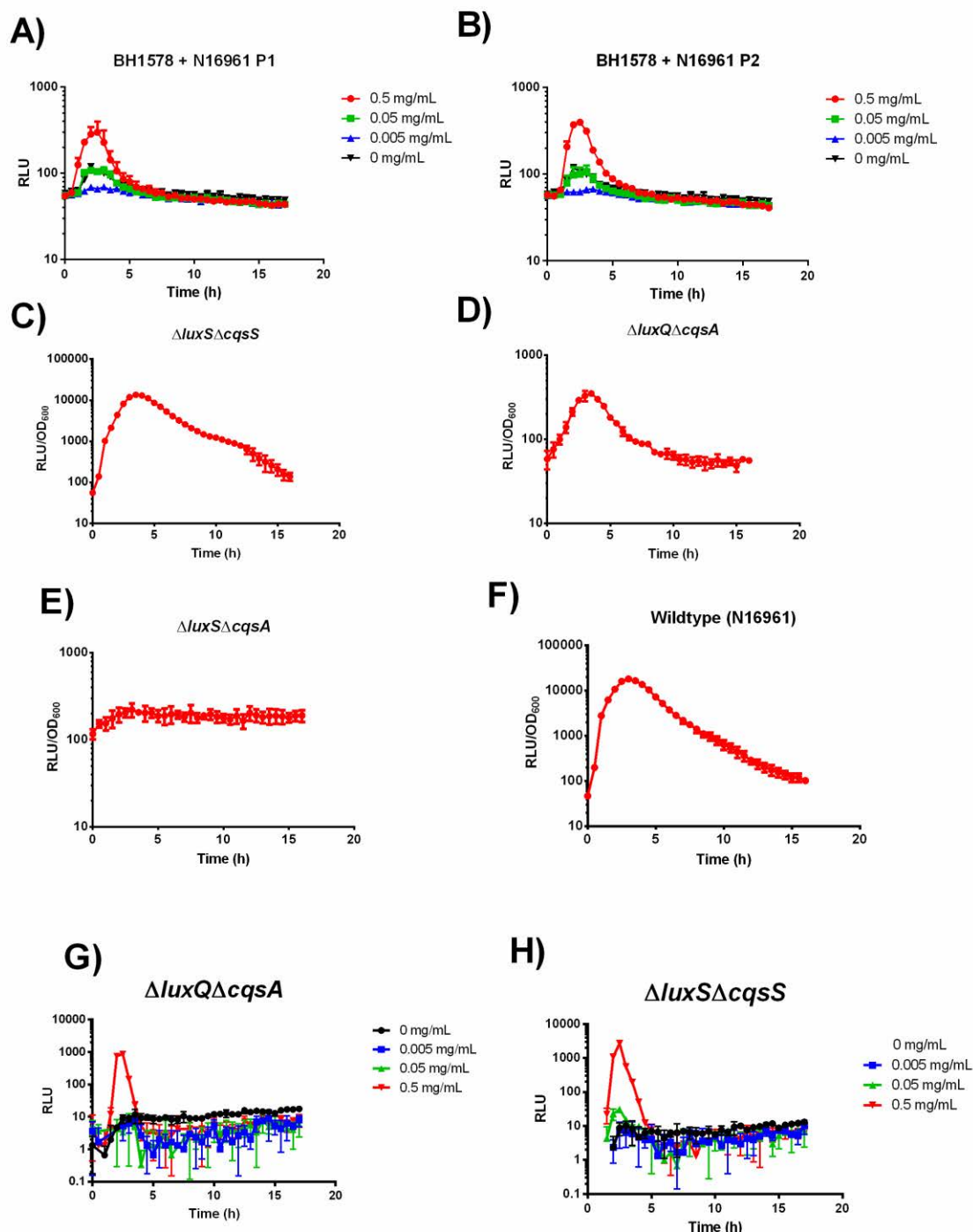
Figure 6.4. Polymer clustering enhances the synthesis of autoinducers. *V. cholerae* BH1578 (Δ*luxS*Δ*cqsA*) was exposed to supernatant from *V. cholerae* N16961 clustered 16-hours with different concentrations of A) P1 and B) P2 in artificial marine water. The two-main route of quorum sensing was tested by exposing supernatant from C) DH231 (Δ*luxS*Δ*cqsS*), D) WN1103 (Δ*luxQ*Δ*cqsA*), E) BH1578 and F) wildtype N16961 incubated in LB against BH1578. Co-cultures of *V. cholerae* N16961 with quorum sensing mutant under clustering with P1 were followed to determine the contribution of each route during activation of luminescence in artificial marine water. G) N16961+ WN1103 and H) N16961 + DH231. Luminescence was recorded every 30 minutes incubating at 37 °C with shaking at 200 rpm on the plate reader for 16-18 hours. C to F Luminescence and OD_{600} were recorded.

6.3 Discussion

This chapter investigated a quorum-dependent effect of bacterial clustering which is the induction of bioluminescence as a result of the expression of the *luxCDABE* operon. This type of quorum sensing phenotype has been described before in the naturally luminescent *V. harveyi* during clustering (Lui *et al.*, 2013). Considering that the components of the quorum sensing pathway are highly conserved in *Vibrio* species, the *lux* operon was expressed from the pBB1 cosmid in *V. cholerae* to follow induction of luminescence as quorum sensing response during clustering. The activation of luminescence likely occurs through a similar mechanism between *Vibrio* species. However, how the clustering induces the quorum sensing phenotype is not entirely understood.

The cluster-induced luminescence effect occurred predominantly when bacteria were incubated in artificial marine water that mimics the concentration of salts dissolved in marine environments, lacking any nutrients. In fact, *V. cholerae* was unable to proliferate in this media (Fig. 6.2A) which simplified the interpretation of luminescence data. The incubation with P1 or P2 resulted in an enhanced luminescence, clearly at 0.5 mg/mL at the first 4-5 hours of incubation when using a bacterial density of 0.2 (Fig. 6.2 D-E, Fig. 6.2H and 6.2J, Fig. 6.3C-H, Fig. 6.3G-H). After that, the luminescence decayed to undetectable levels. This strong induction of quorum sensing suggests that the clustering creates a micro-environment where the concentration of quorum sensing molecules is high enough to induce related phenotype. Since quorum sensing is dominated by cell density, the dilution of the bacterial density delayed the luminescence peak during clustering, which suggests that before induction of quorum sensing, polymers need to capture bacteria in order to trigger the related phenotype (Fig. 6.2B-G). Interestingly, the diluted culture also had reduced intensity of the luminesce peak that may be related to the fact that fewer bacteria resulted in smaller clusters where quorum sensing

molecules can more readily diffuse. However, opposite to the effect in artificial marine water, in minimal media DMEM the effect was abolished, and no luminescence was appreciable (Fig. 6.2I). The poor/non-boron content of DMEM maybe impacts the production of AI-2 since DPD and $B(OH)_3$ are essential during its synthesis (Lui *et al.*, 2013). Artificial marine water boron content is 5.6 mg/mL whereas DMEM does not contain boron (Sigma).

The induction of luminescence was also observed through a time-lapse experiment, where the luminescence of clusters was activated simultaneously and at nearly 4 hours which was also measured by the pixel intensity of individual clusters, replicating the plate reader experiments. Since luminescence was induced during clustering in artificial marine water but not in DMEM, starvation seems to be a cue for the luminescence burst. Limited diffusion of nutrients stimulates cAMP-CRP (cAMP receptor protein) which is capable of modulating the *lux* operon in *V. fischeri* (Friedrich and Greenberg, 1983). Here, the presence of CRP in strains during incubation and clustering in artificial marine water was important to activate the luminescence. In addition, by supplementing artificial marine water with external nutrients glucose and peptone, the luminescence was enhanced 10-fold with glucose (10^3 RLU to 10^4 RLU) without polymers and almost 100-fold (10^3 RLU to 10^5 RLU) with peptone. This induction challenges the idea that within clusters the diffusion of nutrients is limited.

In order to determine if the quorum sensing phenotype observed resulted in increased synthesis of autoinducers, the strain BH1578 which lacks both autoinducer synthetases LuxS and CqsA and can only sense external autoinducers was used. The clustering with P1 and P2 showed an increase of about 10-fold at higher concentration of polymers. This positive feedback in the quorum sensing circuit that controls autoinducer production has been observed in *V. fischeri* where high cell density modulates the expression of *luxI*, which is responsible for the synthesis of autoinducer homoserine lactone (HSL), (Engebrecht *et al.*, 1983).

At least four cascades have been identified in the *V. cholerae* quorum sensing pathway converging in LuxU (Jung *et al.*, 2015), where the two most studied are CAI-1 and AI-2. Considering that the activation of quorum sensing has an impact on the production of autoinducers, the contribution of CAI-1 and AI-2 was determined during clustering. The contribution of CAI-1 to the induction of quorum sensing phenotype was considerably higher than AI-2 (Fig. 6.4C-D, 6.4G-H) which is in agreement with previous reports (Rutherford and Bassler, 2012, Ng and Bassler, 2009). CAI-1 is responsible for the *Vibrio*-specific communication which might be favoured since the system is mono-species.

These experiments shed light on the induction of quorum sensing as result of the clustering, but open questions remain regarding the mechanism by which polymers enhance this phenotype. Specifically, if the binding with the bacterial cell wall and the perturbation of the outer membrane can contribute to this quorum sensing-controlled phenotype. Immediately, a hypothesis appears suggesting that the interaction with cationic polymers increases the permeability of the outer membrane due to mild permeabilisation induced by P1 and P2. This idea is supported by the fact that these polymers do not compromise the bacterial viability as shown in Chapter 4. Additionally, these results are in agreement with work done with similar materials that expose similar cationic groups (primary amine), as materials with higher toxicity also increase the luminescence in *V. harveyi* (Leire *et al.*, 2016).

Another interesting observation was the effect of nutrients on the induction of luminescence without polymers. In this sense, peptone which is rich in amino acids elevates the luminescence to similar levels as during clustering suggesting a shared feature between both molecules (Fig. 6.3E-H). Cationic polymers share features with naturally occurring small cationic peptides that can induce different phenotypes such as polyamines. Polyamines are small cationic peptides commonly found in nature that help the innate immune system to control pathogens (Shah and Swiatlo, 2008). These molecules coat the pathogen's surface by electrostatic binding with the

membrane in a similar fashion as polymers. This binding results in different responses regarding quorum sensing phenotypes, including the inhibition of *tcpA* expression or biofilm enhancement or inhibition (Goforth *et al.*, 2013, Sobe *et al.*, 2017).

Chapter 7: Polymer sequestration abolishes *Vibrio cholerae* virulence at the transcriptional level and infection *in vitro* and *in vivo*

Part of the results of this chapter has been published as part of a paper (Perez-Soto et al.,

2017).

7.1 Background

V. cholerae is an important human pathogen that causes watery diarrhoea, the characteristic symptom of the cholera disease. In nature, the bacteria are commonly associated with chitinous surfaces forming a biofilm or are found as planktonic cells. The ingestion of biofilm leads to bacterial dispersion prior to rapid colonisation and infection since virulent phenotypes are associated with a sessile lifestyle. However, the control of virulence is a complex network of positive and negative regulators that not only impact on virulence but many other cellular functions such as biofilm formation, quorum sensing or stress (Fong *et al.*, 2010, Acosta *et al.*, 2015). Within the regulation of virulence, the ToxR regulon is highlighted below as it controls most of the virulence factors of *V. cholerae*.

7.1.1 Activation of virulence through ToxR regulon in V. cholerae.

In *V. cholerae*, virulence-related genes are under the control of ToxT, which in turn is controlled by ToxR and TcpP in a cascade mode (DiRita *et al.*, 1991, Häse and Mekalanos, 1998). The interaction of ToxR with the promoter is not sufficient to trigger *toxT* transcription, and this only happens when TcpP is recruited and promotes a tight interaction with the promoter (Krukonis *et al.*, 2000). Further accessory proteins are needed to stabilise the ToxR/TcpP complex at the promoter and to recruit the RNA polymerase. ToxR is accompanied by ToxS, an intramembrane protein that stabilises the transcriptionally active conformation of ToxR, and prevents premature intramembrane proteolysis under starvation, alkaline pH or late stationary phase (Almagro-Moreno *et al.*, 2015b). Meanwhile, TcpH acts as a chaperone to stabilise TcpP, and its expression is highly dependent on pH and temperature (Beck *et al.*, 2004). The active complex comprises two ToxR/ToxS dimers, covering between -100 until -69 and TcpP/TcpH covering from -51 to -32 at *toxT* promoter relative to the transcription

157

initiation site (Krukonis *et al.*, 2000) (Fig. 7.1). Also, environmental signals play an essential role in the modulation of virulence factor expression as they can control ToxT activity. Bile concentration and temperature play an important role in inhibiting the activity of ToxT but not its expression. High levels of CTx and TCP expression are observed at 30 ºC, while at 37 ºC or in the presence of 0.4% of bile they are reduced even though the expression of *toxT* under these conditions is unchanged (Schuhmacher and Klose, 1999). At the same time, ToxR function can be affected by low or high osmolarity as these affect the conformation of membrane proteins. Optimal conditions for the expression of ToxR in the classical biotype are not affected in the same manner as in strains of the El Tor biotype; both biotypes express ToxR but only classical strain express ToxT in rich media (DiRita *et al.*, 1996). Nevertheless, *V. cholerae* El Tor strains incubated in high-salt LB supplemented with 0.3% $NaHCO_3$, known as AKI media, produce high levels of CTx and TCP when incubated at 37 °C in stationary tubes for 4 hours and then with shaking for 16 hours (Iwanaga and Yamamoto, 1985). The amino acids asparagine, serine, glutamate and arginine have been shown to modulate the expression of CTx and TCP inhibiting them and changing the ratio between OmpU and OmpT (Miller and Mekalanos, 1988). Also, early studies determined that the presence of carbon dioxide also regulates the expression of virulence factors as at 10% CO_2 atmosphere, the expression of the cholera toxin is at a maximum (Shimamura *et al.*, 1985). Although under these conditions the expression of virulence factors is affected, only temperature has a high impact on the transcription of *toxT* (Skorupski and Taylor, 1997).
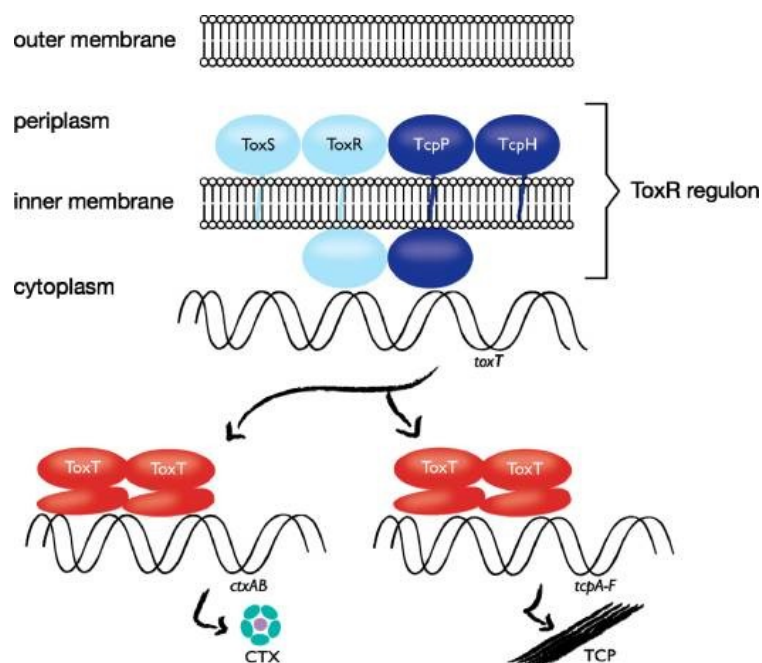
Figure 7.1. Regulatory proteins of the ToxR regulon. The ToxR/ToxS together with TcpP and TcpH control the expression for virulence master regulator ToxT by dimerising at the DNA binding site. When in position at the DNA binding site, the conformational changes of the promoter expose the ribosome binding site, and virulence factors are expressed accordingly (Haas *et al.*, 2014).

Global regulators also play a role in controlling the ToxR regulon. The cAMP-CRP system can repress the ToxR regulon, binding to a -35 motif in TCP and CTx promoters preventing the RNA polymerase or other transcriptional factors from binding (Skorupski and Taylor, 1997). Environmental cues that lead to accumulation of cAMP downregulate virulence via the cAMP-CRP system. For example, under glucose starvation, the activity of the adenylate cyclase CyaA is enhanced leading to accumulation of cAMP during biofilm formation (Fong and Yildiz, 2008). Similarly, the histone-like nucleoid-structuring (H-NS) protein represses virulence by blocking transcription of the ToxR regulon. Signals that promote the accumulation of H-NS include elevated osmolarity, temperature, anaerobiosis, pH and stationary phase (Nye *et al.*, 2000). The aminopeptidase PepA controls virulence according to the environmental pH, possibly by modifying the exopeptidase activity on regulators such as AphA and AphB, or by targeting the intergenic site between *tcpPH* (Behari *et al.*, 2001).

7.1.2 Cell envelope stress and the control of virulence

In Gram-negatives, cell envelope stress plays a key role in controlling pathogenesis. Studies in *E. coli* have shown the relationship between the expression of virulence factors with the Cpx pathway implicated in the synthesis of type IV secretion systems and expression of virulence regulators, and sigmaE which is key for intracellular survival and protection against oxidative stress (Raivio, 2005). The most reviewed pathways are Cpx and σ^E discussed below.

7.1.2.1 Vibrio cholerae Cpx pathway

The CpxRA is a two-component system to detect membrane perturbations. Activation of this pathway occurs when a disruption is sensed by the periplasmic protein CpxP which will transduce a signal by a yet unknown process to the inner membrane sensor kinase CpxA. The

160

kinase activity of CpxA sequentially will phosphorylate the response regulator CpxR, leading to transcription of cell wall maintenance genes (Slamti and Waldor, 2009). Phosphorylated CpxR has a dual function on the ToxR regulon; on one side it promotes the transcription of *toxRS* while on the other inhibits the expression of TcpPH and ultimately TCP and CTx through an unknown mechanism. Moreover, virulence may be regulated through indirect routes via CRP due to the CpxR-dependent repression of OmpT, and in a similar fashion to AphB (Acosta *et al.*, 2015).

7.1.2.2 Vibrio cholerae σ^E.

The alternative sigma factor σ^E is also important during cell envelope stress as well as virulence and host survival. The function of this sigma factor has been observed in *E. coli* as a response to conditions such as high temperature or exposure to ethanol and the accumulation of immature outer membrane proteins in the periplasm (Mecsas *et al.*, 1993). Although the response of σ^E to temperature and ethanol works differently in *V. cholerae*, Δ*rpoE* mutants were unable to colonise the digestive tract of infant mice (Kovacikova and Skorupski, 2002a).

7.1.3 The role of cell density in the expression of virulence

Cell density plays an important role controlling the expression of virulence. Virulence and quorum sensing networks share regulatory proteins which allow this crosstalk. The expression of the regulatory protein HapR, which is homologous with LuxR from *V. harveyi,* is enhanced during high cell density (Jobling and Holmes, 1997). Although HapR acts as an activator of the quorum sensing pathway, it is a repressor for virulence, inhibiting the expression of the *tcpPH* locus (Zhu *et al.*, 2002). During low cell density, the opposing quorum sensing regulator AphA helped by its cognate protein AphB enhances the transcription of the *tcpPH* locus by

binding to the promoter motif (Kovacikova *et al.*, 2004) (Fig. 7.2). The expression of secretion systems is also essential during virulence and is controlled by cell density. Especially, type III and type IV secretion systems, which are highly conserved across *Vibrio* species, can be induced when the quorum sensing route is stopped (Zheng *et al.*, 2010)

Figure 7.2. Quorum sensing circuit at low cell density. All four QS pathways are not detecting autoinducer, so LuxO remains phosphorylated and AphA accumulates. Other pathways that interact with the quorum sensing circuit, RpoN and RpoS have opposite effects, inducing Qrr1-4 and inhibiting HapR. Interestingly, CRP induces quorum sensing phenotypes in *V. fischeri*, but the opposite effect has been observed in *E. coli* (Dunlap and Greenberg, 1988). CRP prevents the action of Fis and enhances the activity of CqsA. VarA/VarS system contributes to induce the LuxO-P through CrsA.

7.1.4 The zebrafish as a model host for V. cholerae

The study of *V. cholerae* infection in animal models started back in 1884 when Nicati and Rietsch reproduced a cholera-like disease by inoculating bacterial cells into the duodenum of guinea pigs since oral inoculation did not result in illness; then, in 1894 Metchnikoff proved that oral infection was achieved with newborn rabbits without a mature intestinal flora (Ritchie and Waldor, 2009). After that until today, numerous reports have used primarily rabbits and mice to describe the disease and the dynamics of the bacteria within the host. In this regard, many genes required during colonisation such as those encoding for cell surface structures, transport, motility, metabolism gene regulation and others with yet not known function have been characterised from suckling mouse intestine (Ritchie and Waldor, 2009). However, mammalian models are expensive as they need intensive care, and at the same time sample processing is complex. The zebrafish (*Danio rerio*) has emerged as a powerful tool to study developmental biology as well as human diseases (Dooley and Zon, 2000). This model presents many advantages compared to traditional models, such as a large number of offspring and short generation time, relative ease of maintenance, and its transparency during larval and infant life stages, which is ideal for microscopy. At the same time, as a vertebrate, it shares many physiological features with humans. Foodborne diseases, including *Vibrio* species, *P. aeruginosa* and opportunistic fungi, have been studied using this model to monitor the colonisation, pathogenicity and transmission (Runft *et al.*, 2014, Mitchell *et al.*, 2017, Engeszer *et al.*, 2007).

Vibrio infections have been studied using the zebrafish model. These two organisms overlap in their endemic geographical zone, which suggests a close evolutionary relationship (Engeszer *et al.*, 2007). Infection of zebrafish with the fish pathogen *Vibrio anguillarum* showed the possibility to trace the pathogen during its infective cycle by fluorescent microscopy in live fish (O'Toole *et al.*, 2004). More recent studies using the human pathogen *V. parahaemolyticus*,

demonstrate that bacteria can infect similarly as in humans and fish develop a similar immune response to humans with activation of proinflammatory cytokines Tnfα and Il-1β during sepsis (Zhang *et al.*, 2016). Likewise, *V. cholerae* can infect zebrafish and be transmitted to naive hosts achieving a normal infection cycle (Runft *et al.*, 2014). Further, the enterotoxicity due to cholera toxin can be quantified by measuring the volume of diarrhoea in infected fish (Mitchell *et al.*, 2017).

Since the clustering resulted in the induction of a controlled quorum sensing activated phenotype, virulence repression was determined. For this aim, V. cholerae virulence was characterised using phenotypical and transcriptional assays.

7.2 Results

7.2.1 Transcription of virulence factors is reduced in sessile V. cholerae.

The sequestration into polymers induces a sessile lifestyle where motility stops and a biofilm-like state is induced (Chapter 4 and Chapter 5). Also, it has been reported that the clustering activates a quorum sensing controlled phenotype as activation of bioluminescence in *V. harveyi* is achieved (Lui *et al.*, 2013). Since virulence in largely affected by cell density, key virulence factor genes were investigated in order to shed light on the virulence regulation during clustering. To achieve this aim, β-galactosidase assays were done using strains expressing pRW50-oriT vector containing specific promoter regions of selected virulence-related genes transcriptionally fused to *lacZ*. The promoter regions were derived from the virulence regulator *toxT* (202 bp upstream from the transcription initiation site), virulence factors *ctxAB* (cholera toxin; 173 bp upstream from the transcription initiation site) and *tcpA* (subunit of the Toxin Co-regulated Pilus TCP; 542 bp upstream from the transcription initiation site), and low cell density-related quorum sensing regulator *aphA* (366 bp upstream from the transcription initiation site). These regions contained important regulatory elements related to infection: ToxR boxes in *toxT* promoter, ToxT boxes in *ctxAB* and *tcpA* promoters, and HapR binding motif on *aphA* promoter (Fig. 7.2). Since virulence is strongly induced during attachment (Dey *et al.*, 2013), β-galactosidase assays were done from reporter strains infecting Caco-2 cells. *V. cholerae* at a multiplicity of infection (MOI) of 10 were incubated with polymers for 1 hour prior to infection at 30 ℃ in 1 mL of clear DMEM. Then the bacterial solution was added to a monolayer of Caco-2 epithelial cells and incubated 7 hours at 37 ℃ with 5 % CO_2. After that cells were washed with PBS and 1 mL of triton 0.5 % triton X-100 was added to recover attached cells, the solution of cells was then treated with toluene and 1 % sodium deoxycholate and then enzymatic assays were done with 0.2 mM ortho-nitrophenyl-β-galactoside as substrate

in buffer. Genes were actively downregulated when clusters were used for infection (Fig. 7.3). *toxT-lacZ* was reduced almost 4-fold with P1 or P2 compared with vector control. Similarly, transcription of *ctxAB-lacZ* was reduced 3-fold upon clustering with P1 or P2 respectively compared with control vector. The down-regulation effect was less pronounced with *tcpA* as P1 showed a mild suppression of hardly 0.5-fold compared with control vector. Oddly, with P2, there seems to be an induction of nearly 2-fold. Finally, the quorum sensing regulator *aphA* showed a reduction of nearly 2-fold and 4-fold when clustering with P1 and P2 respectively, compared with empty vector. Induction of the reporter was followed overtime in absence of epithelial cells with similar results obtained. Interestingly, the peak of induction for the reporters seems to be around 4 hours until 7 hours (Appendix 2), in line with results with the cytotoxicity assays in section 7.2.4.

These results suggest that clustering inhibit the expression of virulence factors as their transcription is down-regulated. Similarly, the low cell density regulator *aphA* is downregulated upon clustering supporting the hypothesis that clustering induces a controlled-quorum sensing phenotype that resembles high cell density.
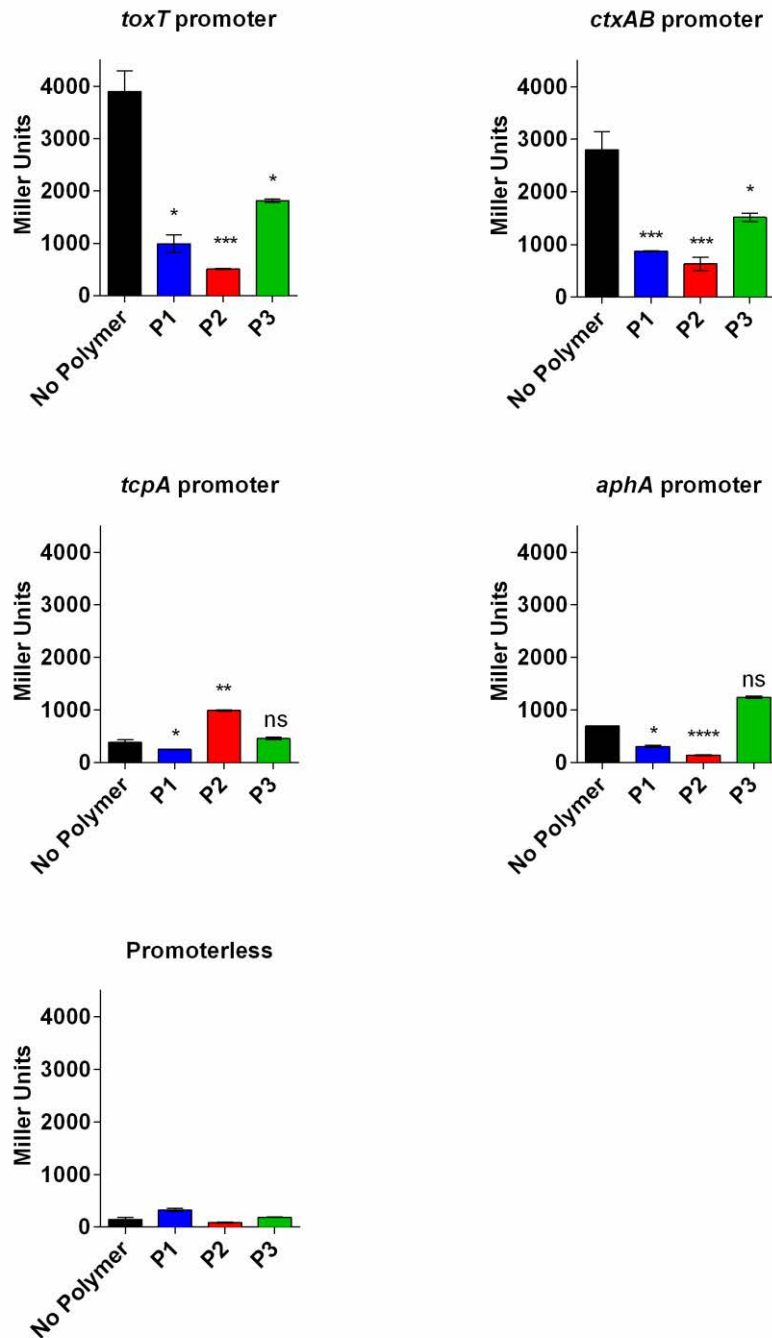
Figure 7.3. Transcriptional expression of virulence-related genes. The activity of promoter regions from *toxT*, *ctxAB*, *tcpA* and *aphA* were cloned into pRW50-oriT. The activity was measured from bacteria recovered from infected epithelial cells. N16961 bearing constructs of pRW50-oriT were incubated with P1 at 0.05 mg/mL or 0.5 mg/mL for P2 and P3 for 1 hour prior to infection and then added to a monolayer of Caco-2 cells at an MOI of 10. After 7 hours, bacterial cells were recovered and β-galactosidase activity measured. Enzymatic activity was adjusted to the number of attached bacteria using serial dilution plating and colony counts. Results are presented as means ± s.e.m. of triplicates. Analysis of variance (ANOVA), followed by Tukey's post hoc test, was used to test for significance. Statistical significance was defined as $p<0.05$ (*), $p<0.001$ (**), $p<0.001$ (***), or $p<0.0001$(****).

7.2.2 Clustered V. cholerae cells are defective in infecting Caco-2 cells.

Sequestration of *V. cholerae* cells into clusters by polymers induces a switching from planktonic to a sessile lifestyle that we hypothesized, would interfere with the normal course of infection. Moreover, the immobilisation of *V. cholerae* cells resulted in down-regulation of key genes related to virulence and cell density. Going further, the impact of the clustering was assessed upon infection of epithelial cells Caco-2. Here, three key events of *V. cholerae* pathogenesis were tested: attachment, cytotoxicity and induction of intracellular cAMP in response to the cholera toxin. It is worth to mention that conditions used for infection were optimised after several experiments. A pre-incubation at 30 ℃ without shaking improved the virulence of *V. cholerae*, similarly to the induction through AKI media (Iwanaga and Yamamoto, 1985). Also, a 7 hours timeframe for infection was optimum to detect differences in cytotoxicity and attachment between treated and untreated cells.

7.2.2.1 Polymers interfere with attachment of Vibrio cholerae.

The first contact between pathogen and host is through adhesion, which is key to stablish an initial colonisation and infection (Almagro-Moreno *et al.*, 2015a). In order to determine if the clustering is detrimental to the attachment to epithelial cell, a monolayer of Caco-2 cells was infected with clustered *V. cholerae*. Bacterial cells were adjusted to an MOI of 10 and clustered with poly(*N*-(3-aminopropyl) methacrylamide) (P1), poly(*N*-[3-dimethylamino)propyl] methacrylamide) (P2) or poly(acryloyl hydrazide) imidazole (P3) at concentrations ranging from 0.005 mg/mL to 0.5 mg/mL in 1 mL of clear DMEM prior the infection. Samples were incubated for 1 h at 30 ℃ and then were added to Caco-2 monolayer using a 24-well plate. The plate was incubated for 7 hours at 37 ℃ with 5% CO_2. Following that, cells were washed to remove unattached cells and Caco-2 were disrupted with 1 mL of 0.5 % triton X-100 to release attached cells. Once the debris was dislodged from the bottom of the well, bacterial cells were

169

vortexed, and serially diluted in PBS. 100 μL aliquots of each dilution were plated onto TCBS agar and incubated for 16 hours at 37 ºC. Then, colony forming units were counted and plotted as CFU/mL versus polymer concentration. Sequestration of *V. cholerae* mediated by polymers resulted in significantly less CFU counted as the concentration of polymers increased. The abolition of attachment was particularly apparent when using P1 at concentrations low as 0.005 mg/mL were sufficient to prevent attachment almost 100-fold. P2 and P3 had a mild detrimental effect on attachment the reduction was small but still significant (Fig. 7.4B).

To visualise the infection, imaging of infected Caco-2 cells with either planktonic cells of clustered bacterial was done. GFP-labelled *V. cholerae* carrying the pMW-*gfp* vector were used to infect a monolayer of Caco-2 at a MOI of 10 in similar conditions as for the attachment assay. After 7 hours unattached cells were removed, and samples were washed with PBS. The 0.5 mL of 4 % paraformaldehyde (PFA) was added for fixation incubating at room temperature for 15 minutes. After that PFA was removed, cells washed, and permeabilisation was done by adding 1 mL of 0.1 % triton X-100 and incubated for 5 minutes, then staining was done adding 66 ng/mL rhodamine-phalloidin and 10 μg/mL Hoechst to stain the actin filaments and the nuclei respectively. After 10 minutes, samples were washed with PBS and mounted into microscope slides with a drop of antifade gold with the cells facing downwards. After 16 hours of curing, imaging was done using an epifluorescence microscope (Zeiss) at 63x magnification and Apotome grid to enhance resolution. The images support the results obtained for the CFU counting as using a higher concentration of polymer, fewer bacteria were observed per field. Moreover, the exposure to polymers affected the epithelial cells similar as with unclustered bacteria. At higher concentrations of polymers, cell shape changed turning into rounded and compact nuclei with strong red patches suggesting morphological changes of the cytoskeleton (Fig. 7.4A and Appendix 3).

Taken together, these results suggest that clustering has a detrimental effect on attachment, preventing *V. cholerae* from colonising the surface of epithelial cells as less CFU were counted when infected with clustered bacteria. These results were supported by images showing fewer bacteria when polymer concentration increased. Since virulence is tightly coordinated with cell density, these results were contrasted using a mutant strain of *V. cholerae* (BH1651) with a mutation in the quorum sensing integrator LuxO mimicking a permanent phosphorylated state (*luxO*^{D47E}), (Ng and Bassler, 2009). Even though it has been reported that BH1651 is slightly more toxic than wild type (Jung *et al.*, 2015), the clustering resulted in slightly less counts when increasing the concentration of polymers. In the same sense, images of the infection polymers were slightly less effective as with wild type (Fig. 7.4C-D).
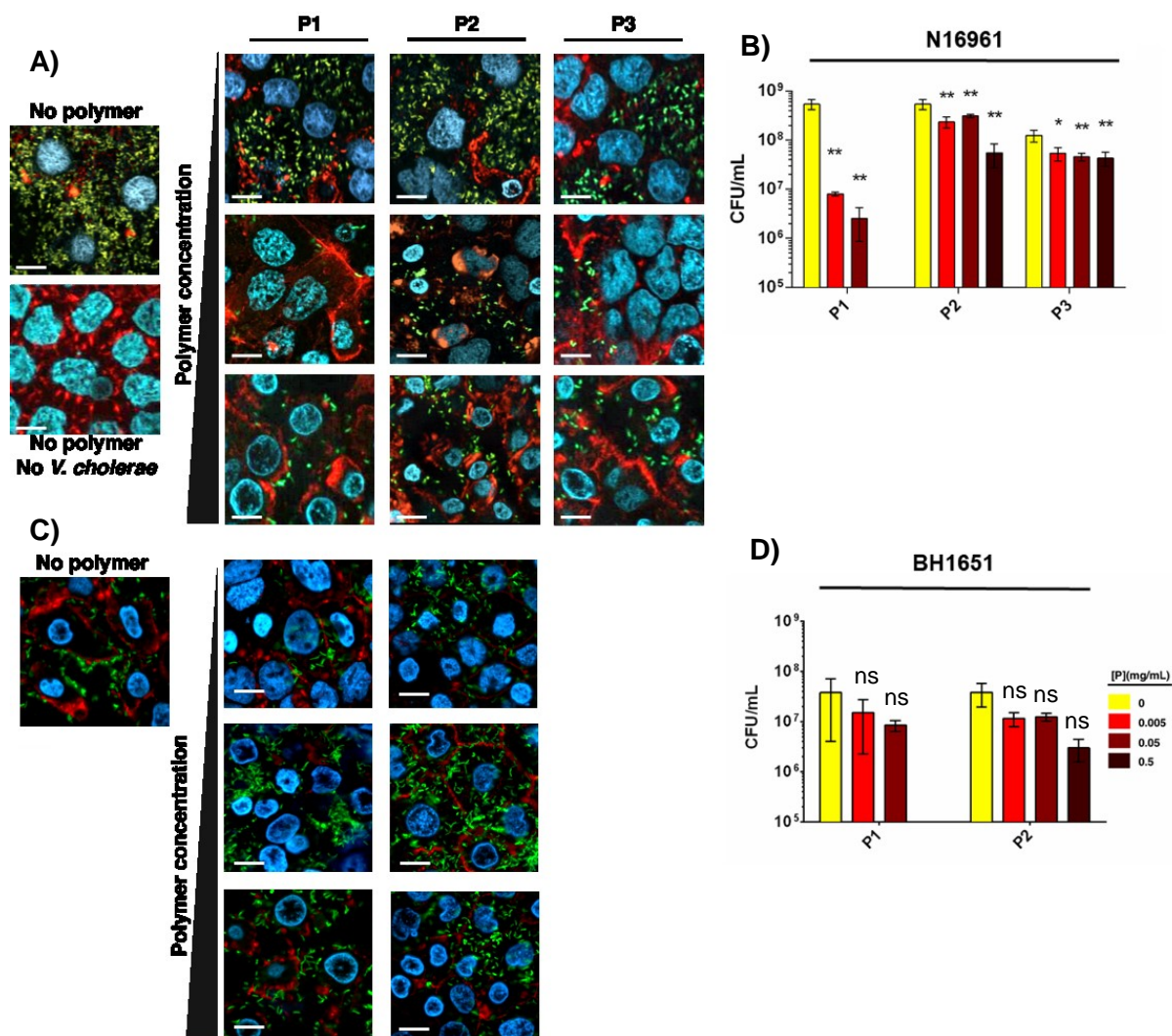
Figure 7.4. Impairment of attachment due to the clustering of *V. cholerae*. *V. cholerae* at a MOI of 10 was incubated with different concentrations of polymers for one hour prior to infection of a monolayer of Caco-2 cells. A) Visualisation of attachment of GFP-labelled *V. cholerae* N16961. Caco-2 cells were stained with Hoechst (blue) and rhodamine-phalloidin (red). B) Attachment assay of *V. cholerae* N16961 clustered with different concentrations of P1, P2 or P3. C) Visualisation of the attachment of GFP-labelled *V. cholerae* BH1651. Caco-2 cells were stained under the same conditions as for N16961. D) Attachment assay of *V. cholerae* BH1651 clustered with different concentrations of P1 or P2. Results are presented as means ± s.e.m. of triplicates. Analysis of variance, followed by Tukey's post hoc test was used to test significance. Statistical significance was defined as $p < 0.05$ (*), or $p < 0.01$ (**).

7.2.4 Protective effect of polymers against V. cholerae cytotoxicity in epithelial cells

Since clustering of *V. cholerae* cells induced repression of key virulence factor genes and interfered with adhesion of the pathogen to the host, the toxicity against Caco-2 cells was determined by measuring the release of lactate dehydrogenase (LDH) after infection. Also, the cytotoxicity of the materials was assessed since micrographs of infection suggested a detrimental effect on the epithelial cell shape. Cytotoxicity was determined by clustering *V. cholerae* N16961 with P1, P2 or P3 at concentrations of 0.00005 mg/mL to 0.5 mg/mL in 1 mL of clear DMEM and incubating for 1 hour prior to the infection at 30 ℃ without shaking. At the same time, polymers were diluted to the same concentrations in 1 mL of clear DMEM using 24-well plates. Samples were added to wells with monolayers of Caco-2 cells. After 7 hours of incubation at 37 ℃ with 5 % CO_2, plates were centrifuged, and clear supernatant was transferred into a 96-well plate dividing each sample volume into 3 wells of 200 μL in order to have three independent and three technical replicates for each sample. The plates were centrifuged again and 100 μL were used for the assay. 100 % cytotoxicity control was Caco-2 cells treated with 1 % triton X-100. Firstly, exposing the Caco-2 cells to each polymer at different concentrations resulted in cytotoxicity at higher concentrations of P1 and P2 in a concentration-dependent manner, while P3 did not cause membrane disruption (Fig. 7.5A-C upper pannels). Once polymers cluster *V. cholerae*, there is a protective effect on host cells, as cytotoxicity is reduced by about 50% at 0.05 mg/mL for P1 and 0.5 mg/mL for P2 and P3. Below these concentrations, or above in the case of P1, the cytotoxicity was high at similar levels as untreated bacteria (Fig. 7.5A-C middle row). *V. cholerae* BH1651 was used to contrast these results in order to determine if the protective effect of polymers can prevent BH1651 cytotoxicity. Under similar conditions for infections as for wildtype and with P1 and P2 at concentration ranging from 0.00005 mg/mL to 0.5 mg/mL, clustered BH1651 was used to infect Caco-2 cells. The protective effect of P1 was observed at 0.05 mg/mL similarly as with

the wild type. However, no significant differences were obtained when using P2 at any concentration (Fig. 7.5A-B bottom row). Moreover, the infection performed by wildtype and BH15651 were different as wildtype reached nearly 75 % of cytotoxicity while under the same conditions BH1651 reached nearly 50 % cytotoxicity. In order to rule out if this difference might be related to the physiology of the bacteria in a minimal media such a DMEM, the growth of both bacteria was compared. GFP-labelled BH1651 and N16961 carrying pMW-*gfp* plasmid were diluted to an OD_{600} of 0.02 in clear DMEM in a total volume of 200 μL and then incubated at 37 ºC with shaking and fluorescence as relative fluorescence units was recorded every 30 minutes for 25 hours. BH1651 reached a stationary phase at a lower bacterial load than N16961 under the same conditions (Fig. 7.8D).

Together these results suggest a therapeutic window where polymers can be used to control *V. cholerae* cytotoxicity. Concentrations of 0.05 mg/mL of P1 and 0.5 mg/mL of P2 and P3 were enough to induce clustering, induce a less virulence phenotype and prevent polymer toxicity against host cells. This observation is in agreement with previous assays as reduction in the transcription of virulence factor genes and minimising the bacteria burden attached to host cells contribute to interfere with the course of infection. Also, the low cell density locked strain BH1651 showed reduced virulence only with P1 at 0.05 mg/mL. However, the strain seemed less infective overall compared with the wildtype. Although the cytotoxicity is reduced and there is reduction in virulence factor expression, it was not clear if the polymers are preventing the production of the major *V. cholerae* virulence factor, cholera toxin.

A)
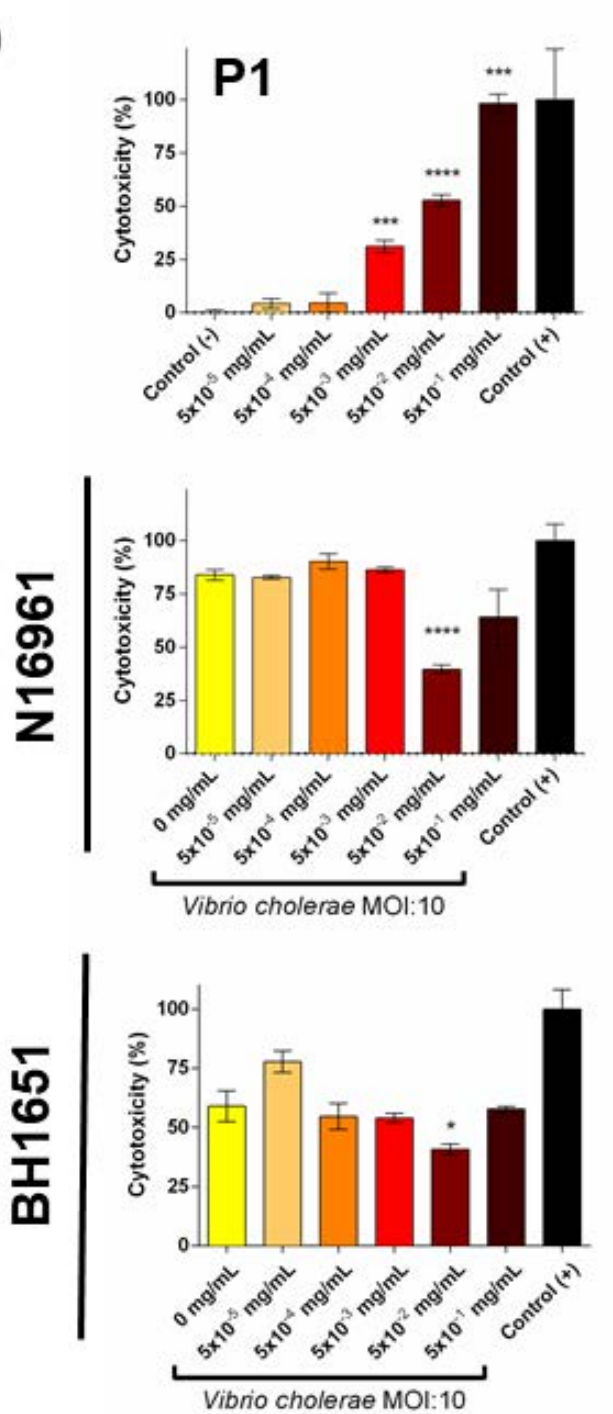
B)
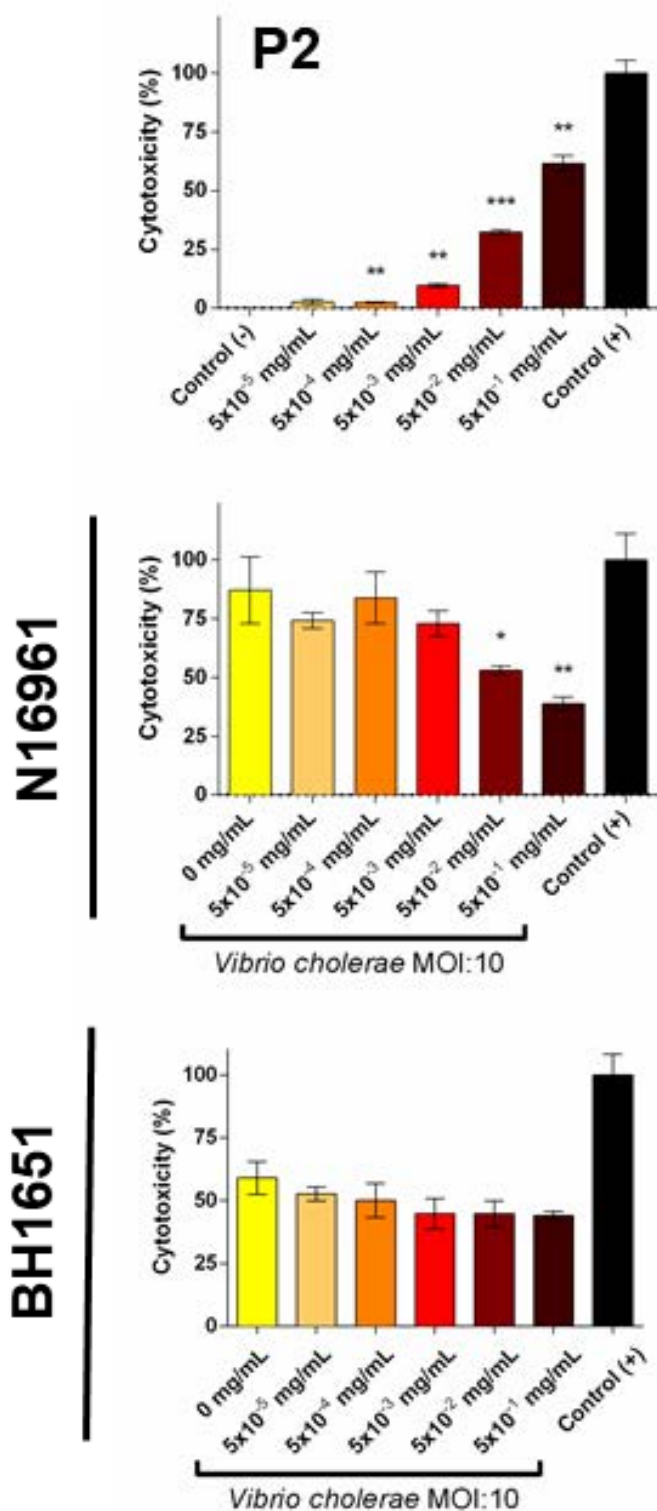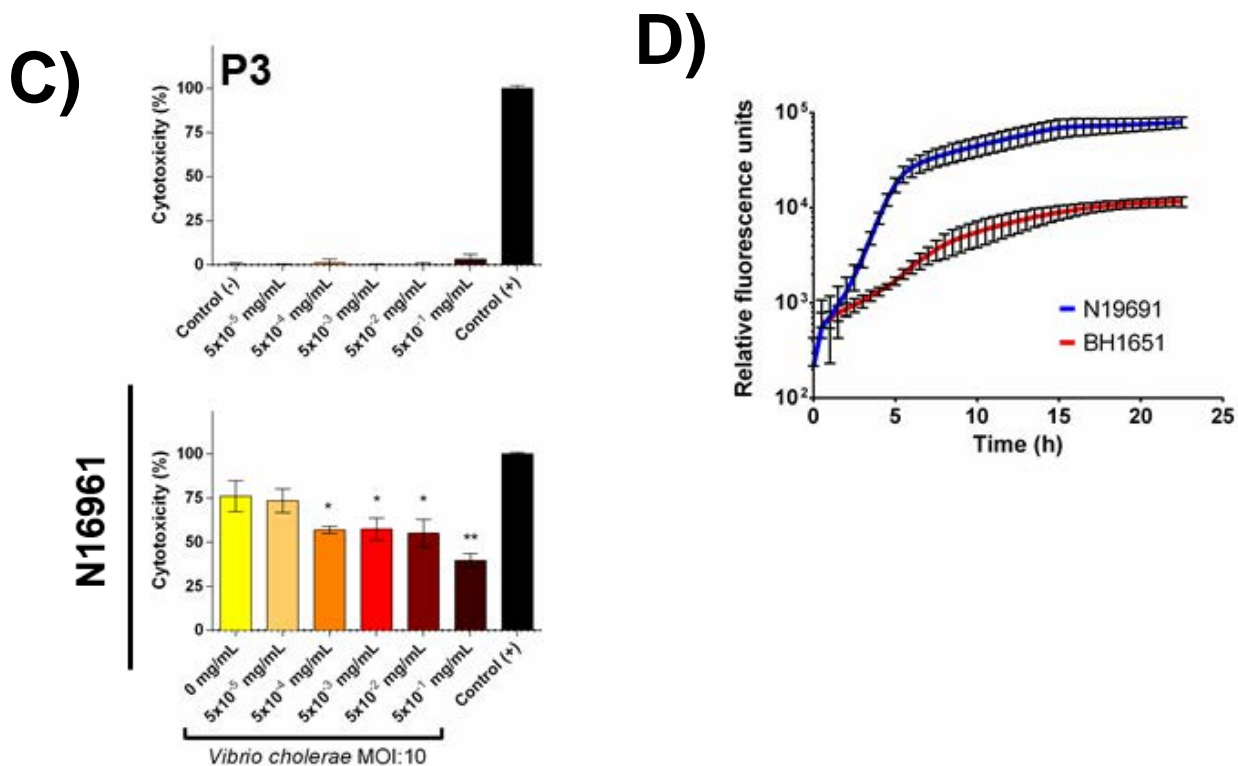
Figure 7.5. Cytotoxicity effect of clustered *V. cholerae* on epithelial cells. Caco-2 cells were seeded forming a monolayer and *V. cholerae* was added at an MOI of 10. Seven hours post infection, LDH activity was measured. P1 (A), P2 (B) and P3 (C) at different concentration were added to epithelial cell layer to determine the cytotoxicity of the materials (upper pannels). N16961 was incubated for 1 hour with different concentrations of P1 (A), P2 (B) and P3 (C) at 30 ºC and added to Caco-2, followed by measurement of LDH activity in the culture supernatant (middle row). BH1651 was incubated 16 hours with a different concentration of P1 (A) and P2 (B) at 30 ºC and added to Caco-2 cells, and LDH activity was measured (bottom row). Results were normalised to untreated cells (0%) and cells lysed with the detergent Triton X-100 (100%). D) Comparison of growth rates between N16961 (red line) and BH1651 (blue line) following the expression of GFP. The measurement was done in clear DMEM, and GFP was measured every 30 min. Results are means ± s.e.m. of three independent experiments. Analysis of variance, followed by Tukey's post hoc test was used to test significance. Statistical significance was defined as $p < 0.05$ (*), $p < 0.01$ (**) or $p < 0.0001$ (****).

7.2.5 Protective effect of polymers reduced cholera toxin activity on Caco-2 cells.

Capturing *V. cholerae* into clusters resulted in decreased transcription of virulence-related genes and a protective effect against bacterial toxicity as well as bacterial attachment to Caco-2 cells. It remained to be answered if the protective effect was due to lowered production of cholera toxin or if the protection occurred through other means. Since cholera toxin is responsible for the accumulation of intracellular cAMP which in turn leads to the high volume of fluid excretion observed in diseases patients, the intracellular concentration was measured by enzyme-linked immunosorbent assay (ELISA). Worth to mention that numerous attempts to detect by western blot both virulence factors, cholera toxin and TCP, fails under these conditions (Appendix 4). *V. cholerae* N16961 wildtype and quorum sensing mutant BH1651 were clustered with P1 and P2 at concentrations from 0.005 mg/mL to 0.5 mg/mL, to infect a monolayer of Caco-2 at an MOI of 10 under the same conditions as infection assays were performed. After 7 hours of incubation at 37 °C under 5 % CO_2, Caco-2 cells were washed with PBS and treated with 0.1 M HCl. Debris was removed by centrifugation and the immunoassay was done and readouts detected at 405 nm. The concentration of cAMP was determined by a calibration curve. There was an inverse relationship between the amount of cAMP produced and the concentration of polymer. Clustering *V. cholerae* with a higher concentration of either P1 or P2 resulted in a smaller amount of intracellular cAMP in Caco-2 cells, suggesting lower levels of cholera toxin activity (Fig. 7.6A). This effect was also observed when the infection was done with BH1651 clustered with P1, while P2 seemed to not have any relation with the cAMP, similar with the cytotoxicity assay (Fig. 7.6B).

These results indicate that clustering and down-regulation of *ctxAB* resulted in less cholera toxin in the media. Higher concentrations of both P1and P2 resulted in less cAMP especially at 0.05 mg/mL and 0.5 mg/mL for P1 and P2 respectively, which is in line with the cytotoxicity assay. Similarly, to the cytotoxicity assays, BH1651 showed important reduction at 0.05

mg/mL of P1 and no protective effect with P2. This result suggests that even though the cells could be clustering with P2 is not enough to induce the less virulent phenotype. Also, slightly less cAMP is observed in BH1651 compared with wildtype.
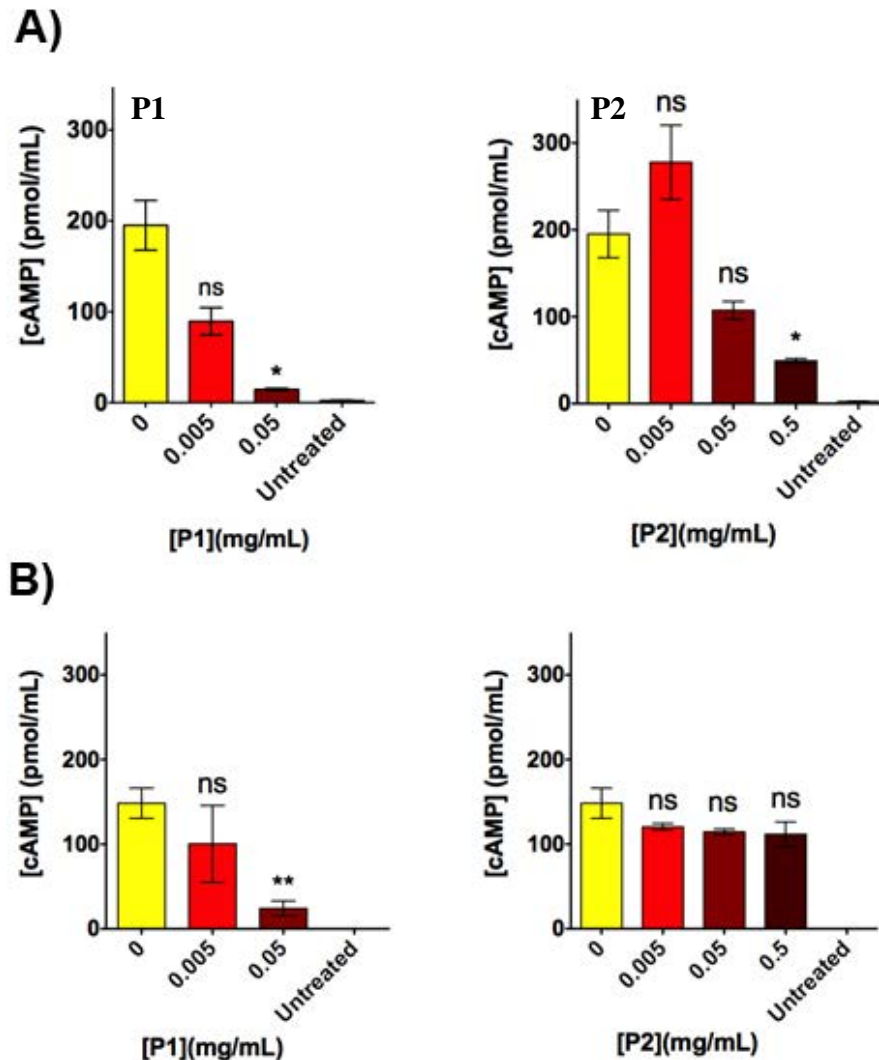
Figure 7.6. Levels of intracellular cAMP after infection. A monolayer of Caco-2 cells was infected with clustered or unclustered *V. cholerae* at a MOI of 10. Bacterial cells were incubated prior infection with different concentrations of polymers P1 or P2 for 1 hour and then added to epithelial cells. Seven hours later, Caco-2 cells were homogenised and intracellular cAMP detected and quantified by ELISA against a calibration curve with known concentrations of pure cAMP. "Untreated" condition refers to the basal level of cell cAMP, to discard potential problems of the kit. A) Intracellular levels of cAMP after infection with *V. cholerae* N16961. B) Intracellular levels of cAMP after infection with *V. cholerae* BH1651. Results are presented as means ± s.e.m. of triplicates. Analysis of variance, followed by Tukey's post hoc test was used to test significance. Statistical significance was defined as $p < 0.05$ (*), or $p < 0.01$ (**).

7.2.6 Polymer-induced clustering mimics the lack of toxin co-regulated pilus (TCP).

A phenotypic characterisation of a Δ*tcpA* mutant was done to compare the effect of clustering in *V. cholerae* with the absence of the toxin co-regulated pilus (TCP). Together with cholera toxin, TCP is the second most important virulence factor of *V. cholerae*. Although it is not directly involved in cell attachment, it is actively expressed during infection and its absence is detrimental to virulence (Almagro-Moreno *et al.*, 2015a). TCP is a pilus used during colonisation, and is formed by multiple subunits of TcpA forming a filament of 7 nm in diameter (Li *et al.*, 2008).

The Δ*tcpA* mutant (AC2764; kindly provided by D. Grainger) is a derivative of E7946 *V. cholerae* Ogawa El Tor. AC2764 was used to quantify colony forming units attached to Caco-2, to quantify the cytotoxicity against Caco-2 and to quantify the intracellular cAMP when infecting Caco-2. These results were compared with the isogenic background E7946 and with the wildtype *V. cholerae* N16961, the main strain characterised in this work. The conditions for the experiment were the same as for the other experiments; the strains were adjusted to an MOI of 10 in 1 mL of clear DMEM and then used to infect a monolayer of Caco-2 epithelial cells for 7 hours at 37 °C under 5% CO_2. *V. cholerae* was plated onto TCBS agar after homogenisation of epithelial cells with 0.5% triton X-100. LDH assays were done to quantify the cytotoxicity, and cAMP ELISA was done from homogenised cells with 0.1 M HCl. The colonisation of clustered *V. cholerae* N16961 onto Caco-2 at 0.005mg/mL was reduced 100-fold similarly to AC2764 (10^7-10^5 CFU/mL) (Fig. 7.7A and 7.7D). The absence of TCP resulted in reduced cytotoxicity reaching 30 % compared with E7946 which was around 70%. Clustered N16961 with P1 at 0.05 mg/mL and P2 at 0.5 mg/mL had similar reduction in cytotoxicity reaching 30 % as well (Fig. 7.7B). Regarding the accumulation of cAMP in Caco-

2 cells, there were no significant differences as the samples were highly variable, but the mean value was lower in AC2764 (Fig. 7.7C).

These results suggest that the absence of TCP resembles an avirulent phenotype exhibited by *V. cholerae* when clustered with cationic polymers. Despite the fact that the expression of *tcpA-lacZ* was not clear as P1 reduced but P2 increased its transcription in the β-galactosidase assay, the down-regulation of the regulator *toxT-lacZ* and *ctxAB-lacZ* indicates that virulence is impeded at the transcriptional level. The absence of TCP resulted in less colonisation and less cytotoxicity. Since ToxT and virulence itself are affected during clustering pressumably, the functions of TCP regarding colonisation and toxicity could be affected as well.
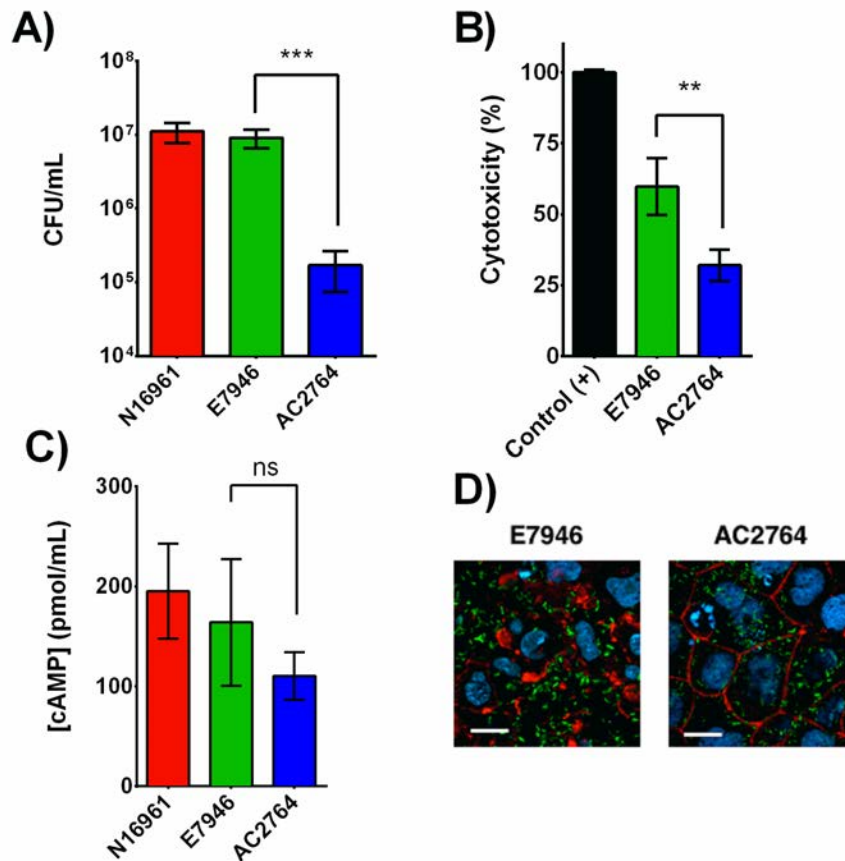
Figure 7.7. Infection of Caco-2 with a Δ*tcpA* background and its isogenic strain. Infection of *V. cholerae* N16961 compared with an Ogawa El Tor (E7946) and a Δ*tcpA* strain (AC2764). This strain was used to compare a virulence-defective phenotype with the clustered-phenotype of N16961. A) N16961 and E7946 showed similar levels of attachment while AC2764 was deficient to adhere. Although the colonisation was lower than with clustered N16961, it is relatively similar to P1 at its protective concentration (0.05 mg/mL). B) LDH assay with Ogawa El Tor strains. Level of cytotoxicity of the wild type was about 10% low compared with N16961 however, the lack of TcpA showed levels of cytotoxicity compared with the protective concentrations of any of the polymers. C) Intracellular cAMP levels were not significantly different between strains probably due to the variability of E7946. In any case, there seems to be a trend downward toward the absence of TcpA. Results are presented as means ± s.e.m. of triplicates. Analysis of variance, followed by Tukey's post hoc test was used to test significance. Statistical significance was defined as $p<0.01$(**), or $p<0.001$ (***). D) Micrographs of infection with E7946 and AC2764. Caco-2 cells under the same condition for infection as for N16961 has a change in morphology with the wildtype while, infection with AC2764, cells showed a normal phenotype.

7.2.7 Clustering of V. cholerae diminishes colonization of zebrafish larvae.

Zebrafish (*Danio rerio*) have been established as an animal model for *V. cholerae* colonisation and transmission as well as for other *Vibrio* species (Mitchell *et al.*, 2017, O'Toole *et al.*, 2004, Runft *et al.*, 2014, Zhang *et al.*, 2016). The protective effect seen during infection of Caco-2 cells led us to test whether a similar effect may be observed in an *in vivo* host model.

As zebrafish can be infected with *Vibrio* species, larvae were infected and imaged. *V. cholerae* at a concentration of 10^7 CFU/mL were clustered with 0.05 mg/mL of P1 and 0.5 mg/mL of P2 for 16 hours prior to incubation in E3 media at 30 ℃ without shaking. After that, supernatants, where mostly planktonic cells are located, were separated from aggregates formed at the bottom where mostly clustered bacteria are located. Both samples were used to infect larvae, and bacterial burdens compared to those achieved with untreated *V. cholerae.* Zebrafish larvae were immersed in media containing *V. cholerae* planktonic or clustered in 1 mL of E3 under rotation for 6 hours at 25 ℃. After that larvae were euthanised and homogenised with 1% triton X-100. Serial dilutions of the homogenised larvae were plated onto TCBS agar and incubated for 16 hours at 37 ℃ and CFUs were counted. The infection with sessile bacteria resulted in less burden compared with infection with planktonic bacteria, which is in agreement with attachment assays done on Caco-2 cells (Fig. 7.8A-B). This result was supported with images of larvae infected GFP labelled *V. cholerae* under the same conditions as above.Larvae were immobilised by sedating with 160 µg/mL tricaine and pictures were taken at 10X. Less green signal was observed in the digestive tract when larvae were infected with clusters, while planktonic bacteria normally infected (Fig. 7.8C).

These results suggest that the polymers were able to reduce the bacterial burden after uptake by zebrafish embryos. The defective colonisation is comparable to the reduction in attached bacteria seen on epithelial cells. At the same time, the bacterial burden was visibly lower compared with planktonic bacteria, as a 100-fold reduction in CFU/mL was quantified. Under

the conditions were zebrafish infection was done it seems that bacteria were efficiently removed from contaminated media subjected to polymer treatment, which could be useful for *ex vivo* applications such as enhancement of filtration in water treatment.
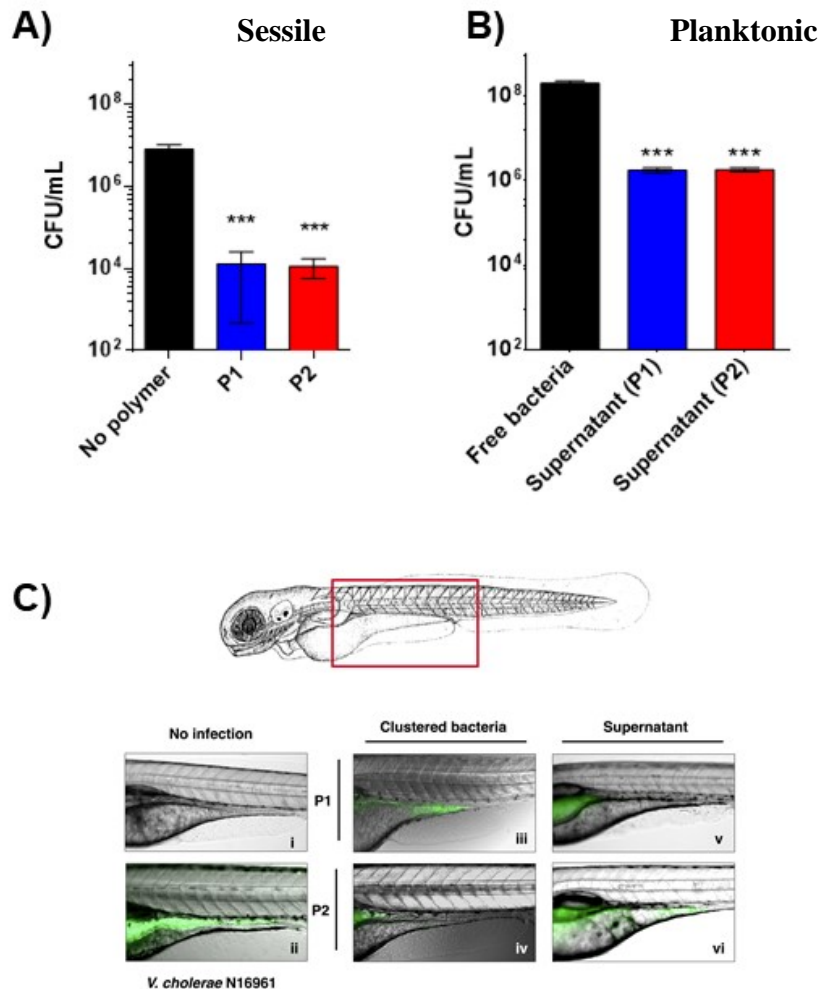
Figure 7.8. Colonisation of zebrafish digestive tract with clustered *V. cholerae*. Zebrafish larvae were infected by immersion with subpopulations of planktonic or clustered *V. cholerae* N16961 from the same clustering process. Bacteria were incubated with polymer 16 hours in 1 mL of E3 media, then supernatants (mainly planktonic cells) were separated from sedimented (mainly clustered bacteria). Larvae were immersed and incubated 16 hours to facilitate colonisation. The colonisation was quantified and imaged. A) Number of colony forming units per mL (CFU/mL) of sessile *V. cholerae* N16961 from homogenised larvae (N=10). B) Number of colony forming units per mL (CFU/mL) of planktonic *V. cholerae* N16961 from homogenised larvae (N=10). Results are presented as means ± s.e.m. of triplicates. Analysis of variance, followed by Tukey's post hoc test was used to test significance. Statistical significance was defined as $p<0.001$ (***). C) Overlay of fluorescence and optical micrographs of zebrafish larvae left uninfected (panel i), infected with GFP-*V. cholerae* (ii), GFP-*V. cholerae* clustered with P1 (iii) or P2 (iv), or the remaining decanted supernatant following removal of clustered *V. cholerae* with P1 (v) of P2 (vi). P1 was added at 0.05 mg/mL and P2 at 0.5 mg/mL.

7.3 Discussion

This chapter described the reduction of *V. cholerae* virulence as a result of clustering. The reduction in virulence was a result of both effects at transcriptional level that translated into less toxicity as a result of less cholera toxin produced, and less attachment and less cell damage at particular polymer concentrations. This effect was observed with an epithelial cell model and colonisation in an animal model. Also, this is the first report to show that clustering reduces the virulence of *V. cholerae*.

Clustering *V. cholerae* with cationic polymers was demonstrated to be an effective way to control virulence, as host cell damage was prevented and colonisation of the digestive tract was impaired. By capturing the bacteria, there is a forced transition from planktonic to a sessile lifestyle, detrimental for expression of virulence factors (Fig. 7.3). Since the binding of these polymers to the bacteria occurs through non-specific interactions, it is hard to pin down the mechanism by which virulence is downregulated. Considering that immobilisation interferes with virulence, the clustering might be a signal to induce an avirulent phenotype. This avirulent phenotype seems to be expressed when the clustering occurs at a high concentration of polymer but before the polymer's toxic threshold (concentration where the polymer alone induces cell damage of the host; Fig. 7.5A-C upper row and Appendix 3) is reached. The strong cationic nature of P1 causes *V. cholerae* to develop this avirulent phenotype at a concentration 10-fold less compared with P2 and P3. At the same time, beyond this concentration, P1 starts to affect also the host as the excess of cationic charges could be interacting with the membrane of epithelial cells. Likewise, below 0.05 mg/mL for P1 and 0.5 mg/mL for P2 and P3, there is a major unclustered population able to develop infection normally (Fig. 7.5A-C middle row). Using the strain BH1651 which is more toxigenic compared with wildtype due to a mutation in LuxO, P1 was able to protect Caco-2 cells. The mutation on this quorum sensing regulator

mimics a low cell density phenotype, however since quorum sensing controls many cell functions, the metabolism of the strain is slower compared with the wildtype which can explain the difference in the percentage of cytotoxicity (Fig. 7.5A-B bottom row). Also, the physical capturing and immobilization is detrimental for motility which is important during infection as it is directly related to attachment (Utada *et al.*, 2014). Taking together these results, polymers prevent virulence at a defined concentration which opens a therapeutic window where polymers can be used. Since the binding activity from these materials lies in the cationic binding groups, at higher concentrations they were harmful to the host. Therefore efforts are put into developing strategies with a focus on the specificity toward a microorganism. Ligands recognised by receptors in the pathogen may increase the specificity toward *V. cholerae*, discussed in Chapter 5.

At the transcriptional level, the avirulent phenotype caused by polymers is associated with low induction of virulence-related genes. The transcription of the regulator *toxT* and the cholera toxin *ctx* were significantly lowered, while *tcpA* had low levels even in untreated cells. The low transcriptional levels of *toxT-lacZ* may explain the reduction of *ctxAB-lacZ* transcription. This was observed in a Δ*toxT* background by Lee et al. showing almost undetectable levels of CTx and TCP (Lee *et al.*, 1999). Under these conditions, a mutant in *toxT* would be appropriate to determine if the presence of polymers is enough to downregulate virulence through ToxT or if the regulation responds to other proteins.

On the other hand, the low levels of *tcpA-lacZ* transcription could be explained by the length of the promoter region used. This region corresponds to a fragment of the intergenic region between *tcpPH* and *tcpA* of 542 bp that include not only the regulatory elements associated with ToxT (toxbox) but others such as CRP binding sequence. In a study done with a Classical O395 strain, different fragments of this promoter were used for beta-galactosidase assays, and a 95 base pair fragment gave the highest activity, fragments shorter or longer than this length

were low in reporter activity (Hulbert and Taylor, 2002). However, the segment in *V. cholerae* N16961 was different, and the ToxT binding motif was located far upstream nearly 300 bp from the transcription initiation site; further improvements could be done with this reporter removing the upstream region from the ToxT binding site. Another relevant regulator is AphA which respond to low cell density. Although the transcription was low and slightly variable for this gene, *aphA* was significantly downregulated during clustering. This effect may indicate that polymers were able to induce a signal of high cell density locally. Quorum sensing responds to the ratio between AphA and HapR to regulate downstream genes. Ideally, one would measure the expression of HapR to capture bacterial response to polymers in more detail. However, the transcription of this regulator is constitutive, while the translation is dictated by Qrr1-4 sRNAs. A time-course β-galactosidase assay done with the *aphA-lacZ*, *toxT-lacZ* and *ctxAB-lacZ* showed that the peak of induction for *ctxAB-lacZ* occurs at around 7 hours which is correlated with the optimum time found for the LDH assays under these conditions.

The poor transcription of virulence-related genes, especially cholera toxin, was correlated with low levels of intracellular cAMP. The cAMP produced by Caco-2 cells infected with clustered *V. cholerae* showed a dose-dependency with polymer concentration (Fig. 7.6A). This effect could be because less concentration of polymer is equal to more planktonic cells similarly to what is seen with the cytotoxicity assay. This effect was contrasted with a BH1651 strain which showed a similar result with wildtype using P1, while the cAMP levels when P2 was clustering were similar as un-clustered condition (Fig. 7.6B). This indirect method to determine the action of cholera toxin was adopted after multiple failed attempts to detect cholera toxin by western blot. In clustering conditions, it is challenging to normalise the biomass between samples, as OD_{600} measurements commonly used elsewhere, are not appropriate. Measuring total protein concentration under optimised conditions seemed to work better as a means of normalisation. However, the detection of either the whole toxin or the subunit B gave strong and unspecific

signals possibly due to poor performance of the antibody in the tested conditions which may require further purification of the toxin

Clustered *V. cholerae* exhibited poor attachment to Caco-2 cells. Together with the reduction in the expression of virulence factors, the attachment was compromised as fewer bacteria were obtained from homogenising Caco-2 cells. The immobilisation interferes directly with the motility and ultimately with colonisation (Fig. 4.3 and Fig. 7.4). The reduction of virulence could be due to physical impairment of motility and transcriptional effect on adhesion production which could be subject to future studies.

This effect was also observed by fluorescent microscopy, as not many bacteria were found attached to epithelial cells especially at high concentrations of any of the polymers (Fig. 7.4). Also, it can be observed the effect that polymers have upon contact with the host, this agrees with the LDH assay. This is in contrast to results with strain BH1651, where attachment seems not to be affected to a big extent as there were no significant differences in the number of bacteria attached to cells. This observation was supported by the images, as a green signal from the bacteria was more appreciable in all samples. These differences between strains could be explained by the fact that BH1651 expresses higher levels of TCP than N16961 which is translated into better colonisation (Krebs and Taylor, 2011). This advantage in colonisation has been reported before, but toxicity of this strain is not significant compared with the wildtype (Jung *et al.*, 2015). Using a *tcpA* deletion background confirmed the obtained results, as the absence of the TCP filament has been described to be critical for the infective process showing low attachment, reduced cytotoxicity and poor induction of cAMP in the host cell (Fig. 7.7). However, the effect of polymer on this virulence factor is not as clear as with cholera toxin judging from the transcriptional assays. During clustering, cholera toxin seems to be more affected than TCP (Fig. 7.3), which is enough to reduce the virulence.

Finally, an animal model was used to test the hypothesis of the protective effect of polymers *in vivo*. Zebrafish larvae were able to be infected with clustered, and unclustered *V. cholera*e and the infection could be seen in real time. *V. cholerae* seemed to accumulate and attach preferentially at the mid-intestine, which is similar to a human cholera infection where the corresponding small intestine is the main site of infection (Hsiao *et al.*, 2014).

Larvae were infected with different subpopulations of the same clustering treatment, i.e. supernatant and aggregates. Both populations were able to be taken up, as green signal is strong especially in the foregut region, which is anatomically equivalent to the stomach. Then, only the planktonic population signal is observed within the intestine. The CFU counting shows more bacteria within the fish with planktonic cells rather than clustered bacteria. Moreover, the values of attached bacteria were similar with both tested polymers (Fig. 7.8). These results suggest that, even though *V. cholerae* is inside the fish, it is not able to accumulate in the digestive tract as colonisation is impeded.

Chapter 8: General Discussion

This work describes the impact of clustering on *V. cholerae* with cationic polymers. This clustering resulted in a lifestyle transition from planktonic to sessile cells and induces a quorum sensing controlled phenotype that included the downregulation of virulence-related genes, and an increase in biofilm synthesis. This avirulent sessile lifestyle was characterised by phenotypic and transcriptional assays using cellular and animal models.

Vibrio cholerae pandemics has been historically associated to the O1 classical biotype, but the ongoing pandemic has been attributed to the El Tor biotype *(Dziejman et al., 2002)*. The genome sequence of this strain has helped to explain the displacement from classical to El Tor, showing that the a 13.5 % of the genome is differentially expressed under ToxR-inducing conditions *(Beyhan et al., 2006)*. These differences are mainly related to biofilm synthesis, chemotaxis and transport of amino acids, iron and peptides, in other words, cellular functions that enhance the ability of the pathogen to persist in the environment *(Beyhan et al., 2006)*. Within El Tor biotypes, there are three subclasses, Inaba, Ogawa and Hikojima. At immunochemical level, the LPS O- A, B and C for Hikojima. Between Inaba and Ogawa, an 2-O-Methyl group is present at the O-specific polysaccharide of the LPS in Ogawa and absent in Inaba (Villeneuve *et al.*, 1999). Differences in the LPS resulted in reduced cross-reactivity when the Ogawa specific vaccine is used against Inaba (Johnson *et al.*, 2012). At genetic level, Inaba present differences in the quorum sensing regulator HapR, since the open reading frame present an early stop codon that result in a frameshift mutation on hapR (Joelsson *et al.*, 2006). Since only a fragment of HapR is present, the strain could fail to control the virulence properly through cell density, as the affinity of HapR might be reduced as result of the early stop codon. Therefore, even if the cell density is high, N16961 will remain virulent. These differences might explain how N16961 El Tor has replace Classical strain in the ongoing cholera pandemic and highlights the importance to study the virulence in relation to this strain.

Clustering bacterial cells with cationic materials under sublethal conditions has been described before (Louzao *et al.*, 2015) and induction of bioluminescence in *V. harveyi* has been described (Lui *et al.*, 2013, Xue *et al.*, 2011), but no studies have addressed the effect on virulence by a physical capturing. This clustering effect, although simple, seems to be detrimental for the course of infection as cell density and movement are critical to starting an infection. The polymers used mainly differ in the cationic group exposed, using a primary amine, a secondary amine and an imidazole ring covering a pKa of nearly 10, 9.5 and 6.5, respectively (Fig. 2.1). Therefore, it is expected that all polymers would be protonated at physiological pH.

Several reviews have suggested the potential of non-conventional approaches to control pathogen's virulence either interfering with at the host-pathogen interface, disrupting the effect of toxins or interrupting the cell-cell communication (Clatworthy *et al.*, 2007, Rutherford and Bassler, 2012, Defoirdt, 2017, Defoirdt *et al.*, 2013). The cationic polymers used in this work appear to be potent tools to manipulate the physiology of bacterial cells. These materials are easily "tuneable" allowing the control of their cytotoxic properties by the rational design of the structure. As is demonstrated in Chapter 4 and Chapter 7, at defined concentrations cytotoxicity is prevented, but the polymers are still able to modify bacterial physiology. Usually, cationic polymers are used for their cytotoxic properties which are mainly due to their charge and hydrophobicity interfering with membrane structures (Yang *et al.*, 2017). As reported by others (Grace *et al.*, 2016) and here, by modifying the charged group, there is less cytotoxicity since the fine-tuning of structural features can modulate the polymer toxicity against bacterial cells. Even though the binding mediated by electrostatic interaction is non-specific, the bacterial membrane was not largely affected (Fig. 4.5). Studies have hypothesised that the binding of cationic compounds to LPS portions allows the formation of phospholipid channels were lipophilic compounds can cross while the overall integrity of the membrane remains (Vaara, 1992).

The physical capturing also suggests the inhibition of movement which is critical in some motile bacteria to start virulence. As shown in Chapter 4 figure 4.3A, polymers are able to reduce the motility and the increase of the ionic strength restore the motility as electrostatic interaction are displaced. Motility is an important cue for virulence as in the related species *V. parahaemolyticus* this occurs mediated by the surface sensing program where the bacterium switch from swimming to swarming to initiate colonisation and virulence. This switching is correlated with lower concentration of the second messenger c-di-GMP that modulates gene expression accordingly (Gode-Potratz *et al.*, 2011). Although the surface sensing program in *V. cholerae* and *V. parahaemolyticus* differs, the inhibition of flagella movement or the absence of it reduces the colonisation ability of *V. cholerae* (Richardson, 1991, Almagro-Moreno *et al.*, 2015a). Non-motile mutants of *V. cholerae* N16961 are unable to properly colonise rabbit ileal mucosae (Richardson, 1991) and tend to auto agglutinate when growing in liquid media under permissive conditions (LB pH 8.5), reducing the adhesion as the fewer adhesion factors fucose-sensitive hemagglutinin and HEp-2 adhesins are produced (Gardel and Mekalanos, 1996). The relation between motility regulatory proteins and their impact on virulence expression in *V. cholerae* is still not fully understood, but it has been suggested that the movement of the flagellum allows for the correct spatiotemporal expression of colonisation-related genes (Syed *et al.*, 2009). Although non-motile mutants upregulate virulence genes (Gardel and Mekalanos, 1996), the inability to colonise leads to a reduced bacterial burden and thus toxicity overall. It would be useful to compare the colonisation under clustering conditions with a non-flagellar mutant.

Virulence and biofilm in *V. cholerae* are tightly related processes and the activation of both mostly simultaneous (Silva and Benitez, 2016). Activation of such processes have in common quorum sensing regulators, therefore, the cell density plays an important role. A relevant phenotype observed was the active production of biofilm during clustering with any of the three

polymers, discussed in Chapter 5. It is known that biofilm is a form of defence against toxic compounds (Teschler *et al.*, 2015, Hansen *et al.*, 2007). Despite the fact that P1, P2 and P3 showed low antimicrobial potential, biofilm was induced significantly (Fig. 5.2). The synthesis of biofilm seems to respond to many other pathways and not only cell density. As explained above, the induction of biofilm is subjected to modulation by c-di-GMP (Tischler and Camilli, 2005), the stationary phase alternative sigma factor *rpoS* (Yildiz *et al.*, 2004) or carbon starvation via cAMP receptor protein (CRP) molecule (Fong and Yildiz, 2008). The clustering mediated by P1, P2 or P3, although they increase the local cell density, the induction of biofilm seems to not correlate to cell density, and could be the result of other signals in a strategy to defend from the binding groups. Furthermore, the capturing and biofilm synthesis might form a hybrid matrix between polymers and exopolysaccharide which prevents the bacteria to disperse by normal enzymatic rearrangement of the matrix. The impediment to disperse from the clusters might also explain the defects on colonisation of Caco-2 cells and zebrafish intestinal tract in the sense that the bacteria cannot dissociate from the polymer, discussed in Chapter 7.

Within the biofilm structural component, extracellular DNA draws our attention. Here we developed a simple microscope-based method to detect and quantify it by staining with Hoechst and rendering orthogonal projection of the biofilm of digested and undigested eDNA (Fig. 5.2 and Fig. 5.3). There was more eDNA when *V. cholerae* was clustered at higher concentration of polymer. The wide role of eDNA within biofilm suggest that is a versatile component and easily manipulable by the bacteria (Okshevsky and Meyer, 2015, Seper *et al.*, 2011). It is likely that the presence of eDNA in the cluster mediated biofilm responds to a charge buffering effect to control the cationic groups.

Results presented in Chapter 5, 6 and 7 may suggest that clustering is a cue of high cell density at local level. This effect might be helping to induce the quorum sensing route as the

concentration of autoinducers within clusters might be higher, and possibly the permeabilisation of the outer membrane helps the autoinducers to reach their receptors. The clustering with P1, P2 or P3 had a significant impact on the expression of virulence genes as discussed in Chapter 7. In *V. cholerae* virulence is related to high cell density as the absence of AphA will prevent the ToxR regulon expression. Similarly to biofilm production, virulence is modulated by numerous regulators (Skorupski and Taylor, 1997). Despite the fact that virulence is usually active during low cell density, its control is tightly regulated by environmental conditions as well. Although there was a reduction in the transcription of virulence-related genes which correlates with less cAMP due to poor expression of cholera toxin, it is necessary to support this protective effect with a non *toxT* or non-virulence factors background, allowing to compare phenotypic switch from virulent to avirulent phenotype.

In order to shed light on the effect of the clustering induced quorum sensing phenotype, the quorum sensing route was dissected using *V. cholerae* mutants, discussed in Chapter 6. So far, the quorum sensing route seems to be intact upon clustering and phenotypic output has been observed in *V. harveyi*. The clustering enhances the *V. harveyi* luminescence, similarly to the effect showed here with *V. cholerae* pBB1, with polymers and dendrimer with similar amine groups as P1 and P2 (Lui *et al.*, 2013, Leire *et al.*, 2016). Introducing the *lux* operon in *V. cholerae* resulted in its heterologous expression during clustering when using P1 and P2. The maximum induction of luminescence mainly occurs at 4 hours, after that the luminescence peak drops to undetectable levels (Fig. 6.2). This luminescence pattern was observed also when nutrient was added to the media, especially peptone which increase the luminescence at levels similar to the clustering by polymers suggesting that nutrients such as amino acids and polymers may share an inductive property of the luminescence (Fig. 6.3).

In the same sense, iron starvation triggers HapR independent luminescence activation in *V. fischeri* (Haygood and Nealson, 1985). Likewise, carbon starvation induces *lux* operon in *V.*

fischeri via CRP. Under starvation conditions adenylate cyclises increase the cAMP concentration inducing the regulatory activity of cAMP-CRP which not only interact with the quorum sensing route but with other important cell functions (Friedrich and Greenberg, 1983). Activation of a quorum sensing phenotype due to limited diffusion of nutrients within the clusters has been suggested. Here, it was demonstrated that nutrients can diffuse across the clusters while quorum sensing phenotype is still induced. Also, the presence of CRP is important for the induction as no CRP background resulted in no induction of luminescence which correlates with phenotype exhibit by *E. coli* Δ*crp* (Dunlap and Greenberg, 1988). The activation of luminescence was followed by pictures showing a coordinated effect since every cluster glow simultaneously (Fig 6.2H). The microenvironment formed within the cluster lead to think that diffusion of nutrients induced a starvation state that seems to modulate the luminescence through cAMP receptor protein (CRP), however, the addition of nutrients maintains the luminescence of clusters suggesting that diffusion is not limited within clusters and starvation is not happening in the clusters. Moreover, the CRP is vital to maintaining the luminescence. Since the quorum sensing circuit has a positive feedback, the phenotype induced by clustering seems to induce a normal activation of quorum sensing since this feedback is unaltered. At the same time, the *Vibrio*-specific communication (CAI-1) has been reported to be dominant over the inter-species communication (AI-2) (Rutherford and Bassler, 2012). The clustering does not represents negative effect over the quorum sensing route and autoinducer production is normal.

The potential of polymers to reduce virulence and adhesion was tested in an *in vivo* model. Zebrafish are a natural host model for *V. cholerae* colonisation and transmission (Wang *et al.*, 2012, Runft *et al.*, 2014) since the gastrointestinal tract of the fish is similar to the mammalian in terms of physiology and development (Ng *et al.*, 2005). A decrease in the colonisation suggests a protective effect of polymers in this model and images support this as less bacterial

burden was observed (Fig. 7.8). Due to animal licence restrictions, the survival could not be assessed in order to test if the protective effect of polymers would persist over an extended period.

The reduction of the virulence due to polymer-mediated clustering indicates the complexity of the interaction between the polymers and the bacterial cell envelope. These interactions could result in perturbations on the bacterial cell envelope which activate cell envelope stress pathways like σ^E or Cpx (Grabowicz and Silhavy, 2017). Such pathways have been associated with diminished virulence in *Vibrio* species. Mutants of *V. parahaemolyticus* in *rpoE*, homologous to *E. coli* σ^E, are defective in their ability to colonise adult mice (Haines-Menges *et al.*, 2014). Moreover, insults on the *V. cholerae* outer membrane activate the Cpx pathway inhibiting the expression of *toxT* through an unknown CRP-dependent pathway (Acosta *et al.*, 2015).

Another question that remains open is how to improve the selectivity of these materials. Since the interaction of these materials is non-specific and their toxicity on mammalian cells is significant, studies are necessary to improve and enhance their selectivity. Chitinous materials were used to explore their potential to capture *V. cholerae*. In nature, *V cholerae* is usually found attached to the exoskeleton of zooplankton and crustacean where uses the chitin as carbon source (Svitil *et al.*, 1997). Therefore, it seems feasible to explore chitinous materials as source of attachment for *V. cholerae*. Here, *V. cholerae* chitin metabolism was active when in contact with chitin flakes or chitin beads; extracellular chitinases and regulator *chiS* were transcribed 3-4-fold compared with bacteria growing in the absence of the material (Fig. 5.5A). Then, the clustering with P1 and P2 resulted in no changes in the expression of the *lacZ* reporters which may suggest that chitin metabolism is active in clustered cells and chitinous oligomers are in contact with the ChiS cognate periplasmic chitin binding protein (Li and Roseman, 2004). In addition, the adhesion of *V. cholerae* to chitin flakes and chitin bead was

quick since after 5 minutes of exposure, both materials were colonised in high numbers (Fig. 5.5C). The adhesion is mediated by chitin binding proteins (CBP) which mediated specific binding with the surface. This sessile lifestyle usually leads to the formation of biofilm (Watnick *et al.*, 1999). Two type IV pili used by the *V. cholerae* to establish the adhesions are GbpA and MSHA. GbpA is especially important since it has been reported that mediates specific binding to chitin as well as the binding to mucin during infection of mammalian host due to carbohydrate binding domains in its structure (Wong *et al.*, 2012). Also, the MSHA pilus mediates both adhesion to chitin and to non-metabolisable mannose residues during host infection (Utada *et al.*, 2014). Moreover, since the adhesion is mediated by conserved structures across *Vibrio* species, chitin seems to be a good candidate to enhance the selectivity not only to *V. cholerae* but for example to the important human pathogen *V. parahaemolyticus*. These two structures highlight the potential to use chitin-derivates as ligands to increase the specificity towards *V. cholerae*.

Finally, this work demonstrates how the clustering of non-bactericidal cationic polymer reduced the virulence of *V. cholerae* at transcriptional level, at the same time quorum sensing is induced and biofilm as well. Since clustering creates micro-environments where nutrients can diffuse freely, the sensing of quorum-sensing autoinducers is enhanced due to the short distances between bacteria. The bacteria within the cluster exhibit a sessile avirulent lifestyle which is similar to high cell density where virulence and quorum sensing are activated. However the induction of biofilm is high. Biofilm regulation is complex and responds to several other cues than quorum sensing such as the second messenger c-di-GMP. Since the impact of the clustering at global level is still unclear, it is not surprising that routes other than quorum sensing is being activated, where motility seems to be important to explore due to immobilisation by clustering. Still is important to explore new polymers and new binding groups to improve the specificity of the material and reduce the side effect over the host. With

this cationic polymer, the clustering induces a sessile non-virulent phenotype with an increase in the biofilm production as result of a force immobilisation switching from planktonic to sessile lifestyle (Fig. 8.2). The capturing by electrostatic interaction perturbs the structure of the outer membrane favouring the permeability where autoinducers movement and sensing is improved. A high cell density phenotype is induced in the cluster with reduction of virulence and motility and enhancement of quorum sensing traits and biofilm through a yet unclear mechanism.
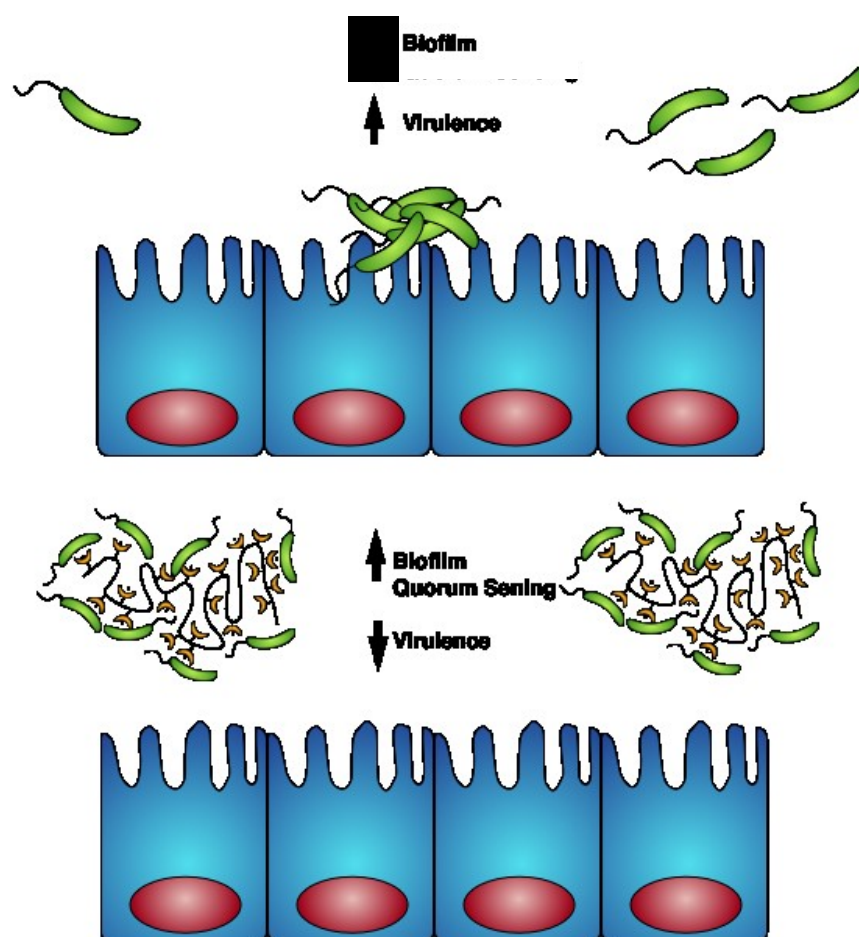
Figure 8.1. Schematic representation of *V. cholerae* infection and effect of polymers reported in this work. A) During infection *V. cholerae* is associated with colonisation of the intestinal tract and increase levels of virulence and biofilm. Once polymers cluster the bacteria, the colonisation is impeded.

List of references.

ACOSTA, N., PUKATZKI, S. & RAIVIO, T. L. 2015. The Cpx system regulates virulence gene expression in Vibrio cholerae. *Infect Immun,* 83**,** 2396-408.

ALLEGRANZI, B., BAGHERI NEJAD, S., CHRAITI, M., CASTILLEJOS, G., KILPATRICK, C. & KELLEY, E. 2011. Report on the burden of endemic health care-associated infection worldwide. *Geneva, Switzerland: World Health Organization*.

ALLEN, T. M. & CULLIS, P. R. 2004. Drug delivery systems: entering the mainstream. *Science,* 303**,** 1818-22.

ALMAGRO-MORENO, S. & BOYD, E. F. 2009a. Insights into the evolution of sialic acid catabolism among bacteria. *BMC Evol Biol,* 9**,** 118.

ALMAGRO-MORENO, S. & BOYD, E. F. 2009b. Sialic acid catabolism confers a competitive advantage to pathogenic vibrio cholerae in the mouse intestine. *Infect Immun,* 77**,** 3807-16.

ALMAGRO-MORENO, S., PRUSS, K. & TAYLOR, R. K. 2015a. Intestinal Colonization Dynamics of Vibrio cholerae. *PLoS Pathog,* 11**,** e1004787.

ALMAGRO-MORENO, S., ROOT, M. Z. & TAYLOR, R. K. 2015b. Role of ToxS in the proteolytic cascade of virulence regulator ToxR in Vibrio cholerae. *Mol Microbiol,* 98**,** 963-76.

ANTONOVA, E. S. & HAMMER, B. K. 2011. Quorum-sensing autoinducer molecules produced by members of a multispecies biofilm promote horizontal gene transfer to Vibrio cholerae. *FEMS Microbiol Lett,* 322**,** 68-76.

ATTRIDGE, S. R., VOSS, E. & MANNING, P. A. 1999. Pathogenic and vaccine significance of toxin-coregulated pili of Vibrio cholerae E1 Tor. *J Biotechnol,* 73**,** 109-17.

BARDILL, J. P., ZHAO, X. & HAMMER, B. K. 2011. The Vibrio cholerae quorum sensing response is mediated by Hfq-dependent sRNA/mRNA base pairing interactions. *Mol Microbiol,* 80**,** 1381-94.

BARNETT, R. & COLLECTION, W. 2014. *The Sick Rose, Or, Disease and the Art of Medical Illustration*, Thames & Hudson.

BARTLETT, T. M., BRATTON, B. P., DUVSHANI, A., MIGUEL, A., SHENG, Y., MARTIN, N. R., NGUYEN, J. P., PERSAT, A., DESMARAIS, S. M., VANNIEUWENHZE, M. S., HUANG, K. C., ZHU, J., SHAEVITZ, J. W. & GITAI, Z. 2017. A Periplasmic Polymer Curves Vibrio cholerae and Promotes Pathogenesis. *Cell,* 168**,** 172-185 e15.

BASSLER, B. L., WRIGHT, M., SHOWALTER, R. E. & SILVERMAN, M. R. 1993. Intercellular signalling in Vibrio harveyi: sequence and function of genes regulating expression of luminescence. *Mol Microbiol,* 9**,** 773-86.

BECK, N. A., KRUKONIS, E. S. & DIRITA, V. J. 2004. TcpH influences virulence gene expression in Vibrio cholerae by inhibiting degradation of the transcription activator TcpP. *Journal of bacteriology,* 186**,** 8309-8316.

BEHARI, J., STAGON, L. & CALDERWOOD, S. B. 2001. pepA, a gene mediating pH regulation of virulence genes in Vibrio cholerae. *J Bacteriol,* 183**,** 178-88.

BELL, A. I., GASTON, K. L., COLE, J. A. & BUSBY, S. J. 1989. Cloning of binding sequences for the Escherichia coli transcription activators, FNR and CRP: location of bases involved in discrimination between FNR and CRP. *Nucleic Acids Res,* 17**,** 3865-74.

BERK, V., FONG, J. C., DEMPSEY, G. T., DEVELIOGLU, O. N., ZHUANG, X., LIPHARDT, J., YILDIZ, F. H. & CHU, S. 2012. Molecular architecture and assembly principles of Vibrio cholerae biofilms. *Science,* 337**,** 236-9.

BEYHAN, S., ODELL, L. S. & YILDIZ, F. H. 2008. Identification and characterization of cyclic diguanylate signaling systems controlling rugosity in Vibrio cholerae. *J Bacteriol,* 190**,** 7392-405.

BEYHAN, S., TISCHLER, A. D., CAMILLI, A. & YILDIZ, F. H. 2006. Differences in gene expression between the classical and El Tor biotypes of Vibrio cholerae O1. *Infection and immunity,* 74**,** 3633-3642.

BOCHICCHIO, D., PANIZON, E., MONTICELLI, L. & ROSSI, G. 2017. Interaction of hydrophobic polymers with model lipid bilayers. *Sci Rep,* 7**,** 6357.

BOEDICKER, J. Q., VINCENT, M. E. & ISMAGILOV, R. F. 2009. Microfluidic confinement of single cells of bacteria in small volumes initiates high-density behavior of quorum sensing and growth and reveals its variability. *Angew Chem Int Ed Engl,* 48**,** 5908-11.

BOLES, B. R., THOENDEL, M. & SINGH, P. K. 2004. Self-generated diversity produces "insurance effects" in biofilm communities. *Proc Natl Acad Sci U S A,* 101**,** 16630-5.

BORGEAUD, S., METZGER, L. C., SCRIGNARI, T. & BLOKESCH, M. 2015. The type VI secretion system of Vibrio cholerae fosters horizontal gene transfer. *Science,* 347**,** 63-7.

BRAUNECKER, W. A. & MATYJASZEWSKI, K. 2007. Controlled/living radical polymerization: Features, developments, and perspectives. *Progress in Polymer Science,* 32**,** 93-146.

BROWN, R. C. & TAYLOR, R. K. 1995. Organization of tcp, acf, and toxT genes within a ToxT‐dependent operon. *Molecular microbiology,* 16**,** 425-439.

BUROW, M., PETERLIN, A. & TURNER, D. 1964. Increasing viscosity of polymer solutions with increasing shear stress. *Journal of Polymer Science Part C: Polymer Letters,* 2**,** 67-70.

CARMICHAEL, A. J., HADDLETON, D. M., BON, S. A. & SEDDON, K. R. 2000. Copper (I) mediated living radical polymerisation in an ionic liquid. *Chemical Communications***,** 1237-1238.

CASAS, V. & MALOY, S. 2011. Role of bacteriophage-encoded exotoxins in the evolution of bacterial pathogens. *Future microbiology,* 6**,** 1461-1473.

CASH, R. A., MUSIC, S. I., LIBONATI, J. P., SNYDER, M. J., WENZEL, R. P. & HORNICK, R. B. 1974. Response of man to infection with Vibrio cholerae. I. Clinical, serologic, and bacteriologic responses to a known inoculum. *J Infect Dis,* 129**,** 45-52.

CERVIN, J., WANDS, A. M., CASSELBRANT, A., WU, H., KRISHNAMURTHY, S., CVJETKOVIC, A., ESTELIUS, J., DEDIC, B., SETHI, A., WALLOM, K. L., RIISE, R., BACKSTROM, M., WALLENIUS, V., PLATT, F. M., LEBENS, M., TENEBERG, S., FANDRIKS, L., KOHLER, J. J. & YRLID, U. 2018. GM1 ganglioside-independent intoxication by Cholera toxin. *PLoS Pathog,* 14**,** e1006862.

CHATTERJEE, S. & CHAUDHURI, K. 2003. Lipopolysaccharides of Vibrio cholerae: I. Physical and chemical characterization. *Biochimica et Biophysica Acta (BBA)-Molecular Basis of Disease,* 1639**,** 65-79.

CHEN, C. Z. & COOPER, S. L. 2002. Interactions between dendrimer biocides and bacterial membranes. *Biomaterials,* 23**,** 3359-3368.

CHIEFARI, J., CHONG, Y. K., ERCOLE, F., KRSTINA, J., JEFFERY, J., LE, T. P. T., MAYADUNNE, R. T. A., MEIJS, G. F., MOAD, C. L., MOAD, G., RIZZARDO, E. & THANG, S. H. 1998. Living free-radical polymerization by reversible addition-fragmentation chain transfer: The RAFT process. *Macromolecules,* 31**,** 5559-5562.

CHILDERS, B. M. & KLOSE, K. E. 2007. Regulation of virulence in Vibrio cholerae: the ToxR regulon.

CLARK, M. & DESIMONE, J. CATIONIC POLYMERIZATIONS IN SUPERCRITICAL CARBON-DIOXIDE. ABSTRACTS OF PAPERS OF THE AMERICAN

CHEMICAL SOCIETY, 1994. AMER CHEMICAL SOC 1155 16TH ST, NW, WASHINGTON, DC 20036, 88-POLY.

CLATWORTHY, A. E., PIERSON, E. & HUNG, D. T. 2007. Targeting virulence: a new paradigm for antimicrobial therapy. *Nat Chem Biol,* 3**,** 541-8.

COLOMBANI, D. 1997. Chain-growth control in free radical polymerization. *Progress in polymer science,* 22**,** 1649-1720.

COLOMBANI, O., LANGELIER, O., MARTWONG, E. & CASTIGNOLLES, P. 2010. Polymerization Kinetics: Monitoring Monomer Conversion Using an Internal Standard and the Key Role of Sample t 0. *Journal of Chemical Education,* 88**,** 116-121.

CONTRERAS, G. A., BELL, C. S., DEL BIANCO, G. P., PEREZ, N., KLEINOSKY, M. T., MURPHY, J. R. & HERESI, G. P. 2013. Prevalence and risk factors associated with resistance-associated mutations to etravirine in a cohort of perinatally HIV-infected children. *J Antimicrob Chemother,* 68**,** 2344-8.

CORFIELD, A., MYERSCOUGH, N., LONGMAN, R., SYLVESTER, P., ARUL, S. & PIGNATELLI, M. 2000. Mucins and mucosal protection in the gastrointestinal tract: new prospects for mucins in the pathology of gastrointestinal disease. *Gut,* 47**,** 589-594.

CRISAN, D. N., CREESE, O., BALL, R., BRIOSO, J. L., MARTYN, B., MONTENEGRO, J. & FERNANDEZ-TRILLO, F. 2017. Poly(acryloyl hydrazide), a versatile scaffold for the preparation of functional polymers: synthesis and post-polymerisation modification. *Polymer Chemistry,* 8**,** 4576-4584.

DANESE, P. N., PRATT, L. A. & KOLTER, R. 2000. Exopolysaccharide production is required for development of Escherichia coli K-12 biofilm architecture. *J Bacteriol,* 182**,** 3593-6.

DAVIES, D. G., PARSEK, M. R., PEARSON, J. P., IGLEWSKI, B. H., COSTERTON, J. W. & GREENBERG, E. P. 1998. The involvement of cell-to-cell signals in the development of a bacterial biofilm. *Science,* 280**,** 295-8.

DEAN, J. A. & LANGE, N. A. 1973. Lange's handbook of chemistry. New York: McGraw-Hill.

DEFOIRDT, T. 2017. Quorum-Sensing Systems as Targets for Antivirulence Therapy. *Trends Microbiol.*

DEFOIRDT, T., BRACKMAN, G. & COENYE, T. 2013. Quorum sensing inhibitors: how strong is the evidence? *Trends in microbiology,* 21**,** 619-624.

DELPLACE, V. & NICOLAS, J. 2015. Degradable vinyl polymers for biomedical applications. *Nat Chem,* 7**,** 771-84.

DEY, A. K., BHAGAT, A. & CHOWDHURY, R. 2013. Host cell contact induces expression of virulence factors and VieA, a cyclic di-GMP phosphodiesterase, in Vibrio cholerae. *J Bacteriol,* 195**,** 2004-10.

DIGGLE, S. P., GRIFFIN, A. S., CAMPBELL, G. S. & WEST, S. A. 2007. Cooperation and conflict in quorum-sensing bacterial populations. *Nature,* 450**,** 411-4.

DIRITA, V. J., NEELY, M., TAYLOR, R. K. & BRUSS, P. M. 1996. Differential expression of the ToxR regulon in classical and E1 Tor biotypes of Vibrio cholerae is due to biotype-specific control over toxT expression. *Proc Natl Acad Sci U S A,* 93**,** 7991-5.

DIRITA, V. J., PARSOT, C., JANDER, G. & MEKALANOS, J. J. 1991. Regulatory cascade controls virulence in Vibrio cholerae. *Proc Natl Acad Sci U S A,* 88**,** 5403-7.

DOOLEY, K. & ZON, L. I. 2000. Zebrafish: a model system for the study of human disease. *Curr Opin Genet Dev,* 10**,** 252-6.

DRAMSI, S., MAGNET, S., DAVISON, S. & ARTHUR, M. 2008. Covalent attachment of proteins to peptidoglycan. *FEMS microbiology reviews,* 32**,** 307-320.

DUNLAP, P. V. & GREENBERG, E. 1988. Control of Vibrio fischeri lux gene transcription by a cyclic AMP receptor protein-luxR protein regulatory circuit. *Journal of bacteriology,* 170**,** 4040-4046.

DZIEJMAN, M., BALON, E., BOYD, D., FRASER, C. M., HEIDELBERG, J. F. & MEKALANOS, J. J. 2002. Comparative genomic analysis of Vibrio cholerae: genes that correlate with cholera endemic and pandemic disease. *Proceedings of the National Academy of Sciences,* 99**,** 1556-1561.

ENGEBRECHT, J., NEALSON, K. & SILVERMAN, M. 1983. Bacterial bioluminescence: isolation and genetic analysis of functions from Vibrio fischeri. *Cell,* 32**,** 773-81.

ENGESZER, R. E., PATTERSON, L. B., RAO, A. A. & PARICHY, D. M. 2007. Zebrafish in the wild: a review of natural history and new notes from the field. *Zebrafish,* 4**,** 21-40.

ENGLAND, N. 2015. Improving outcomes for patients with sepsis: a cross-system action plan. *London: NHS England.*

FIGURSKI, D. H., POHLMAN, R. F., BECHHOFER, D. H., PRINCE, A. S. & KELTON, C. A. 1982. Broad host range plasmid RK2 encodes multiple kil genes potentially lethal to Escherichia coli host cells. *Proc Natl Acad Sci U S A,* 79**,** 1935-9.

FISCHER, H. 2001. The persistent radical effect: a principle for selective radical reactions and living radical polymerizations. *Chem Rev,* 101**,** 3581-610.

FISHMAN, P. H., MOSS, J. & VAUGHAN, M. 1976. Uptake and metabolism of gangliosides in transformed mouse fibroblasts. Relationship of ganglioside structure to choleragen response. *J Biol Chem,* 251**,** 4490-4.

FLEMMING, H. C., WINGENDER, J., SZEWZYK, U., STEINBERG, P., RICE, S. A. & KJELLEBERG, S. 2016. Biofilms: an emergent form of bacterial life. *Nat Rev Microbiol,* 14**,** 563-75.

FONG, J. C., SYED, K. A., KLOSE, K. E. & YILDIZ, F. H. 2010. Role of Vibrio polysaccharide (vps) genes in VPS production, biofilm formation and Vibrio cholerae pathogenesis. *Microbiology,* 156**,** 2757-69.

FONG, J. C. & YILDIZ, F. H. 2008. Interplay between cyclic AMP-cyclic AMP receptor protein and cyclic di-GMP signaling in Vibrio cholerae biofilm formation. *J Bacteriol,* 190**,** 6646-59.

FRIEDRICH, W. & GREENBERG, E. 1983. Glucose repression of luminescence and luciferase in Vibrio fischeri. *Archives of microbiology,* 134**,** 87-91.

FRISCHKORN, K. R., STOJANOVSKI, A. & PARANJPYE, R. 2013. Vibrio parahaemolyticus type IV pili mediate interactions with diatom-derived chitin and point to an unexplored mechanism of environmental persistence. *Environ Microbiol,* 15**,** 1416-27.

FULLNER, K. J. & MEKALANOS, J. J. 2000. In vivo covalent cross‐linking of cellular actin by the Vibrio cholerae RTX toxin. *The EMBO journal,* 19**,** 5315-5323.

GAN, L., CHEN, S. & JENSEN, G. J. 2008. Molecular organization of Gram-negative peptidoglycan. *Proceedings of the National Academy of Sciences,* 105**,** 18953-18957.

GARDEL, C. L. & MEKALANOS, J. J. 1996. Alterations in Vibrio cholerae motility phenotypes correlate with changes in virulence factor expression. *Infection and immunity,* 64**,** 2246-2255.

GARNER, A. L., PARK, J., ZAKHARI, J. S., LOWERY, C. A., STRUSS, A. K., SAWADA, D., KAUFMANN, G. F. & JANDA, K. D. 2011. A multivalent probe for AI-2 quorum-sensing receptors. *J Am Chem Soc,* 133**,** 15934-7.

GHIGO, J. M. 2001. Natural conjugative plasmids induce bacterial biofilm development. *Nature,* 412**,** 442-5.

GLINEUR, C. & LOCHT, C. 1994. Importance of ADP-ribosylation in the morphological changes of PC12 cells induced by cholera toxin. *Infect Immun,* 62**,** 4176-85.

GODE-POTRATZ, C. J., KUSTUSCH, R. J., BREHENY, P. J., WEISS, D. S. & MCCARTER, L. L. 2011. Surface sensing in Vibrio parahaemolyticus triggers a programme of gene expression that promotes colonization and virulence. *Mol Microbiol,* 79**,** 240-63.

GOFORTH, J. B., WALTER, N. E. & KARATAN, E. 2013. Effects of polyamines on Vibrio cholerae virulence properties. *PLoS One,* 8**,** e60765.

GOLDBERG, J. B. & OHMAN, D. E. 1984. Cloning and expression in Pseudomonas aeruginosa of a gene involved in the production of alginate. *J Bacteriol,* 158**,** 1115-21.

GRABOWICZ, M. & SILHAVY, T. J. 2017. Envelope Stress Responses: An Interconnected Safety Net. *Trends Biochem Sci,* 42**,** 232-242.

GRACE, J. L., HUANG, J. X., CHEAH, S.-E., TRUONG, N. P., COOPER, M. A., LI, J., DAVIS, T. P., QUINN, J. F., VELKOV, T. & WHITTAKER, M. R. 2016. Antibacterial low molecular weight cationic polymers: dissecting the contribution of hydrophobicity, chain length and charge to activity. *RSC advances,* 6**,** 15469-15477.

GRIFFITH, L. 2000. Polymeric biomaterials. *Acta materialia,* 48**,** 263-277.

GRUBBS, R. B. 2011. Nitroxide-Mediated Radical Polymerization: Limitations and Versatility. *Polymer Reviews,* 51**,** 104-137.

HAAS, B. L., MATSON, J. S., DIRITA, V. J. & BITEEN, J. S. 2014. Imaging live cells at the nanometer-scale with single-molecule microscopy: obstacles and achievements in experiment optimization for microbiology. *Molecules,* 19**,** 12116-12149.

HACKER, M. C. & MIKOS, A. G. 2011. Synthetic Polymers. *Principles of Regenerative Medicine, 2nd Edition***,** 587-622.

HAINES-MENGES, B., WHITAKER, W. B. & BOYD, E. F. 2014. Alternative Sigma Factor RpoE Is Important for Vibrio parahaemolyticus Cell Envelope Stress Response and Intestinal Colonization. *Infection and Immunity,* 82**,** 3667-3677.

HALL-STOODLEY, L. & STOODLEY, P. 2005. Biofilm formation and dispersal and the transmission of human pathogens. *Trends Microbiol,* 13**,** 7-10.

HAMMER, B. K. & BASSLER, B. L. 2003. Quorum sensing controls biofilm formation in Vibrio cholerae. *Molecular microbiology,* 50**,** 101-104.

HANG, L., JOHN, M., ASADUZZAMAN, M., BRIDGES, E. A., VANDERSPURT, C., KIRN, T. J., TAYLOR, R. K., HILLMAN, J. D., PROGULSKE-FOX, A., HANDFIELD, M., RYAN, E. T. & CALDERWOOD, S. B. 2003. Use of in vivo-induced antigen technology (IVIAT) to identify genes uniquely expressed during human infection with Vibrio cholerae. *Proc Natl Acad Sci U S A,* 100**,** 8508-13.

HANKINS, J. V., MADSEN, J. A., GILES, D. K., BRODBELT, J. S. & TRENT, M. S. 2012. Amino acid addition to Vibrio cholerae LPS establishes a link between surface remodeling in gram-positive and gram-negative bacteria. *Proc Natl Acad Sci U S A,* 109**,** 8722-7.

HANSEN, S. K., RAINEY, P. B., HAAGENSEN, J. A. & MOLIN, S. 2007. Evolution of species interactions in a biofilm community. *Nature,* 445**,** 533-6.

HARKEY, C. W., EVERISS, K. D. & PETERSON, K. M. 1994. The Vibrio cholerae toxin-coregulated-pilus gene tcpI encodes a homolog of methyl-accepting chemotaxis proteins. *Infection and immunity,* 62**,** 2669-2678.

HARMSEN, M., LAPPANN, M., KNOCHEL, S. & MOLIN, S. 2010. Role of extracellular DNA during biofilm formation by Listeria monocytogenes. *Appl Environ Microbiol,* 76**,** 2271-9.

HÄSE, C. C. & MEKALANOS, J. J. 1998. TcpP protein is a positive regulator of virulence gene expression in Vibrio cholerae. *Proceedings of the National Academy of Sciences,* 95**,** 730-734.

HAYGOOD, M. G. & NEALSON, K. H. 1985. Mechanisms of iron regulation of luminescence in Vibrio fischeri. *J Bacteriol,* 162**,** 209-16.

HEIDELBERG, J. F., EISEN, J. A., NELSON, W. C., CLAYTON, R. A., GWINN, M. L., DODSON, R. J., HAFT, D. H., HICKEY, E. K., PETERSON, J. D., UMAYAM, L., GILL, S. R., NELSON, K. E., READ, T. D., TETTELIN, H., RICHARDSON, D., ERMOLAEVA, M. D., VAMATHEVAN, J., BASS, S., QIN, H., DRAGOI, I., SELLERS, P., MCDONALD, L., UTTERBACK, T., FLEISHMANN, R. D., NIERMAN, W. C., WHITE, O., SALZBERG, S. L., SMITH, H. O., COLWELL, R. R., MEKALANOS, J. J., VENTER, J. C. & FRASER, C. M. 2000. DNA sequence of both chromosomes of the cholera pathogen Vibrio cholerae. *Nature,* 406**,** 477-83.

HELANDER, I. M. & MATTILA-SANDHOLM, T. 2000. Fluorometric assessment of gram-negative bacterial permeabilization. *J Appl Microbiol,* 88**,** 213-9.

HENDRICKX, L., HAUSNER, M. & WUERTZ, S. 2003. Natural genetic transformation in monoculture Acinetobacter sp. strain BD413 biofilms. *Appl Environ Microbiol,* 69**,** 1721-7.

HIBBING, M. E. & FUQUA, C. 2012. Inhibition and dispersal of Agrobacterium tumefaciens biofilms by a small diffusible Pseudomonas aeruginosa exoproduct(s). *Arch Microbiol,* 194**,** 391-403.

HOLMGREN, J., LONNROTH, I., MANSSON, J. & SVENNERHOLM, L. 1975. Interaction of cholera toxin and membrane GM1 ganglioside of small intestine. *Proc Natl Acad Sci U S A,* 72**,** 2520-4.

HOOK, A. L., CHANG, C.-Y., YANG, J., LUCKETT, J., COCKAYNE, A., ATKINSON, S., MEI, Y., BAYSTON, R., IRVINE, D. J. & LANGER, R. 2012. Combinatorial discovery of polymers resistant to bacterial attachment. *Nature biotechnology,* 30**,** 868.

HSIAO, A., AHMED, A. M., SUBRAMANIAN, S., GRIFFIN, N. W., DREWRY, L. L., PETRI, W. A., JR., HAQUE, R., AHMED, T. & GORDON, J. I. 2014. Members of the human gut microbiota involved in recovery from Vibrio cholerae infection. *Nature,* 515**,** 423-6.

HU, J., ZHANG, G. & LIU, S. 2012. Enzyme-responsive polymeric assemblies, nanoparticles and hydrogels. *Chemical Society Reviews,* 41**,** 5933-5949.

HUGHES, K. J., EVERISS, K. D., HARKEY, C. W. & PETERSON, K. M. 1994. Identification of a Vibrio cholerae ToxR-activated gene (tagD) that is physically linked to the toxin-coregulated pilus (tcp) gene cluster. *Gene,* 148**,** 97-100.

HULBERT, R. R. & TAYLOR, R. K. 2002. Mechanism of ToxT-dependent transcriptional activation at the Vibrio cholerae tcpA promoter. *J Bacteriol,* 184**,** 5533-44.

INSUA, I., LIAMAS, E., ZHANG, Z., PEACOCK, A. F., KRACHLER, A. M. & FERNANDEZ-TRILLO, F. 2016. Enzyme-responsive polyion complex (PIC) nanoparticles for the targeted delivery of antimicrobial polymers. *Polym Chem,* 7**,** 2684-2690.

IWANAGA, M. & YAMAMOTO, K. 1985. New medium for the production of cholera toxin by Vibrio cholerae O1 biotype El Tor. *J Clin Microbiol,* 22**,** 405-8.

JOBLING, M. G. & HOLMES, R. K. 1997. Characterization of hapR, a positive regulator of the Vibrio cholerae HA/protease gene hap, and its identification as a functional homologue of the Vibrio harveyi luxR gene. *Mol Microbiol,* 26**,** 1023-34.

JOELSSON, A., LIU, Z. & ZHU, J. 2006. Genetic and phenotypic diversity of quorum-sensing systems in clinical and environmental isolates of Vibrio cholerae. *Infect Immun,* 74**,** 1141-7.

JOFRE, E., LAGARES, A. & MORI, G. 2004. Disruption of dTDP-rhamnose biosynthesis modifies lipopolysaccharide core, exopolysaccharide production, and root colonization in Azospirillum brasilense. *FEMS Microbiol Lett,* 231**,** 267-75.

JOHNSON, R. A., UDDIN, T., AKTAR, A., MOHASIN, M., ALAM, M. M., CHOWDHURY, F., HARRIS, J. B., LAROCQUE, R. C., BUFANO, M. K., YU, Y., WU-FREEMAN,

Y., LEUNG, D. T., SARRACINO, D., KRASTINS, B., CHARLES, R. C., XU, P., KOVAC, P., CALDERWOOD, S. B., QADRI, F. & RYAN, E. T. 2012. Comparison of immune responses to the O-specific polysaccharide and lipopolysaccharide of Vibrio cholerae O1 in Bangladeshi adult patients with cholera. *Clin Vaccine Immunol,* 19**,** 1712-21.

JOHNSON, T. L., FONG, J. C., RULE, C., ROGERS, A., YILDIZ, F. H. & SANDKVIST, M. 2014. The Type II secretion system delivers matrix proteins for biofilm formation by Vibrio cholerae. *J Bacteriol,* 196**,** 4245-52.

JOSENHANS, C. & SUERBAUM, S. 2002. The role of motility as a virulence factor in bacteria. *Int J Med Microbiol,* 291**,** 605-14.

JUDE, B. A. & TAYLOR, R. K. 2011. The physical basis of type 4 pilus-mediated microcolony formation by Vibrio cholerae O1. *Journal of structural biology,* 175**,** 1-9.

JUNG, S. A., CHAPMAN, C. A. & NG, W.-L. 2015. Quadruple quorum-sensing inputs control Vibrio cholerae virulence and maintain system robustness. *PLoS pathogens,* 11**,** e1004837.

KANEHISA, M., FURUMICHI, M., TANABE, M., SATO, Y. & MORISHIMA, K. 2016. KEGG: new perspectives on genomes, pathways, diseases and drugs. *Nucleic acids research,* 45**,** D353-D361.

KAPER, J. B., MORRIS, J. G., JR. & LEVINE, M. M. 1995. Cholera. *Clin Microbiol Rev,* 8**,** 48-86.

KATO, N., MOROHOSHI, T., NOZAWA, T., MATSUMOTO, H. & IKEDA, T. 2006. Control of gram-negative bacterial quorum sensing with cyclodextrin immobilized cellulose ether gel. *Journal of inclusion phenomena and macrocyclic chemistry,* 56**,** 55-59.

KAUFMAN, M. R., SEYER, J. M. & TAYLOR, R. K. 1991. Processing of TCP pilin by TcpJ typifies a common step intrinsic to a newly recognized pathway of extracellular protein secretion by gram-negative bacteria. *Genes & development,* 5**,** 1834-1846.

KEYHANI, N. O. & ROSEMAN, S. 1999. Physiological aspects of chitin catabolism in marine bacteria. *Biochim Biophys Acta,* 1473**,** 108-22.

KIRN, T. J., JUDE, B. A. & TAYLOR, R. K. 2005. A colonization factor links Vibrio cholerae environmental survival and human infection. *Nature,* 438**,** 863-6.

KLARE, W., DAS, T., IBUGO, A., BUCKLE, E., MANEFIELD, M. & MANOS, J. 2016. Glutathione-Disrupted Biofilms of Clinical Pseudomonas aeruginosa Strains Exhibit an Enhanced Antibiotic Effect and a Novel Biofilm Transcriptome. *Antimicrob Agents Chemother,* 60**,** 4539-51.

KOCH, H., LUCKER, S., ALBERTSEN, M., KITZINGER, K., HERBOLD, C., SPIECK, E., NIELSEN, P. H., WAGNER, M. & DAIMS, H. 2015. Expanded metabolic versatility of ubiquitous nitrite-oxidizing bacteria from the genus Nitrospira. *Proc Natl Acad Sci U S A,* 112**,** 11371-6.

KOJIMA, S. & BLAIR, D. F. 2004. Solubilization and purification of the MotA/MotB complex of Escherichia coli. *Biochemistry,* 43**,** 26-34.

KOSTRITSKII, A. Y., KONDINSKAIA, D. A., NESTERENKO, A. M. & GURTOVENKO, A. A. 2016. Adsorption of Synthetic Cationic Polymers on Model Phospholipid Membranes: Insight from Atomic-Scale Molecular Dynamics Simulations. *Langmuir,* 32**,** 10402-10414.

KOVACIKOVA, G., LIN, W. & SKORUPSKI, K. 2004. Vibrio cholerae AphA uses a novel mechanism for virulence gene activation that involves interaction with the LysR-type regulator AphB at the tcpPH promoter. *Mol Microbiol,* 53**,** 129-42.

KOVACIKOVA, G. & SKORUPSKI, K. 2002a. The alternative sigma factor sigma(E) plays an important role in intestinal survival and virulence in Vibrio cholerae. *Infect Immun,* 70**,** 5355-62.

KOVACIKOVA, G. & SKORUPSKI, K. 2002b. Regulation of virulence gene expression in Vibrio cholerae by quorum sensing: HapR functions at the aphA promoter. *Mol Microbiol,* 46**,** 1135-47.

KOZLOVA, N. O., BRUSKOVSKAYA, I. B., OKUNEVA, I. B., MELIK-NUBAROV, N. S., YAROSLAVOV, A. A., KABANOV, V. A. & MENGER, F. M. 2001. Interaction of a cationic polymer with negatively charged proteoliposomes. *Biochim Biophys Acta,* 1514**,** 139-51.

KRACHLER, A. M., HAM, H. & ORTH, K. 2011. Outer membrane adhesion factor multivalent adhesion molecule 7 initiates host cell binding during infection by gram-negative pathogens. *Proceedings of the National Academy of Sciences,* 108**,** 11614-11619.

KRASTEVA, P. V., FONG, J. C., SHIKUMA, N. J., BEYHAN, S., NAVARRO, M. V., YILDIZ, F. H. & SONDERMANN, H. 2010. Vibrio cholerae VpsT regulates matrix production and motility by directly sensing cyclic di-GMP. *Science,* 327**,** 866-8.

KRATOCHVIL, M. J., TAL-GAN, Y., YANG, T., BLACKWELL, H. E. & LYNN, D. M. 2015. Nanoporous Superhydrophobic Coatings that Promote the Extended Release of Water-Labile Quorum Sensing Inhibitors and Enable Long-Term Modulation of Quorum Sensing in Staphylococcus aureus. *ACS Biomater Sci Eng,* 1**,** 1039-1049.

KREBS, S. J. & TAYLOR, R. K. 2011. Protection and attachment of Vibrio cholerae mediated by the toxin-coregulated pilus in the infant mouse model. *J Bacteriol,* 193**,** 5260-70.

KRUKONIS, E. S., YU, R. R. & DIRITA, V. J. 2000. The Vibrio cholerae ToxR/TcpP/ToxT virulence cascade: distinct roles for two membrane-localized transcriptional activators on a single promoter. *Mol Microbiol,* 38**,** 67-84.

KUBOTA, N., TATSUMOTO, N., SANO, T. & TOYA, K. 2000. A simple preparation of half N-acetylated chitosan highly soluble in water and aqueous organic solvents. *Carbohydr Res,* 324**,** 268-74.

KUMAR, N. & KUMAR, R. 2013. *Nanotechnology and Nanomaterials in the Treatment of Life-threatening Diseases*, William Andrew.

KURODA, K. & CAPUTO, G. A. 2013. Antimicrobial polymers as synthetic mimics of host-defense peptides. *Wiley Interdisciplinary Reviews: Nanomedicine and Nanobiotechnology,* 5**,** 49-66.

LANGER, R. 2000. Biomaterials in drug delivery and tissue engineering: one laboratory's experience. *Acc Chem Res,* 33**,** 94-101.

LAZAZZERA, B. A. 2000. Quorum sensing and starvation: signals for entry into stationary phase. *Curr Opin Microbiol,* 3**,** 177-82.

LEE, S. H., HAVA, D. L., WALDOR, M. K. & CAMILLI, A. 1999. Regulation and temporal expression patterns of Vibrio cholerae virulence genes during infection. *Cell,* 99**,** 625-34.

LEIRE, E., AMARAL, S. P., LOUZAO, I., WINZER, K., ALEXANDER, C., FERNANDEZ-MEGIA, E. & FERNANDEZ-TRILLO, F. 2016. Dendrimer mediated clustering of bacteria: improved aggregation and evaluation of bacterial response and viability. *Biomater Sci,* 4**,** 998-1006.

LENZ, D. H., MOK, K. C., LILLEY, B. N., KULKARNI, R. V., WINGREEN, N. S. & BASSLER, B. L. 2004. The small RNA chaperone Hfq and multiple small RNAs control quorum sensing in Vibrio harveyi and Vibrio cholerae. *Cell,* 118**,** 69-82.

LEWNARD, J. A., ANTILLÓN, M., GONSALVES, G., MILLER, A. M., KO, A. I. & PITZER, V. E. 2016. Strategies to prevent cholera introduction during international personnel

deployments: a computational modeling analysis based on the 2010 Haiti outbreak. *PLoS medicine,* 13**,** e1001947.

LI, J., LIM, M. S., LI, S., BROCK, M., PIQUE, M. E., WOODS, V. L. & CRAIG, L. 2008. Vibrio cholerae toxin-coregulated pilus structure analyzed by hydrogen/deuterium exchange mass spectrometry. *Structure,* 16**,** 137-148.

LI, X. & ROSEMAN, S. 2004. The chitinolytic cascade in Vibrios is regulated by chitin oligosaccharides and a two-component chitin catabolic sensor/kinase. *Proc Natl Acad Sci U S A,* 101**,** 627-31.

LIANG, W., PASCUAL-MONTANO, A., SILVA, A. J. & BENITEZ, J. A. 2007. The cyclic AMP receptor protein modulates quorum sensing, motility and multiple genes that affect intestinal colonization in Vibrio cholerae. *Microbiology,* 153**,** 2964-75.

LIU, Z., MIYASHIRO, T., TSOU, A., HSIAO, A., GOULIAN, M. & ZHU, J. 2008. Mucosal penetration primes Vibrio cholerae for host colonization by repressing quorum sensing. *Proc Natl Acad Sci U S A,* 105**,** 9769-74.

LODGE, J., FEAR, J., BUSBY, S., GUNASEKARAN, P. & KAMINI, N. R. 1992. Broad host range plasmids carrying the Escherichia coli lactose and galactose operons. *FEMS microbiology letters,* 95**,** 271-276.

LOUZAO, I., SUI, C., WINZER, K., FERNANDEZ-TRILLO, F. & ALEXANDER, C. 2015. Cationic polymer mediated bacterial clustering: Cell-adhesive properties of homo-and copolymers. *European Journal of Pharmaceutics and Biopharmaceutics,* 95**,** 47-62.

LU, H. D., SPIEGEL, A. C., HURLEY, A., PEREZ, L. J., MAISEL, K., ENSIGN, L. M., HANES, J., BASSLER, B. L., SEMMELHACK, M. F. & PRUD'HOMME, R. K. 2015. Modulating Vibrio cholerae quorum-sensing-controlled communication using autoinducer-loaded nanoparticles. *Nano Lett,* 15**,** 2235-41.

LUI, L. T., XUE, X., SUI, C., BROWN, A., PRITCHARD, D. I., HALLIDAY, N., WINZER, K., HOWDLE, S. M., FERNANDEZ-TRILLO, F. & KRASNOGOR, N. 2013. Bacteria clustering by polymers induces the expression of quorum-sensing-controlled phenotypes. *Nature chemistry,* 5**,** 1058-1065.

MAITZ, M. 2015. Applications of synthetic polymers in clinical medicine. *Biosurface and Biotribology,* 1**,** 161-176.

MANNING, P. A. 1997. The tcp gene cluster of Vibrio cholerae. *Gene,* 192**,** 63-70.

MARQUIS, R. E., MAYZEL, K. & CARSTENSEN, E. L. 1976. Cation exchange in cell walls of gram-positive bacteria. *Canadian journal of microbiology,* 22**,** 975-982.

MATHIOWITZ, E., JACOB, J. S., JONG, Y. S., CARINO, G. P., CHICKERING, D. E., CHATURVEDI, P., SANTOS, C. A., VIJAYARAGHAVAN, K., MONTGOMERY, S. & BASSETT, M. 1997. Biologically erodable microspheres as potential oral drug delivery systems. *Nature,* 386**,** 410.

MATSON, J. S., WITHEY, J. H. & DIRITA, V. J. 2007. Regulatory networks controlling Vibrio cholerae virulence gene expression. *Infection and immunity,* 75**,** 5542-5549.

MATYJASZEWSKI, K. 2003. The synthesis of functional star copolymers as an illustration of the importance of controlling polymer structures in the design of new materials. *Polymer international,* 52**,** 1559-1565.

MECSAS, J., ROUVIERE, P. E., ERICKSON, J. W., DONOHUE, T. J. & GROSS, C. A. 1993. The activity of sigma E, an Escherichia coli heat-inducible sigma-factor, is modulated by expression of outer membrane proteins. *Genes Dev,* 7**,** 2618-28.

MEIBOM, K. L., BLOKESCH, M., DOLGANOV, N. A., WU, C. Y. & SCHOOLNIK, G. K. 2005. Chitin induces natural competence in Vibrio cholerae. *Science,* 310**,** 1824-7.

MEIBOM, K. L., LI, X. B., NIELSEN, A. T., WU, C. Y., ROSEMAN, S. & SCHOOLNIK, G. K. 2004. The Vibrio cholerae chitin utilization program. *Proc Natl Acad Sci U S A,* 101**,** 2524-9.

MILLER, V. L., DIRITA, V. J. & MEKALANOS, J. J. 1989. Identification of Toxs, a Regulatory Gene Whose Product Enhances Toxr-Mediated Activation of the Cholera-Toxin Promoter. *Journal of Bacteriology,* 171, 1288-1293.

MILLER, V. L. & MEKALANOS, J. J. 1988. A novel suicide vector and its use in construction of insertion mutations: osmoregulation of outer membrane proteins and virulence determinants in Vibrio cholerae requires toxR. *J Bacteriol,* 170, 2575-83.

MILLET, Y. A., ALVAREZ, D., RINGGAARD, S., VON ANDRIAN, U. H., DAVIS, B. M. & WALDOR, M. K. 2014. Insights into Vibrio cholerae intestinal colonization from monitoring fluorescently labeled bacteria. *PLoS Pathog,* 10, e1004405.

MITCHELL, K. C., BREEN, P., BRITTON, S., NEELY, M. N. & WITHEY, J. H. 2017. Quantifying Vibrio cholerae enterotoxicity in a zebrafish infection model. *Appl Environ Microbiol.*

MIYASHIRO, T. & RUBY, E. G. 2012. Shedding light on bioluminescence regulation in Vibrio fischeri. *Mol Microbiol,* 84, 795-806.

MOGHIMI, S. M., SYMONDS, P., MURRAY, J. C., HUNTER, A. C., DEBSKA, G. & SZEWCZYK, A. 2005. A two-stage poly(ethylenimine)-mediated cytotoxicity: implications for gene transfer/therapy. *Mol Ther,* 11, 990-5.

MOISI, M., JENUL, C., BUTLER, S. M., NEW, A., TUTZ, S., REIDL, J., KLOSE, K. E., CAMILLI, A. & SCHILD, S. 2009. A novel regulatory protein involved in motility of Vibrio cholerae. *J Bacteriol,* 191, 7027-38.

MULCAHY, H., CHARRON-MAZENOD, L. & LEWENZA, S. 2008. Extracellular DNA chelates cations and induces antibiotic resistance in Pseudomonas aeruginosa biofilms. *PLoS Pathog,* 4, e1000213.

MÜLLER, A. H. E. & MATYJASZEWSKI, K. 2009. Controlled and living polymerizations. *From Mechanisms to Applications,* 555-597.

MUÑOZ-BONILLA, A. & FERNÁNDEZ-GARCÍA, M. 2012. Polymeric materials with antimicrobial activity. *Progress in Polymer Science,* 37, 281-339.

NESVADBA, P. 2012. Radical polymerization in industry. *Encyclopedia of Radicals in Chemistry, Biology and Materials.*

NG, A. N. Y., DE JONG-CURTAIN, T. A., MAWDSLEY, D. J., WHITE, S. J., SHIN, J., APPEL, B., DONG, P. D. S., STAINIER, D. Y. R. & HEATH, J. K. 2005. Formation of the digestive system in zebrafish: III. Intestinal epithelium morphogenesis. *Developmental biology,* 286, 114-135.

NG, W.-L., PEREZ, L., CONG, J., SEMMELHACK, M. F. & BASSLER, B. L. 2012. Broad spectrum pro-quorum-sensing molecules as inhibitors of virulence in vibrios. *PLoS pathogens,* 8, e1002767.

NG, W. L. & BASSLER, B. L. 2009. Bacterial quorum-sensing network architectures. *Annu Rev Genet,* 43, 197-222.

NIELSEN, A. T., DOLGANOV, N. A., OTTO, G., MILLER, M. C., WU, C. Y. & SCHOOLNIK, G. K. 2006. RpoS controls the Vibrio cholerae mucosal escape response. *PLoS Pathog,* 2, e109.

NIJVIPAKUL, S., WONGRATANA, J., SUADEE, C., ENTSCH, B., BALLOU, D. P. & CHAIYEN, P. 2008. LuxG is a functioning flavin reductase for bacterial luminescence. *J Bacteriol,* 190, 1531-8.

NYE, M. B., PFAU, J. D., SKORUPSKI, K. & TAYLOR, R. K. 2000. Vibrio cholerae H-NS silences virulence gene expression at multiple steps in the ToxR regulatory cascade. *J Bacteriol,* 182, 4295-303.

O'TOOLE, G. A. 2011. Microtiter dish biofilm formation assay. *J Vis Exp.*

O'TOOLE, R., VON HOFSTEN, J., ROSQVIST, R., OLSSON, P. E. & WOLF-WATZ, H. 2004. Visualisation of zebrafish infection by GFP-labelled Vibrio anguillarum. *Microb Pathog,* 37**,** 41-6.

OGIERMAN, M. A. & MANNING, P. A. 1992. TCP pilus biosynthesis in Vibrio cholera O1: gene sequence of tcpC encoding an outer membrane lipoprotein. *FEMS microbiology letters,* 97**,** 179-184.

OKSHEVSKY, M. & MEYER, R. L. 2015. The role of extracellular DNA in the establishment, maintenance and perpetuation of bacterial biofilms. *Crit Rev Microbiol,* 41**,** 341-52.

OLIVER, J. D. 2005. The viable but nonculturable state in bacteria. *J Microbiol,* 43 Spec No**,** 93-100.

PACK, D. W., HOFFMAN, A. S., PUN, S. & STAYTON, P. S. 2005. Design and development of polymers for gene delivery. *Nat Rev Drug Discov,* 4**,** 581-93.

PAGE, L., GRIFFITHS, L. & COLE, J. A. 1990. Different physiological roles of two independent pathways for nitrite reduction to ammonia by enteric bacteria. *Arch Microbiol,* 154**,** 349-54.

PALERMO, E. F. & KURODA, K. 2009. Chemical structure of cationic groups in amphiphilic polymethacrylates modulates the antimicrobial and hemolytic activities. *Biomacromolecules,* 10**,** 1416-1428.

PALERMO, E. F., LEE, D.-K., RAMAMOORTHY, A. & KURODA, K. 2010. Role of cationic group structure in membrane binding and disruption by amphiphilic copolymers. *The Journal of Physical Chemistry B,* 115**,** 366-375.

PARSOT, C. & MEKALANOS, J. J. 1992. Structural analysis of the acfA and acfD genes of Vibrio cholerae: effects of DNA topology and transcriptional activators on expression. *Journal of bacteriology,* 174**,** 5211-5218.

PEREZ-SOTO, N., MOULE, L., CRISAN, D. N., INSUA, I., TAYLOR-SMITH, L. M., VOELZ, K., FERNANDEZ-TRILLO, F. & KRACHLER, A. M. 2017. Engineering microbial physiology with synthetic polymers: cationic polymers induce biofilm formation in Vibrio cholerae and downregulate the expression of virulence genes. *Chem Sci,* 8**,** 5291-5298.

PERRIER, S. B. 2017. 50th Anniversary Perspective: RAFT Polymerization · A User Guide. *Macromolecules,* 50**,** 7433-7447.

PERRIN, D. D., DEMPSEY, B. & SERJEANT, E. P. 1981. *pKa prediction for organic acids and bases*, Springer.

PESCHEL, A. 2002. How do bacteria resist human antimicrobial peptides? *Trends in microbiology,* 10**,** 179-186.

PHILLIPS, D. J., HARRISON, J., RICHARDS, S.-J., MITCHELL, D. E., TICHAUER, E., HUBBARD, A. T., GUY, C., HANDS-PORTMAN, I., FULLAM, E. & GIBSON, M. I. 2017. Evaluation of the antimicrobial activity of cationic polymers against mycobacteria: toward antitubercular macromolecules. *Biomacromolecules,* 18**,** 1592-1599.

PILETSKA, E. V., STAVROULAKIS, G., KARIM, K., WHITCOMBE, M. J., CHIANELLA, I., SHARMA, A., EBOIGBODIN, K. E., ROBINSON, G. K. & PILETSKY, S. A. 2010. Attenuation of Vibrio fischeri quorum sensing using rationally designed polymers. *Biomacromolecules,* 11**,** 975-980.

PILETSKA, E. V., STAVROULAKIS, G., LARCOMBE, L. D., WHITCOMBE, M. J., SHARMA, A., PRIMROSE, S., ROBINSON, G. K. & PILETSKY, S. A. 2011. Passive control of quorum sensing: prevention of Pseudomonas aeruginosa biofilm formation by imprinted polymers. *Biomacromolecules,* 12**,** 1067-1071.

PILLAI, O. & PANCHAGNULA, R. 2001. Polymers in drug delivery. *Curr Opin Chem Biol,* 5**,** 447-51.

PLASTICEUROPE. 2015. *Plastics - the Facts 2014/2015* [Online]. Available: http://www.plasticseurope.org/Document/plastics-the-facts-20142015.aspx [Accessed].

PROUTY, M. G., CORREA, N. E. & KLOSE, K. E. 2001. The novel $\sigma 54$‐ and $\sigma 28$‐ dependent flagellar gene transcription hierarchy of Vibrio cholerae. *Molecular microbiology,* 39**,** 1595-1609.

PROUTY, M. G. & KLOSE, K. E. 2006. Vibrio cholerae: the genetics of pathogenesis and environmental persistence. *The biology of vibrios.* American Society of Microbiology.

PROVENZANO, D. & KLOSE, K. E. 2000. Altered expression of the ToxR-regulated porins OmpU and OmpT diminishes Vibrio cholerae bile resistance, virulence factor expression, and intestinal colonization. *Proceedings of the National Academy of Sciences of the United States of America,* 97**,** 10220-10224.

PYUN, J., KOWALEWSKI, T. & MATYJASZEWSKI, K. 2003. Synthesis of polymer brushes using atom transfer radical polymerization. *Macromolecular Rapid Communications,* 24**,** 1043-1059.

QIU, J., CHARLEUX, B. & MATYJASZEWSKI, K. 2001. Controlled/living radical polymerization in aqueous media: homogeneous and heterogeneous systems. *Progress in Polymer Science,* 26**,** 2083-2134.

RAETHER, B., NUYKEN, O., WIELAND, P. & BREMSER, W. Free‐radical synthesis of block copolymers on an industrial scale. Macromolecular Symposia, 2002. Wiley Online Library, 25-42.

RAIVIO, T. L. 2005. Envelope stress responses and Gram-negative bacterial pathogenesis. *Mol Microbiol,* 56**,** 1119-28.

RAJANNA, C., WANG, J., ZHANG, D., XU, Z., ALI, A., HOU, Y.-M. & KARAOLIS, D. 2003. The vibrio pathogenicity island of epidemic Vibrio cholerae forms precise extrachromosomal circular excision products. *Journal of bacteriology,* 185**,** 6893-6901.

REICHHARDT, C., FONG, J. C., YILDIZ, F. & CEGELSKI, L. 2015. Characterization of the Vibrio cholerae extracellular matrix: a top-down solid-state NMR approach. *Biochim Biophys Acta,* 1848**,** 378-83.

REIMSCHUESSEL, H. K. 1975. General aspects in polymer synthesis. *Environ Health Perspect,* 11**,** 9-20.

RICHARDSON, K. 1991. Roles of motility and flagellar structure in pathogenicity of Vibrio cholerae: analysis of motility mutants in three animal models. *Infect Immun,* 59**,** 2727-36.

RITCHIE, J. M., RUI, H., BRONSON, R. T. & WALDOR, M. K. 2010. Back to the future: studying cholera pathogenesis using infant rabbits. *MBio,* 1**,** e00047-10.

RITCHIE, J. M., RUI, H., ZHOU, X., IIDA, T., KODOMA, T., ITO, S., DAVIS, B. M., BRONSON, R. T. & WALDOR, M. K. 2012. Inflammation and disintegration of intestinal villi in an experimental model for Vibrio parahaemolyticus-induced diarrhea. *PLoS pathogens,* 8**,** e1002593.

RITCHIE, J. M. & WALDOR, M. K. 2009. Vibrio cholerae interactions with the gastrointestinal tract: lessons from animal studies. *Curr Top Microbiol Immunol,* 337**,** 37-59.

RUNFT, D. L., MITCHELL, K. C., ABUAITA, B. H., ALLEN, J. P., BAJER, S., GINSBURG, K., NEELY, M. N. & WITHEY, J. H. 2014. Zebrafish as a natural host model for Vibrio cholerae colonization and transmission. *Applied and Environmental Microbiology,* 80**,** 1710-1717.

RUTHERFORD, S. T. & BASSLER, B. L. 2012. Bacterial quorum sensing: its role in virulence and possibilities for its control. *Cold Spring Harb Perspect Med,* 2.

SAALWÄCHTER, K. & REICHERT, D. 2010. Polymer applications of NMR.

SAHARIAH, P., BENEDIKTSSDOTTIR, B. E., HJALMARSDOTTIR, M. A., SIGURJONSSON, O. E., SORENSEN, K. K., THYGESEN, M. B., JENSEN, K. J. & MASSON, M. 2015a. Impact of chain length on antibacterial activity and hemocompatibility of quaternary N-alkyl and n,n-dialkyl chitosan derivatives. *Biomacromolecules,* 16**,** 1449-60.

SAHARIAH, P., OSKARSSON, B. M., HJALMARSDOTTIR, M. A. & MASSON, M. 2015b. Synthesis of guanidinylated chitosan with the aid of multiple protecting groups and investigation of antibacterial activity. *Carbohydr Polym,* 127**,** 407-17.

SALGADO-PABON, W., DU, Y., HACKETT, K. T., LYONS, K. M., ARVIDSON, C. G. & DILLARD, J. P. 2010. Increased expression of the type IV secretion system in piliated Neisseria gonorrhoeae variants. *J Bacteriol,* 192**,** 1912-20.

SCHELLHORN, H. E. & STONES, V. L. 1992. Regulation of katF and katE in Escherichia coli K-12 by weak acids. *J Bacteriol,* 174**,** 4769-76.

SCHMALJOHANN, D. 2006. Thermo-and pH-responsive polymers in drug delivery. *Advanced drug delivery reviews,* 58**,** 1655-1670.

SCHUHMACHER, D. A. & KLOSE, K. E. 1999. Environmental signals modulate ToxT-dependent virulence factor expression in Vibrio cholerae. *J Bacteriol,* 181**,** 1508-14.

SCOTT, R. W., DEGRADO, W. F. & TEW, G. N. 2008. De novo designed synthetic mimics of antimicrobial peptides. *Current opinion in biotechnology,* 19**,** 620-627.

SENOH, M., HAMABATA, T. & TAKEDA, Y. 2015. A factor converting viable but nonculturable Vibrio cholerae to a culturable state in eukaryotic cells is a human catalase. *Microbiologyopen,* 4**,** 589-96.

SEPER, A., FENGLER, V. H., ROIER, S., WOLINSKI, H., KOHLWEIN, S. D., BISHOP, A. L., CAMILLI, A., REIDL, J. & SCHILD, S. 2011. Extracellular nucleases and extracellular DNA play important roles in Vibrio cholerae biofilm formation. *Mol Microbiol,* 82**,** 1015-37.

SHAH, P. & SWIATLO, E. 2008. A multifaceted role for polyamines in bacterial pathogens. *Mol Microbiol,* 68**,** 4-16.

SHAHIN, J., HARRISON, D. A. & ROWAN, K. M. 2012. Relation between volume and outcome for patients with severe sepsis in United Kingdom: retrospective cohort study. *Bmj,* 344**,** e3394.

SHAI, Y. 2002. Mode of action of membrane active antimicrobial peptides. *Peptide Science,* 66**,** 236-248.

SHAO, Y. & BASSLER, B. L. 2012. Quorum-sensing non-coding small RNAs use unique pairing regions to differentially control mRNA targets. *Mol Microbiol,* 83**,** 599-611.

SHIMAMURA, T., WATANABE, S. & SASAKI, S. 1985. Enhancement of enterotoxin production by carbon dioxide in Vibrio cholerae. *Infect Immun,* 49**,** 455-6.

SHINODA, H. & MATYJASZEWSKI, K. 2001. Improving the structural control of graft copolymers. Copolymerization of poly (dimethylsiloxane) macromonomer with methyl methacrylate using RAFT polymerization. *Macromolecular Rapid Communications,* 22**,** 1176-1181.

SIEDENBIEDEL, F. & TILLER, J. C. 2012. Antimicrobial polymers in solution and on surfaces: overview and functional principles. *Polymers,* 4**,** 46-71.

SILHAVY, T. J., KAHNE, D. & WALKER, S. 2010. The bacterial cell envelope. *Cold Spring Harbor perspectives in biology,* 2**,** a000414.

SILVA, A. J. & BENITEZ, J. A. 2016. Vibrio cholerae biofilms and cholera pathogenesis. *PLoS neglected tropical diseases,* 10**,** e0004330.

SIMON, R., PRIEFER, U. & PUHLER, A. 1983. A Broad Host Range Mobilization System for Invivo Genetic-Engineering - Transposon Mutagenesis in Gram-Negative Bacteria. *Bio-Technology,* 1**,** 784-791.

SKORUPSKI, K. & TAYLOR, R. K. 1997. Control of the ToxR virulence regulon in Vibrio cholerae by environmental stimuli. *Mol Microbiol,* 25**,** 1003-9.

SLAMTI, L. & LERECLUS, D. 2002. A cell-cell signaling peptide activates the PlcR virulence regulon in bacteria of the Bacillus cereus group. *EMBO J,* 21**,** 4550-9.

SLAMTI, L. & WALDOR, M. K. 2009. Genetic analysis of activation of the Vibrio cholerae Cpx pathway. *J Bacteriol,* 191**,** 5044-56.

SMITH, D. R., MAESTRE-REYNA, M., LEE, G., GERARD, H., WANG, A. H. & WATNICK, P. I. 2015. In situ proteolysis of the Vibrio cholerae matrix protein RbmA promotes biofilm recruitment. *Proc Natl Acad Sci U S A,* 112**,** 10491-6.

SOBE, R. C., BOND, W. G., WOTANIS, C. K., ZAYNER, J. P., BURRISS, M. A., FERNANDEZ, N., BRUGER, E. L., WATERS, C. M., NEUFELD, H. S. & KARATAN, E. 2017. Spermine inhibits Vibrio cholerae biofilm formation through the NspS-MbaA polyamine signaling system. *J Biol Chem,* 292**,** 17025-17036.

SOM, A., VEMPARALA, S., IVANOV, I. & TEW, G. N. 2008. Synthetic mimics of antimicrobial peptides. *Peptide Science,* 90**,** 83-93.

SPANGLER, B. D. 1992. Structure and function of cholera toxin and the related Escherichia coli heat-labile enterotoxin. *Microbiol Rev,* 56**,** 622-47.

SRIVASTAVA, D., HARRIS, R. C. & WATERS, C. M. 2011. Integration of cyclic di-GMP and quorum sensing in the control of vpsT and aphA in Vibrio cholerae. *J Bacteriol,* 193**,** 6331-41.

STAUDER, M., HUQ, A., PEZZATI, E., GRIM, C. J., RAMOINO, P., PANE, L., COLWELL, R. R., PRUZZO, C. & VEZZULLI, L. 2012. Role of GbpA protein, an important virulence-related colonization factor, for Vibrio cholerae's survival in the aquatic environment. *Environ Microbiol Rep,* 4**,** 439-45.

STEWART, B. J. & MCCARTER, L. L. 2003. Lateral flagellar gene system of Vibrio parahaemolyticus. *Journal of bacteriology,* 185**,** 4508-4518.

SUCKOW, G., SEITZ, P. & BLOKESCH, M. 2011. Quorum sensing contributes to natural transformation of Vibrio cholerae in a species-specific manner. *Journal of bacteriology,* 193**,** 4914-4924.

SVITIL, A. L., CHADHAIN, S., MOORE, J. A. & KIRCHMAN, D. L. 1997. Chitin Degradation Proteins Produced by the Marine Bacterium Vibrio harveyi Growing on Different Forms of Chitin. *Appl Environ Microbiol,* 63**,** 408-13.

SYED, K. A., BEYHAN, S., CORREA, N., QUEEN, J., LIU, J., PENG, F., SATCHELL, K. J., YILDIZ, F. & KLOSE, K. E. 2009. The Vibrio cholerae flagellar regulatory hierarchy controls expression of virulence factors. *J Bacteriol,* 191**,** 6555-70.

SZABADY, R. L., YANTA, J. H., HALLADIN, D. K., SCHOFIELD, M. J. & WELCH, R. A. 2011. TagA is a secreted protease of Vibrio cholerae that specifically cleaves mucin glycoproteins. *Microbiology,* 157**,** 516-525.

TANG, W., TSAREVSKY, N. V. & MATYJASZEWSKI, K. 2006. Determination of equilibrium constants for atom transfer radical polymerization. *Journal of the American Chemical Society,* 128**,** 1598-1604.

TARSI, R. & PRUZZO, C. 1999. Role of surface proteins in Vibrio cholerae attachment to chitin. *Appl Environ Microbiol,* 65**,** 1348-51.

TAYLOR, K. C. & NASR-EL-DIN, H. A. 1998. Water-soluble hydrophobically associating polymers for improved oil recovery: A literature review. *Journal of Petroleum Science and Engineering,* 19**,** 265-280.

TAYLOR, R. G., WALKER, D. C. & MCINNES, R. R. 1993. E. coli host strains significantly affect the quality of small scale plasmid DNA preparations used for sequencing. *Nucleic Acids Res,* 21**,** 1677-8.

TESCHLER, J. K., ZAMORANO-SANCHEZ, D., UTADA, A. S., WARNER, C. J., WONG, G. C., LININGTON, R. G. & YILDIZ, F. H. 2015. Living in the matrix: assembly and control of Vibrio cholerae biofilms. *Nat Rev Microbiol,* 13**,** 255-68.

THANH NGUYEN, H. & GOYCOOLEA, F. M. 2017. Chitosan/Cyclodextrin/TPP Nanoparticles Loaded with Quercetin as Novel Bacterial Quorum Sensing Inhibitors. *Molecules,* 22.

THOMAS, M. S. & WIGNESHWERARAJ, S. 2014. Regulation of virulence gene expression. *Virulence,* 5**,** 832-4.

TIELEN, P., KUHN, H., ROSENAU, F., JAEGER, K. E., FLEMMING, H. C. & WINGENDER, J. 2013. Interaction between extracellular lipase LipA and the polysaccharide alginate of Pseudomonas aeruginosa. *BMC Microbiol,* 13**,** 159.

TILLER, J. C., LEE, S. B., LEWIS, K. & KLIBANOV, A. M. 2002. Polymer surfaces derivatized with poly (vinyl‐N‐hexylpyridinium) kill airborne and waterborne bacteria. *Biotechnology and Bioengineering,* 79**,** 465-471.

TILLER, J. C., LIAO, C.-J., LEWIS, K. & KLIBANOV, A. M. 2001. Designing surfaces that kill bacteria on contact. *Proceedings of the National Academy of Sciences,* 98**,** 5981-5985.

TIMOFEEVA, L. & KLESHCHEVA, N. 2011. Antimicrobial polymers: mechanism of action, factors of activity, and applications. *Appl Microbiol Biotechnol,* 89**,** 475-92.

TISCHLER, A. D. & CAMILLI, A. 2005. Cyclic diguanylate regulates Vibrio cholerae virulence gene expression. *Infect Immun,* 73**,** 5873-82.

TOKIWA, Y., CALABIA, B. P., UGWU, C. U. & AIBA, S. 2009. Biodegradability of plastics. *Int J Mol Sci,* 10**,** 3722-42.

UTADA, A. S., BENNETT, R. R., FONG, J. C. N., GIBIANSKY, M. L., YILDIZ, F. H., GOLESTANIAN, R. & WONG, G. C. L. 2014. Vibrio cholerae use pili and flagella synergistically to effect motility switching and conditional surface attachment. *Nat Commun,* 5**,** 4913.

VAARA, M. 1992. Agents that increase the permeability of the outer membrane. *Microbiol Rev,* 56**,** 395-411.

VAN DONGEN, M. A., SILPE, J. E., DOUGHERTY, C. A., KANDULURU, A. K., CHOI, S. K., ORR, B. G., LOW, P. S. & BANASZAK HOLL, M. M. 2014. Avidity mechanism of dendrimer–folic acid conjugates. *Molecular pharmaceutics,* 11**,** 1696-1706.

VILLENEUVE, S., BOUTONNIER, A., MULARD, L. A. & FOURNIER, J. M. 1999. Immunochemical characterization of an Ogawa-Inaba common antigenic determinant of Vibrio cholerae O1. *Microbiology,* 145 (Pt 9)**,** 2477-84.

VLASSOV, V. V., LAKTIONOV, P. P. & RYKOVA, E. Y. 2007. Extracellular nucleic acids. *Bioessays,* 29**,** 654-667.

WALDOR, M. K. & MEKALANOS, J. J. 1996. Lysogenic conversion by a filamentous phage encoding cholera toxin. *Science,* 272**,** 1910-4.

WANG, H., CHEN, S., ZHANG, J., ROTHENBACHER, F. P., JIANG, T., KAN, B., ZHONG, Z. & ZHU, J. 2012. Catalases promote resistance of oxidative stress in Vibrio cholerae. *PloS one,* 7**,** e53383.

WANG, Y. & GRAYSON, S. M. 2012. Approaches for the preparation of non-linear amphiphilic polymers and their applications to drug delivery. *Advanced drug delivery reviews,* 64**,** 852-865.

WATERS, C. M. & BASSLER, B. L. 2005. Quorum sensing: cell-to-cell communication in bacteria. *Annu. Rev. Cell Dev. Biol.,* 21**,** 319-346.

WATNICK, P. I., FULLNER, K. J. & KOLTER, R. 1999. A role for the mannose-sensitive hemagglutinin in biofilm formation by Vibrio cholerae El Tor. *J Bacteriol,* 181**,** 3606-9.

WATNICK, P. I., LAURIANO, C. M., KLOSE, K. E., CROAL, L. & KOLTER, R. 2001. The absence of a flagellum leads to altered colony morphology, biofilm development and virulence in Vibrio cholerae O139. *Mol Microbiol,* 39**,** 223-35.

WEBER, G. G. & KLOSE, K. E. 2011. The complexity of ToxT-dependent transcription in Vibrio cholerae. *The Indian journal of medical research,* 133**,** 201.

WEST, S. A., WINZER, K., GARDNER, A. & DIGGLE, S. P. 2012. Quorum sensing and the confusion about diffusion. *Trends Microbiol,* 20**,** 586-94.

WESTERFIELD, M. 1995. *The zebrafish book: a guide for the laboratory use of zebrafish (Brachydanio rerio)*, University of Oregon press.

WHEELDON, I., FARHADI, A., BICK, A. G., JABBARI, E. & KHADEMHOSSEINI, A. 2011. Nanoscale tissue engineering: spatial control over cell-materials interactions. *Nanotechnology,* 22**,** 212001.

WHITCHURCH, C. B., TOLKER-NIELSEN, T., RAGAS, P. C. & MATTICK, J. S. 2002. Extracellular DNA required for bacterial biofilm formation. *Science,* 295**,** 1487.

WHITEHEAD, N. A., BARNARD, A. M., SLATER, H., SIMPSON, N. J. & SALMOND, G. P. 2001. Quorum-sensing in Gram-negative bacteria. *FEMS Microbiol Rev,* 25**,** 365-404.

WHO 1996. Infectious diseases kill over 17 million people a year. *Malaria Weekly,* 3**,** 11-16.

WIBBENMEYER, J. A., PROVENZANO, D., LANDRY, C. F., KLOSE, K. E. & DELCOUR, A. H. 2002. Vibrio cholerae OmpU and OmpT porins are differentially affected by bile. *Infect Immun,* 70**,** 121-6.

WILLIAMS, T. C., AYRAPETYAN, M. & OLIVER, J. D. 2014. Implications of chitin attachment for the environmental persistence and clinical nature of the human pathogen Vibrio vulnificus. *Appl Environ Microbiol,* 80**,** 1580-7.

WITHEY, J. H. & DIRITA, V. J. 2005. Vibrio cholerae ToxT independently activates the divergently transcribed aldA and tagA genes. *J Bacteriol,* 187**,** 7890-900.

WITHEY, J. H. & DIRITA, V. J. 2006. The toxbox: specific DNA sequence requirements for activation of Vibrio cholerae virulence genes by ToxT. *Molecular microbiology,* 59**,** 1779-1789.

WONG, E., VAAJE-KOLSTAD, G., GHOSH, A., HURTADO-GUERRERO, R., KONAREV, P. V., IBRAHIM, A. F., SVERGUN, D. I., EIJSINK, V. G., CHATTERJEE, N. S. & VAN AALTEN, D. M. 2012. The Vibrio cholerae colonization factor GbpA possesses a modular structure that governs binding to different host surfaces. *PLoS pathogens,* 8**,** e1002373.

XUE, X., PASPARAKIS, G., HALLIDAY, N., WINZER, K., HOWDLE, S. M., CRAMPHORN, C. J., CAMERON, N. R., GARDNER, P. M., DAVIS, B. G. & FERNÁNDEZ-TRILLO, F. 2011. Synthetic polymers for simultaneous bacterial sequestration and quorum sense interference. *Angewandte Chemie International Edition,* 50**,** 9852-9856.

YANG, Y., CAI, Z., HUANG, Z., TANG, X. & ZHANG, X. 2017. Antimicrobial cationic polymers: from structural design to functional control. *Polymer Journal*.

YILDIZ, F., FONG, J., SADOVSKAYA, I., GRARD, T. & VINOGRADOV, E. 2014. Structural characterization of the extracellular polysaccharide from Vibrio cholerae O1 El-Tor. *PLoS One,* 9**,** e86751.

YILDIZ, F. H., LIU, X. S., HEYDORN, A. & SCHOOLNIK, G. K. 2004. Molecular analysis of rugosity in a Vibrio cholerae O1 El Tor phase variant. *Mol Microbiol,* 53**,** 497-515.

YU, R. K., USUKI, S., ITOKAZU, Y. & WU, H. C. 2016. Novel GM1 ganglioside-like peptide mimics prevent the association of cholera toxin to human intestinal epithelial cells in vitro. *Glycobiology,* 26**,** 63-73.

ZAHOUANI, S., HURMAN, L., DE GIORGI, M., VIGIER-CARRIERE, C., BOULMEDAIS, F., SENGER, B., FRISCH, B., SCHAAF, P., LAVALLE, P. & JIERRY, L. 2017. Step-by-step build-up of covalent poly(ethylene oxide) nanogel films. *Nanoscale,* 9**,** 18379-18391.

ZHANG, Q., DONG, X., CHEN, B., ZHANG, Y., ZU, Y. & LI, W. 2016. Zebrafish as a useful model for zoonotic Vibrio parahaemolyticus pathogenicity in fish and human. *Dev Comp Immunol,* 55**,** 159-68.

ZHAO, B. & BRITTAIN, W. J. 2000. Polymer brushes: surface-immobilized macromolecules. *Progress in Polymer Science,* 25**,** 677-710.

ZHENG, J., SHIN, O. S., CAMERON, D. E. & MEKALANOS, J. J. 2010. Quorum sensing and a global regulator TsrA control expression of type VI secretion and virulence in Vibrio cholerae. *Proc Natl Acad Sci U S A,* 107**,** 21128-33.

ZHU, J. & MEKALANOS, J. J. 2003. Quorum sensing-dependent biofilms enhance colonization in Vibrio cholerae. *Developmental cell,* 5**,** 647-656.

ZHU, J., MILLER, M. B., VANCE, R. E., DZIEJMAN, M., BASSLER, B. L. & MEKALANOS, J. J. 2002. Quorum-sensing regulators control virulence gene expression in Vibrio cholerae. *Proceedings of the National Academy of Sciences of the United States of America,* 99**,** 3129-3134.

Appendix

Brightfield images were acquired at the same time as the images showing clustering of *V. cholerae* pBB1 expressing bioluminescence. Each still shown follows the dark images shown in figure 6.2H and 6.2I. The conditions of incubation are detailed in section 2.11.2.

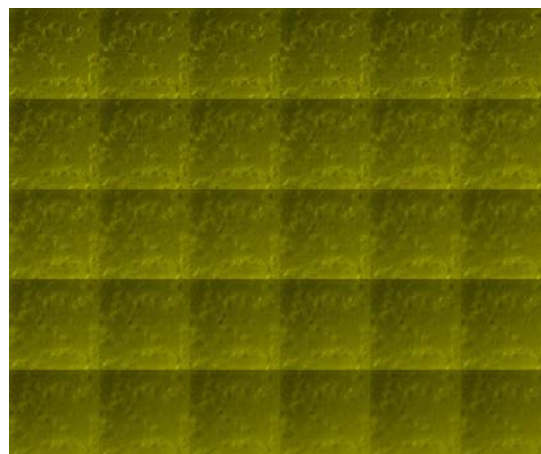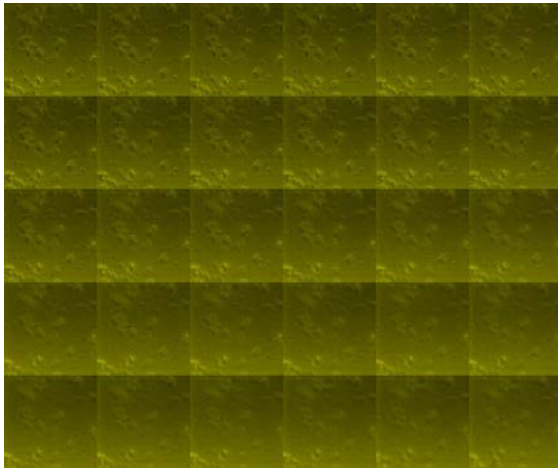**<u>Artificial marine water</u>**

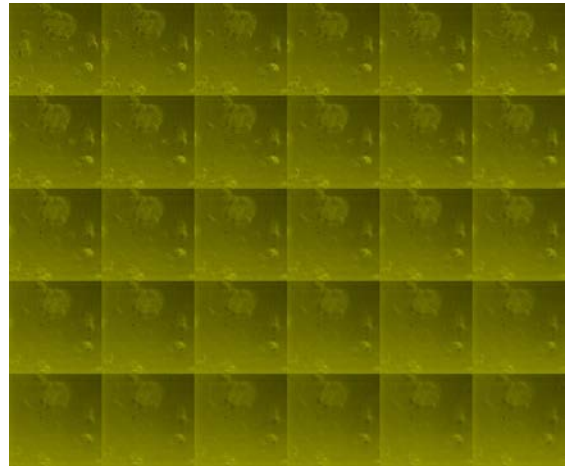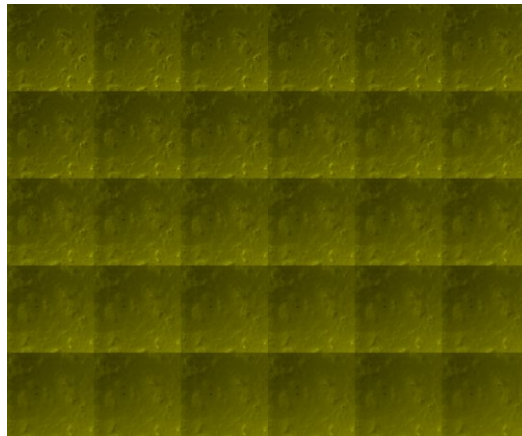0 mg/mL
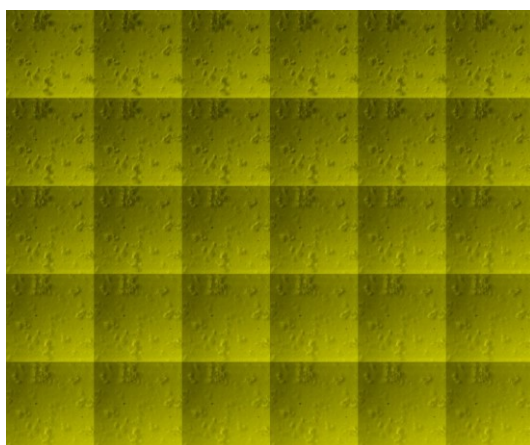
P1 0.005 mg/mL
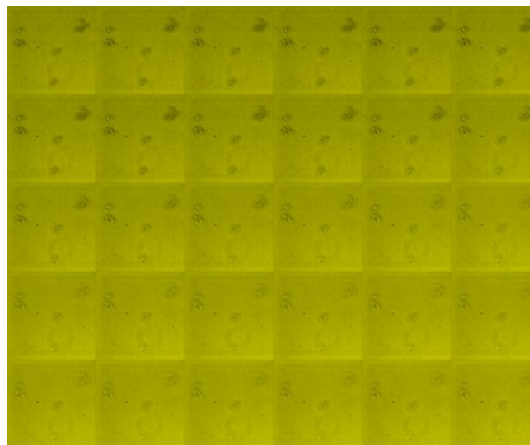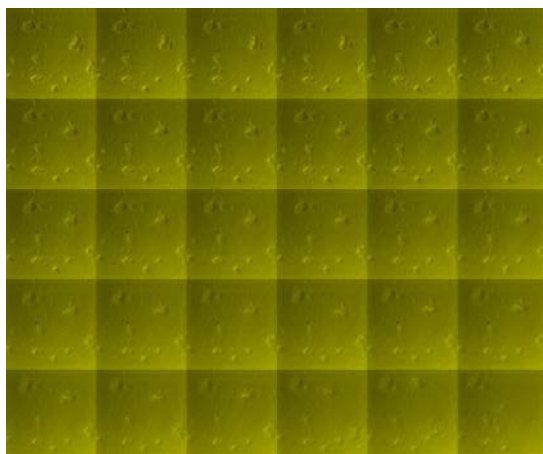
P1 0.05 mg/mL

P1 0.5 mg/mL

P2 0.005 mg/mL

P2 0.05 mg/mL
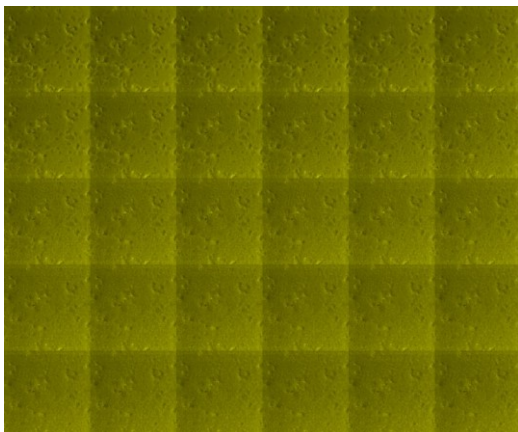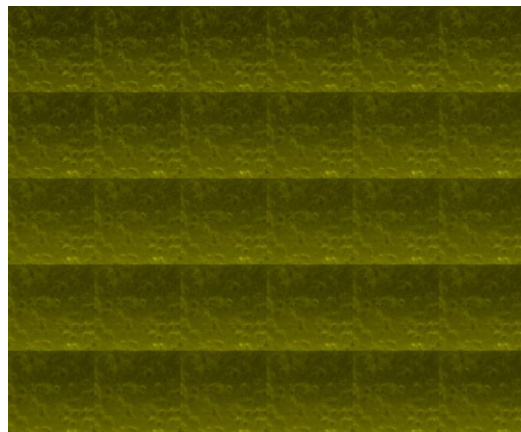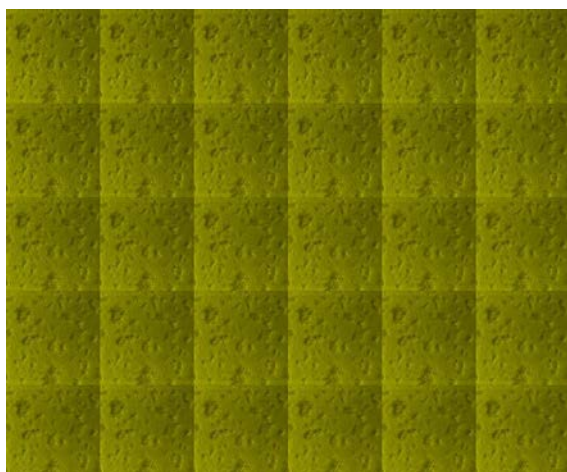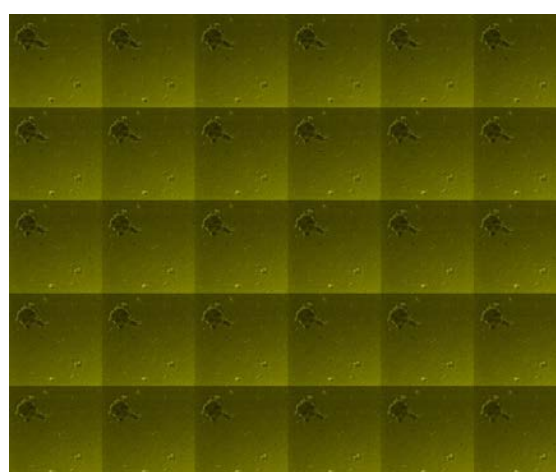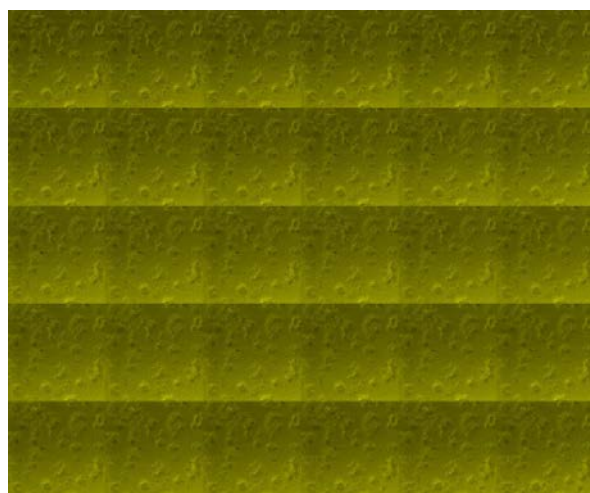

P2 0.5 mg/mL

<u>DMEM</u>

0 mg/mL

P1 0.005 mg/mL
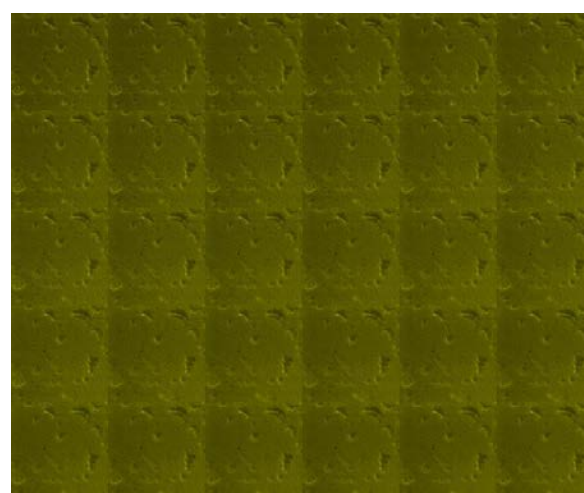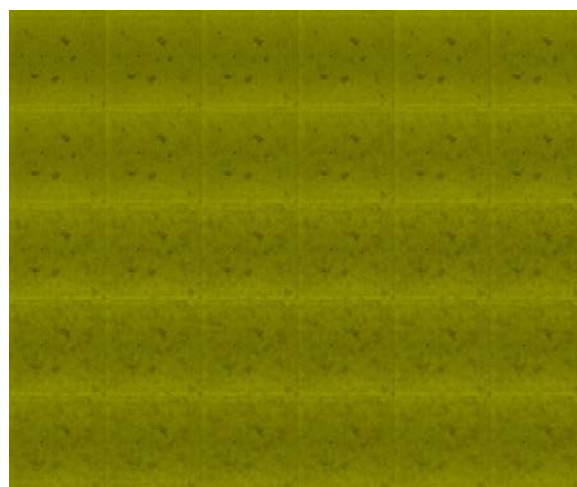
P1 0.05 mg/mL

P1 0.5 mg/mL

P2 0.005 mg/mL


P2 0.05 mg/mL

P2 0.5 mg/mL

During the clustering of *V. cholerae* reporter strains (NP5002, NP5003 and NP5005) with P1 (0.05 mg/ mL), P2 (0.5 mg/ mL) and P3 (0.5 mg/mL), LacZ activity was measured. Strains were adjusted to an OD_{600} of 0.2 with polymers at indicated concentrations in 1 mL of DMEM. Next, cells were washed with 200 mM PBS and a β-galactosidase assay was conducted as described in section 2.10.

In line with the assays presented in section 7.2.1, clustering reduced the transcription of the reporters tested. Interestingly, the untreated *ctxAB-lacZ* reporter showed increased transcription, with a maximum level at around 6-7 hours of incubation. In agreement with this, multiple LDH assays (Sec. 7.2.4) done prior to the β-galactosidase assays, showed that 7 hours was an optimal time frame to observe significant differences under the conditions assayed.
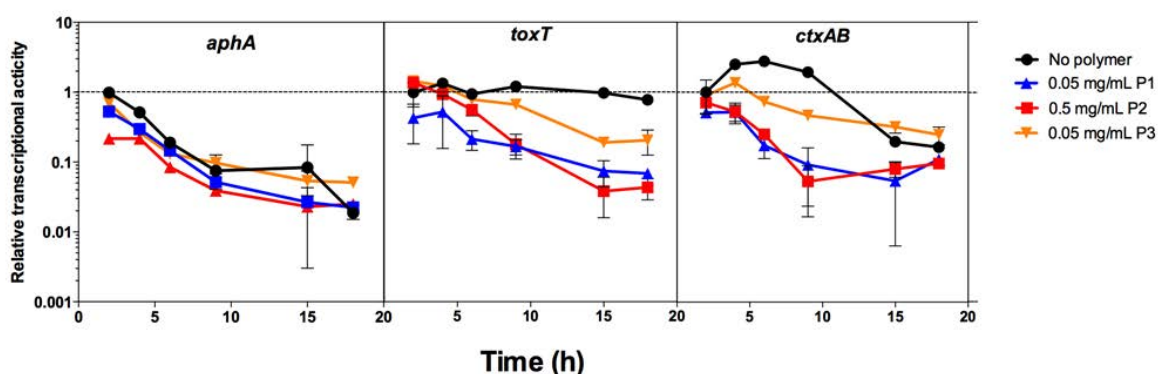
Appendix 3. Caco-2 cells exposed to P1.

At the same time that Caco-2 cells were infected with clustered *V. cholerae*, cells were exposed to the same concentration of polymer without bacteria (results shown in section 7.2.4). Samples were prepared for imaging by fluorescence microscopy. The figures below are representative images of Caco-2 exposed to different concentrations of P1. The morphology changes observed are appreciable. Cells turned from irregular to round, with denser nuclei (Hoechst). The cytoskeleton (rhodamine phalloidin) is packed into spots, suggesting that higher concentration of polymers induced cellular changes, possibly due to toxicity. The same pattern was observed with P2.

P1

| 0 mg/mL | 0.005 mg/mL | 0.05 mg/mL | 0.5 mg/mL |
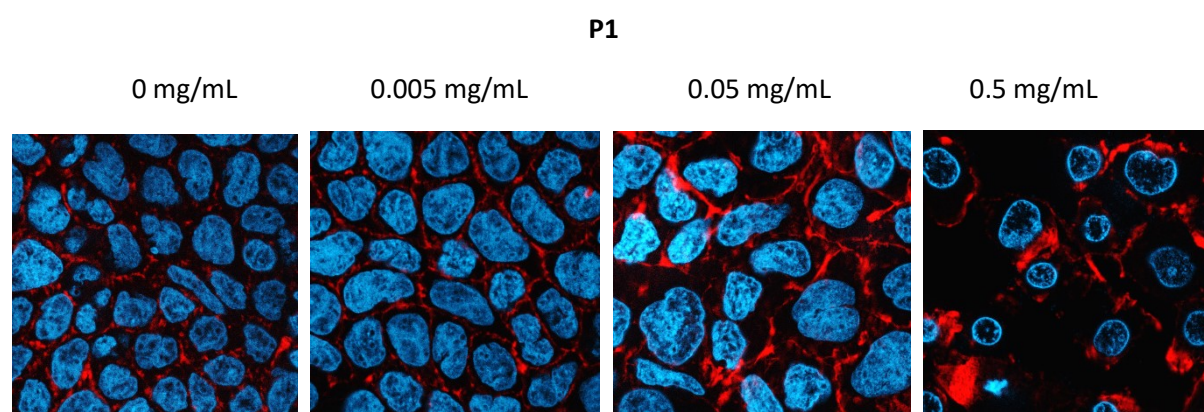
The main virulence factors of *V. cholera* N16961 (and 623-39) were immunodetected from clustered cells. Bacterial cells at an OD_{600} of 1.0 were incubated with P1, P2 and P3 at indicated concentrations in DMEM for 16 hours at 30 °C. Western blot analysis was done with anti-TcpA, custom made from an immunogenic fragment of TCP, and anti-CTxB.

Despite multiple attempts to detect the virulence factor, the conditions tested made it difficult to normalise the biomass to load equal amounts of sample. Initially, OD_{600} was not consistent as explained is section 4.2.4, and the quantification of protein from lysates that were previously clustered showed cross-reactivity with the material. In order to avoid these issues, the presence of cholera toxin was estimated by measuring the second messenger cAMP from infected epithelial cells (section 7.2.5). The detection of cholera did not show a defined band at the expected molecular weight (12 kDa), but a considerably bigger band appeared. In the case of TcpA, the detection was clean, but there was poor consistency and poor reproducibility across the experiments. The image shown was the best detection obtained, nevertheless, the loading control is inconsistent, so reliable conclusions cannot be made.